Water, carbon and nitrogen dynamics in soil - Influence of crop residue location and quality

Filip Coppens

▶ **To cite this version:**

Filip Coppens. Water, carbon and nitrogen dynamics in soil - Influence of crop residue location and quality. Earth Sciences. Institut national agronomique paris-grignon - INA P-G; Université Catholique de Louvain, 2005. English. NNT : . tel-00121922

HAL Id: tel-00121922

https://theses.hal.science/tel-00121922

Submitted on 22 Dec 2006

HAL is a multi-disciplinary open access archive for the deposit and dissemination of scientific research documents, whether they are published or not. The documents may come from teaching and research institutions in France or abroad, or from public or private research centers.

L'archive ouverte pluridisciplinaire **HAL**, est destinée au dépôt et à la diffusion de documents scientifiques de niveau recherche, publiés ou non, émanant des établissements d'enseignement et de recherche français ou étrangers, des laboratoires publics ou privés.

Katholieke Universiteit Leuven

Faculteit Bio-ingenieurswetenschappen

Institut National Agronomique Paris-Grignon

Ecole Doctorale ABIES

DISSERTATIONES DE AGRICULTURA

Doctoraatsproefschrift Nr. 648 aan de Faculteit Bio-ingenieurswetenschappen
van de K.U.Leuven

Water, carbon and nitrogen dynamics in soil

Influence of crop residue location and quality

Thèse pour obtenir le grade de
Docteur de l'Institut National
Agronomique Paris-Grignon
présentée et soutenue publiquement

Proefschrift voorgedragen tot
het behalen van de graad van
Doctor in de Toegepaste
Biologische Wetenschappen

par

door

Filip COPPENS

Promotoren / Directeurs de thèse:
Prof. R. Merckx, K.U.Leuven
Dr. S. Recous, INRA Unité d'Agronomie Laon-Reims-Mons
Dr. P. Garnier, INRA Unité d'Agronomie Laon-Reims-Mons

Leden van de examencommissie / Jury:
Prof. J. Coosemans, K.U.Leuven, voorzitter - président
Dr. J. Balesdent, INRA - CEA
Prof. J. Feyen, K.U.Leuven
Prof. J. Roger-Estrade, INA P-G
Prof. E. Smolders, K.U.Leuven

MEI 2005

Dankwoord - Remerciements

“En Filip, heb je geen zin om naar Frankrijk te verhuizen...”

Zo werd ik bijna vier jaar geleden door Roel verwelkomd tijdens een koffiepauze - en het resultaat is dat ik een doctoraat, maar vooral een hele levenservaring rijker ben geworden. Bedankt Roel, voor deze unieke kans, voor het uitwisselen van ideeën en voor het vele verbeterwerk tussen (en tijdens) alle reizen door.

Merci Sylvie, pour l’accueil chaleureux à Laon, pour ton aide et tes conseils - malgré un agenda aussi trop chargé. Mais surtout merci, parce que tu étais toujours là avec un mot de soutien dans les moments un peu difficiles.

Merci Patricia, pour m’avoir introduit dans le monde de la modélisation, et parce que ta porte était toujours ouverte pour une bonne discussion.

Merci Florence pour l’assistance au labo - sans toi je ferais toujours ‘plouf - plouf’. Je n’oublie pas non plus Olivier, Gonzague et Sylvie pour les milliers d’analyses; Eric, Daniel, Yves, Fred B. et Fred M. pour l’assistance technique. Sans Valérie et Brigitte, je n'aurais pas survécu “l’administration française”. Merci à toute l’Unité d’Agronomie pour l’accueil formidable tout au long de ces trois années que j’ai vécu avec vous.

Merci Roy Kasteel, Monique Carnol et Jean Roger-Estrade, pour vos remarques et les discussions très utiles pendant les Comités de Pilotage. Je remercie également Antoine Findeling, qui nous a sauvé chaque fois quand nous étions en train de nous noyer dans le PASTIS.

Je suis reconnaissant à l’INRA et la Région Picardie, ainsi qu'au GICC 2002 et le projet bilatéral franco-flamand ‘Tournesol’, pour le support financier qui a permis de réaliser ce travail.

Bedankt Frans, voor de plastieken buizen die door jou omgetoverd werden tot heuse bodemkolommen; Kristin en Karla, voor de hulp tijdens de late uurtjes in Laon (en de lekkere broccoli-taart); Steven en Heleen, voor de nuttige aggregaattips, en iedereen van het Laboratorium voor Bodem- en Waterbeheer voor de fijne momenten die ik bij jullie heb doorgebracht. Bedankt Katrien, voor de telefoontjes tussen Laon en Reims als ik dan toch eens een Nederlandstalige babbel wou doen.

Graag wil ik ook mijn ouders bedanken voor de kans die ze me hebben gegeven om verder te studeren. Wees gerust, nu ga ik écht beginnen werken...

Tenslotte: bedankt Elke, voor je eindeloos geduld tijdens de afgelopen maanden en voor de honderden SMS'jes morele steun die de Belgisch-Franse grens zijn overgevlogen.

Filip Coppens, 2002-2005

Summary

At present, the mechanisms for carbon sequestration in soil are not well identified and there is still a great deal of uncertainty about its quantification. In particular, little information is available on the impact of modifications in tillage practice (e.g. conversion from conventional tillage towards no-tillage) or changes in land use on carbon stocks and fluxes in soil. Land use and management are principal factors affecting the transformation of organic matter, determining the mineralization of carbon and nitrogen or their retention in soil. In addition, different ecosystems (e.g. arable land, pasture and forest) offer a large variety of vegetation types and likewise plant residues of different nature and quality.

The main objective of this work was to identify the physical and biological processes that are affected by plant residue location in soil, in interaction with residue quality. The initial location of plant residues acts directly on some soil physical properties: the water dynamics, solute transport and soil temperature. The biochemical quality of crop residues influences the soil (micro-)biological processes: biotransformations of carbon and nitrogen, and the activity and composition of the soil microbial biomass. These soil physical and biological changes may interact, modify the soil structure (e.g. by aggregation) and in turn influence the decomposition of soil organic matter.

In a first part, the influence of residue quality and soil type on C and N mineralization was investigated with 'optimal' soil-residue contact, i.e. with homogenous incorporation of finely chopped plant material. It has been demonstrated that, under controlled and non-limiting N conditions, the quality of the substrate added was the first factor determining the residue decomposition rate and that soil type had little or no effect on the short-term dynamics of residue decomposition. However on a longer term, carbon mineralization was slightly influenced by soil type, which was probably due to differences in the capacity to stabilize soluble carbon and/or microbial derived carbon.

In a second part, the effect of plant residue location on C and N mineralization was examined for oilseed rape residues in a silt loam soil. Soil columns were constructed with incorporated or surface applied residues and periodically placed under a rainfall simulator to simulate field conditions. Soil evaporation was reduced with surface placed residues, resulting in a larger soil water content than with residue incorporation. At the same time, fast desiccation of the residue mulch was observed. Mulch-derived C and N were concentrated near the soil surface, while residue-C and -N were distributed more deeply in the soil profile with residue

incorporation. Microbial activity was closely related to soluble carbon concentrations in the soil profile. Differences in water and nutrient availability resulted in a slower decomposition rate of residues left at the soil surface than when incorporated in soil. Net nitrogen mineralization was larger in soil under mulch than with residue incorporation.

Further, the influence of crop residue location on the fate of C and N in soil and soil aggregates was investigated to elucidate the mechanisms controlling carbon storage in soil. On the short term, a large fraction of particulate organic matter (POM) was left at the soil surface, while almost all of the POM had disappeared with residue incorporation. Residue addition increased the aggregate mean weight diameter (MWD) compared to the control soil, and a larger MWD was obtained in the 0-5 cm soil layer under mulch than with residue incorporation. The total amount of residue-C recovered in the aggregate fractions did not significantly differ between treatments. However, this carbon was mostly located in the upper soil layer with mulch, while it was almost equally distributed over the two soil layers with residue incorporation. Despite the different way for new C to enter the soil, the relative distribution of residue-C in the various aggregate fractions did not differ between the two treatments on the longer term - probably because in both treatments residue-C mainly entered the aggregate fractions as soluble C.

Finally, the interaction of crop residue location with residue quality regarding C and N mineralization was examined. Residue mulch significantly reduced soil water evaporation, the extent of reduction depended on physical properties of the mulch layer. Changes in mulch water content, assumed as the main factor controlling surface residue decomposition, also depended on (physical) residue quality. When incorporated, C mineralization rates were mainly influenced by the biochemical residue quality, e.g. C:N ratio and soluble compounds. The strongest interactions between residue location and quality were observed in the N dynamics: net N mineralization was determined by the interaction between soil water content (depending on residue location) and N availability (depending on residue quality). Our results contributed to the development and calibration of a submodule of the PASTIS model (Garnier *et al*., 2003), describing the decomposition of mulched residues. Modelling with $PASTIS_{mulch}$ allowed to access gross N fluxes, to estimate nitrate transport and potential leaching in the soil profile and to quantify the impact of residue location and quality on C and N mineralization in soil.

Keywords: carbon, nitrogen, decomposition, crop residue location and quality, modelling

Résumé

Les mécanismes qui contrôlent le stockage du carbone dans le sol ne sont pas tous clairement identifiés et il reste une grande incertitude concernant leur quantification. Peu d'information est disponible sur l'impact des changements de pratiques culturales ou de gestion des sols sur les stocks et les flux de carbone dans le sol. L'usage et la gestion des sols sont les facteurs principaux qui influencent les transformations de la matière organique, déterminant la minéralisation du carbone et de l'azote ou leur rétention dans le sol. De plus, les différents écosystèmes (grande culture, prairie et forêt) offrent une grande variété de végétation et donc de caractéristiques de résidus végétaux.

L'objectif principal de cette thèse est l'identification des processus physiques et biologiques qui sont influencés par la localisation des résidus dans le sol, en interaction avec la qualité de ces résidus. La localisation initiale des résidus modifie des propriétés physiques du sol : les dynamiques d'eau, le transport des solutés ou la température du sol. La qualité biochimique des résidus influence les processus (micro-) biologiques : les biotransformations du carbone et de l'azote, l'activité et la composition des populations microbiennes dans le sol. Ces changements physiques et biologiques interagissent, peuvent modifier la structure du sol (par l'agrégation) et, en retour, influencer la décomposition de la matière organique.

La première partie de ce travail traite de l'influence de la qualité des résidus végétaux et du type de sol sur la minéralisation du C et N en contact 'optimal' avec le sol (incorporation homogène des résidus finement coupés). Il est montré que sous conditions contrôlées et d'azote non limitant, la qualité des résidus est le facteur principal déterminant la vitesse de décomposition. Le type de sol a un effet négligeable sur les dynamiques de décomposition à court terme. Par contre, la minéralisation du carbone à plus long terme dépend du type de sol, ce qui est probablement lié aux différences dans la capacité du sol à stabiliser du carbone soluble ou d'origine microbienne.

La deuxième partie traite de l'effet de la localisation des résidus sur la minéralisation du C et N pour des résidus de colza dans un sol limoneux. Des colonnes de sol sont construites avec des résidus soit incorporés soit appliqués à la surface du sol. Les colonnes sont placées périodiquement sous un simulateur de pluie pour simuler des conditions hydriques relativement similaires au champ. L'évaporation du sol est fortement réduite avec le mulch, ce qui conduit à une humidité du sol plus grande que lorsque les résidus sont incorporés. Simultanément, on observe un dessèchement rapide du mulch de résidus. Le C et N issu des

résidus est distribué différemment dans le sol selon que ceux-ci sont à la surface ou incorporés. Les différences dans la disponibilité d'eau et des nutriments conduisent à une vitesse de décomposition plus lente pour des résidus à la surface que pour des résidus incorporés dans le sol. Cependant, la minéralisation nette de l'azote est plus grande dans le sol sous mulch qu'avec incorporation des résidus en raison de l'humidité plus grande qui favorise la minéralisation et d'une moindre organisation d'azote.

L'influence de la localisation des résidus sur le devenir du C et N dans le sol et dans les agrégats est examinée afin d'évaluer les mécanismes qui contrôlent le stockage du carbone dans le sol. A court terme, une grande partie de la matière organique particulaire (MOP) est retenue à la surface du sol avec le traitement mulch alors que toute la MOP a disparu quand les résidus sont incorporés. La présence des résidus augmente la taille moyenne des agrégats comparé au sol témoin et des agrégats plus larges sont trouvés dans la couche de sol 0-5 cm sous le mulch que dans la couche ou les résidus sont incorporés. La quantité totale du C des résidus récupérée dans les agrégats est similaire avec les résidus laissés à la surface et les résidus incorporés, mais elle est distribuée différemment dans le profil du sol. Malgré les différences dans la façon dont le C 'nouveau' entre dans le sol, la distribution relative du C des résidus dans les micro et macro agrégats est la même pour les deux localisations, probablement parce que dans les deux cas le C des résidus entre dans les agrégats sous forme soluble.

Finalement, l'interaction entre la localisation des résidus et leur qualité est étudiée. Un mulch réduit fortement l'évaporation du sol et l'importance de cette réduction dépend de la qualité physique du mulch. Des changements dans l'humidité du mulch, identifié comme facteur principal qui détermine la décomposition du mulch, dépend aussi de la qualité (physique) des résidus. Avec l'incorporation des résidus, la vitesse de minéralisation de C est principalement influencée par la qualité biochimique des résidus. L'interaction la plus forte entre localisation et qualité des résidus est observée sur les dynamiques de l'azote : la minéralisation nette de l'azote est déterminée par l'interaction entre l'humidité du sol (effet localisation) et la disponibilité de l'azote (effet qualité). Ces résultats permettent de développer et de calibrer un module du modèle PASTIS (Garnier *et al*., 2003), conçu pour simuler la décomposition d'un mulch. La modélisation avec $PASTIS_{mulch}$ a permis d'avoir accès au flux brut d'azote, d'estimer le transport des nitrates et le lessivage potentiel dans le profil du sol, et de quantifier l'impact de la localisation et qualité des résidus sur la minéralisation du C et N dans le sol.

Mot clés : carbone, azote, décomposition, localisation et qualité du résidu, modélisation

Samenvatting

Op dit ogenblik zijn de mechanismen die koolstofopslag in de bodem bepalen nog niet helemaal gekend en bestaat er grote onzekerheid over de hoeveelheid koolstof, afkomstig van plantenresten of "residu's", die de bodem kan stockeren. Meer in het bijzonder is er weinig informatie beschikbaar over de impact van een veranderd bodemgebruik of bodembewerking op de koolstofflux in bodems, bijvoorbeeld bij de overgang van conventioneel ploegen naar 'no-tillage'. Nochtans zijn bodemgebruik en -bewerking belangrijke factoren die de afbraak van organische stof beïnvloeden. Daarenboven heeft elk ecosysteem (bv. akker, weide of bos) zijn eigen vegetatietype en daardoor komen plantenresten met zeer verschillende karakteristieken in of op de bodem terecht.

De doelstelling van deze studie is de bodemfysische en -biologische processen te identificeren die worden beïnvloed door de plaats waar residu's in de bodem terechtkomen: ingemengd of op het bodemoppervlak. Hierbij zal ook de interactie met de kwaliteit van de residu's worden nagegaan. De locatie van residu's in de bodem heeft een rechtstreekse invloed op bodemfysische eigenschappen, zoals op het transport van water en opgeloste stoffen. Biochemische karakteristieken van de residu's beïnvloeden hun C- en N-mineralisatie en bepalen de activiteit en samenstelling van de microbiële biomassa. Wijzigingen in deze fysische en biologische eigenschappen werken op elkaar in en kunnen op hun beurt een invloed uitoefenen op de afbraak van organisch materiaal in de bodem (bv. door een verandering in bodemaggregatie).

In een eerste deel van dit werk is de invloed van de residu-kwaliteit en het bodemtype op C- en N-mineralisatie bestudeerd. Dit gebeurde met 'optimaal' contact tussen bodem en residu door fijn plantenmateriaal in de bodem te vermengen. Er werd aangetoond dat, onder gecontroleerde omstandigheden, de residu-kwaliteit de voornaamste factor was die de afbraaksnelheid bepaalde en dat bodemtype op korte termijn een verwaarloosbare rol speelde. Op lange termijn werd het effect van bodemtype wel belangrijker; waarschijnlijk omwille van verschillen in potentiële stabilisatie van opgeloste koolstof of biomassa-C door de minerale bodemfractie.

In een tweede deel werd het effect van residu-locatie op C- en N-mineralisatie onderzocht. Er werden bodemkolommen opgezet waarbij koolzaad-residu's werden ingemengd of waarbij ze als mulch op het bodemoppervlak bleven liggen. De kolommen werden regelmatig onder een regensimulator geplaatst om veldomstandigheden na te bootsen. Bedekking van het

bodemoppervlak met mulch reduceerde de evaporatie van de bodem, hetgeen resulteerde in een verhoogd vochtgehalte in de bodem. De mulch zelf droogde sterk uit telkens na een regenval. De residu-C en -N waren verschillend verdeeld over het bodemprofiel naargelang de initiële locatie van de residu's. Verschillen in de beschikbaarheid van water en nutriënten resulteerden in een tragere afbraak van residu-mulch dan van ingemengde residu's in de bodem. Netto N-mineralisatie was groter in de bodem onder mulch dan met ingemengde residu's, doordat het hogere vochtgehalte van de bodem N-mineralisatie stimuleerde en doordat de scheiding van bodem-N en residu-C de N-immobilisatie verminderde.

Daarnaast werd ook de invloed van residu-locatie op de bestemming van C en N in de bodem en in bodemaggregaten nagegaan, om de mechanismen te verhelderen die verantwoordelijk zijn voor de koolstofopslag in de bodem. Op korte termijn bleef er een grote hoeveelheid residu-deeltjes (> 2 mm) achter op het bodemoppervlak met mulch, terwijl bijna geen residu-deeltjes konden worden gerecupereerd na inmenging in de bodem. Hier zat residu-C voornamelijk in de fijne bodemfractie (< 2 mm). Het toevoegen van residu's aan de bodem resulteerde in grotere bodemaggregaten dan in de controle-bodem. De meest stabiele macroaggregaten werden gevonden in de 0-5 cm bodemlaag onder mulch. Voor de twee residu-locaties was er weinig verschil in de relatieve verdeling van residu-C over de verschillende aggregaatklassen; waarschijnlijk omdat in beide gevallen aggregaten door diffusie van opgeloste residu-C werden aangerijkt.

Tenslotte werd het effect van de interactie tussen residu-locatie en -kwaliteit op C- en N-mineralisatie bestudeerd. Een mulch reduceerde de evaporatie van de bodem en de mate waarin dit gebeurde hing af van de fysische eigenschappen van de mulch-laag. De variaties in het watergehalte van de mulch, die eerder werden aangeduid als belangrijkste factor in de controle van de afbraaksnelheid, werden ook beïnvloed door de fysische eigenschappen van de residu's. Voor ingemengde residu's daarentegen was de residu-kwaliteit (bv. C:N-verhouding of de fractie aan oplosbare stoffen) bepalend voor de C-mineralisatie-snelheid. De sterkste interacties tussen residu-locatie en -kwaliteit werden waargenomen bij de N-dynamiek. Onze resultaten hebben bijgedragen tot de ontwikkeling en calibratie van een module in het PASTIS-model (Garnier *et al*., 2003), dat toelaat de afbraak van een residu mulch te simuleren. Dankzij dit model konden bruto N-mineralisatie en transport van nitraat in de bodem worden geëvalueerd en kon een kwantitatieve schatting gemaakt worden van het effect van residu-locatie en -kwaliteit op C- en N-mineralisatie in de bodem.

Sleutelwoorden: koolstof, stikstof, decompositie, residu-locatie en -kwaliteit, modelleren

List of Abbreviations

a.e. %	atom % excess
AGRI	referring to arable soil
BIO	microbial biomass
CANTIS	Carbon And Nitrogen Transformations In Soil
CEC	cation exchange capacity
CEL	cellulose
CTRL	control soil, without residue addition
CWE	cold water extractable
DIC	dissolved inorganic carbon
DOC	dissolved organic carbon
DOC_m	mobile dissolved organic carbon
DOC_{pa}	potentially available dissolved organic carbon
DPM	decomposable plant material
FOR	referring to forest soil
HEM	hemicellulose
HOM	humified organic matter
INC	soil with residue incorporation in the 0-10 cm soil layer
IOM	inert organic matter
FOM	fresh organic matter
LIG	lignin
MWD	mean weight diameter
NDF	neutral detergent fraction
NDS	neutral detergent solution
Nmin	mineral nitrogen (NH_4^+-N + NO_3^--N)
PAST	refering to pasture soil
PASTIS	Prediction of Agricultural Solute Transport In Soil
POM	particulate organic matter
R0-3-6-9	artificial rainfall after 0, 3, 6 and 9 weeks of incubation
RAPE	decomposition experiment with oilseed rape residues
RDM	rapidly decomposable material
RPM	resistant plant material

RYE	decomposition experiment with rye residues
SOC	soil organic carbon
SOL	soluble residue fraction
SURF	soil with surface placed residues
wt. %	gravimetric %

List of Symbols

α	scaling factor of the matric potential / m^{-1}
B_Z	carbon content in zymogenous biomass / mg C kg^{-1}
E_f	model efficiency coefficient / -
E_{os}	potential daily soil evaporation / mm
$F_{1,2}$	reduction factor for soil-residue contact / -
F_{decomp}	residue decay rate / day^{-1}
f_b	biomass reduction factor / -
f_N	nitrogen reduction factor / -
f_t	temperature reduction factor / -
f_w	moisture reduction factor / -
h_A	humification coefficient by the autochthonous biomass / -
h_Z	humification coefficient by the zymogenous biomass / -
$h(\theta)$	soil water retention curve
K_{MZ}	soil-residue contact factor connected to the zymogenous biomass / mg C kg^{-1}
K_s	saturated soil hydraulic conductivity / cm $hour^{-1}$
$K(\theta)$	soil hydraulic conductivity curve
k	potential decompostion rate constant / day^{-1}
k_A	decomposition rate constant of the autochthonous biomass / day^{-1}
k_H	decomposition rate constant of the humified organic matter / day^{-1}
k_Z	decomposition rate constant of the zymogenous biomass / day^{-1}
m	empirical shape parameter / -
n	empirical shape parameter / -
R	residue mass / t ha^{-1}
R_{min}	residue mass above which the decomposition rate is reduced (for F_1) / t ha^{-1}
R_{max}	residue mass above which the decomposition rate is mass-independent / t ha^{-1}
R_{crit}	residue mass above which the decomposition rate is reduced (for F_2) / t ha^{-1}
θ_r	residual volumetric water content / $m^3\ m^{-3}$
θ_s	saturated volumetric water content / $m^3\ m^{-3}$

Contents

INTRODUCTION 1

General context 1
Scientific context 2
Research strategy 4
Choice of methodologies 6
Organization of the manuscript 7

1. ACCOUNTING FOR DIFFERENCES IN CONTACT BETWEEN SOIL AND PLANT RESIDUES IN DECOMPOSITION STUDIES: CONCEPTS AND MODELLING 9

1.1 Introduction 9
1.2 Factors influencing soil-residue contact 10
1.3 Effect of soil-residue contact on crop residue decomposition 13
1.3.1 Residue particle size 13
1.3.2 Residue location 15
1.4 Soil-residue contact in decomposition models 17
1.5 Conclusion 22

2. IMPACT OF PLANT QUALITY AND SOIL CHARACTERISTICS IN THE MINERALIZATION OF C AND N FROM GRASSLAND, FOREST AND ANNUAL CROP SOILS 25

2.1 Introduction 25
2.2 Materials and methods 26
2.2.1 Soil and plant residues 26
2.2.2 Incubation conditions 28
2.2.3 Sample treatment and analysis 28
2.2.4 Model description: Roth-C 26.3 29
2.2.5 Simulation method 29
2.3 Results 30
2.3.1 Characterization of agricultural, pasture and forest soils 30
2.3.2 Influence of plant residue quality 35
2.3.3 Influence of soil type 38
2.3.4 Simulation of plant residue biotransformations with Roth-C 40
2.4 Discussion 43
2.5 Conclusion 45

3. SOIL MOISTURE, CARBON AND NITROGEN DYNAMICS FOLLOWING INCORPORATION VERSUS SURFACE APPLICATION OF LABELLED RESIDUES IN SOIL COLUMNS 47

3.1 Introduction 47
3.2 Materials and methods 48
3.2.1 Soil 48
3.2.2 Crop residue 48
3.2.3 Soil column preparation 49
3.2.4 Experimental conditions 49
3.2.5 Experimental design 50

3.2.6 Destructive soil analysis *50*
3.2.7 Semi-continuous measurements *51*
3.3 RESULTS 52
3.3.1 Influence of crop residue location on water dynamics *52*
3.3.2 pH in soil and soil solution *54*
3.3.3 Distribution of soluble carbon *55*
3.3.4 Microbial activity: substrate induced respiration *55*
3.3.5 Residue decomposition *59*
3.3.6 Distribution of residue-C and -N in soil *61*
3.3.7 Nitrogen mineralization *62*
3.4 DISCUSSION 67
3.4.1 Soil water dynamics *67*
3.4.2 Soluble carbon *68*
3.4.3 Residue decomposition *69*
3.4.4 Distribution of residue-C and –N in soil *70*
3.4.5 Nitrogen mineralization-immobilization *70*
3.5 CONCLUSION 71

4. IMPACT OF CROP RESIDUE LOCATION ON CARBON AND NITROGEN DISTRIBUTION IN SOIL AND IN WATER-STABLE AGGREGATES 73

4.1 INTRODUCTION 73
4.2 MATERIALS AND METHODS 75
4.2.1 Soil and crop residues *75*
4.2.2 Experimental conditions *75*
4.2.3 Aggregate separation *76*
4.2.4 Soil analysis *76*
4.3 RESULTS 77
4.3.1 Characteristics of the soil samples *77*
4.3.2 Dynamics of residue-C and –N and its distribution in soil *78*
4.3.3 Aggregate dynamics *79*
4.3.4 Aggregate enrichment with ^{13}C and ^{15}N *85*
4.3.5 Distribution of residue-C and -N in aggregate fractions at week 33 ..... *85*
4.4 DISCUSSION 92
4.4.1 Soil aggregation *92*
4.4.2 Residue-C and –N stored in aggregate fractions *94*
4.5 CONCLUSION 96

5. COMPARING WATER, CARBON AND NITROGEN DYNAMICS IN SOIL COLUMNS WITH INCORPORATED OR SURFACE APPLIED CROP RESIDUES USING THE PASTIS MODEL 99

5.1 INTRODUCTION 99
5.2 MATERIALS AND METHODS 100
5.2.1 Experimental set-up *100*
5.2.2 Model description *103*
5.2.3 Boundary conditions *104*
5.2.4 Initial conditions *104*
5.2.5 Parameter optimization: water flow parameters *107*
5.2.6 Parameter optimization: biological parameters *107*
5.2.7 Model efficiency coefficient *107*
5.3 RESULTS 108

5.3.1 Water dynamics ... *108*
5.3.2 Residue decomposition ... *112*
5.3.3 Carbon dioxide fluxes ... *115*
5.3.4 Nitrogen dynamics ... *118*
5.4 DISCUSSION ... 122
5.4.1 Influence of residue location and quality on water dynamics ... *122*
5.4.2 Effects of residue location and quality, and their interactions ... *122*
5.4.3 Combined effects of residue location and quality on soil nitrogen dynamics and transport ... *126*
5.5 CONCLUSION ... 131

6. GENERAL DISCUSSION AND PERSPECTIVES ... 133

6.1 OBJECTIVES ... 133
6.2 GENERAL CONCLUSION ... 134
6.3 EVALUATION OF RESEARCH STRATEGY ... 136
6.4 PERSPECTIVES ... 140

APPENDIX A - DESCRIPTION PASTIS$_{MULCH}$ ... 145

ABSTRACT ... 146
INTRODUCTION ... 147
THEORETICAL BACKGROUND ... 148
The PASTIS model ... *148*
Adaptation of PASTIS model ... *151*
MATERIALS AND METHODS ... 155
Main experiment ... *155*
Specific soil incubations ... *158*
Analytical methods ... *158*
Modeling conditions ... *159*
Model parameters ... *159*
Model calibration and evaluation ... *163*
Sensitivity analysis ... *163*
RESULTS AND DISCUSSION ... 164
Model calibration ... *164*
Model evaluation ... *165*
Sensitivity analysis ... *181*
CONCLUSION ... 184

APPENDIX B - ILLUSTRATION EXPERIMENTAL DESIGN ... 187

APPENDIX C - BIBLIOGRAPHY ... 191

List of Tables

Table 1.1 The total surface area measured by gas adsorption, and the calculated maximum surface area available to an enzyme of molecular weight > 20 kDa of a number of typical forage plants. The surface area associated with pores of 3×10^{-3} µm diameter or less was excluded in calculating the available surface area. (Chesson, 1997) 11

Table 2.1 Selected properties of the soil sampled at Mons-en-Chausseé (AGRI), Theix (PAST) and Hesse (FOR). 26

Table 2.2 Selected chemical and biochemical properties of the plant residues used 27

Table 2.3 Nitrogen mineralization in AGRI, FOR and PAST, without and with incorporation of plant residues 35

Table 2.4 Characterization of biochemical plant residue properties in Roth-C. Average values of Decomposable Plant Material (DPM) and Resistant Plant Material (RPM) are obtained by optimization on experimental data of C mineralization of AGRI, PAST and FOR 40

Table 3.1 Carbon and nitrogen content of the biochemical fractions of the applied oilseed rape residue 49

Table 3.2 Distribution of ^{13}C and ^{15}N in the fine (<2 mm) and coarse (>2 mm) fraction with surface applied residues (SURF) or residues incorporated in the 0-10 cm soil layer (INC), expressed as % of added C and N (mean values, with standard errors in parentheses, n = 3). 63

Table 4.1 Distribution of (a) the soil water content, (b) microbial activity measured by substrate induced respiration and (c) dissolved organic carbon of CTRL, SURF and INC in the 0-5 cm and 5-10 cm soil layer at sampling. Different lowercase letters indicate significant differences over time ($P < 0.05$), for given soil layer and treatment. Different uppercase letters indicate significant differences between treatments and soil layers ($P < 0.05$), at given sampling point. 77

Table 4.2 Evolution over time of the distribution of residue-C and –N in particulate organic matter (> 2 mm) and the bulk soil (< 2 mm), for SURF and INC. 80

Table 4.3 Evolution of the mean weight diameter (MWD) of soil aggregates in the 0-5 cm and 5-10 cm soil layer of CTRL, SURF and INC. Different lowercase letters indicate significant differences over time ($P < 0.05$), for given soil layer and treatment. Different uppercase letters indicate significant differences between treatments and soil layers ($P < 0.05$), at given sampling point. 84

Table 4.4 Initial mass distribution and total C and N in the large macroaggregates (> 2000 µm), small macroaggregates (2000-250 µm), microaggregates (250-53 µm) and the silt and clay fraction (< 53 µm) of the control soil. 90

Table 4.5 Recapitulative of the distribution of residue-C and -N in soil aggregate and particulate organic matter (POM) fractions in the 0-5 cm and 5-10 cm soil layer, after 33 weeks of incubation. In this table, there is no overlap between residue-C and -N in soil aggregates and POM. Residue-C present at the soil surface as mulch is not taken into account. Values between parentheses indicate the standard error. 90

Table 5.1 Selected soil properties of the soil sampled at the experimental site in Mons-en-Chaussée (France) 101

Table 5.2 Selected chemical and biochemical properties of the oilseed rape and rye residues 101

Table 5.3 Description of initial conditions for the RAPE and RYE experiment..... 102

Table 5.4 Initial conditions of the organic pools and microbial biomass used in the PASTIS model (SOIL refers to parameters used by PASTIS, MULCH refers to parameters used by the submodule $PASTIS_{mulch}$) 106

Table 5.5 Distribution of the soil water content in the soil profile after 3, 6 and 9 weeks of incubation, for CTRL, SURF and INC of the RAPE and RYE treatment. Values are the average of 3 replicates; maximum standard error was 0.01 $cm^3\ cm^{-3}$. 108

Table 5.6 Model efficiency coefficients (E_f) for evaluation of $PASTIS_{mulch}$ 109

Table 5.7 Hydraulic parameters of soil retention and soil conductivity curves for RAPE and RYE used in $PASTIS_{mulch}$ 112

Table 5.8 Symbols, units and values of biological parameters used in $PASTIS_{mulch}$ 115

Table 5.9 Distribution of the amount of NO_3^--N in the soil profile after 3, 6 and 9 weeks of incubation, for CTRL, SURF and INC of the RAPE and RYE treatment. Values are the average of 3 replicates; standard errors are indicated between parentheses. 119

Table A.1 Biological parameters used in the CANTIS (Carbon And Nitrogen Transformations In Soil) submodel..... 151

Table A.2 Mulch parameters used in the mulch module of $PASTIS_{mulch}$ (Prediction of Agricultural Solute Transfer In mulched Soils) model 152

Table A.3 Characteristics of the used soil, rape and the rye residues 155

Table A.4 Description of experimental conditions for the rape and rye experiments..... 156

Table A.5 Initial condition of organic pools and microbial biomasses used in the CANTIS (Carbon And Nitrogen Transformations In Soil) submodel..... 161

Table A.6 Hydraulic parameters of soil retention and soil conductivity curves for the rape and the rye experiments 162

Table A.7 Optimal value of the parameters and statistical performance of the calibrated model for the rape and the rye experiments 166

List of Figures

Figure 0.1 Conceptual diagram of interactions between soil physical and biological processed, as influenced by land use and management practices 3

Figure 1.1 Simplified diagram of interactions between soil and plant residue particles (Fruit *et al*., 1999)..... 12

Figure 1.2 The default functions for the four factors that limit residue decomposition in APSIM-Residue due to: (a) temperature (T_{opt} = 25°C); (b) moisture (potential daily soil evaporation E_{os}, max = 25 mm); (c) initial residue C:N ratio ($C:N_{opt}$ = 25); (d) residue-soil contact (R_{min} = 1.5 t ha^{-1}, R_{max} = 3 t ha^{-1} and $F_{contact,min}$ = 0.46). The dashed line in (d) shows the new residue-soil contact function (Eq. 1.3) with R_{crit} = 1.5 t ha^{-1}. (Thorburn *et al.*, 2001) 20

Figure 1.3 Conceptual diagram of residue on the soil surface showing two layers: layer 1, in contact with the soil and decomposing; and layer 2, the residue above layer 1 that is not decomposing. The thickness of layer 1 remains constant through time as long as there is residue in layer 2. The thickness of layer 2 decreases through time as residue from that layer replaces the residue decomposed from layer 1. (Thorburn *et al.*, 2001)..... 21

Figure 2.1 Cumulative carbon mineralization in an arable (AGRI), pasture (PAST) and forest (FOR) soil, without addition of residue-C (control soil). Error bars indicate the standard error (n = 3). 30

Figure 2.2 Relationship between cumulative C mineralization after 142 days of incubation and the amount of initial biomass-C for the control soil of AGRI, PAST and FOR 31

Figure 2.3 Change of NH_4^+-N and total mineral nitrogen (NH_4^+-N + NO_3^--N) in the control soil of AGRI, PAST and FOR over time. Error bars indicate the standard error (n = 3). 32

Figure 2.4 (a) Cumulative carbon mineralization, expressed in % of added C, in AGRI with incorporation of oilseed rape and rye, calculated from evolved CO_2 or by difference with residual ^{13}C. Error bars represent the standard error (n = 3). 33

Figure 2.4 (b) Cumulative carbon mineralization, expressed in % of added C, in FOR with beech leaves and in PAST with Lolium roots, calculated from evolved CO_2 or by difference with residual ^{13}C (no ^{13}C data available for Lolium). Error bars represent the standard error (n = 3)..... 34

Figure 2.5 (a) Cumulative carbon mineralization, expressed in % of added C, and (b) change in mineral N content, in the arable soil (AGRI) with incorporation of rye and oilseed rape residues, Lolium and Dactylis roots, and beech leaves. Error bars indicate the standard error (n = 3). 36

Figure 2.6 (a) Relationship between cumulative C mineralization after 3 days of incubation and the soluble residue fraction, and (b) relationship between cumulative C mineralization after 142 days of incubation and the lignin-like residue fraction..... 37

Figure 2.6 (c) Relationship between the accumulation of mineral N in soil after 142 days of incubation and the plant residue N content. 38

Figure 2.7 Cumulative C mineralization, expressed in % of added C, for rye in AGRI, FOR and PAST, beech leaves in AGRI and FOR, and Lolium roots in AGRI and PAST..... 39

Figure 2.8 Simulation of carbon mineralization in the different soil-residue combinations with the Roth-C model. Only the parameter $DPM.(DPM+RPM)^{-1}$ was optimized. 41

Figure 2.9 Observed values with prediction of the fate of carbon in FOR on the long term, with incorporation of rye residues and beech leaves..... 42

Figure 2.10 Estimation of the parameter $DPM.(DPM+RPM)^{-1}$ from biochemical plant residue characteristics. Data from three soils and five residues are used. 42

Figure 3.1 Distribution of the gravimetric soil water content through the soil profile of the control (CTRL ○), surface (SURF ●) and incorporation treatment (INC ▼), at the end of a 3-week evaporation period. Values are the average of the three wetting-drying cycles (bars represent the standard error, n = 9) 53

Figure 3.2 Change in the gravimetric water content of residues at the soil surface over the 3 wetting-drying cycles (△) and the residual mass of surface applied residues (SURF ●) (mean values, bars represent the standard error, n = 3)..... 54

Figure 3.3 (a) Distribution of the 'mobile' dissolved organic carbon concentration (DOC_m) in the soil solution after rainfall R0 and R3 of the control (CTRL ○), surface (SURF ●) and incorporation treatment (INC ▼) (mean values, bars represent the standard error, n = 2) 56

Figure 3.3 (b) Distribution of the 'mobile' dissolved organic carbon concentration (DOC_m) in the soil solution after rainfall R6 and R9 of the control (CTRL ○), surface (SURF ●) and incorporation treatment (INC ▼) (mean values, bars represent the standard error, n = 2) 57

Figure 3.4 Distribution of the amount 'potentially available' dissolved organic carbon (DOC_{pa}) in different soil layers after 3, 6 and 9 weeks of incubation (before re-wetting) in the control (CTRL ○), surface (SURF ●) and incorporation treatment (INC ▼) (mean values, bars represent the standard error, n = 3)..... 58

Figure 3.5 Distribution of the soil microbial activity in different soil layers, measured by substrate induced respiration, after 3, 6 and 9 weeks of incubation (before re-wetting) of the control (CTRL ○), surface (SURF ●) and incorporation treatment (INC ▼) (mean values, bars represent the standard error, n = 3)..... 60

Figure 3.6 Change in the CO_2 flux for soil without residues (CTRL ○), residues left at the soil surface (SURF ●) or incorporated in the 0-10 cm soil layer (INC ▼). Arrows indicate the application of artificial rain (R0-R9) (mean values, bars represent the standard error, n = 2 for CTRL and SURF, n = 3 for INC) 61

Figure 3.7 (a) The concentration of NO_3^--N in the soil solution at different soil depths after rainfall R0 and R3, for soil without residues (CTRL ○), residues left at the soil surface (SURF ●) or incorporated in the 0-10 cm soil layer (INC ▼) (mean values, bars represent the standard error, n = 2) 64

Figure 3.7 (b) The concentration of NO_3^--N in the soil solution at different soil depths after rainfall R6 and R9, for soil without residues (CTRL ○), residues left at the soil surface (SURF ●) or incorporated in the 0-10 cm soil layer (INC ▼) (mean values, bars represent the standard error, n = 2) 65

Figure 3.8 Distribution of NO_3^--N in different soil layers after 3, 6 and 9 weeks of incubation (before re-wetting), for soil without residues (CTRL ○), residues left at the soil surface (SURF ●) or incorporated in the 0-10 cm soil layer (INC ▼) (mean values, bars represent the standard error, n = 3) 66

Figure 3.9 Change in CO_2 flux with changing mulch water content during the 3 evaporation periods (Week 0-3, Week 3-6 and Week 6-9)..... 68

Figure 4.1 (a) Evolution of the distribution of aggregate fraction mass over time for the large macroaggregates (> 2000 µm), small macroaggregates (2000-250 µm), microaggregates (250-53 µm) and the silt and clay fraction (< 53 µm), for (A) the 0-5 cm and (B) the 5-10 cm soil layer of CTRL. Error bars show the 95% confidence interval. 81

Figure 4.1 (b) Evolution of the distribution of aggregate fraction mass over time for the large macroaggregates (> 2000 µm), small macroaggregates (2000-250 µm), microaggregates (250-53 µm) and the silt and clay fraction (< 53 µm), for (A) the 0-5 cm and (B) the 5-10 cm soil layer of SURF. Error bars show the 95% confidence interval. 82

Figure 4.1 (c) Evolution of the distribution of aggregate fraction mass over time for the large macroaggregates (> 2000 µm), small macroaggregates (2000-250 µm), microaggregates (250-53 µm) and the silt and clay fraction (< 53 µm), for (A) the 0-5 cm and (B) the 5-10 cm soil layer of INC. Error bars show the 95% confidence interval. 83

Figure 4.2 (a) Evolution of the ^{13}C atom % excess over time, measured in the large macroaggregates (> 2000 µm), small macroaggregates (2000-250 µm), microaggregates (250-53 µm) and the silt and clay fraction (< 53 µm), for (A) the 0-5 cm and (B) the 5-10 cm soil layer of SURF. Error bars show the 95% confidence interval. 86

Figure 4.2 (b) Evolution of the ^{13}C atom % excess over time, measured in the large macroaggregates (> 2000 µm), small macroaggregates (2000-250 µm), microaggregates (250-53 µm) and the silt and clay fraction (< 53 µm), for (A) the 0-5 cm and (B) the 5-10 cm soil layer of INC. Error bars show the 95% confidence interval. 87

Figure 4.3 (a) Evolution of the ^{15}N atom % excess over time, measured in the large macroaggregates (> 2000 µm), small macroaggregates (2000-250 µm), microaggregates (250-53 µm) and the silt and clay fraction (< 53 µm), for (A) the 0-5 cm and (B) the 5-10 cm soil layer of SURF. Error bars show the 95% confidence interval. 88

Figure 4.3 (b) Evolution of the ^{15}N atom % excess over time, measured in the large macroaggregates (> 2000 µm), small macroaggregates (2000-250 µm), microaggregates (250-53 µm) and the silt and clay fraction (< 53 µm), for (A) the 0-5 cm and (B) the 5-10 cm soil layer of INC. Error bars show the 95% confidence interval. 89

Figure 5.1 (a) Comparison between the observed and simulated change in soil matric potential over time, determined at 6 cm and 14 cm soil depth, with incorporation (INC) of RAPE and RYE residues. 110

Figure 5.1 (b) Comparison between the observed and simulated change in soil matric potential over time, determined at 6 cm and 14 cm soil depth, with surface application (SURF) of RAPE and RYE residues. 111

Figure 5.2 (a) Comparison between the observed and simulated change in total residual ^{13}C over time, expressed in % of added ^{13}C, with incorporation (INC) of RAPE and RYE residues. 113

Figure 5.2 (b) Comparison between the observed and simulated change in total residual ^{13}C over time, expressed in % of added ^{13}C, with surface application (SURF) of RAPE and RYE residues. 114

Figure 5.3 (a) Comparison between the observed and simulated change in CO_2 fluxes over time, expressed in kg C ha^{-1} day^{-1}, with incorporation (INC) of RAPE and RYE residues. 116

Figure 5.3 (b) Comparison between the observed and simulated change in CO_2 fluxes over time, expressed in kg C ha^{-1} day^{-1}, with incorporation (INC) of RAPE and RYE residues. 117

Figure 5.4 (a) Comparison between the observed and simulated change in the amount of nitrate in the 0-5 cm soil layer, expressed in mg NO_3^--N kg^{-1}, with incorporation (INC) of RAPE and RYE residues. 120

Figure 5.4 (b) Comparison between the observed and simulated change in the amount of nitrate in the 0-5 cm soil layer, expressed in mg NO_3^--N kg^{-1}, with surface application (SURF) of RAPE and RYE residues. 121

Figure 5.5 Simulation of the cumulative carbon mineralization for the control (CTRL), surface (SURF) and incorporation (INC) treatment with RAPE and RYE residues. 125

Figure 5.6 (a) Evolution of the simulated gross fluxes of nitrogen mineralization and immobilization, and comparison between simulated and observed net nitrogen mineralization in the 0-25 cm soil layer with incorporation (INC) of RAPE and RYE residues. 127

Figure 5.6 (b) Evolution of the simulated gross fluxes of nitrogen mineralization and immobilization, and comparison between simulated and observed net nitrogen mineralization in the 0-25 cm soil layer with surface application (SURF) of RAPE and RYE residues. 128

Figure 5.7 (a) Simulation of the nitrate concentration through the soil profile after 0, 1, 3 and 21 days of evaporation, with incorporation (INC) of RAPE and RYE residues. 129

Figure 5.7 (b) Simulation of the nitrate concentration through the soil profile after 0, 1, 3 and 21 days of evaporation, with surface application (SURF) of RAPE and RYE residues. 130

Figure 6.1 Soil aggregate size distribution as observed in the field (Mons) 138

Figure 6.2 Residue particle size distribution as observed in the field (wheat straw) 138

Figure A.1 Flow diagram of the CANTIS (Carbon And Nitrogen Transformations In Soil) submodel from Garnier *et al.*(2003). 150

Figure A.2 Conceptual diagram of mulch decomposition processes based on a two mulch compartments approach. 154

Figure A.3 Simulated and measured matric potentials in the soil at -6 and -14 cm: (A) rape experiment and (B) rye experiment. 167

Figure A.4 Simulated and measured gravimetric water content: (A) rape experiment and (B) rye experiment. 169

Figure A.5 Simulated and measured total dry mass of mulch: (A) rape experiment and (B) rye experiment. 170

Figure A.6 Simulated and measured total CO_2 fluxes: (A) rape experiment and (B) rye experiment. 172

Figure A.7 Simulated and measured ^{13}C remaining in mulch: (A) rape experiment and (B) rye experiment. 174

Figure A.8 Simulated and measured nitrate content in the 0-5 cm topsoil layer: (A) rape experiment and (B) rye experiment. 176

Figure A.9 Simulated and measured nitrate concentration in soil solution at -2 cm: (A) rape experiment and (B) rye experiment. 179

Figure A.10 Simulated and measured nitrate content in the 0-25 cm topsoil layer: (A) rape experiment and (B) rye experiment. 180

Figure A.11 Sensitivity analysis of the model outputs (cumulative CO_2 emission (A), final mulch residue carbon (B), and final nitrogen content in the 0-5 cm topsoil layer (C)) on 5 key parameters describing the mulch. 183

Introduction

General context

Conservation tillage, i.e. no-tillage with at least 30% of the arable land area covered with crop residues, has been shown to be an effective strategy to reduce soil erosion. On a global scale, the surface of arable land under conservation tillage has been estimated between 50 and 60 millions of hectare, which are mainly located in the USA, Brazil, Argentina and Australia (FAO, 2002). At present, conservation tillage is becoming increasingly important even in temperate regions, given its capacity to enhance the C level in soils (Paustian *et al.*, 1997b; West & Marland, 2002).

Over the last 5 decades, about 50 Gt of organic carbon has been globally lost from arable land (FAO, 2002). Conventional tillage increases aeration of the soil and enhances disruption of soil aggregates protecting soil organic matter, which results in an increased mineralization of organic carbon. Management practices to build up the carbon stock in agricultural land should delay the carbon output due to mineralization and/or increase the input of organic matter (Arrouays *et al.*, 2002). The annual increase in the level of soil carbon resulting from conservation tillage has been estimated between 0.2 and 0.5 t C ha^{-1} $year^{-1}$ for tropical regions and between 0.5 and 1.0 t C ha^{-1} $year^{-1}$ for temperate regions (FAO, 2002). These rates are maintained until a new equilibrium in the soil organic carbon stock is established, i.e. 30 to 50 years after changing tillage practice.

However, there are also side effects of reducing or suppressing soil tillage. For example Darwis *et al*. (1993) observed that the soil nitrate content and nitrate leaching increased in no-till situations. Similarly, enhanced N_2O emissions in no-tilled systems counter-balanced the positive effect of increasing C sequestration in soil (Six *et al*., 2002). There is a rather general agreement that both the short-term and long-term effects of management practices should be considered, and that the environmental impacts of land use and management should be assessed by simultaneously examining the various processes.

In other eco-systems such as grasslands and forests, the ‘new’ C also enters the soil after deposition at the soil surface with senescent leaves and shoots. The understanding of processes that affect surface residue decomposition and its impact on fate of C into the soil is therefore not only relevant in relation with conservation tillage in arable soils. Still little is

known about these processes because the interactions between physical and biological processes and their hierarchy are difficult to assess. In this context, the present study will investigate the relative importance of the main physical and biological processes in residue decomposition as a function of crop residue location and quality.

Scientific context

Changing tillage intensity significantly changes the distribution of fresh crop residues in the soil (Balesdent *et al.*, 2000). While residues are distributed over the soil profile with conventional tillage, they are concentrated at the soil surface with conservation tillage. These differences in residue location have been shown to affect the decomposition dynamics: in the field, residue mulch has been reported to decompose at a slower rate than residues incorporated in the soil (e.g. Douglas *et al.*, 1980). However, studies under controlled laboratory conditions tended to show little or no effect of residue placement on C and N mineralization (Abiven & Recous, submitted). This apparent contradiction suggests that other factors are influenced by the initial crop residue location and interact to determine residue decomposition.

The initial location of crop residues determines gradients of organic matter and microbial activity in the soil profile. Differences in residue location also modify water dynamics in soil, solute transport and physical soil properties (e.g. soil aggregation). These changes in physical characteristics affect by turn the dynamics of microbial populations and consequently the decomposition of organic matter (Figure 0.1). Initial gradients in soil organic matter and microbial biomass, and fluctuating moisture content of soil and residues are most often not taken into account in 'classical' incubation experiments, which partly explains the differences between field observations and laboratory results.

In addition, the biochemical quality of the residues interacts with the soil (micro-) biological processes. The decomposition rate of organic carbon depends on the amount of soluble compounds and the lignin content of the residues, and nitrogen dynamics are strongly influenced by N availability as determined by the C:N ratio of the residues (Trinsoutrot *et al.*, 2000b; Jensen *et al.*, in press). It has been demonstrated that the influence of crop residue location on net N mineralization decreased with increasing N availability (Abiven & Recous, submitted). Crop residue quality also modifies the activity and functional diversity of the soil microbial biomass (Bending *et al.*, 2002).

There are still very few attempts to clarify the complex interaction between changes in soil physical and biological properties, as affected by crop residue location and quality. Also most often the biological and physical functioning of soils are considered separately. However, this interaction determines the dynamics of residue decomposition and may explain the observed differences between field and laboratory data.

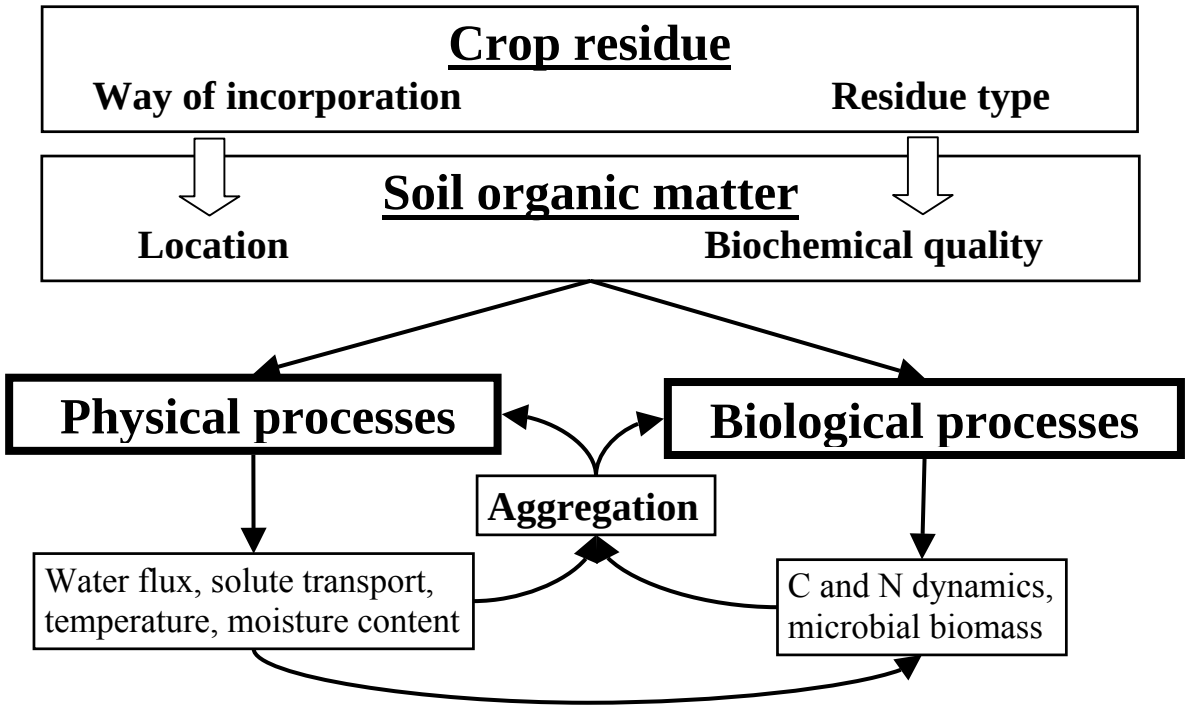

Figure 0.1 Conceptual diagram of interactions between soil physical and biological processed, as influenced by land use and management practices

Research strategy

The aim of this dissertation was to investigate the specific effect of crop residue location (incorporated or surface applied) on C and N mineralization in soil. In addition, the interaction with crop residue quality and soil type was examined.

Within this context, the specific questions addressed in this work are:

(i) Can the actually established relationships between the biochemical quality of arable crops and their decomposition kinetics be generalized for plant residues of very different origin (e.g. agro-, pasture, forest ecosystem) and are these concepts soil-type dependent (Chapter 2)?

(ii) Which physical and biological factors that affect residue decomposition are modified with changing plant residue location (surface placed vs. incorporation) (Chapter 3)?

(iii) How does residue location and the way new C enters the soil affect the fate of residue-C and -N in soil and in soil aggregates, and what are the consequences for C storage in soil on the longer term (Chapter 4)?

(iv) How does the interaction between crop residue location and quality affect residue decomposition, C mineralization and potential nitrate leaching, and can these processes be modelled (Chapter 5)?

In the first place, the influence of residue quality and soil type on C and N mineralization was investigated with ‘optimal’ soil-residue contact, i.e. with homogenous incorporation of finely chopped plant material. It is hypothesized that

(i) the initial residue decomposition rate is determined by the release of rapidly decomposable compounds,

(ii) this release depends on plant residue quality and is determined by the amount of soluble compounds,

(iii) this release, and consequently the initial residue decomposition rate, is independent of soil type.

Secondly, the effect of residue location on C and N mineralization was examined for one residue quality in one soil type. It is hypothesized that

(i) surface application of residues reduces soil evaporation and consequently results in a larger soil water content than with residue incorporation. In addition, fluctuations in residue water content are expected to be more important with residue mulch than with residue incorporation.

(ii) spatial separation of soil and residues with mulch reduces the accessibility of residue-C and availability of mineral soil-N to the microbial biomass compared to soil with residue incorporation

(iii) these differences in water and nutrient availability affect microbial activity, resulting in a slower decomposition rate of residues left at the soil surface than when incorporated in soil.

Further, the impact of crop residue location on the fate of C and N in soil and soil aggregates was assessed to elucidate the mechanisms controlling the storage of organic matter in soil. It is hypothesized that

(i) more stable macroaggregates are formed near the soil surface under mulch than with residue incorporation, due to the larger concentration of organic matter and microbial activity

(ii) the distribution of residue-C and -N in the different aggregate size classes depends on residue location, due to the different way organic matter enters the soil (leaching of soluble compounds with residue mulch vs. direct contact between soil and residue particles with incorporation).

Finally, the interaction between crop residue location and residue quality, with their combined effect on C and N mineralization was examined. It is hypothesized that

(i) physical residue properties (i.e. residue morphology) modify the water dynamics of soil and residue, due to differences in the physical characteristics of the mulch layer (e.g. porosity, water retention capacity)

(ii) biochemical residue properties determine the ability of (soluble) residue components to diffuse and/or to be leached down into the soil, affecting the distribution of nutrients in the soil profile, their availability to the microbial biomass and consequently the decomposition rate of organic matter.

Choice of methodologies

The interaction between soil physical and biological properties was examined under controlled conditions in the laboratory, in repacked soil columns. The objective of this approach was to simulate a simplified soil profile in which simultaneously the transformations of C and N, the transport of water and solutes, and the emission of CO_2 can be measured. The main methodological options were the following:

(i) Crop residues were left at the soil surface (to simulate no-tilled situations), or homogeneously incorporated in the upper 10 cm of the soil column (to simulate reduced tillage situations).

(ii) The various residue treatments (quality x placement) were all investigated in similarly repacked soil columns. Therefore, differences in soil characteristics due to soil history (tilled vs. no-tilled systems) were eliminated in this study.

(iii) We hypothesized a major role of water dynamics on the fate of C: special attention was paid to simulate kinetics of water infiltration and water evaporation. This was achieved by using a laboratory rain simulator and incubating soil columns at a constant temperature in a chamber that controls air humidity, with several rain/evaporation sequences.

(iv) To investigate the influence of crop residue quality, mature oilseed rape (simulating a typical mature crop residue at harvest) and young rye (simulating a situation with a cover crop residue) were used. Beside representing two types of plant residues that are returned to soil in cropped arable systems, both residues were firstly chosen because they largely differ in their physical and biochemical quality and consequently in their decomposition kinetics, although the physical quality of crop residue is rather difficult to characterize.

(v) The residues used were doubly labelled with ^{13}C and ^{15}N. The use of stable isotopes is the unique method that ensures enough sensitivity to trace the short term fate of residue-C and -N in the soil, to distinguish accurately the ‘new’ and the ‘old’ carbon in soil and to make balances.

(vi) A model has been used that simulates both the biotransformations of C and N in the soil and the transport of heat and water, and for which a mulch module was currently under development.

Organization of the manuscript

The manuscript is organized into five chapters plus a paper given in Appendix. This latter section corresponds to a modelling work that was mainly written by another author, but with a major contribution of our data to the calibration and testing of the model.

The first chapter of this thesis reviews the state-of-the-art of how contact between soil and plant residues affects residue decomposition. Given the importance of plant residue size and location in soil - factors that can be modified by soil tillage practices - it was evaluated how the effects of residue size and location are conceptualized in crop residue decomposition models. In the second chapter, C and N mineralization was determined for five plant residues and soils coming from three different ecosystems (agro-, pasture and forest ecosystem), to investigate the impact of land use on the soil carbon storage capacity. In particular, the interaction between plant residue quality and soil type was examined. In the third and the fourth chapter, the influence of crop residue location on decomposition was investigated, with oilseed rape taken as single residue type. The third chapter focuses on the dynamics of water, mineralization of C and N, and microbial biomass in soil. The fourth chapter describes the fate of residue-C and -N in soil and soil aggregates as a function of initial residue location, with its consequences on C storage in soil. In the fifth chapter, the PASTIS model (Lafolie, 1991; Garnier *et al.*, 2003) was used to assess and compare the influence of crop residue quality on water dynamics and decomposition. Modelling gives access to extra information that cannot be measured directly, i.e. cumulative C mineralization, nitrate transport in soil and gross fluxes of N mineralization and immobilization, which are key-variables from environmental point of view. The model also allows extrapolation to other climatic and residue quality scenarios, although this has not been done within the time available. In Appendix, the development of a new module of the PASTIS model is described in detail. This module allowed to simulate decomposition of mulched residues, and was necessary for running our modelling work. Data of rape and rye decomposition in small recipients and in soil columns were used to improve the mulch parameters and to test the mulch module.

Chapter 1

Accounting for differences in contact between soil and plant residues in decomposition studies: concepts and modelling

1.1 Introduction

Plant residues are an important and obvious natural source of nutrients in forest, pasture and agricultural ecosystems. The loss of organic matter, especially observed in many agro-ecosystems, can have detrimental effects on soil physical and biological properties. Therefore, a regular supply of organic matter is necessary to maintain or improve soil fertility. In combination with an adapted tillage system, crop residues contribute to the preservation of a stable soil structure and to the reduction of soil erosion (Blevins & Frye, 1993).

Mineralization of organic carbon and nitrogen is controlled by the interaction between physical and biochemical properties of the plant residues, the physical-chemical environment in which they decompose (e.g. pH, temperature, moisture content, soil texture and structure or N availability) and, for agricultural soils, the applied tillage system (Kumar & Goh, 2000). A major determinant of decomposition is also the so-called contact area between soil and residue, depending on soil and residue characteristics.

Soil-residue contact is assumed to be a significant factor in regulating the decomposition of surface litter in forest or pasture ecosystems and of heterogeneously incorporated crop residues in agricultural land. In addition, soil-residue contact actually becomes increasingly important for crop residue decomposition in agro-ecosystems where more and more land is converted from conventional tillage to no-tillage systems, in which residues are left at the soil surface. Therefore, it is imperative to investigate, conceptualize and simulate the impact of soil-residue contact on residue decomposition.

In general, a faster decomposition rate was observed with an increased contact between soil and residues, but contradictory results are reported, especially with residues rich in nitrogen (Bremer *et al.*, 1991; Jensen, 1994). Given the ambiguity in those results, the influence of

soil-residue contact in residue decomposition processes should be better understood when dealing with environmental issues as C storage or nitrate leaching. In particular, soil-residue contact may interfere in the translation of laboratory incubation results, where plant material is often ground to reduce heterogeneity, to field conditions with crop residues of larger dimension. Computer modelling is an essential part in those investigations. The actual uncertainty in decomposition modelling can be partly ascribed to a lack of understanding of the complex interactions between soil-residue contact and residue decomposition.

The aim of this review is to evaluate: (i) which factors influence the surface area of contact between soil and residue; (ii) how soil-residue contact affects residue decomposition; and (iii) how these concepts are incorporated in the existing models describing crop residue decomposition.

1.2 Factors influencing soil-residue contact

Four main factors influencing the contact between soil and residue particles are distinguished: (i) morphology and nature of the residue, (ii) physical soil properties, (iii) residue particle size and (iv) residue location.

In the first place, the potential surface of contact between soil and plant residues (e.g. maize stem, wheat straw) depends on the morphology and nature of the residues (Table 1.1). Only a fraction of the total residue surface area, as determined by gas adsorption, is directly in contact with soil particles. The residue surface area within micropores ($< 3 \times 10^{-3}$ µm) is physically protected from microbial attack and reduces the available residue surface for micro-organisms (Chesson, 1997). Further, both biochemical and physical properties of the plant residues influence the substrate availability to the microbial biomass. The rate of organic matter breakdown not only depends on the relative proportions of the biochemical fractions (e.g. soluble substances, nitrogen, lignin or polyphenol content) (Trinsoutrot *et al.*, 2000b), but the arrangement of those different compounds within plant tissues may also be considered as a physico-chemical component of residue quality (Paustian *et al.*, 1997a). Decomposition of cellulose and hemicellulose in plant tissue is thought to be restricted by the presence of lignified secondary plant cell walls, inhibiting the accessibility of enzymes to the more decomposable structural polysaccharides (Swift *et al.*, 1979, Chesson, 1997).

Table 1.1 The total surface area measured by gas adsorption, and the calculated maximum surface area available to an enzyme of molecular weight > 20 kDa of a number of typical forage plants. The surface area associated with pores of 3×10^{-3} μm diameter or less was excluded in calculating the available surface area. (Chesson, 1997)

Plant sample	Total surface area / $m^2\ g^{-1}$	Available surface area / $m^2\ g^{-1}$
Lucerne	2.1	0.8
Maize stem	2.4	0.9
Grass (Timothy)	4.9	2.6
Wheat straw	3.2	1.7

When plant residues are applied to the soil, physical soil properties (e.g. texture, aggregate and pore-size distribution and water content) determine the actual contact between residue and mineral soil particles (Figure 1.1). Firstly, the soil surface area increases as clay content increases, thereby enhancing the potential contact between the mineral soil fraction and incorporated residues. Secondly, reducing the inter-aggregate soil porosity (by compaction) increases soil-residue contact, which was suggested to affect nitrogen diffusion or microbial colonization of the straw particles (Fruit *et al*., 1999). Finally, the percentage water filled pore space (WFPS), defined by soil texture and soil water potential, does not only control gas diffusion, but also the substrate diffusion to soil microbes and their movement (Hassink *et al*., 1993). However, even though the soil water content is important in regulating soil-residue contact, Scott *et al*. (1996) found that the % WFPS was more related to the decomposition of native organic matter than of the applied plant litter.

Changing particle size of plant residues can be considered as a physical quality component which is manifested indirectly (Paustian *et al.*, 1997a). For example, reducing particle size increases the surface area of residues potentially in contact with soil, in turn increasing the microbial colonization potential. The direct association of microbial biomass with organic matter was observed by Chenu *et al.* (2001) with low temperature scanning electron microscopy: bacteria occurred as isolated cells or as small colonies often located on organic remnants. Data of Nunan *et al.* (2003) also suggested that bacterial 'patches' may be associated with local deposits of organic substrate. Further, reducing particle size increases the number of particles per unit of volume soil, which, combined with homogenous incorporation, results in a more even distribution of decomposition sites, allowing for better access to nutrients and water (Angers & Recous, 1997; Tarafdar *et al.*, 2001). In decomposition studies, plant residues are often ground to reduce sampling errors and to

increase homogeneity in microcosm incubation experiments. In agricultural land, crop residue size is managed by incorporation techniques and mechanical treatment of the residues, but fine grinding of plant residues as in laboratory conditions is unlikely to be a feasible practice.

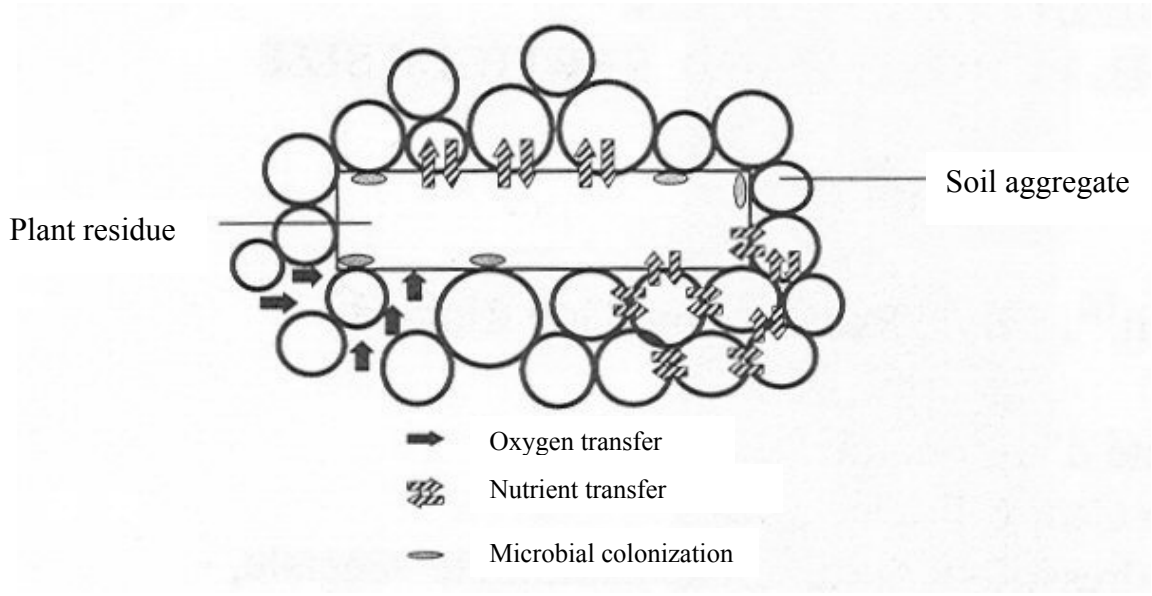

Figure 1.1 Simplified diagram of interactions between soil and plant residue particles (Fruit *et al.*, 1999)

However, in agricultural systems, soil-residue contact is strongly influenced by tillage operations which determine the location of crop residues in soil (Balesdent *et al.*, 2000). Heterogeneous incorporation of crop residues with conventional tillage results in a reduced contact between soil and residues that are completely surrounded by other residue fragments. In no-till systems, most residues are spatially separated from the soil at the soil surface. The method of residue amendment to the soil provides a different degree of accessibility to the soil micro-organisms, which, in turn, affects residue decomposition rates as well as the mineralization-immobilization process (Kumar & Goh, 2000). Soil fauna such as earthworms and arthropods also enhance the biodegradation and humification of organic residues by comminuting and thereby decreasing residue particle size and changing their location in the soil (Tian *et al.*, 1997). This soil fauna is reported to be more abundant under no-till than under conventional tillage system (e.g. Jordan *et al.*, 1997).

Given the importance of plant residue size, especially in laboratory incubation experiments, and of crop residue location in the decomposition of residue mulch in no-till systems, the

influence of soil-residue contact on crop residue decomposition as determined by those two factors was evaluated.

1.3 Effect of soil-residue contact on crop residue decomposition

1.3.1 Residue particle size

Particle size of crop residues influences the extent to which residue carbon and nitrogen are mineralized in soil, but the nature of this effect seems variable. In general, an increased C mineralization rate has been observed with reduced particle size (Sims & Frederick, 1970). However, some studies reported a lower C mineralization rate with decreasing particle size (Bremer *et al*., 1991; Jensen, 1994), especially for N-rich residues like rye (Angers & Recous, 1997). These results are explained by the interaction between three important factors that are affected by residue particle size: (i) accessibility of the residue particles to micro-organisms, (ii) nitrogen availability and (iii) physical protection by the soil matrix.

Ground or finely chopped residue material is more accessible to micro-organisms than intact plant parts. This is due to the increased surface area of the residues exposed to decomposition (Angers & Recous, 1997) and lack of intact lignified barrier tissues (Summerell & Burgess, 1989). Further, reduction in particle size improves the access to catabolic enzymes and increases the ease with which soluble compounds are leached (Swift *et al*., 1979). The latter was confirmed by Vanlauwe *et al*. (1997), who demonstrated that a reduced residue particle size led to a significant increase in the quantity of extracted biochemical plant components (e.g. soluble compounds), due to an increased contact between extractant and residue. An increased accessibility of the smaller residue particles suggests that the initial microbial colonization rate of the residues is favoured with reduced particle size. Although the largest effect of reducing particle size on C and N mineralization is observed in the early stages of decomposition (Sorensen *et al*., 1996), no direct evidence of a faster microbial colonization of residue particles with reduced size has been found.

For residues with a high C:N ratio, nitrogen present in the residues is often limiting for the developing micro-organisms and therefore soil inorganic N is immobilized by the microbial biomass. The availability of this soil-N to the microbial biomass increases with increasing soil-residue contact, i.e. with decreasing residue particle size, resulting in enhanced decomposition of the smaller residue particles. This was confirmed by Bremer *et al.* (1991),

who observed a larger CO_2 evolution for ground than for unground wheat straw (C:N = 80) over a period of 98 days. Angers & Recous (1997) also showed the largest amount of C mineralized for the finest particles of wheat straw (C:N = 270, ≤ 0.1 cm) after 102 days. In exceptional cases however, reducing particle size of residues with a high C:N resulted in an inhibition of microbial respiration in the very early stages of decomposition (Bending & Turner, 1999), which was attributed to a more rapid release of water soluble compounds, including inhibitory substances like phenols. For residues with a narrow C:N ratio, the nitrogen available in the residue itself may be sufficient for the developing biomass, and be responsible for the fact that mineralization does not increase with decreasing particle size as often observed with N-depleted residues. This was demonstrated by Bending & Turner (1999), who found that reducing particle size of potato shoots (C:N = 10) had no effect on the microbial respiration rate. Jensen (1994) showed that the total evolution of CO_2 from pea residues (C:N = 19) was not significantly influenced by residue particle size after 30 days of decomposition. Irrespective of the C:N ratio, the increased N availability with decreasing residue particle size enhanced N immobilization during the early stages of decomposition (< 14 days). Ambus & Jensen (1997) showed with ^{15}N tracers that N immobilization as well as mineralization of residue-N was enhanced with reduced particle size of barley (C:N = 86) and pea residue (C:N = 21). On the longer term however (> 90 days), particle size had no significant effect on net N mineralization (Jensen, 1994; Ambus & Jensen, 1997).

Grinding of plant residues, when added to the soil, results in a more intimate contact between the plant constituents and the soil matrix, thereby enhancing opportunities for colonization by decomposer organisms that are more protected against predation. The greater association of cells protected by the soil matrix results in a higher retention of substrate-derived C in the microbial biomass and a less extensive turnover of substrate-C. This was confirmed by Sorensen *et al*. (1996), who demonstrated with ^{14}C labelled subclover and wheat leaves that more biomass ^{14}C was found in soil with ground than with unground residues. The hypothesis of physical protection was earlier assessed by Jensen (1994), who concluded that decomposition of plant residues, microbial biomass and metabolites formed during the early decomposition was slower with small than with coarse residues, probably due to a better protection of the residues and the biomass by clay minerals.

1.3.2 Residue location

As observed for residue particle size, the effect of residue location on decomposition is rather ambiguous. Some authors showed an enhanced decomposition of incorporated residues compared to residue mulch (Douglas *et al.*, 1980; Holland & Coleman, 1987; Curtin *et al.*, 1998), while others found that surface applied residues decomposed at similar or even higher rates than incorporated residues (Aulakh *et al.*, 1991; Scott *et al.*, 1996; Abiven & Recous, submitted). In general, the influence of residue location on decomposition can be explained by the interaction between the same factors explaining the influence of residue particle size: accessibility of the residue to the microbial biomass, N availability and the stabilization of residue-C by the mineral soil fraction. However, the main factor determining decomposition of residue mulch is probably the micro-environmental condition applied to the mulch (e.g. moisture content).

In no-till systems, residues are left as mulch at the soil surface. Only a fraction of the total residue mass is in direct contact with the soil, depending on its morphology and on the residue quantity left after harvest. The reduced soil-residue contact with residue mulch reduces the accessibility to the biomass present in soil and therefore in a delay in the initial C mineralization (0-3 days). Henriksen & Breland (2002) suggested that the mechanism underlying the latter observation was a slower initial colonization of the residues by soil micro-organisms degrading cellulose and hemicellulose.

Mulching of residues apparently results in a lower availability of soil N for litter decomposition than when incorporated in the soil. However, the spatial separation of surface placed residue-C from soil N is not necessarily a limiting factor for residue decomposition. Fungal biomass, which is found to be more abundant with surface applied than with incorporated residues (Holland & Coleman, 1987), is able to utilize both the surface straw carbon and the nitrogen present in soil. Frey *et al*. (2000) estimated a total annual fungal-mediated N flux of 2.4 g m^{-2}, which was nearly equivalent to the N immobilization potential of decomposing wheat straw (i.e. 2.3 g N m^{-2}, predicted from initial N and lignin content of the residue). They suggested that fungal N translocation was a significant mechanism for soil N input.

Consequently, N availability is mainly determined by the C:N ratio of the residue itself and has an influence on N dynamics in the soil. According to Abiven *et al*. (2002), net N mineralization showed no significant differences for rice (C:N = 47), wheat (C:N = 128) and sorghum stems (C:N = 49) either incorporated or left at the soil surface. In contrast, net N

mineralization was higher for N-rich Brachiaria (C:N = 20) and soybean stem (C:N = 23) when located on the soil surface. This was attributed to a lower N immobilization, probably due to a more efficient use of residue-N by decomposers when left at the soil surface, which would provide a significant advantage for N-rich residues (Abiven & Recous, submitted). Mendham *et al*. (2004) confirmed that net N release with surface placed residues was significantly related to residue-N concentration.

With residue incorporation, most of the residue-C that enters the soil is present in the 2-mm soil layer surrounding the residue particles (= detritusphere) (Gaillard *et al*., 1999). The reduced soil-residue contact with residue mulch entails a smaller volume of 'detritusphere'-soil, compared to residue incorporation. As a result, a lower potential stabilization of litter C by the mineral soil fraction is expected with residue mulch than with incorporation, however no direct evidence has been found.

In spite of the reduced soil-residue contact and decreased accessibility to micro-organisms, similar decomposition rates were observed for surface applied and incorporated litter, when micro-environmental conditions were optimal for decomposition (e.g. temperature, moisture content and N availability) (Abiven & Recous, submitted). The lack of contact between litter and soil particles apparently did not delay decomposition of surface litter as long as litter moisture levels were maintained (Scott *et al*., 1996). In contrast, when surface litter undergoes periodic wetting and drying as observed in field situations, Curtin *et al*. (1998) found that the total CO_2 emission from surface applied straw was reduced by 10% after 77 days of incubation, compared to a continuous moist situation.

In addition, Flessa *et al.* (2002) showed the importance of indigenous microflora on mulch decomposition. Surface applied grass mulch was entirely decomposed by microflora already present on the grass residues or introduced from the air, and that – at least for easily biodegradable and N-rich residues – autochtonous soil organisms had no influence on decomposition. The indigenous microflora of surface applied plant residues is normally exposed to a rapid fluctuating environment, and Flessa *et al*. (2002) proposed that humidity was probably the most important factor affecting activity and growth of those micro-organisms. They also suggested that the initial size of the microbial biomass colonizing plant litter may be an important factor determining the decomposition rate of surface applied residues.

1.4 Soil-residue contact in decomposition models

By managing the soil-residue contact, either by changing residue particle size or its location in soil, it is possible to modify the decomposition rate of fresh crop residues and the amount of N mineralized from them. This may be important regarding the storage of C in soil and the synchronisation of the release of N with plant uptake. To this end, it is necessary to know the consequences of a change in crop residue management towards decomposition processes. Because of the complex interactions due to the many factors involved, computer models are needed in the prediction of C and N mineralization, carbon storage and nitrate leaching.

Several models that have been developed to simulate crop residue decomposition under various environmental conditions are listed by Guérif *et al.* (2001). Some models like Expert-N (Engel & Priesack, 1993), CERES-N (Godwin & Jones, 1991), STICS (Brisson *et al.*, 1998) or APSIM (Keating *et al.*, 2003) were developed to predict crop growth and nutrient availability; other models as CENTURY (Parton *et al.*, 1987), NCSOIL (Molina *et al.*, 1983) or Roth-C (Coleman & Jenkinson, 1996) are used to simulate the long-term effects of residue management on C storage in soils. In general, residue decomposition is described by a potential rate of decomposition that is affected by temperature, moisture and N availability (Eq. 1.1):

$$F_{decomp} = k \times f_w \times f_t \times f_N \qquad \text{(Eq. 1.1)}$$

where F_{decomp} is the residue decay rate (day^{-1}), k the potential decomposition rate (day^{-1}), f_w the moisture factor (-), f_t the temperature factor (-) and f_N the nitrogen factor (-).

A first option to take into account the effect of a reduced soil-residue contact on the decomposition of residue mulch is the modification of the decomposition rate constants under non-limiting conditions. On the one hand, in the CENTURY model (Parton *et al.*, 1987), potential decomposition rates of surface residues are arbitrarily set at 20 % lower than those of litter decomposing in soil, to take in account the less optimal moisture conditions at the surface than in the soil. On the other hand, in the CERES-N model, non-limiting decay constants for the carbohydrate and cellulose pool of surface placed residues are determined by fitting on experimental data, obtained from an incubation under optimal conditions of residues applied at the soil surface (Quemada & Cabrera, 1995).

Another approach is to use the same decomposition rate constants for incorporated and surface placed residues, while temperature, moisture and N functions should fully describe the

variability in environmental conditions. The Douglas-Rickman model (Douglas & Rickman, 1992) describes surface residue decomposition using a first-order decay with respect to degree-days. Degree-days for a specific day are taken as the average temperature above 0°C of that day. The rate constant is related to the initial residue N content and the average moisture condition. The reduction function for N limitation is provided by a regression equation; the moisture function takes discrete values, in the range of 0.2 to 1.0, depending on residue placement in bare or cropped soils. The model of Gregory *et al*. (1985) assumes a second order decay with respect to degree-days. Temperature, the residue C:N ratio and a moisture factor are used to calculate weighted degree-days. The moisture factor corresponds to an antecedent moisture index, which is proportional to the precipitation depth over 5 consecutive days. An antecedent moisture index > 0.01 is set to 0.01 to reduce the percent decomposition of surface placed residues during periods of high precipitation. Ma *et al.* (1999) showed that decomposition of surface crop residues during a 13-year period was better simulated with the Douglas-Rickman model than with the Gregory model. Data of Curtin *et al.* (1998) were also reasonably consistent with the Douglas-Rickman model for incorporated and surface applied straw decomposition. It was suggested that even simple straw-decomposition models, based on empirical assumptions, could be useful in estimating annual or seasonal emissions of CO_2 from decomposing straw.

Other models, like CENTURY and CERES-N, also introduced multiplicative factors to reduce the potential decomposition rates for decomposition of residue mulch. In CENTURY, it is assumed that the mineral nitrogen present in the soil layer to which residues are incorporated is readily available for decomposition, while only a limited amount of N translocated from the soil by fungi is available for decomposition of surface placed residues (Wang *et al.,* 2002). A potential N supply from soil to surface residue by fungal translocation is set at 6.6 mg N m^{-2} day^{-1}, which is equal to 2.4 g N m^{-2} $year^{-1}$ as observed by Frey *et al.* (2000), who worked with the same soil and residue type. The model modified, after introduction of the N availability factor, gave improved simulations for CO_2 fluxes and mineral N dynamics of surface straw treatments. In simulations with CERES-N, it is assumed that the temperature of the residue mulch is the same as measured at 5 cm soil depth, and the soil temperature factor is applied to residues decomposing at the soil surface. In analogy, it is assumed that the volumetric water content at 5 cm soil depth could be used to modify decomposition rate constants of the residue mulch. The model uses the same moisture and temperature factors for humus and residue decomposition, which is acceptable for residues incorporated in the soil (Quemada *et al.*, 1997). With surface applied residues, however, it

may be necessary to use different moisture and temperature factors for the decomposition of humus and crop residues (Quemada & Cabrera, 1997).

Finally, models are developed in which separate organic pools are defined for residue mulch decomposition (e.g. Expert-N), or in which specific functions take into account the influence of reduced soil-residue contact with residue mulch (e.g. APSIM or PASTIS).

The central assumptions in the soil surface decomposition submodel of Expert-N are (i) that the potential mineralization rates are the same in the soil and at the surface; and (ii) that differences in microbial activity between soil and surface are mainly caused by N-limiting conditions (Berkenkamp *et al.*, 2002). The submodel introduces three surface organic matter pools, i.e. the litter, the manure and the humus surface pool, plus a standing surface reservoir consisting of dead catch crops and standing crop residues. The three surface pools undergo decomposition, while the standing surface reservoir is considered as a storage capacity which is not decomposed. Organic matter from this standing reservoir can be added to the surface litter pool depending on atmospheric conditions and tillage operations. Different microbial activities are calculated using reduction functions of volumetric water content and temperature. The volumetric water content of the topsoil is compared with the optimal volumetric water content for microbial activity; the temperature function describes the impact of air temperature on the microbial turnover processes. The impact of N limitation is taken into account by the microbial use efficiency factor, the inverse of the C:N ratio of the respective pools and the C:N ratio of the microbial biomass and the newly formed humus at the soil surface.

One of the very few models in which a specific function for soil-residue contact was developed is the APSIM-Residue model. Decomposition of surface residues was described as a function of moisture (defined by potential daily soil evaporation), average daily air temperature, residue C:N ratio and, unlike most other cropping system models, residue mass (Figure 1.2) (Thorburn *et al.*, 2001). Plant residues on the soil surface were treated as a component separated from soil organic matter and incorporated residues. The transfer of surface residue-C into the soil organic matter pools was controlled by incorporation (e.g. during tillage) or by decomposition. The initial contact factor F_1 (-) depended on the residue mass R (t ha^{-1}), which varied between R_{min} (t ha^{-1}), i.e. the residue mass above which the decomposition rate was reduced, and R_{max} (t ha^{-1}), i.e. the residue mass above which the decomposition rate was independent of mass (Eq. 1.2). The minimum value for F_1, when $R > R_{max}$, was set to 0.46 (= F_{min}). However, this relation is based on very limited data.

$$F_1 = 1 - \left(\frac{1 - F_{\min}}{R_{\max} - R_{\min}} \right) (R - R_{\min}) \qquad \text{(Eq. 1.2)}$$

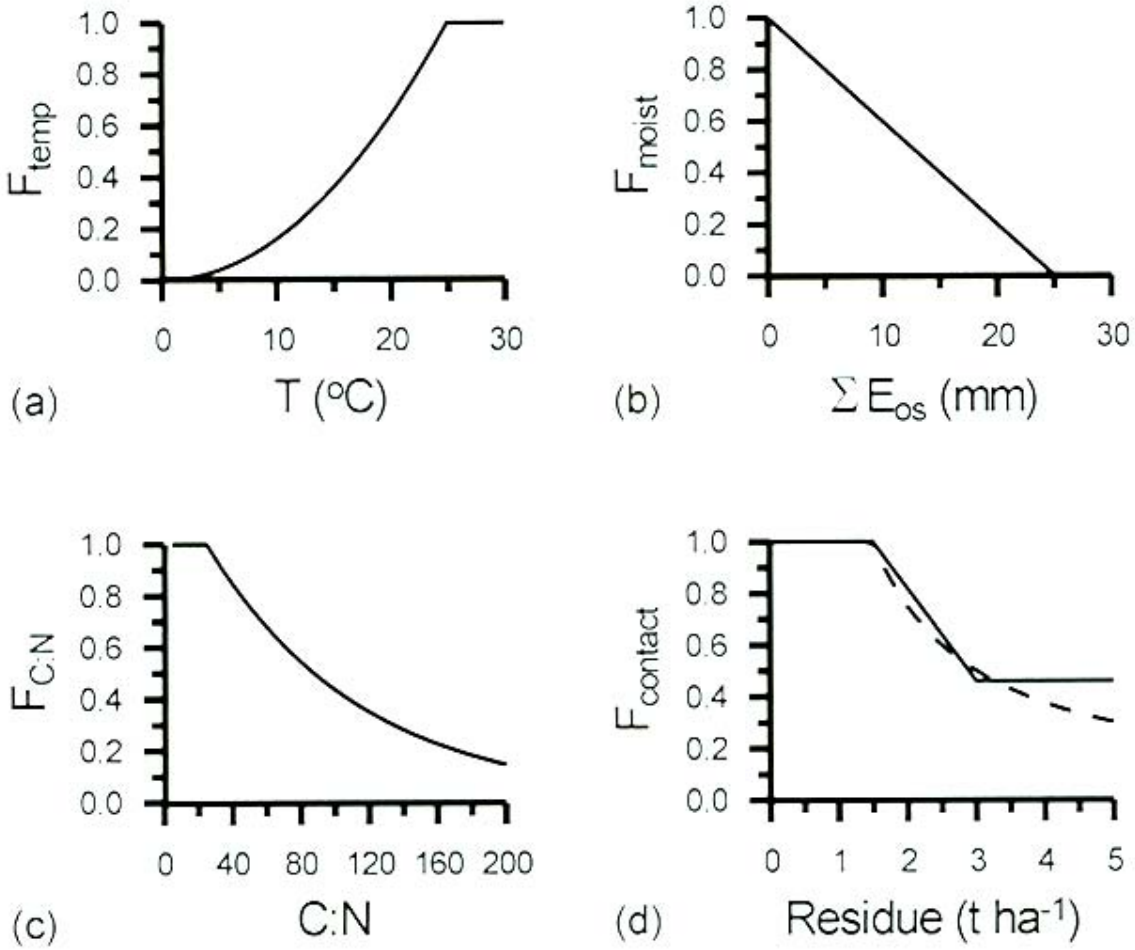

Figure 1.2 The default functions for the four factors that limit residue decomposition in APSIM-Residue due to: (a) temperature (T_{opt} = 25°C); (b) moisture (potential daily soil evaporation E_{os}, max = 25 mm); (c) initial residue C:N ratio ($C:N_{opt}$ = 25); (d) residue-soil contact (R_{min} = 1.5 t ha^{-1}, R_{max} = 3 t ha^{-1} and $F_{contact,min}$ = 0.46). The dashed line in (d) shows the new residue-soil contact function (Eq. 1.3) with R_{crit} = 1.5 t ha^{-1}. (Thorburn *et al.*, 2001)

A new contact factor for APSIM-Residue, F_2 (-), was developed by Thorburn *et al.* (2001), where residue mulch is divided in two separate layers (Fig. 1.3). In the first layer, residues are in contact with the soil and decomposing; the second layer consists of all the residues above the first layer, which are not decomposing. This approach seemed reasonable for a large initial residue mass, as observed for sugar cane (10-20 t dry matter ha^{-1}), which makes a residue

layer of about 50 cm. The residues decomposed from the first layer are replaced by residues from the second layer. Over time, the mass of the second layer is assumed to decrease, while the mass of the first layer remains constant until there is no residue left in the second layer. The decomposition rate would thus be independent of the residue mass R (t ha^{-1}), until layer 2 had disappeared and had reached the critical mass R_{crit} (t ha^{-1}) (Eq. 1.3).

$$F_2 = \begin{cases} \dfrac{R_{crit}}{R} , & R > R_{crit} \\ 1 , & R \le R_{crit} \end{cases} \qquad \text{(Eq. 1.3)}$$

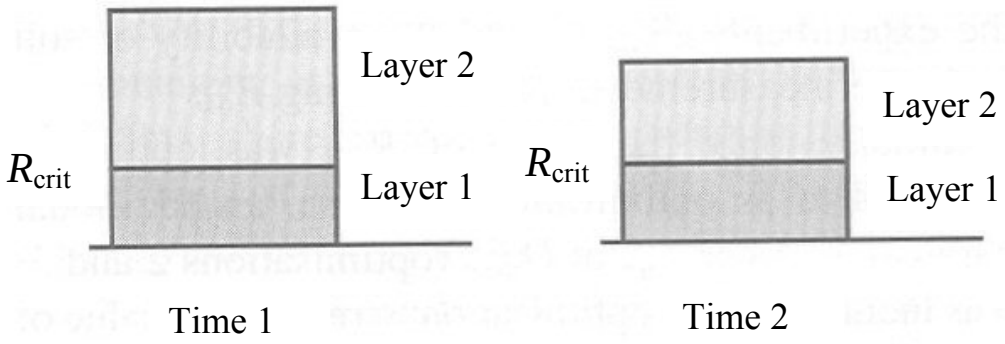

Figure 1.3 Conceptual diagram of residue on the soil surface showing two layers: layer 1, in contact with the soil and decomposing; and layer 2, the residue above layer 1 that is not decomposing. The thickness of layer 1 remains constant through time as long as there is residue in layer 2. The thickness of layer 2 decreases through time as residue from that layer replaces the residue decomposed from layer 1. (Thorburn *et al.*, 2001)

A value for R_{crit} is obtained with numerical optimisation, which was suggested to be residue-specific. Thorburn *et al.* (2001) proposed that the function relating decomposition rate to residue mass may be useful for other decomposition models, in particular when large residue masses are involved.

PASTIS, a mechanistic model that couples the transfer of water and solutes in soil with the biotransformation of carbon and nitrogen (Garnier *et al.*, 2001; Garnier *et al.*, 2003), provides a reduction function for the decomposition of incorporated residues that can take into account the contact between soil and residue (e.g. for ground or chopped residues). This function f_b (-) is related to the zymogenous biomass (Eq. 1.4), with B_Z (mg C kg^{-1}) the carbon content in the

zymogenous biomass and K_{MZ} (mg C kg^{-1}) an empirical factor connected to the size of the zymogenous biomass (Garnier *et al.*, 2003).

$$f_b = \frac{B_Z}{K_{MZ} + B_Z} \qquad \text{(Eq. 1.4)}$$

This function is supposed to describe the limitation in residue decomposition by microbial colonization of the substrate, which is influenced by either the specificity of the substrate or by a reduced soil-residue contact.

For decomposing surface placed residues, the concept of two separate mulch layers, as developed in APSIM, is also adopted in PASTIS (see Appendix A). The decomposition rate of the mulch in contact with the soil is a function of the mass fraction of the residues in contact with the soil, its volumetric water content and its temperature. The availability of soil nitrogen for the zymogenous biomass is supplied from a superficial soil layer with given depth. The supply of the pool of residue mass in contact with the soil with residues not in contact with the soil is also regulated by an empirical factor. Although simulated results were in good agreement with experimental data, a more mechanistic approach of K_{MZ}, taking into account specific residue surface area or biochemical quality, and of the empirical parameters controlling mulch decomposition is desirable.

1.5 Conclusion

The contact between soil and plant residues is influenced by the morphology of residues, their physical and biochemical properties, soil physical properties, residue particle size and location in soil. The influence of soil-residue contact on the decomposition process is the result of a complex interaction between the accessibility of residues to the micro-organisms, nitrogen availability and physical protection of organic carbon by the soil matrix. In general, the lower microbial accessibility of residues with reducing soil-residue contact delayed the initial residue decomposition rate. Largest differences in C mineralization were observed when reducing soil-residue contact of residues with highest C:N ratio, i.e. with smallest N availability. Finally, decomposition of residue mulch was mainly determined by the water content of the residues.

Uncertainty still exists about some processes which are essential to understand mechanisms in the decomposition of residues with reduced soil-residue contact. Firstly, although the association of micro-organisms with organic residues has been demonstrated, no direct evidence has been found on the faster colonization rate of crop residues by the microbial biomass with reducing particle size, as suggested by several authors. Secondly, an important question that needs further investigation is which mechanisms control or affect fungal translocation of soil N to surface placed residues. Fungal N translocation has been demonstrated and quantified for one soil and one type of residue, but it is not clear to what extent the process may be generalized in the reduction of N limitation. Finally, a general relationship between residue particle size (or specific surface area), residue N content and the mineralization rate of C has not been determined, which could be of great importance in the translation of microcosm incubation results (small sized residues) to field conditions (large sized residues).

Given the complex interactions, computer models are imperative to investigate mechanisms in the decomposition process of crop residues and to make predictions of the fate of residue C and N in agricultural systems on the short and on the long term. However, using models for investigating mechanisms can only be done under assumption that the concepts adopted by the model are correct. Most of the decomposition models take into account the effect of soil-residue contact by modifying the decomposition rate constants, temperature and moisture reduction functions and/or a factor controlling N availability. Only few models, like APSIM or PASTIS, made an attempt to treat the effect of soil-residue contact on decomposition by a mechanistic approach. However, current knowledge is insufficient to describe all processes that take place in residue decomposition and some of the functions used are still based on empirical assumptions. This implies the need for further experimental studies that investigate the processes regulating surface residue decomposition.

Chapter 2

Impact of plant quality and soil characteristics in the mineralization of C and N from grassland, forest and annual crop soils

2.1 Introduction

The global change debate has highlighted the importance of the carbon and nitrogen cycle in the prevision of future climatic scenarios and the potential storage capacity of carbon in the terrestrial biosphere (FAO, 2002). A possible option to reduce the impact of greenhouse gases (CO_2, CH_4, NO_x) is a decrease in the emissions and/or an increase in the storage capacity of soils, which largely depend on land use and management factors (e.g. Balesdent *et al.,* 2000). The carbon stock in soil is more important in ecosystems with a permanent vegetation cover (e.g. pasture or forest) than in many agro-ecosystems (Woomer *et al.*, 1998). In the latter, less organic matter is returned to the soil and frequent tillage operations enhance the mineralization of C. Consequently, agricultural land depleted in carbon has a potential for increasing the C stock in soil, especially in combination with no-tillage or by conversion to pasture or afforestation (Paustian *et al.*, 1997).

At present, the mechanisms for carbon sequestration in soil are not well identified, and there is still a great deal of uncertainty about its quantification. In particular, little information is available on the impact of modifications of tillage practice or changes in land use on carbon stocks and fluxes in soil. Land use and management are principal factors affecting the transformation of organic matter, determining the mineralization of carbon and nitrogen or their retention in soil. In addition, different ecosystems (e.g. agriculture, pasture and forest) offer a large variety of vegetation types, and likewise plant residues of different nature and quality. Therefore, it is essential to take into account the effects of soil type and residue quality in the analysis of the global carbon and nitrogen cycles. A better understanding of the interaction between soil type and residue quality will also contribute to the development of conceptual models that can predict carbon and nitrogen mineralization on the longer term.

Those models are indispensable in the evaluation of the impact land use changes (e.g. afforestation of agricultural land) on carbon stocks in soil.

In this study, C and N mineralization of selected plant residues from different ecosystems (pasture, forest and arable land) were investigated. The originality of this work is that for each of the three ecosystems effects of soil type were evaluated, as well as interactions between residue quality and soil type. This strategy allowed to examine the initial mechanisms that determine the fate of plant residues in the soil and if the same concepts and formalisms for residue decomposition can be adopted for plant residues originating from different ecosystems. The Roth-C model was used in the validation of those concepts and as a tool to simulate the fate of C on the longer term in the different ecosystems.

2.2 Materials and methods

2.2.1 Soil and plant residues

Three contrasting soils with different land use history were selected to represent agricultural (Orthic Luvisol, Mons-en-Chaussée, Northern France), pasture (Dystric Cambisol, Theix, Central France) and forest (Gleyic Luvisol, Hesse, Eastern France) soils. The soil was sampled from the 0-10 cm layer, sieved (< 2 mm) and stored at 4°C prior to use. Soil properties are shown in Table 2.1. The soils differed widely in texture, C and N content, C/N ratio and pH. Treatments with agricultural, pasture and forest soil are further referred to as AGRI, PAST and FOR, respectively.

Table 2.1 Selected properties of the soil sampled at Mons-en-Chausseé (AGRI), Theix (PAST) and Hesse (FOR).

		AGRI	PAST	FOR
clay	/ g kg^{-1}	134	163	222
fine silt	/ g kg^{-1}	320	233	353
coarse silt	/ g kg^{-1}	496	124	345
fine sand	/ g kg^{-1}	38	148	59
coarse sand	/ g kg^{-1}	12	332	21
organic carbon	/ g kg^{-1}	6.7	16.0	24.0
total nitrogen	/ g kg^{-1}	0.9	1.7	1.6
C:N		7.3	9.4	14.9
total carbonate	/ g kg^{-1}	7.0	n.a.	n.a.
pH (H_2O)		8.2	6.6	4.9
CEC	/ $cmol_c$ kg^{-1}	8.1	15.9	9.8

Five different plant residues were used for incubation: mature oilseed rape (*Brassica napus* L.), young rye (*Secale cereale*), Dactylis roots (*Dactylis glomerata*), Lolium roots (*Lolium perenne*) and beech leaves (*Fagus sylvatica*). Oilseed rape and rye crops were grown under hydroponic conditions in a plant growth chamber with an atmosphere enriched in ^{13}C-CO_2, and in a nutrient solution labelled with ^{15}N-KNO_3 (Trinsoutrot *et al.*, 2000a). Beech leaves were collected from 10-year old trees, enriched in ^{13}C by continuous labelling with ^{13}C-CO_2 during 4 weeks and 'pulse labelling' during 3 months in a plant growth chamber. Labelling with ^{15}N was effectuated by pulverisation of ^{15}N-urea on the leaves (Zeller *et al.*, in preparation). Roots of Dactylis and Lolium, recovered from soil by wet sieving and hand picking, were unlabelled. Characteristics of the different plant residues are given in Table 2.2. Large variations existed in the amount of nitrogen in the residues, between 2.7 % of total dry matter for young rye and 0.7 % for beech leaves, resulting in C:N ratios between 16 and 70. Residues also differed in biochemical composition, as determined by proximate analysis (Van Soest, 1963). Maximum and minimum amounts of soluble compounds were respectively found in young rye and grass roots. For the lignin-like fraction, amounts were maximal in beech leaves and almost nil in young rye.

Table 2.2 Selected chemical and biochemical properties of the plant residues used

		Oilseed rape	Rye	Beech leaves	Dactylis roots	Lolium roots
C	/ %	42.4	43.4	51.3	44.4	43.8
N	/ %	1.2	2.7	0.7	1.2	1.3
C:N	/ -	36.8	16.1	70.0	37.0	32.7
^{13}C	/ a.e.%[1]	2.89	2.90	1.54	-	-
^{15}N	/ a.e.%[1]	9.49	9.50	1.56	-	-
Biochemical Fractions						
Soluble	/ %	45.6	52.5	28.1	16.2	16.0
Hemicellulose	/ %	14.4	24.9	11.1	35.7	38.7
Cellulose	/ %	33.2	21.2	32.3	33.9	35.5
Lignin-like	/ %	6.7	1.4	28.5	14.3	9.8

[1] atom % excess

2.2.2 Incubation conditions

The three soils were pre-incubated in the dark at 20°C. A solution of KNO_3 was added to bring the initial soil mineral N content at 60 mg kg^{-1} soil. Adding nitrate, not considered as an intrinsic soil property, removed the difference in mineral N availability between the three soils, which is necessary for the non-biased evaluation of residue quality effects on residue decomposition (Trinsoutrot *et al*., 2000a). After 2 weeks of pre-incubation, each soil was divided in 30-g subsamples. Residues, chopped with scissors to an average size of 1 to 3 mm, were mixed into the soil at a rate of 2 g dry matter kg^{-1} soil. The residues were incorporated in their 'original' soil, i.e. oilseed rape and rye in AGRI, Lolium roots in PAST and beech leaves in FOR. Other soil-residue combinations were prepared to have all residues incorporated in AGRI and the rye residue in all soils. Subsamples without residue addition were used as control treatments. The subsamples were compacted at 1.2 g cm^{-3} and incubated in sealed jars at 20°C for 142 days at constant water content, corresponding to a matric potential of -5.0×10^4 Pa. A small recipient with water was added to each jar to limit water loss from the soil during incubation. The jars were periodically opened to prevent oxygen limitation and to allow adjustments for water loss.

2.2.3 Sample treatment and analysis

Three series of subsamples were managed differently. The first series was used for characterization of carbon mineralization. Three replicates of each soil-residue combination (with control soil) were incubated individually in a jar with CO_2-trap (10 ml 0.25 *M* NaOH). On a regular base, the amount of trapped CO_2 was determined by titration. Carbon dioxide in the NaOH solution was precipitated by an excess of 10% $BaCl_2$ and the remaining NaOH was titrated with 0.25 *M* HCl. Solutions of NaOH in the jars were replaced. A second series was used to follow up nitrogen mineralization and residual ^{13}C in soil. At 12 occasions, three replicates of 30-g soil samples were mixed thoroughly and divided in another 2 subsamples. Soil mineral nitrogen was extracted from 25 g of soil, with 100 ml 1 *M* KCl (30 minutes shaking). Soil extracts were centrifuged (20 minutes at 5800 *g*), filtered and stored at –20°C until analysis. The mineral nitrogen (NO_3^--N and NH_4^+-N) was measured by continuous flow colorimetry (TRAACS 2000, Bran & Luebbe). The remaining 5 g of soil was dried, crushed and analyzed for ^{13}C using an elemental analyser (NA 1500, Carlo Erba) coupled to a mass spectrometer (Fisons Isochrom, Manchester, UK). Finally, the third series was used for measuring biomass-C with the fumigation-extraction method (Vance *et al.*, 1987), at 5

different sampling points. Soluble carbon from the 30-g soil samples, unfumigated or fumigated with chloroform, was extracted in triplicate with 120 ml 0.03 *M* K_2SO_4, followed by centrifugation (20 minutes at 5800 *g*) and storage at -40°C. The concentration of soluble carbon in the extracts was measured by a chemical oxidation in a persulphate medium, the CO_2 produced being measured by infrared spectrometry (1010, O.I. Analytical). Microbial biomass carbon was calculated from the difference between soluble C in fumigated and unfumigated soil, after division by a coefficient $K_{EC} = 0.38$ (Vance *et al.*, 1987).

2.2.4 Model description: Roth-C 26.3

The Roth-C model (Coleman & Jenkinson, 1996) is a soil organic matter (SOC) decomposition model in which incoming plant residues are divided in Decomposable Plant Material (DPM) and Resistant Plant Material (RPM). Both decompose to form microbial biomass (BIO) and humified organic matter (HUM). Mineralized residue-C is evolved as CO_2. Each compartment decomposes by first order kinetics, and each has a maximum decomposition rate. The model also includes a pool of inert organic matter (IOM). The actual decomposition rate is calculated using three multiplicative factors taking into account effects of temperature, soil moisture and plant residue type, and is attributed at each time step (month). Clay content of the soil determines the partitioning of SOC between BIO, HUM and evolved CO_2. The Roth-C model was partly validated in several studies (e.g. Powlson *et al.*, 1996), for tropical soils (Diels *et al*., 2004) and in particular for French cereal cropping systems (Balesdent, 1996).

2.2.5 Simulation method

The Roth-C 26.3 model was used as regression model for the C mineralization kinetics. For all parameters the default values of the model were used, with exception for $DPM.(DPM+RPM)^{-1}$ which characterized the biochemical plant residue quality. Decomposition rate constants of the different compartments were multiplied by a climatic factor of 2.83, corresponding to the applied incubation conditions (temperature = 20°C and soil moisture = optimal). The obtained rate constants are: $k_{DPM} = 28.3$ year^{-1}; $k_{RPM} = 0.85$ year^{-1}; $k_{BIO} = 1.87$ year^{-1}; $k_{HUM} = 0.057$ year^{-1}. Clay content of the soils (134, 163 and 222 mg kg^{-1} for AGRI, PAST and FOR) controls the proportion of BIO and HUM that is formed, but there is little effect due to minor contribution of these two pools to residual C. The model was run with a 10-day time step and an optimized numerical approximation over this time period.

2.3 Results

2.3.1 Characterization of agricultural, pasture and forest soils

A large difference in carbon mineralization of native organic matter was observed between the agricultural (AGRI), pasture (PAST) and forest (FOR) soil (Figure 2.1). The C mineralization rate in the FOR treatment was respectively 4 to 7 times larger than for AGRI and PAST. A strong relationship was found between the cumulative C mineralization after 142 days of incubation (y) and the amount of initial biomass-C (x): $y = 2.0\ x + 43.3$; $R^2 = 0.994$ (Figure 2.2). Also the patterns of nitrogen mineralization were very different for the three soils (Figure 2.3). In AGRI, no NH_4^+-N accumulated and during the first 4 weeks of incubation, a net N immobilization was observed. In PAST, the amount of NO_3^--N increased from the beginning of the incubation, while in FOR nitrification was initially inhibited by the low soil-pH. In the latter, the increase in mineral nitrogen during the first 5 weeks of incubation resulted from an accumulation in NH_4^+-N. Net N mineralization of native organic matter after 142 days was 4 to 5 times larger in FOR (+ 99.3 mg N_{min} kg^{-1}) compared to AGRI (+ 19.5 mg N_{min} kg^{-1}) or PAST (+ 27.5 mg N_{min} kg^{-1}).

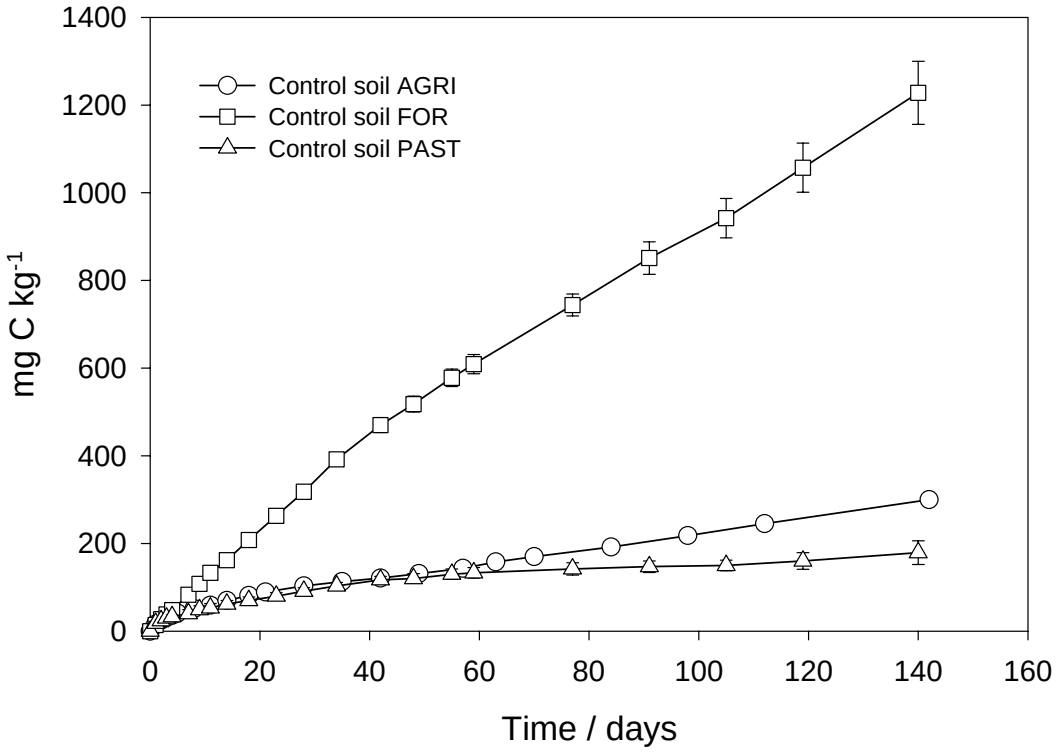

Figure 2.1 Cumulative carbon mineralization in an arable (AGRI), pasture (PAST) and forest (FOR) soil, without addition of residue-C (control soil). Error bars indicate the standard error (n = 3).

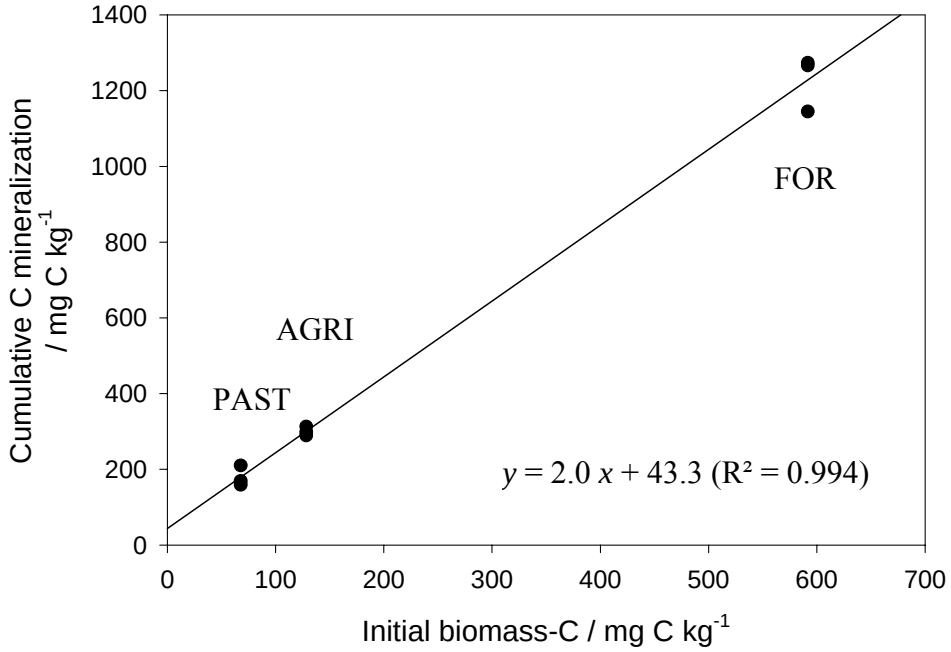

Figure 2.2 Relationship between cumulative C mineralization after 142 days of incubation and the amount of initial biomass-C for the control soil of AGRI, PAST and FOR

With incorporation of plant residues in their 'original' soil, beech leaves in FOR still had the largest total cumulative C mineralization after 142 days of incubation (1520 mg C kg^{-1}), compared to rye (885 mg C kg^{-1}) and oilseed rape (787 mg C kg^{-1}) in AGRI, or Lolium (435 mg C kg^{-1}) in PAST. The contribution of the plant residues to the total mineralization was calculated by difference with the amount of CO_2 evolved from the control soils (Figure 2.4). In this case, cumulative C mineralization (expressed in % of added C) was significantly larger for rye (67.4 %) and oilseed rape (57.5 %) in AGRI than for Lolium in PAST (29.2 %) and beech leaves in FOR (28.5 %).

Carbon mineralization was also calculated from residual ^{13}C in the soil (Figure 2.4). Variability in ^{13}C measurements was initially large for all treatments due to sample heterogeneity. Over time, more advanced residue decomposition allowed more homogenous sampling that reduced variation between replicates. For beech leaves, variability remained large compared to rye and oilseed rape residues due to initially larger residue particles (due to residue morphology) and a slower decomposition rate. For AGRI, residue C mineralization calculated from the difference between amended and control soils are in good agreement with the amounts of mineralized residue-C calculated from residual ^{13}C of rye and oilseed rape. In FOR, the difference between ^{13}C measurements and cumulative C mineralization was larger than for AGRI, which was also attributed to sample heterogeneity.

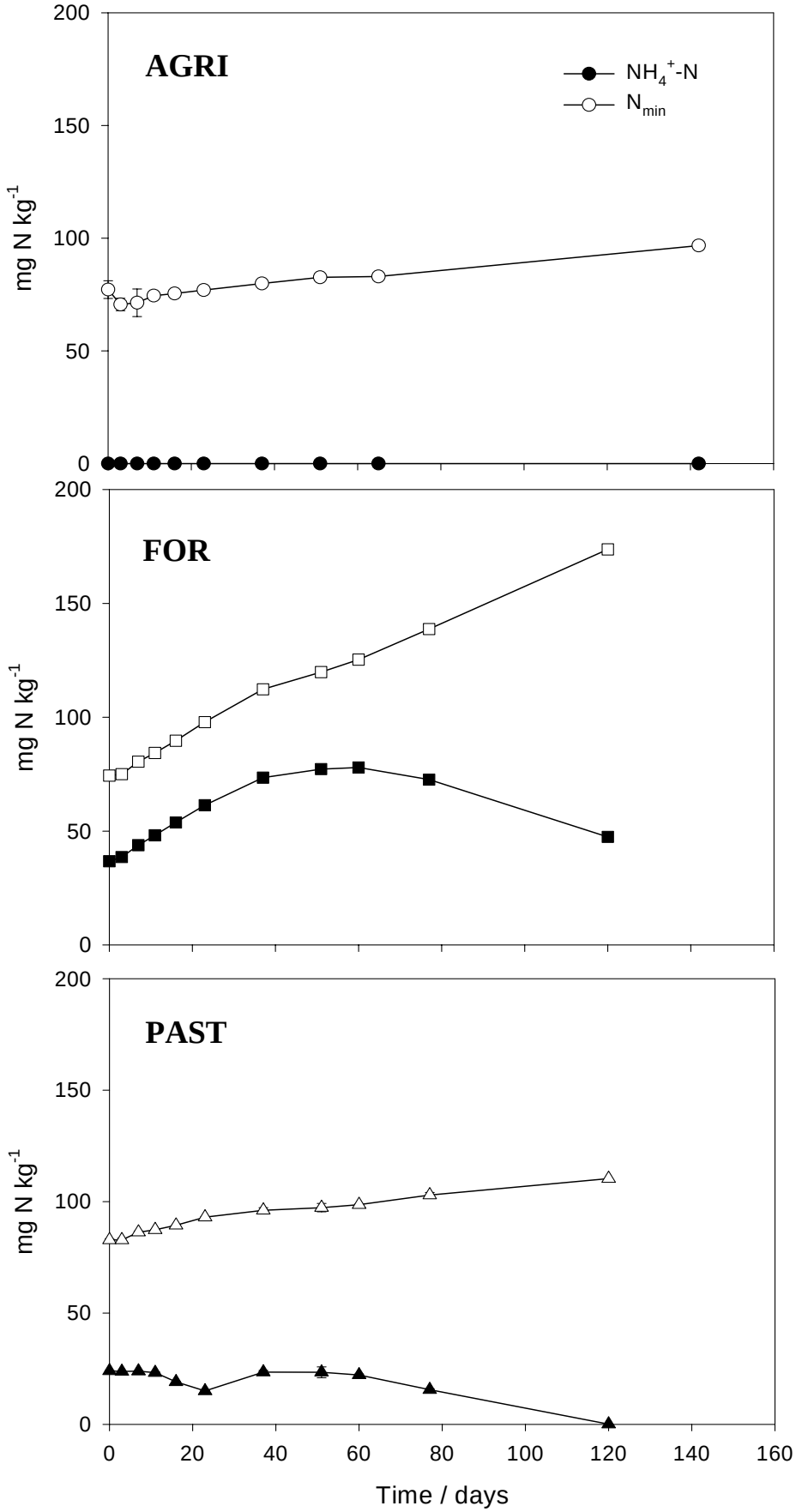

Figure 2.3 Change of NH_4^+-N and total mineral nitrogen (NH_4^+-N + NO_3^--N) in the control soil of AGRI, PAST and FOR over time. Error bars indicate the standard error (n = 3).

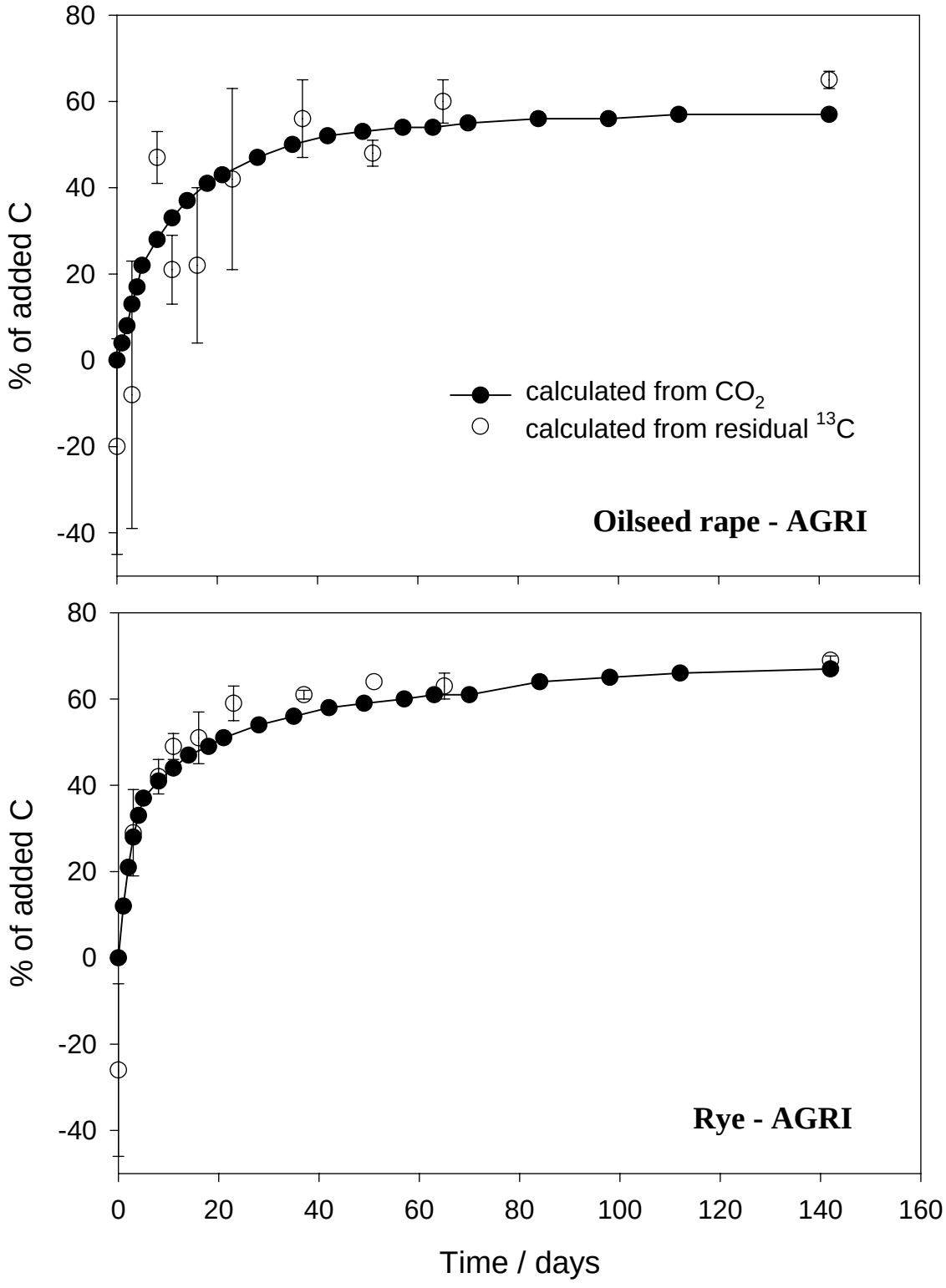

Figure 2.4 (a) Cumulative carbon mineralization, expressed in % of added C, in AGRI with incorporation of oilseed rape and rye, calculated from evolved CO_2 or by difference with residual ^{13}C. Error bars represent the standard error (n = 3).

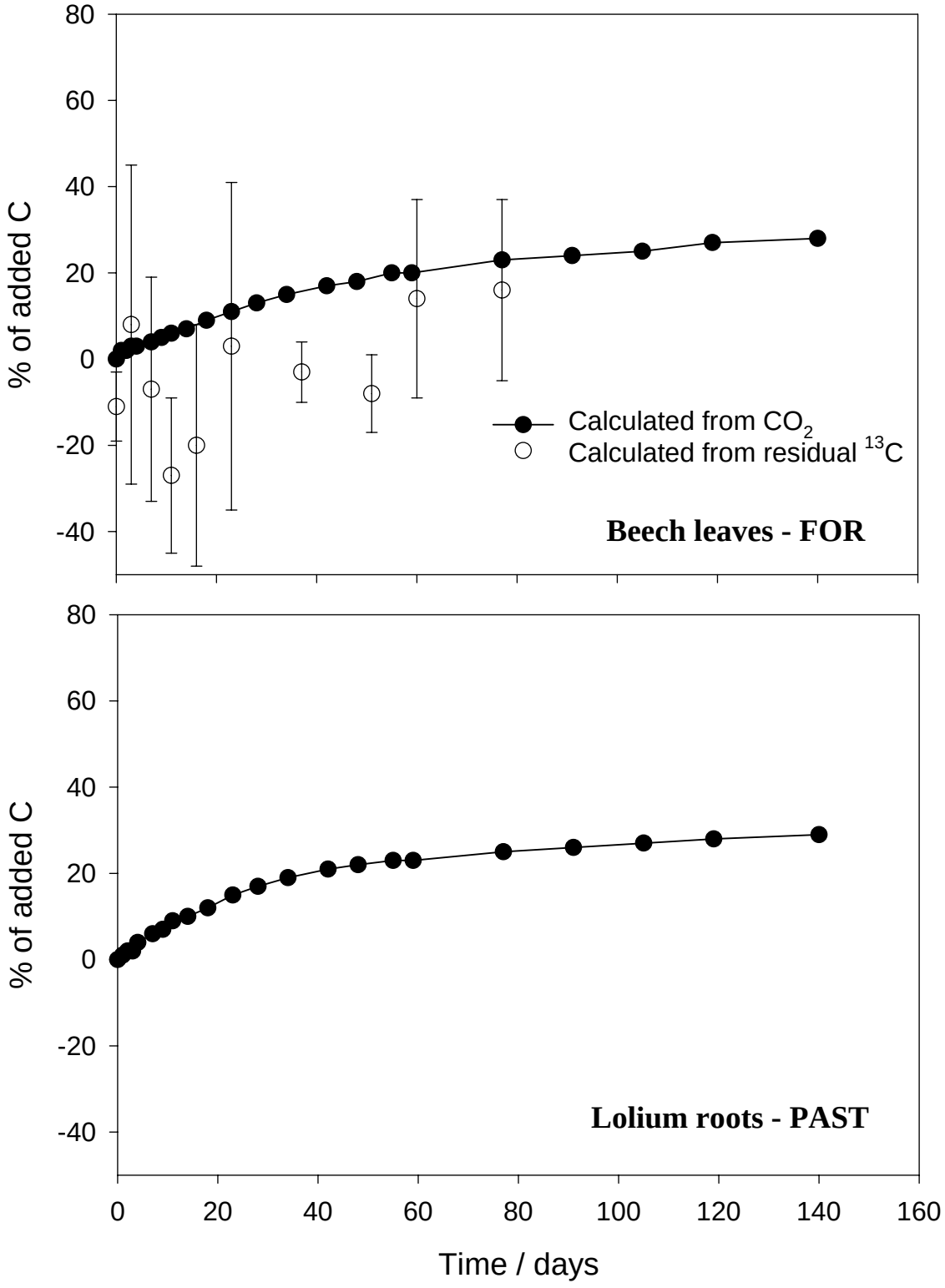

Figure 2.4 (b) Cumulative carbon mineralization, expressed in % of added C, in FOR with beech leaves and in PAST with Lolium roots, calculated from evolved CO_2 or by difference with residual ^{13}C (no ^{13}C data available for Lolium). Error bars represent the standard error (n = 3).

Nitrogen mineralization was also different in the three ecosystems, with the largest net N accumulation for beech leaves in the soil of FOR (Table 2.3). The contribution of the plant residues was calculated from difference with N mineralized in the control soils. Only incorporation of rye residues in AGRI increased the net N mineralization of the soil with +21.4 mg NO_3^--N kg^{-1} over the 0-142 day period. Incorporation of the other residues resulted in a net N mineralization between -6.0 and -11.5 mg NO_3^--N kg^{-1} over the same period.

Table 2.3 Nitrogen mineralization in AGRI, FOR and PAST, without and with incorporation of plant residues

/ mg N_{min} kg^{-1}	AGRI	AGRI + Oilseed rape	AGRI + Rye	FOR	FOR + Beech leaves	PAST	PAST + Lolium roots
Initial N_{min}	77.2	76.6	73.7	74.4	72.1	82.8	80.5
Final N_{min}	96.7	90.1	114.6	204.8	191.0	123.2	110.3
N accumulation (Final - Initial N_{min})	+ 19.5	+ 13.5	+ 40.9	+ 130.4	+ 118.9	+ 40.4	+ 29.8
Net N mineralization (difference with control)		- 6.0	+ 21.4		- 11.5		- 10.6

2.3.2 Influence of plant residue quality

The effect of plant residue quality on decomposition and nitrogen dynamics was examined by incubating oilseed rape, rye, beech leaves and roots of Dactylis and Lolium in the soil of AGRI (Figure 2.5). Using one reference soil eliminated interactions with soil type effects as pH, native soil organic matter, texture or soil microbial biomass. Carbon mineralization rate was much larger for rye and oilseed rape residues than for roots of the two grasses and beech leaves. This resulted after 142 days of incubation in a significantly larger cumulative carbon mineralization, expressed in % of added C, for rye (67.4 ± 1.8 %) and oilseed rape (57.5 ± 1.6 %) compared to the three other residues (between 32.3 ± 1.7 % and 38.7 ± 3.5 %). Net nitrogen mineralization was largest with incorporation of rye (+ 41 mg N_{min} kg^{-1}), while incorporation of all other residues resulted in N immobilization compared to the control soil after 142 days of incubation.

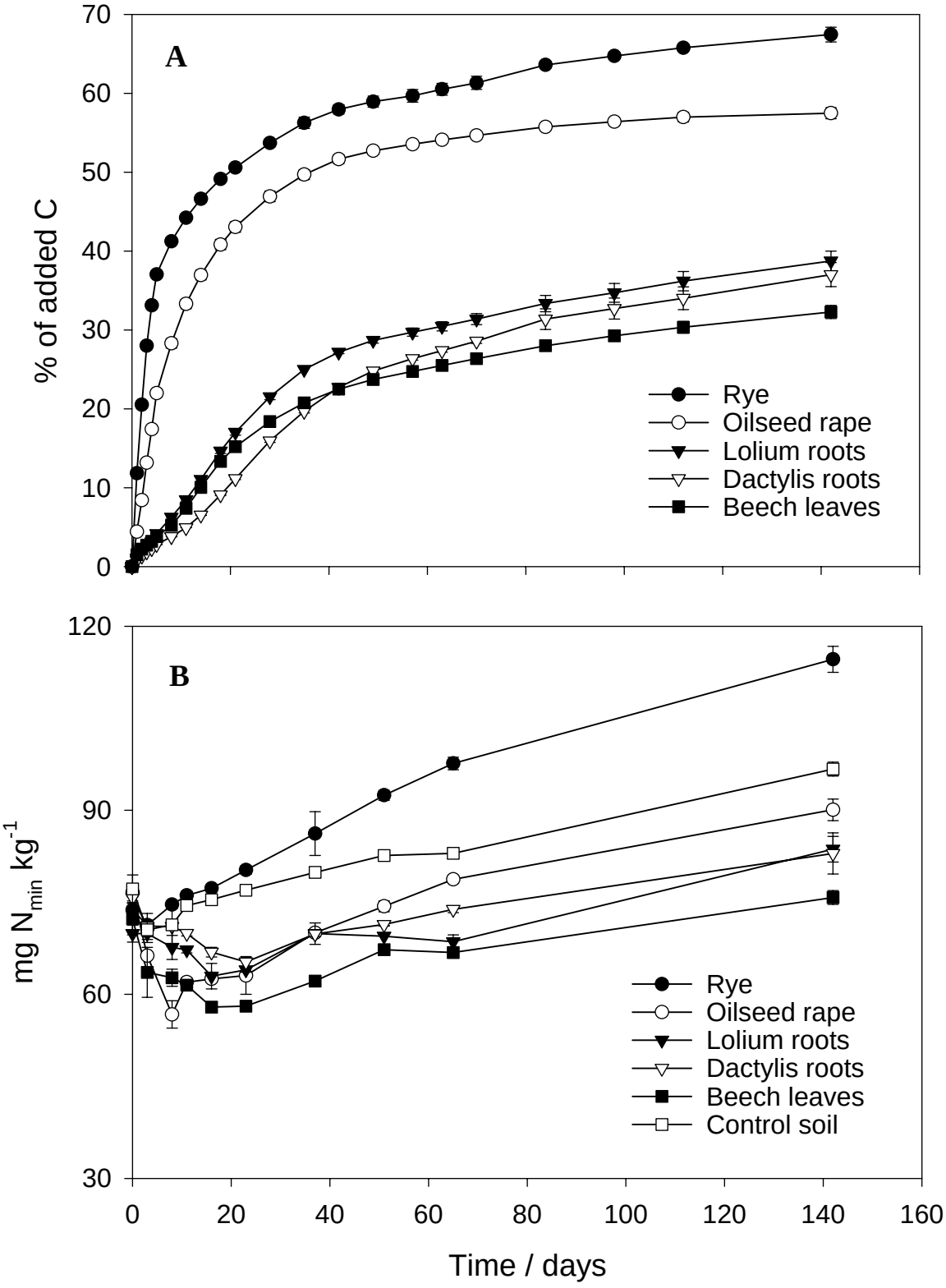

Figure 2.5 (a) Cumulative carbon mineralization, expressed in % of added C, and (b) change in mineral N content, in the arable soil (AGRI) with incorporation of rye and oilseed rape residues, Lolium and Dactylis roots, and beech leaves. Error bars indicate the standard error (n = 3).

Carbon dynamics were mainly explained by the biochemical composition of the plant residues (Figure 2.6.a and 2.6.b). Initial C mineralization (after 3 days of incubation) was well related to the percentage of soluble compounds of the residue mass ($R^2 = 0.84$). After 142 days, a negative linear relationship was observed between cumulative C mineralization and the percentage of lignin-like fraction ($R^2 = 0.70$). The smaller carbon mineralization on the longer term of grass roots and beech leaves compared to oilseed rape and rye was well explained by their larger fraction of lignin-like compounds. Concerning nitrogen dynamics, the amount of N mineralized during the incubation was strongly related to the initial N content of the residues ($R^2 = 0.97$) (Figure 2.6.c).

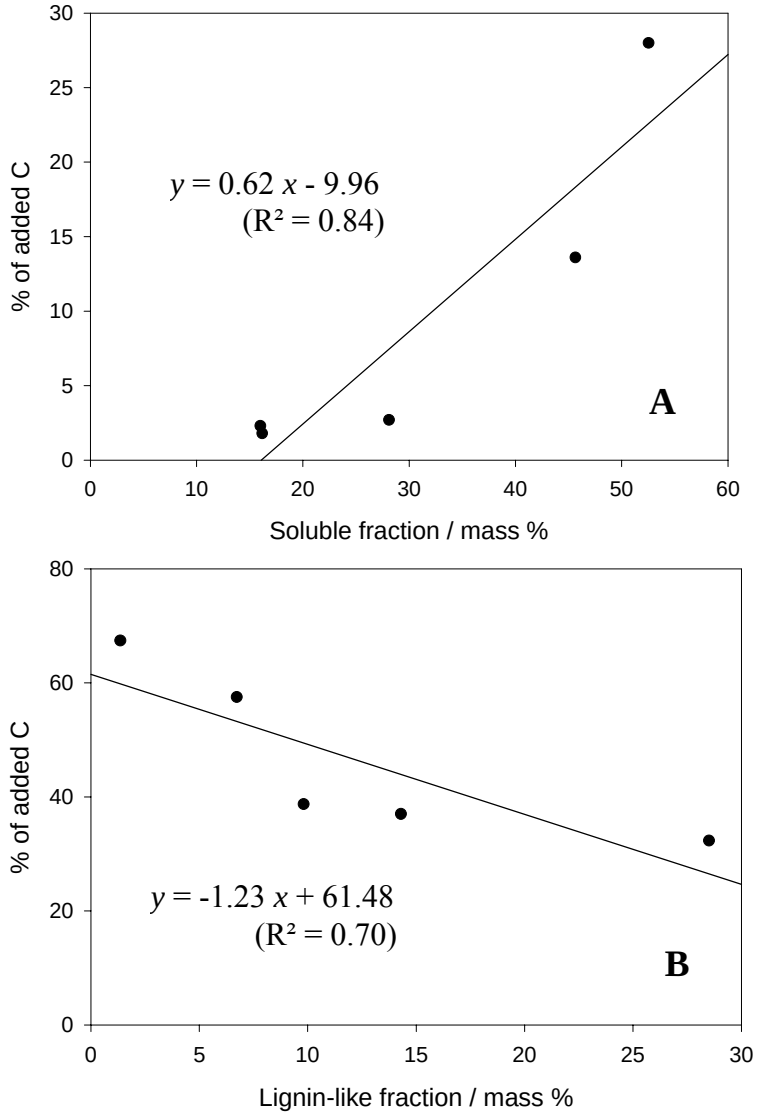

Figure 2.6 (a) Relationship between cumulative C mineralization after 3 days of incubation and the soluble residue fraction, and (b) relationship between cumulative C mineralization after 142 days of incubation and the lignin-like residue fraction.

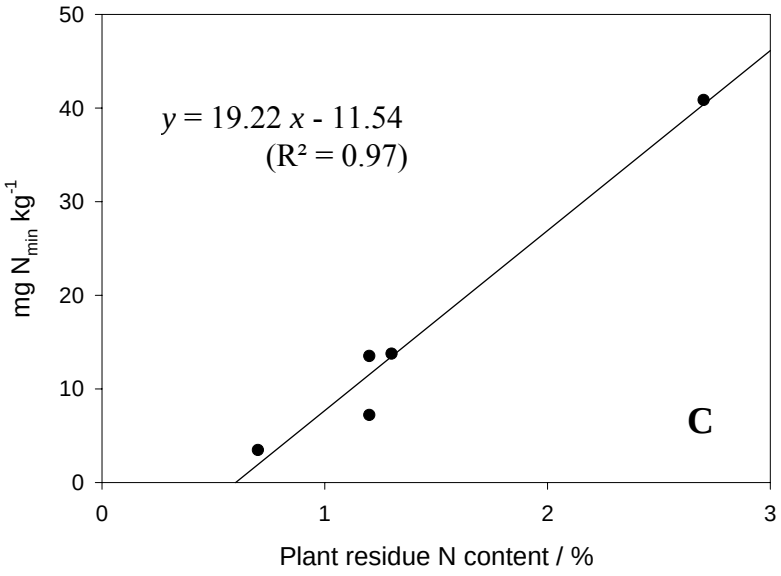

Figure 2.6 (c) Relationship between the accumulation of mineral N in soil after 142 days of incubation and the plant residue N content.

2.3.3 Influence of soil type

To characterize the effect of soil type on residue decomposition and nitrogen mineralization, one residue (rye) was incubated in the three soils and further, beech leaves and Lolium roots were incubated in their 'original' soil and a reference soil, i.e. AGRI. Carbon mineralization of rye, beech leaves and Lolium roots was only little affected by the soil type in which residues were incorporated (Figure 2.7). This was in particular the case during the first two weeks of incubation, where mineralization kinetics were almost identical and this for all of the three residues. Over time, mineralization kinetics slightly diverged for the three soils (with a maximal difference in cumulative mineralization of 10 %), with, in general, a larger carbon mineralization for the residues incubated in AGRI. Net nitrogen accumulation in the soil was mainly determined by the mineralization of native organic N (data not shown).

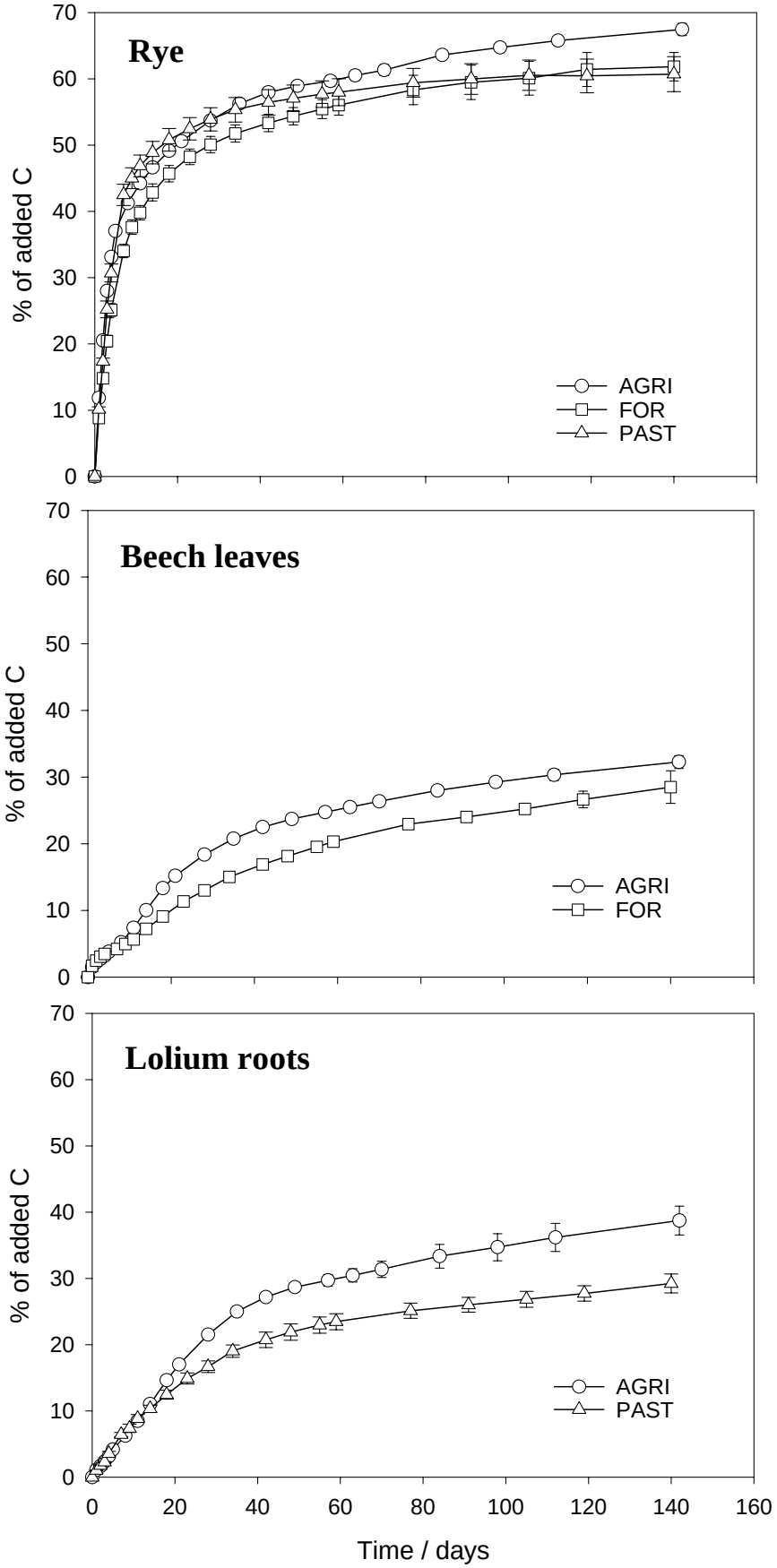

Figure 2.7 Cumulative C mineralization, expressed in % of added C, for rye in AGRI, FOR and PAST, beech leaves in AGRI and FOR, and Lolium roots in AGRI and PAST.

2.3.4 Simulation of plant residue biotransformations with Roth-C

The parameter DPM.(DPM+RPM)$^{-1}$ was estimated by minimizing the sum of squared differences between observed and simulated cumulative CO_2 emission from day 20 to day 140 (Table 2.4). Plant residue decomposition was almost perfectly simulated in AGRI and FOR by optimizing DPM.(DPM+RPM)$^{-1}$ (Figure 2.8). However, in PAST, the mineralization rate of the RPM compartment was overestimated by the model, or the stabilization of carbon in the other compartments was too small. In Roth-C, the yield for the more stable carbon components in HUM varies between 8 % (clay content = 0 g kg^{-1}) and 13 % (clay content = 1000 g kg^{-1}). The yield for BIO also varies between 7 % and 11 %. Increasing yields resulted in a better simulation for PAST, but maximum values were not sufficient to describe C dynamics. A yield of about 20 % for HUM should be necessary to simulate the observed stabilization. A projection of the decomposition dynamics over several years is conceivable (e.g. Figure 2.9), but nevertheless is risky. After 2.7 years, the model still predicted a larger decomposition of 5% for rye residues compared to beech leaves, both incorporated in FOR.

The model underestimated the short term increases in biomass-C, resulting from the stimulated activity of the zymogenous biomass (results not shown). The microbial biomass in Roth-C is attributed to one pool with a relatively slow turnover time, which is not able to simulate the initial flush of microbial activity when adding fresh organic matter to the soil. On the longer term however, the amount of biomass was simulated correctly.

Our dataset was used to estimate the optimized parameter DPM.(DPM+RPM)$^{-1}$ from biochemical plant residue characteristics, determined by proximate analysis (Van Soest, 1963). The parameter (0.18 + soluble fraction - lignin-like fraction) was found to be an excellent estimator for DPM.(DPM+RPM)$^{-1}$ (Figure 2.10). Simulations with this new parameter were validated on residual C data, after 30 and 142 days of incubation (data not shown). The optimization step on observed C mineralization can thus be eliminated, which is a major advantage in scenario analysis for residues of varying biochemical composition.

Table 2.4 Characterization of biochemical plant residue properties in Roth-C. Average values of Decomposable Plant Material (DPM) and Resistant Plant Material (RPM) are obtained by optimization on experimental data of C mineralization of AGRI, PAST and FOR

	Oilseed rape	Rye	Beech leaves	Dactylis roots	Lolium roots
DPM / %	0.61	0.69	0.16	0.22	0.22
RPM / %	0.39	0.31	0.84	0.78	0.79

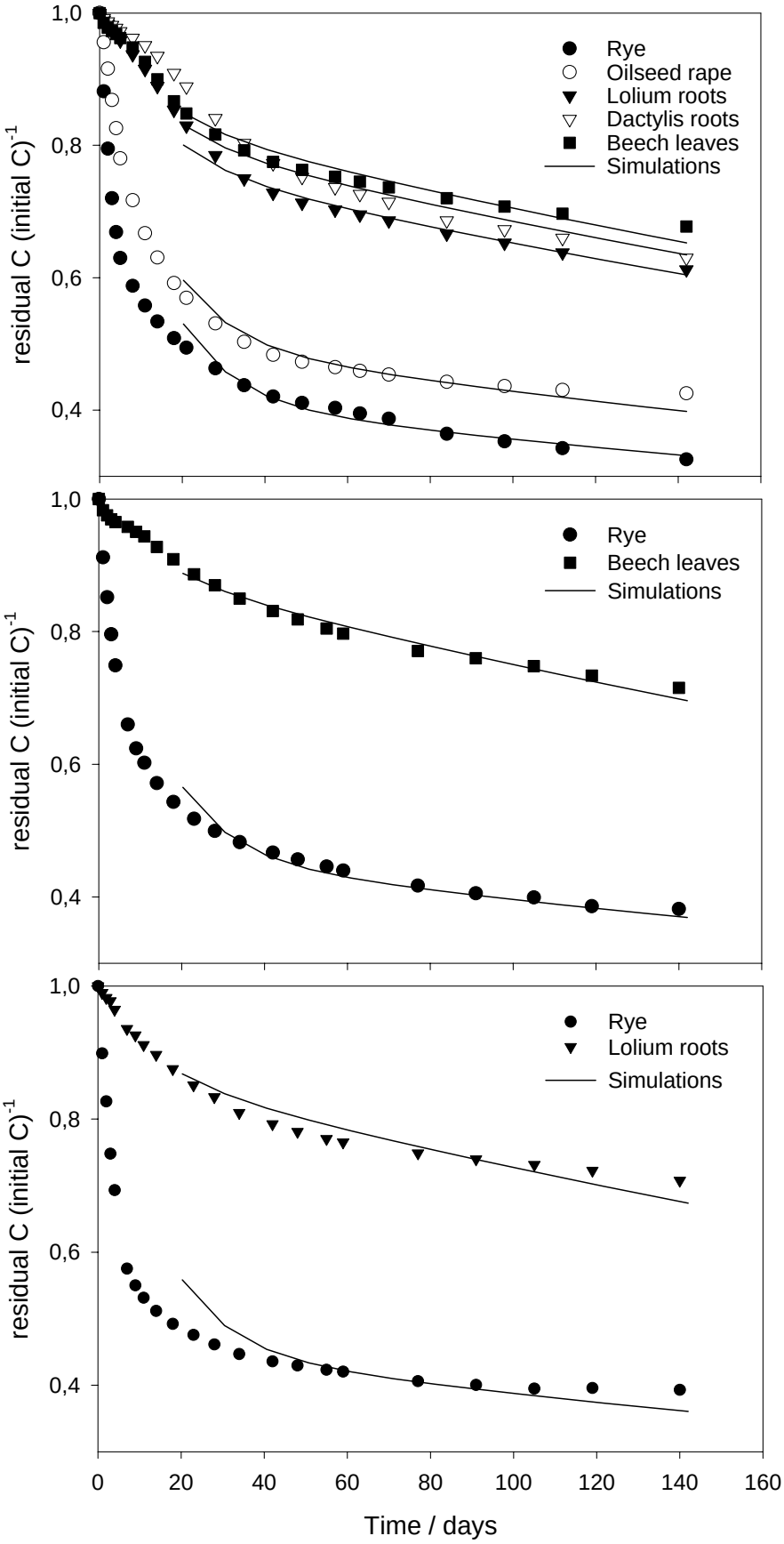

Figure 2.8 Simulation of carbon mineralization in the different soil-residue combinations with the Roth-C model. Only the parameter DPM.(DPM+RPM)$^{-1}$ was optimized.

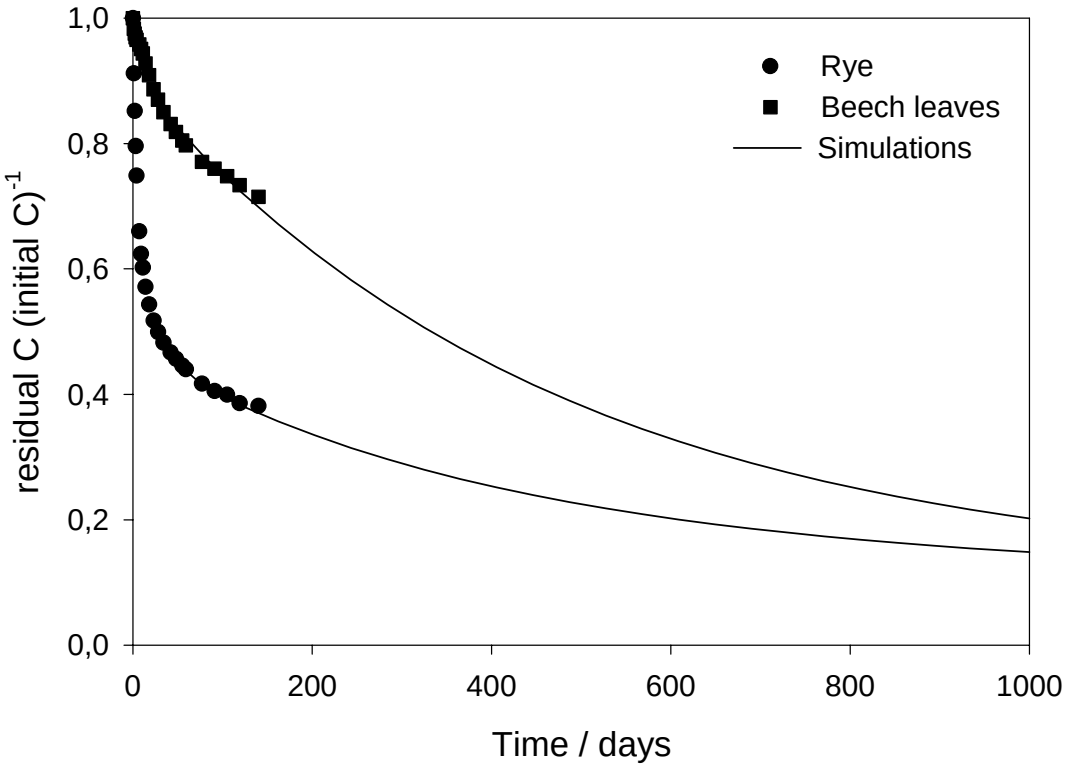

Figure 2.9 Observed values with prediction of the fate of carbon in FOR on the long term, with incorporation of rye residues and beech leaves.

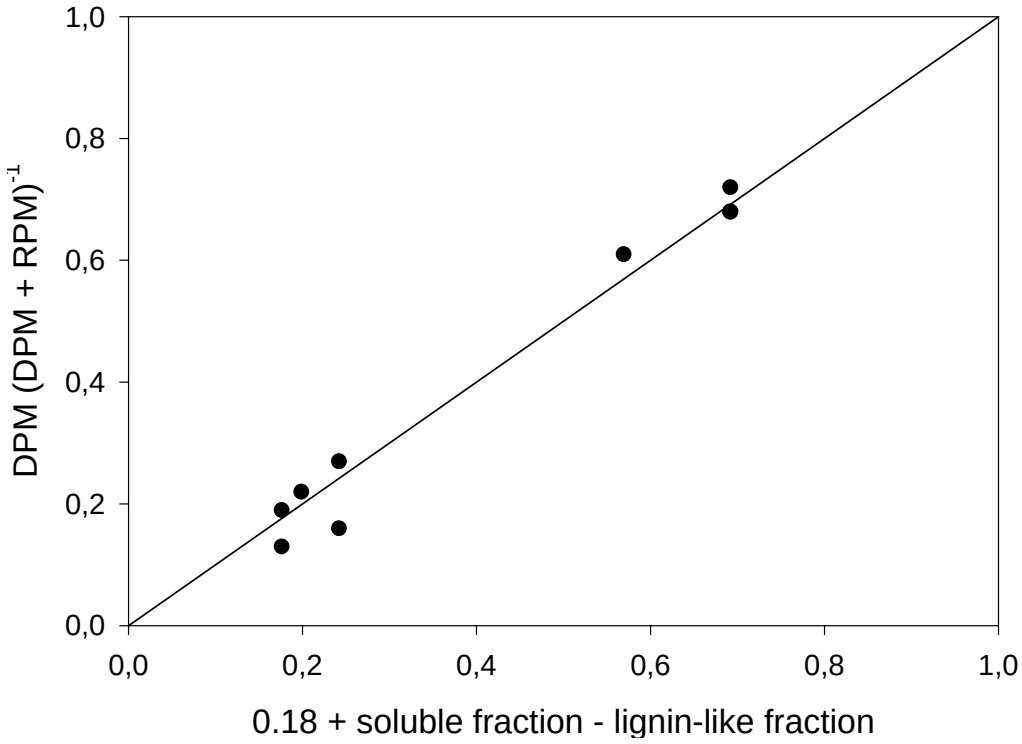

Figure 2.10 Estimation of the parameter DPM.(DPM+RPM)$^{-1}$ from biochemical plant residue characteristics. Data from three soils and five residues are used.

2.4 Discussion

Our results demonstrate that the potential relative contribution to C storage in soil of grass roots and beech leaves is larger than of the aboveground plant parts of oilseed rape and rye, irrespective the soil type in which they decompose. However, the largest fluxes of C and N were observed in the forest soil, when mineralization of native organic matter was taken into account. This is attributed to the larger native organic carbon content of the forest soil compared to the arable and pasture soil, and to the large initial microbial biomass content (592 mg biomass-C kg^{-1}) which was 5 to 9 times the amount of biomass-C in the other soils. A considerable amount of mineral nitrogen was already present in the soil before incubation (37 mg NH_4^+-N kg^{-1}) and it is supposed that the addition of nitrate was not responsible for the observed large C mineralization.

During the initial phase of decomposition, the principal factor determining decomposition kinetics was the nature of the added carbon, which strongly affects the nature and activity of the decomposing microbial biomass. Previously established relationships between C mineralization and the biochemical plant residue quality are confirmed: a linear relationship ($R^2 = 0.79$) between residue-C mineralized at 7 days and the water-soluble C content of the residues was demonstrated by Trinsoutrot *et al.* (2000b). No specific interaction with the origin of the used residues (agro-, pasture or forest ecosystem) was observed, indicating that elaborated mechanisms for describing crop residue decomposition may be generalized for the decomposition of grass roots and tree leaves. Modelling with Roth-C confirmed this hypothesis: using the same concepts and formalisms for modelling the decomposition of different residue types resulted for each residue in a good agreement between simulation and observed data.

The comparison of mineralization kinetics of one residue in three soils with different physico-chemical characteristics and land use history allowed to demonstrate the minor influence of soil type on the initial decomposition of fresh organic matter, which is in agreement with the results of Scott *et al.* (1996). Only during the later stages of decomposition, soil type, and in particular its texture, may have played a role in the degree of stabilization of newly formed microbial biomass and its metabolites. The soil surface area increases as clay content increases, thereby enhancing the potential contact between the mineral soil fraction and incorporated residues or microbial metabolites derived from decomposed residues, resulting in an increased organic matter stabilization potential (Merckx *et al.*, 1985). The larger carbon mineralization in AGRI of about +10%, which had the lowest clay content compared to the

other soils, confirmed this hypothesis. Contribution to the emission of mineral carbon from dissolved carbonates in the soil was considered as negligible, because the amount of mineralized residue-C calculated from cumulative CO_2 emission was in good agreement with amount obtained from residual ^{13}C (e.g. for rye in AGRI). Similar results indicating the negligible contribution of carbonate derived CO_2 in the total CO_2 emission when crop residues are incorporated in this soil were found by Bertrand *et al.* (personal communication). We suggest that soil type affected the mineralization kinetics only when recycling and re-mineralization of C and N of the microbial biomass became important.

As a consequence, decomposition of plant residues is not necessarily favoured in soil that receives regularly the same type of residues. This result is very important regarding to the existing questions on the role and adaptation of indigenous microflora of the soil in the decomposition of organic matter (Pankhurst *et al.*, 1996). Large variation in the initial amount of microbial biomass-C, which was associated to the differences in the mineralization of native organic matter in the three soils (i.e. autochthonous biomass), did not influence the decomposition rate of fresh organic matter. Observations of Lundquist *et al.* (1999) supported this hypothesis. They found that despite long-term differences in agricultural management and differences in active soil organic matter contents, the rates of rye decomposition and C and N mineralization were similar. Rye incorporation produced a short-term flush of microbial growth and activity of similar magnitude, although the initial contents of soil microbial biomass were different. Thus, mineralization of the added residues was controlled by the activity of a "zymogeneous" biomass, developing from the added C, supporting the concept that decomposition of organic matter is regulated by two distinct pools of microbial biomass (autochthonous and zymogeneous) as designed in some decomposition models, e.g. CANTIS (Garnier *et al*., 2003).

Although on the short term no major effect of soil type on residual C was observed, large differences exist in some chemical and biological properties of the soils taken from the three agro-ecosystems (in particular total C and N, biomass-C). Two hypotheses are proposed to explain the origin of these differences. (i) Differences in stabilization of organic carbon by soil texture that were not detectable on a < 1 year time basis, result on the long term in a significant increase of the carbon content in soil and affected the turnover rate of the microbial biomass (soil type effect). (ii) The different agro-ecosystems produce plant residues of different quality with different intrinsic decomposition properties that led to more or less accumulation of residual organic matter (residue quality effect). The latter hypothesis was supported by modelling of the long term decomposition of different plant residues in one

specific soil, where the Roth-C model predicts that residue quality still had an impact on the residual C in soil after almost three years of decomposition.

2.5 Conclusion

It has been demonstrated that, under controlled and non-limiting N conditions, the quality of the substrate added was the first factor determining the residue decomposition kinetics and that the type of soil had little or no effect on the short-term dynamics of decomposition of residues in soils. However on a longer term, carbon mineralization was slightly influenced by soil type, which was probably due to differences in the capacity to stabilize soluble carbon and/or microbial derived carbon. Plant residue decomposition was well simulated by the Roth-C model.

The 'classical' relationship that was observed between carbon mineralization and the biochemical composition of the five residues (i.e. soluble fraction and lignin-like fraction), and the validation of the formalisms describing residue decomposition by the Roth-C model, demonstrate that a general approach can be used to characterise and model the quality impact of plant residues originating from different agro-ecosystems. The lack of soil type effects on the short term kinetics of C mineralization justifies to use a single soil type to investigate the influence of residue quality on C fluxes.

Chapter 3

Soil moisture, carbon and nitrogen dynamics following incorporation versus surface application of labelled residues in soil columns

3.1 Introduction

Reducing tillage intensity has an impact on soil physical properties, such as soil structure and stability, water infiltration rate and soil temperature, and on biological properties such as nutrient availability and the diversity of soil biota (Blevins & Frye, 1993; Tebrügge & Düring, 1999; Holland, 2004). The combined effect of those soil physical and biological properties, climatic factors and their interactions determines the biotransformations of organic matter in soil.

In order to understand these physical-biological changes upon changing tillage practice, it is necessary to first distinguish the influence of the modified residue location from the mechanical effect of soil disturbance. Several authors have examined the effect of crop residue location on the decomposition rate (Douglas *et al.*, 1980), CO_2 emission (Curtin *et al.*, 1998), N mineralization (Corbeels *et al.*, 2003) or microbial activity (Holland & Coleman, 1987). However, residues left at the soil surface also slow down the initial constant rate of water evaporation (Bond & Willis, 1969) and hence change the soil water regime during decomposition.

Studies combining biological and physical processes are lacking, but nevertheless are essential to analyse the interactions of residue location with the carbon and nitrogen cycles. For example, in a laboratory microcosm incubation experiment with sieved soil, conducted under constant temperature and moisture conditions and without nitrogen limitation, significant differences in carbon mineralization remained absent, irrespective of the residue location (Abiven & Recous, 2002). An important factor that could explain the lack of response is the absence of water transport in the microcosm experiment. Under field

Adapted from: F. Coppens, P. Garnier, R. Merckx, S. Recous (submitted) Soil moisture carbon and nitrogen dynamics following incorporation versus surface application of labelled residues in soil columns. *European Journal of Soil Science*

conditions, however, rain is an important modifier of the distribution of carbon and nitrogen derived from the fresh organic matter in the soil, creating gradients in nutrient concentrations through the soil profile (Cannavo *et al.*, 2004). Also the subsequent drying-wetting cycles observed in field situations are not taken into account in the simplified laboratory incubation experiments.

The objective of our experiment was to assess the interactions between soil physical and biological processes that are affected by initial crop residue location in soil. The main hypothesis of this work was that crop residue location influences the soil water dynamics and the distribution of carbon and nitrogen in soil, which in turn affect soil microbial activity and the residue decomposition rate.

3.2 Materials and methods

3.2.1 Soil

The soil used in the experiment was a silt loam, Orthic Luvisol, (clay: 13.4%, silt: 81.6%, sand: 5.0%), obtained from the experimental site of INRA, Mons-en-Chaussée, Northern France. The soil has not been cropped since 1994. The top 25 cm soil layer was sampled, sieved (< 2 mm) at field moist content (0.17 g g^{-1}) and stored in plastic bags at 4°C prior to use. The soil pH (H_20) was 8.2, and soil contained 8.5 g kg^{-1} organic carbon and 0.9 g kg^{-1} nitrogen, resulting in a C:N ratio of 9.4. The organic matter content was 13.3 g kg^{-1}, the total carbonate content 7.0 g kg^{-1} and the cation exchange capacity 8.1 $cmol_c$ kg^{-1}. The soil was preincubated for 2 weeks at 20°C before the start of the experiment.

3.2.2 Crop residue

The fresh organic matter used in this experiment was mature oilseed rape (*Brassica napus* L.), labelled with $^{13}C^{15}N$. The plant residues were obtained by growing a rape crop under hydroponic conditions in a labelling growth chamber, with enriched $^{13}CO_2$ atmosphere (^{13}C atom % excess = 3.13%) and in a nutrient solution with ^{15}N labelled KNO_3 (^{15}N atom % excess = 9.8%). This resulted in a homogeneous labelling of all plant parts. The overall plant growth conditions are described by Trinsoutrot *et al.* (2000a). The residues applied consisted of a mixture of leaves, stalks, branches and pods, chopped at 1 cm. The C and N content of the mixture was 42.2% C and 1.45% N, resulting in a C:N ratio of 29. The isotopic excess was 2.88% for ^{13}C and 9.73% for ^{15}N. Its biochemical composition determined by proximate

analysis (van Soest, 1963) consisted of 45.6% soluble compounds, 14.4% hemicellulose, 33.2% cellulose and 6.7% lignin-like fractions. Details of the C and N content of each fraction are given in Table 3.1.

Table 3.1 Carbon and nitrogen content of the biochemical fractions of the applied oilseed rape residue

	Analysis oilseed rape residue				Analysis biochemical fractions	
	mass / %	C / %[a]	N / %[a]	C/N	C / %[b]	N / %[b]
Total residue	99.9	42.2	1.45	29		
Soluble fraction (CWE)[c]	25.7	29.4	2.12	14	17.8	47.2
Soluble fraction (NDS)[c]	45.6	35.5	1.75	20	39.0	71.0
Hemicellulose	14.4	36.4	0.75	49	12.6	9.6
Cellulose	33.2	48.3	0.39	125	38.7	11.4
Lignin + ash	6.7	59.2	1.33	44	9.6	8.0

[a]% C and N in mass of biochemical fraction; [b]% of total residue-C and -N
[c] The Cold Water-Extractable fraction (CWE) is part of the fraction extracted with Neutral Detergent Solution (NDS)

3.2.3 Soil column preparation

Plastic cylinders (PVC, 15.4 cm inner diameter and 30 cm high) with perforated bases were used to contain 25 cm of soil, compacted at 1.3 g cm^{-3}. To this end, 6.0 kg (dry weight) of the preincubated soil was divided in three subsamples, which were successively compacted in a predefined volume of the cylinder. The surface of a compacted soil layer was loosened before adding the next soil layer to maintain continuity in the arrangement of soil particles over the 25-cm soil profile. Oilseed rape residues were applied at the surface (referred to as SURF) or homogeneously mixed in the upper 10 cm before compaction (referred to as INC) at a rate of 13.8 g dry matter per column, equivalent to a return of 7.4 t ha^{-1}. Control columns (referred to as CTRL) without addition of residues were prepared. When residues were incorporated, a certain volume of soil was replaced by the equivalent volume of the added residues in order to obtain the same apparent bulk density over the whole soil profile for all treatments.

3.2.4 Experimental conditions

At the start of the incubation period, artificial rain was applied with a rainfall simulator on all of the soil columns for 2.5 hours at a rate of 12 mm $hour^{-1}$. The simulator consisted of 380 capillary tubes (inner diameter 0.5 mm) equally distributed over a surface of 1 m^2, at 4 m

above the soil surface. Rain intensity was controlled by adjusting the water pressure. A wire mesh placed at 1 m below the capillary tubes lead to a homogeneous distribution of the raindrops. The applied water was obtained from filtered rain water, with a pH of 6.5 and a composition of 1.5 mg dissolved organic carbon (DOC) litre^{-1}, 1.6 mg dissolved inorganic carbon (DIC) litre^{-1}, 1.3 mg NO_3^--N litre^{-1} and < 0.1 mg NH_4^+-N litre^{-1}. By this treatment, the volumetric water content of the soil was raised from 0.22 to 0.34 cm^3 cm^{-3}, no drainage was observed. Subsequently, the soil columns were transferred to a climate chamber and left uncovered at 20°C and 70% relative air humidity to allow evaporation. After 3, 6 and 9 weeks of incubation, soil columns were again placed under the rainfall simulator until the water lost by evaporation was replaced. The rainfall application at week 9 allowed to extract the soil solution and to determine the final concentrations of dissolved organic carbon and mineral nitrogen. Therefore, the four rainfall events, further referred to as R0, R3, R6 and R9, defined three wetting-drying cycles. The experimental design is illustrated in Appendix B.

3.2.5 Experimental design

At the end of the three evaporation periods (before re-wetting), three independent columns of CTRL, SURF and INC were used for destructive analysis (total : 27 columns). These soil columns were sliced into four layers: 0-5 cm, 5-10 cm, 10-17.5 cm and 17.5-25 cm. For each treatment (CTRL, SURF, INC), another two columns were equiped with a number of probes to provide information about the transport of water and solutes during the 9-week incubation period (total : 6 columns). These columns were also used for CO_2-flux measurements. Finally, for the SURF treatment, three additional columns were constructed with detachable mulch: the residues were placed on a 1-mm mesh to allow measurements of the mulch mass. These data were used to calculate the gravimetric water content of the mulch, after correction of the mass for leached and mineralized C. In this way, a total of 36 soil columns was constructed.

3.2.6 Destructive soil analysis

For the SURF treatment, the mulch was removed from the soil surface and dried at 60°C; for the INC treatment, the coarse residue fraction (>2 mm) was separated from the fine fraction (<2 mm) and also dried at 60°C. Destructive soil analysis was performed on each of the four soil layers. The gravimetric soil water content was determined after 24 hours drying at 105°C. The soil pH was measured after 30 minutes shaking in water (soil-to-solution ratio: 1/2; pH meter 51 – Radiometer, Copenhagen). Soil mineral nitrogen was extracted with 1 *M* KCl (30

minutes shaking, soil-to-solution ratio 1/2.5), soluble carbon was obtained by extracting 30 g of soil in 160 ml 0.03 *M* K_2SO_4 (30 minutes shaking). Soil extracts for mineral N and soluble C were centrifuged (20 minutes at 5800 *g*), filtered and stored at –20°C until analysis. The mineral nitrogen (NO_3^--N and NH_4^+-N) was measured by continuous flow colorimetry (TRAACS 2000, Bran & Luebbe). We distinguished dissolved inorganic and organic carbon in the soluble extract: acidification of the extract by 5% H_3PO_4 (for DIC) was followed by chemical oxidation in a persulfate medium (for DOC), the CO_2 produced being measured by infrared spectrometry (1010, O.I. Analytical).

The total C and N content of the soil and the recovered plant residues, with their isotopic excess, were determined using an elemental analyser (NA 1500, Carlo Erba) coupled to a mass spectrometer (Fisons Isochrom). The soil adhering to the recovered residues was detached and analysed separately for C and N.

Microbial activity in each soil layer was measured using the substrate induced respiration technique (SIR) (Anderson & Domsch, 1978; Lin & Brookes, 1999). A glucose solution was prepared to add 500 µg glucose-C g^{-1} soil by bringing the gravimetric soil water content to 0.24 g g^{-1}. A subsample of 3 g soil was incubated for 6 hours at 20°C in a sealed 10-ml tube. The amount of produced CO_2 was measured on an infrared gas analyser (UNOR 610, Maihak).

3.2.7 Semi-continuous measurements

At 6 and 14 cm soil depth, the volumetric water content was measured by horizontally inserted TDR-probes (3 rods, 8 cm). The measurements were recorded every hour on a TRASE system (Soilmoisture Equipment Corp.). At the opposite side of the columns, at 6 and 14 cm soil depth, the soil water potential was determined, using tensiometers with porous cups of 5 cm (RhizoCera ø 3 mm, Rhizosphere Research Products) which were connected to differential pressure sensors (CZ5022/2, EuroSensor). Measurements of the soil water potential were stored on a CR10X data acquisition central (Campbell). Mass loss of the columns was used to calculate daily evaporation rates.

Soil solution (3x 10 ml) was sampled 12 hours after each rainfall application at 2, 10 and 18 cm soil depth (Rhizon MOM 10 cm, Rhizosphere Research Products). The pH was determined on the 10 ml samples (pH meter 51 – Radiometer, Copenhagen), which were further stored at –20°C until analysis for mineral nitrogen (TRAACS 2000, Bran & Luebbe) and soluble carbon (1010, O.I. Analytical).

The flux of CO_2 from the soil surface to the atmosphere was calculated from the accumulation rate of CO_2 in the headspace of the columns. During a 3-minute period, the columns were sealed with a cover that was connected to an infrared gas analyser (UNOR 610, Maihak). A fan on the inside of the 'closed chamber' provided homogenous mixing of the air. The slope of a linear regression through the increase of CO_2 concentration over time was used to calculate the CO_2 flux. Measurements were performed on a daily basis at the beginning of every evaporation cycle; the frequency of periodic measurements was decreased after the initial flush of microbial activity.

3.3 Results

3.3.1 Influence of crop residue location on water dynamics

Water loss from the soil columns (CTRL, SURF, INC) was determined for each 3-week evaporation period. Leaving crop residues at the soil surface reduced water loss by 47 to 59 % compared to CTRL, while incorporation of residues did not affect the total evaporation (data not shown). The differences in evaporation between CTRL and INC on the one hand and SURF on the other hand strongly influenced the water distribution in the soil profile (Figure 3.1). The greater water loss in CTRL and INC compared to SURF resulted in the development of a more pronounced gradient in the gravimetric soil water content, which increased on average from 0.15 g g^{-1} at the top to 0.20 g g^{-1} at the bottom of the soil columns. The gravimetric soil water content for SURF was significantly larger and more equally distributed over all soil layers (from 0.22 to 0.23 g g^{-1}). The small difference in water content between CTRL and INC could have arisen from the construction of the soil columns, where the soil for INC required longer manipulation and might have lost some water.

Figure 3.2 shows the change in gravimetric mulch water content during the 9-week incubation, combined with the change in residual mulch mass. The first rainfall event (R0) increased the mulch water content from 0.08 to 2.10 g g^{-1}. After 7 days of evaporation, a constant level of 0.33 g g^{-1} was reached. After R3 and R6, a slight increase in water storage capacity (up to 2.25 g g^{-1}) and a faster reduction of the mulch water content to a constant level was observed, while mulch mass decreased over time.

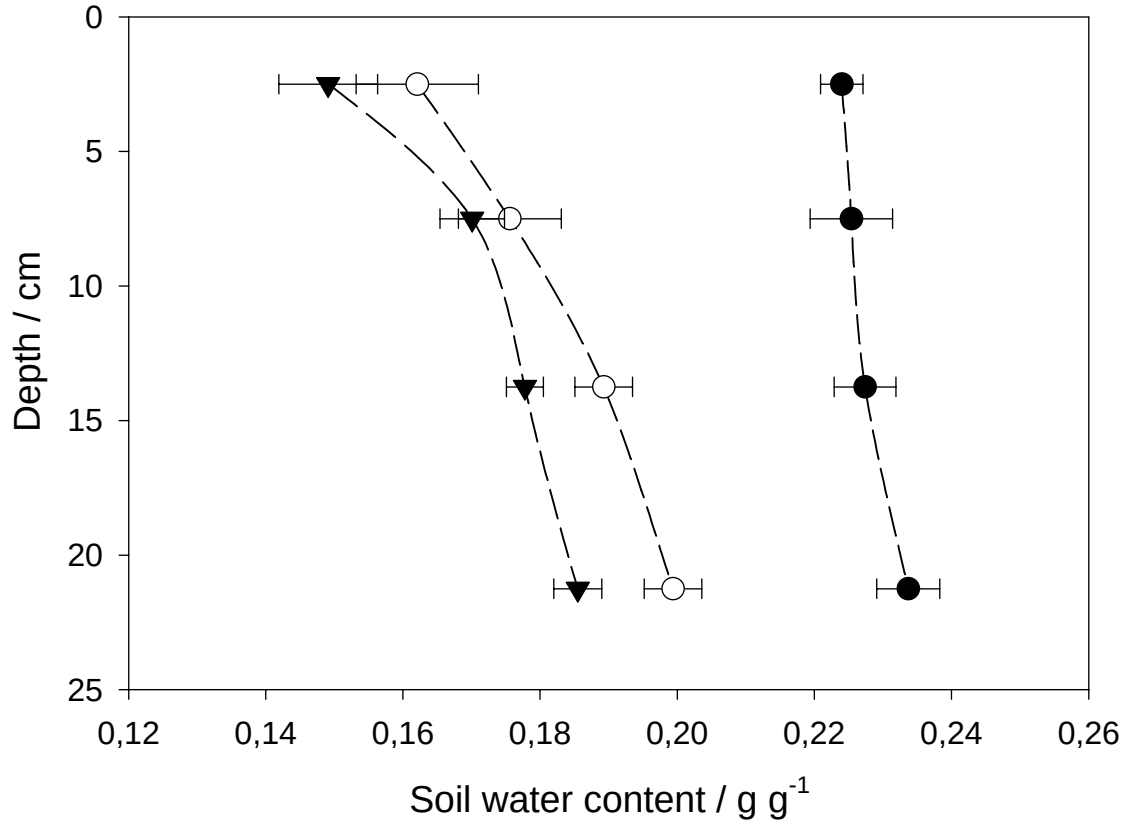

Figure 3.1 Distribution of the gravimetric soil water content through the soil profile of the control (CTRL ○), surface (SURF ●) and incorporation treatment (INC ▼), at the end of a 3-week evaporation period. Values are the average of the three wetting-drying cycles (bars represent the standard error, n = 9)

Water retention curves of the soil were obtained for CTRL, SURF and INC by combining the experimental results of TDR probes and tensiometers (data not shown). Within treatments, a small shift in the water retention curve was measured over each evaporation period, towards a smaller volumetric water content for the same matric potential. The destructive impact of rain on soil aggregates (Le Bissonnais & Arrouays, 1997) and the transport of soil particles with infiltrating water (Nemati *et al.*, 2000) are assumed to be responsible for this change. This effect was less pronounced for SURF, where the soil surface was protected from direct rain impact. No significant differences in water retention due to the presence of fresh organic matter could be observed, irrespective of the mode of application.

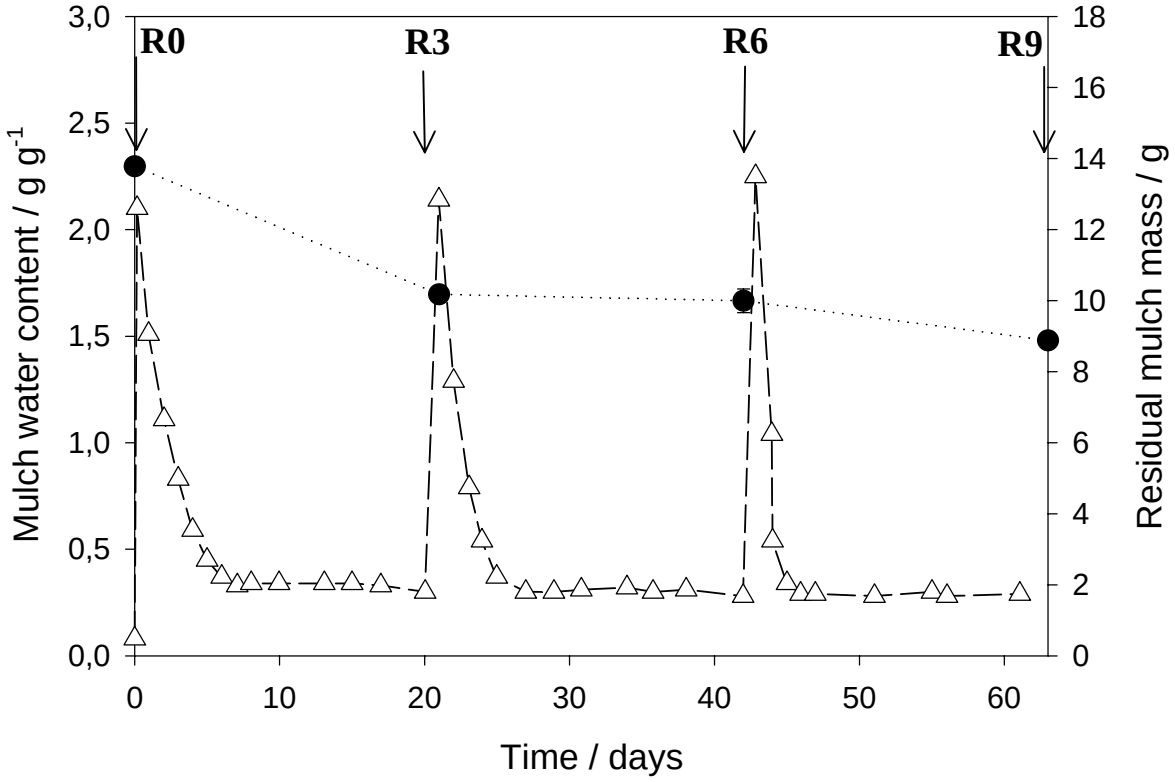

Figure 3.2 Change in the gravimetric water content of residues at the soil surface over the 3 wetting-drying cycles (△) and the residual mass of surface applied residues (SURF ●) (mean values, bars represent the standard error, n = 3).

3.3.2 pH in soil and soil solution

Addition of crop residues (SURF and INC) decreased the pH of the soil solution at all sampling depths after the first rainfall (R0). The decrease in pH ranged from -0.3 to -0.6 units for SURF and between -0.8 and -1.2 units for INC compared to CTRL which had a pH between 8.2 and 8.4. The greater CO_2 partial pressure in SURF and INC due to the increased microbial activity compared to CTRL, resulted in an increased amount of dissolved CO_2 and consequently in an acidification of the soil solution. This effect was less pronounced after the following rainfall events. No clear change with depth or time was observed in the pH measured in soil extracts at the end of the three evaporation periods.

3.3.3 Distribution of soluble carbon

Soluble carbon determined in the soil solution sampled after each rainfall was considered as mobile dissolved organic carbon (DOC_m) (Figure 3.3). The concentration of DOC_m in the soil solution of CTRL was relatively constant over time and distributed homogeneously over the soil profile, with an average concentration of 9 mg DOC_m $litre^{-1}$. After the first rainfall (R0), DOC_m concentrations at 2 and 10 cm soil depth were significantly larger for SURF and INC than for CTRL. In addition, the distribution of DOC_m in the soil profile was different comparing SURF to INC: the maximum DOC_m concentration was measured for SURF at 2 cm soil depth (110 mg DOC_m $litre^{-1}$), and for INC at 10 cm soil depth (117 mg DOC_m $litre^{-1}$). Although smaller concentrations of DOC_m were obtained after the following rainfall events, the same pattern in distribution over the soil profile was observed.

Soluble carbon determined in K_2SO_4 extracts of the soil at the end of each evaporation period (before re-wetting) was considered as potentially available dissolved organic carbon (DOC_{pa}) (Figure 3.4). At week 3, a significantly larger amount of DOC_{pa} was measured in the soil profile of SURF compared to CTRL and INC. At this time, the amount of DOC_{pa} left in the 0-10 cm soil layer for INC was only 46.5% of the amount measured for SURF. At week 6, the amount of DOC_{pa} in the 0-10 cm soil layer had significantly decreased for SURF and increased for INC compared to week 3. Below 10 cm soil depth, no significant differences were observed between treatments. At week 9, no significant changes were observed in the amounts of DOC_{pa} compared to week 6. For CTRL, the amounts of DOC_{pa} were stable over time and distributed homogeneously in the soil profile.

3.3.4 Microbial activity: substrate induced respiration

The application of crop residues stimulated the microbial activity in the soil, irrespective of the addition mode (INC or SURF) (Figure 3.5). The microbial respiration in the 0-10 cm soil layer for SURF was significantly greater than this for CTRL. For the INC treatment, an increase in respiration was observed down to 17.5 cm in the soil profile. In these soil layers, there was no significant change in SIR over time. Maximum respiration rates were found in the 0-5 cm soil layer for SURF (5.3 µg C g^{-1} soil $hour^{-1}$) and in the 5-10 cm soil layer for INC (5.6 µg C g^{-1} soil $hour^{-1}$). Over the total soil profile (0-25 cm), a significant larger average SIR was obtained for INC (21.1 mg C $hour^{-1}$ per column) than for SURF, (17.9 mg C $hour^{-1}$ per column).

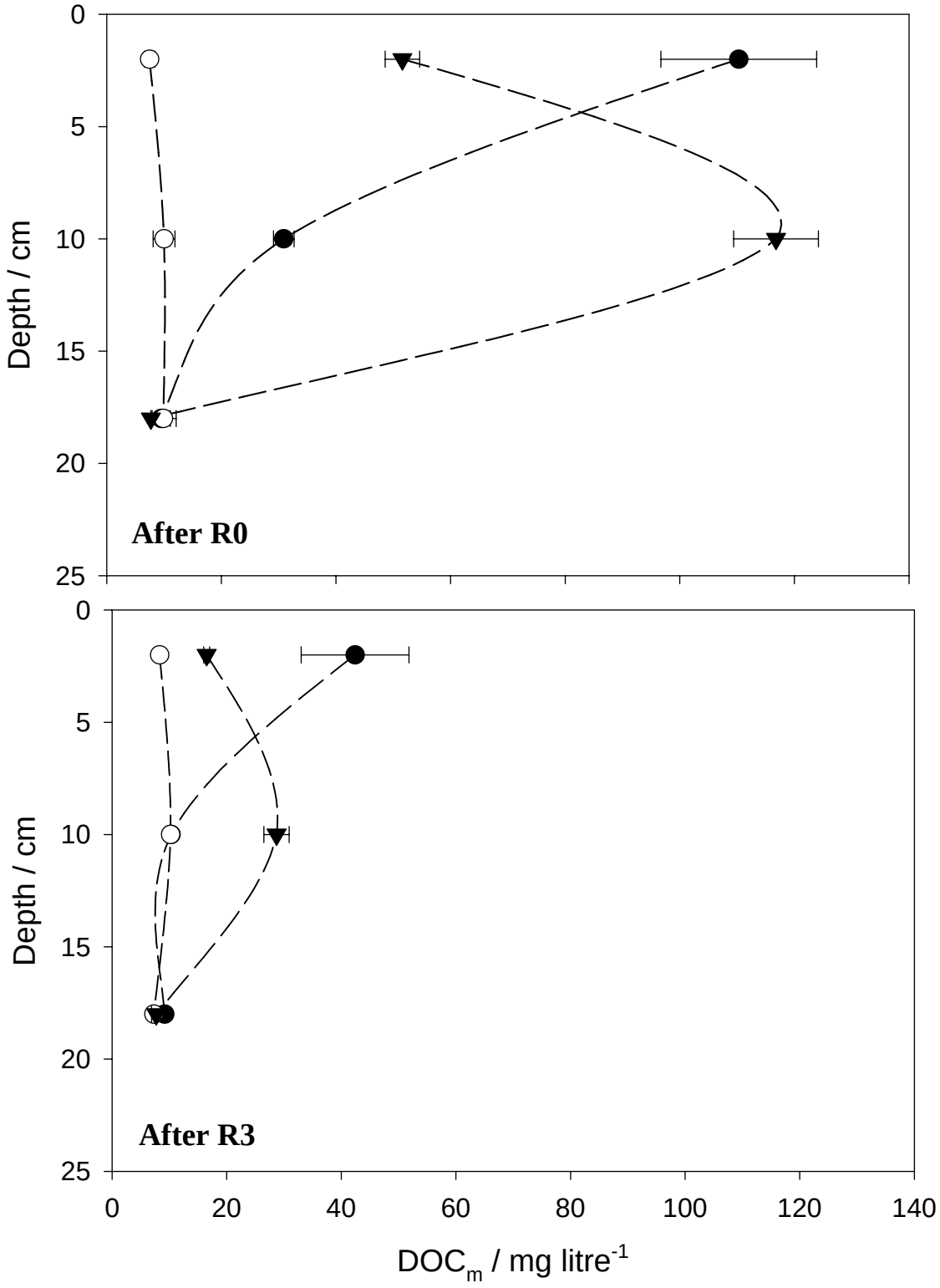

Figure 3.3 (a) Distribution of the 'mobile' dissolved organic carbon concentration (DOC_m) in the soil solution after rainfall R0 and R3 of the control (CTRL ○), surface (SURF ●) and incorporation treatment (INC ▼) (mean values, bars represent the standard error, n = 2)

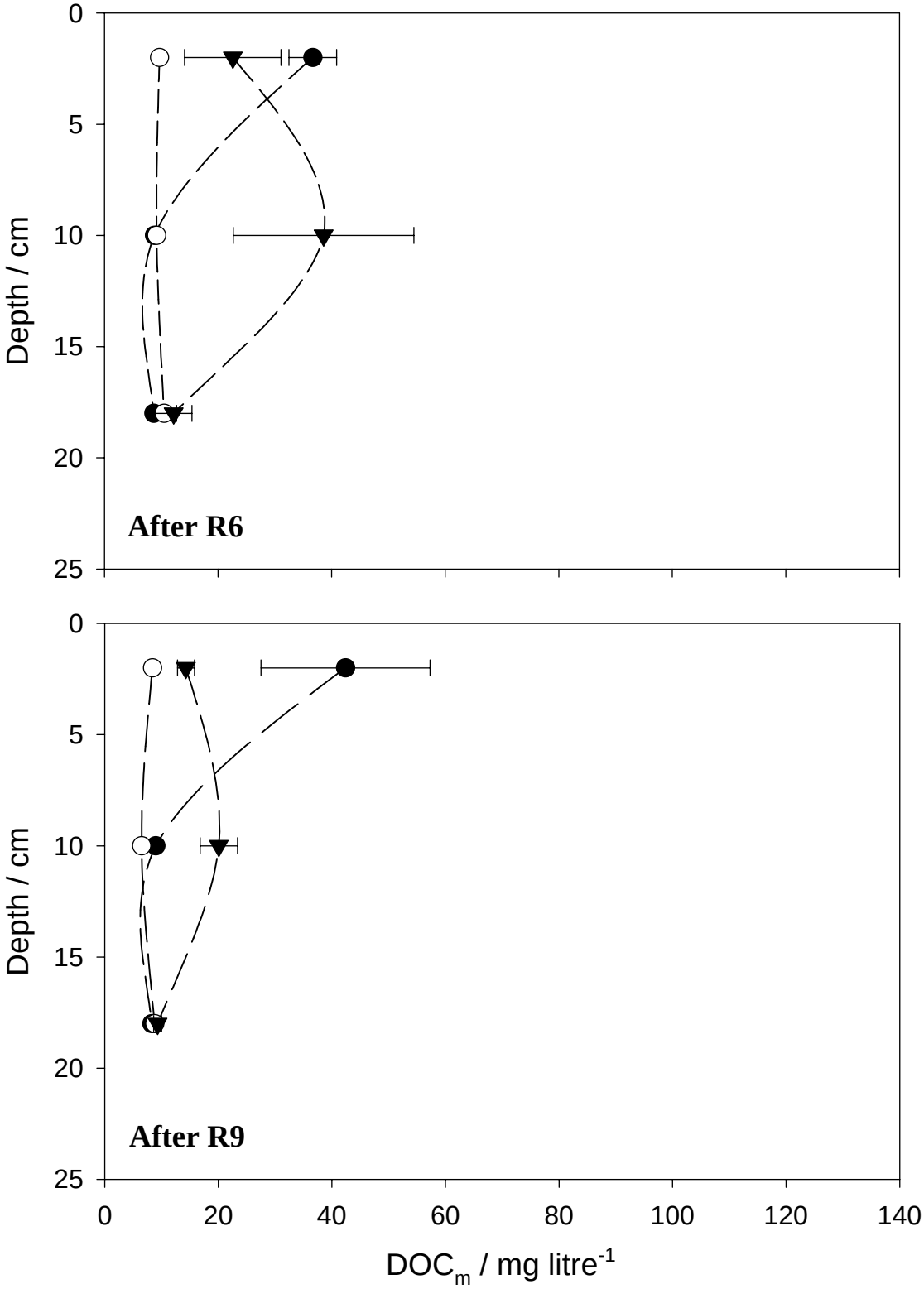

Figure 3.3 (b) Distribution of the 'mobile' dissolved organic carbon concentration (DOC_m) in the soil solution after rainfall R6 and R9 of the control (CTRL ○), surface (SURF ●) and incorporation treatment (INC ▼) (mean values, bars represent the standard error, n = 2)

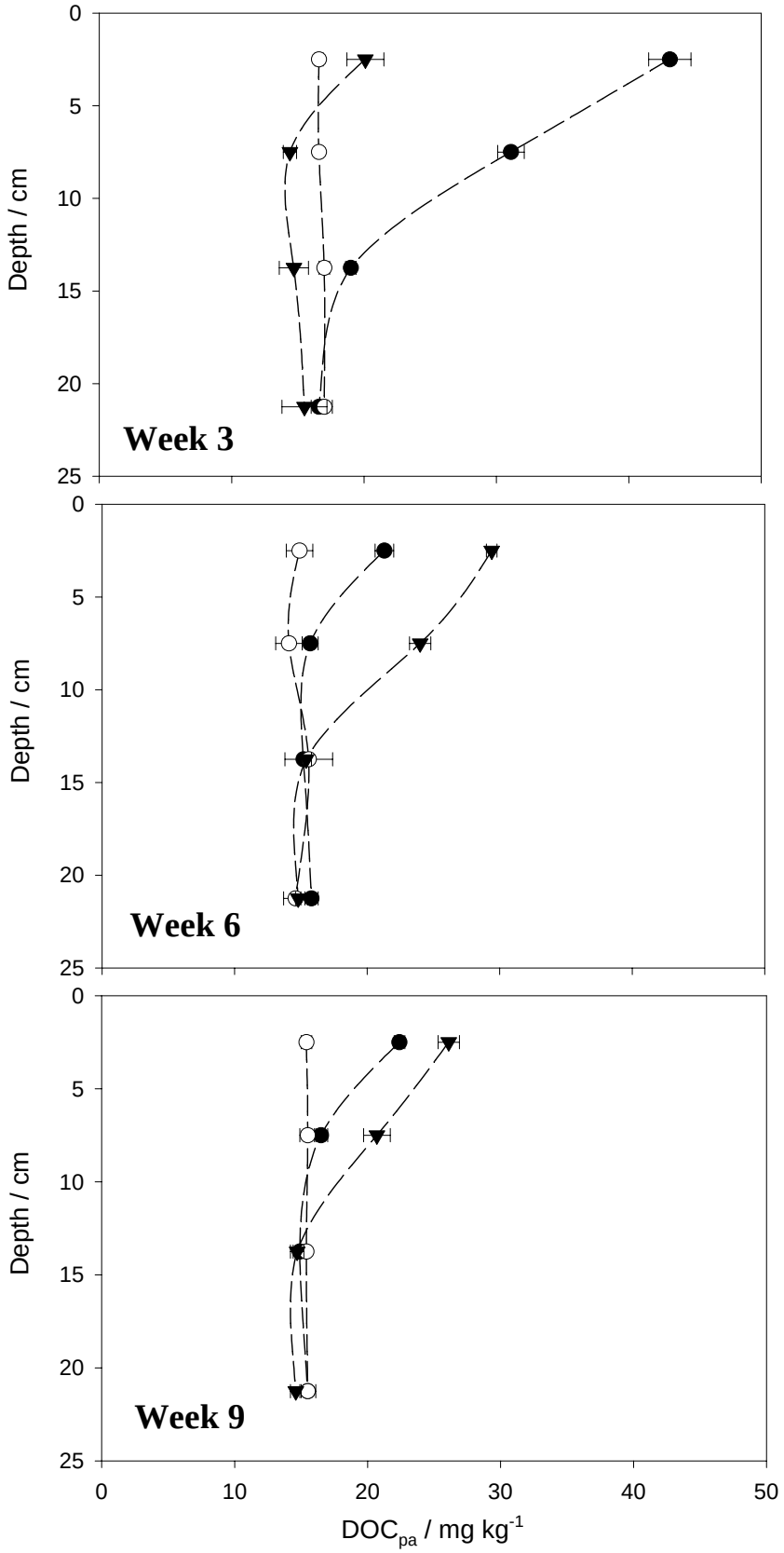

Figure 3.4 Distribution of the amount 'potentially available' dissolved organic carbon (DOC_{pa}) in different soil layers after 3, 6 and 9 weeks of incubation (before re-wetting) in the control (CTRL ○), surface (SURF ●) and incorporation treatment (INC ▼) (mean values, bars represent the standard error, n = 3)

3.3.5 Residue decomposition

For the SURF treatment, 64% of the initial mulch mass was recovered after 9 weeks of incubation (Figure 3.2). For the INC treatment, only 19% of the added residue mass was found in the coarse fraction (>2 mm) at the same date (data not shown). The unrecovered part of the residue mass was mineralized or had entered the fine soil fraction (<2 mm). For the INC treatment, we also observed a different decomposition rate at different soil depths: at week 3, 49% of the initial residue mass was recovered in the 0-5 cm soil layer and only 28% in the 5-10 cm soil layer. At week 9, no significant difference in decomposition was observed between the two soil layers.

The mineralization rate of organic C was calculated from the CO_2 flux emitted from the soil surface (Figure 3.6). In general, a larger CO_2 flux was observed from INC compared to SURF. After a rainfall event however, the increased soil water content reduced the CO_2 emission from CTRL and INC. This is probably due to less diffusion of CO_2 to the atmosphere (Jensen *et al*., 1996) and/or trapping of mineral C in the soil solution as indicated by an increased amount of dissolved inorganic carbon (DIC) in the soil over time (data not shown). This effect was less important for SURF, where CO_2 emitted from the mulch did not interact with the soil, and an increased CO_2 flux was observed after each rain event. For SURF and INC, the C mineralization rate decreased over time, which corresponded to the depletion of the substrate during its decomposition.

Measurements of the CO_2 flux were not used to estimate cumulative mineralization of residue-C, because integrating non-continuous measurements induced inaccuracies and the results did not take into account the consequences of a potential priming effect. Therefore, the cumulative mineralization of residue-C was calculated from the difference in residual ^{13}C in the soil: after 9 weeks of incubation, 18% of the added C was mineralized for SURF and 55% for INC. Cumulative residue-C mineralization was overestimated by + 8% for SURF and underestimated by - 8% for INC when calculated from CO_2-flux measurements.

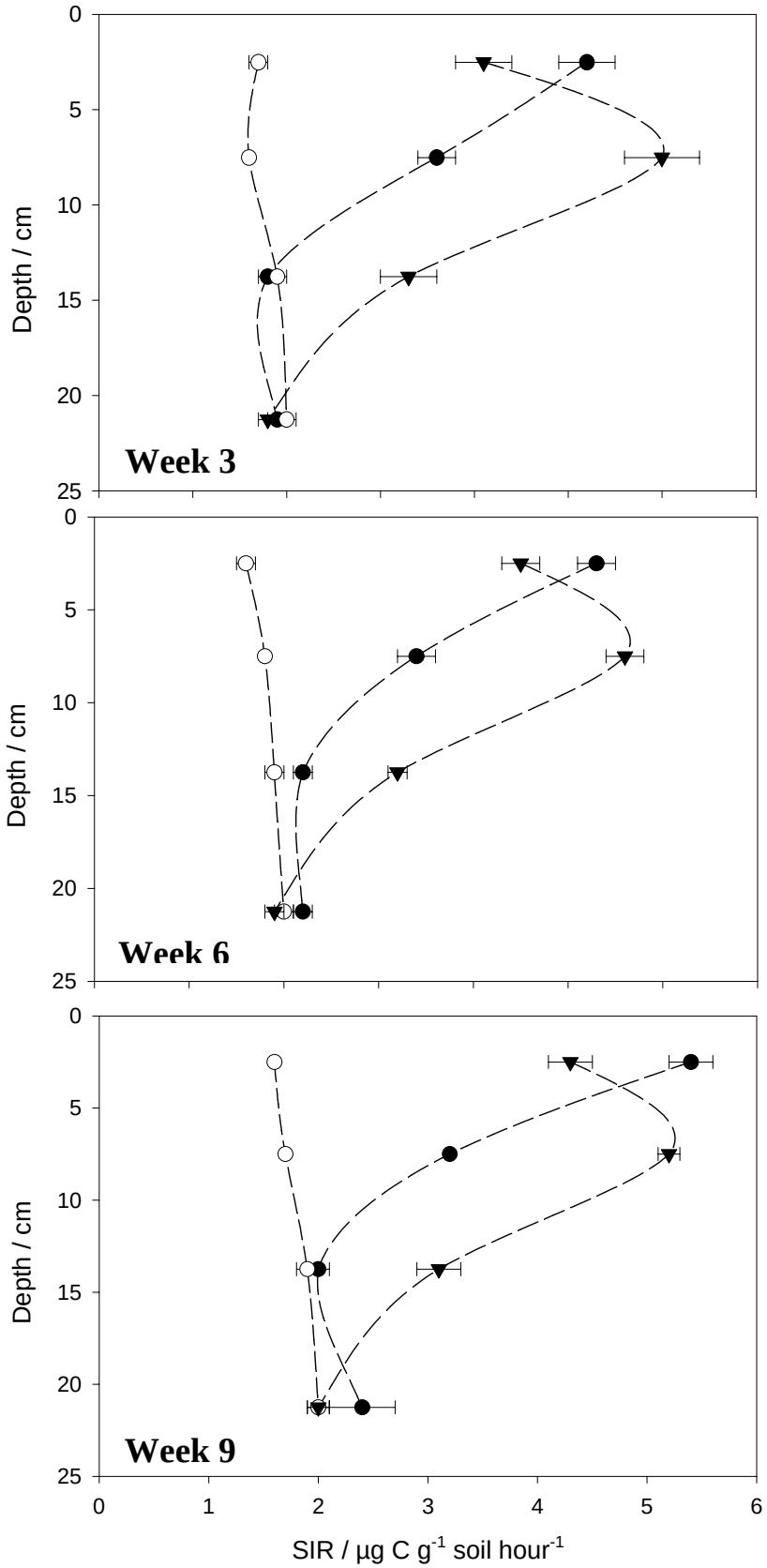

Figure 3.5 Distribution of the soil microbial activity in different soil layers, measured by substrate induced respiration, after 3, 6 and 9 weeks of incubation (before re-wetting) of the control (CTRL ○), surface (SURF ●) and incorporation treatment (INC ▼) (mean values, bars represent the standard error, n = 3)

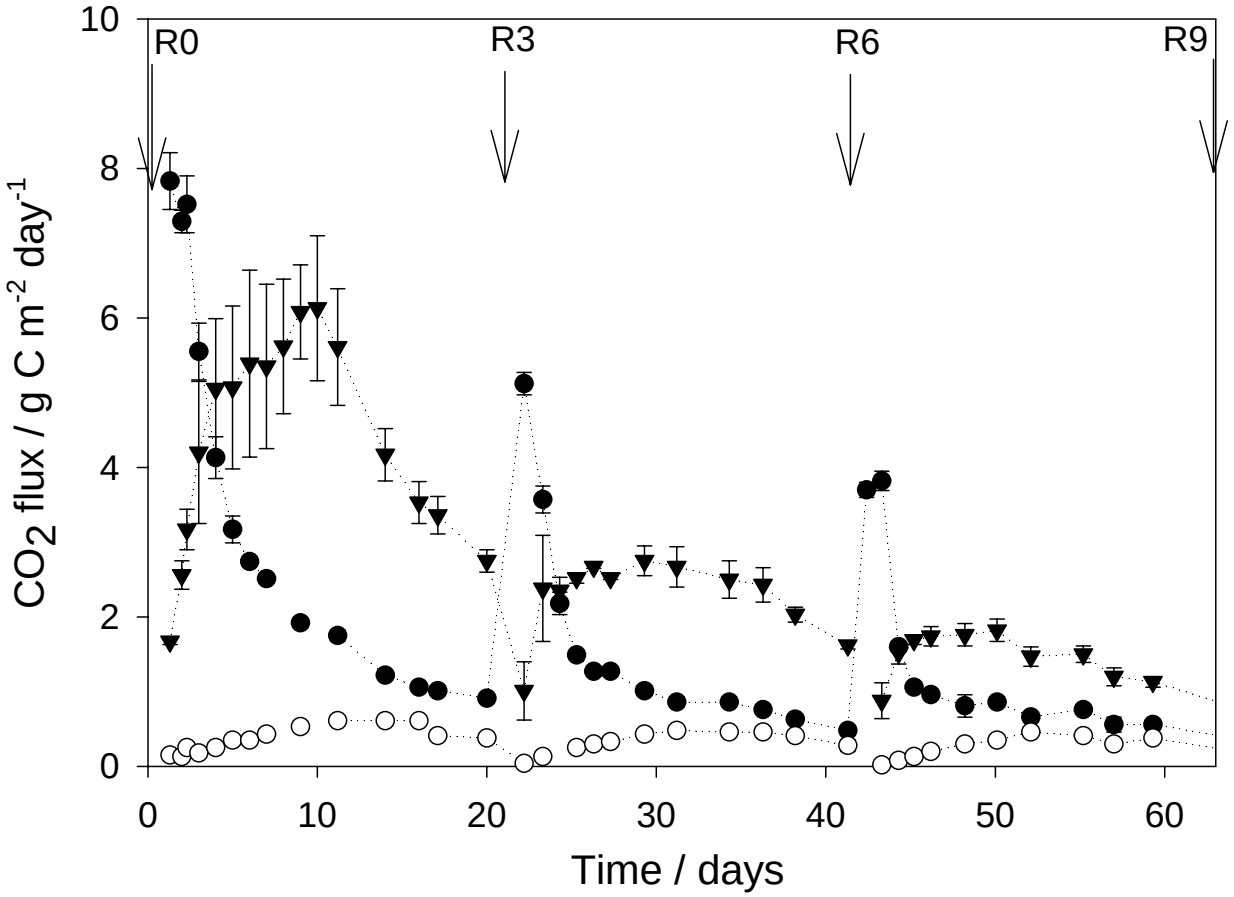

Figure 3.6 Change in the CO_2 flux for soil without residues (CTRL ○), residues left at the soil surface (SURF ●) or incorporated in the 0-10 cm soil layer (INC ▼). Arrows indicate the application of artificial rain (R0-R9) (mean values, bars represent the standard error, n = 2 for CTRL and SURF, n = 3 for INC)

3.3.6 Distribution of residue-C and -N in soil

At the end of each evaporation period, the residual rape-C and -N in the coarse and fine soil fraction was calculated from total C and N measurements with their isotopic excess (Table 3.2). The INC treatment resulted in more transfer of residue-C and -N into the fine soil fraction compared to SURF. This transfer mainly took place in the first 3 weeks of the incubation. In the bulk soil, 21.3% of the residue-C and 63.9% of the residue-N was found. The amount of ^{13}C which was not recovered in soil and residue was considered as having mineralized. Losses of ^{15}N could be due to denitrification.

While initially no residue-C was present in the soil fraction with SURF, 6.6% of the residue-C was leached down to 10 cm soil depth at week 3. This corresponded to 37.1% of the initial

water-extractable residue-C. For INC, 1.9% of the residue-C was measured in the soil layer below 10 cm soil depth. For both treatments, residue-N was more mobile than residue-C. At week 3, 39.1% of the residue-N was leached down to 17.5 cm soil depth, corresponding to 82.8% of the water-extractable residue-N. Amounts of residue-N observed in the 10-25 cm soil layer increased over time for SURF and INC.

During the incubation, an isotopic dilution of the excess of ^{15}N of the residues was observed, due to 'contamination' with non-labelled soil-N by the decomposers growing on the residue particles. Dilution with nitrogen from soil particles was calculated to be negligible. For SURF, 4% of the nitrogen measured in the residues after 9 weeks of incubation originated from the soil. For INC, the amount of soil-N found in the residues was about 25%. At the first sampling time, the isotopic dilution of residues in the 0-5 cm soil layer of INC was half of the dilution in the 5-10 cm layer, which confirms a slower colonisation and decomposition of the residues incorporated in the upper soil layer, as mentioned above.

3.3.7 Nitrogen mineralization

The distribution of NH_4^+-N and NO_3^--N in the soil solution was determined after each rainfall at 2, 10 and 18 cm soil depth (Figure 3.7). The amount of NH_4^+-N was negligible (0.1 mg litre^{-1}). After the first rainfall (R0) there was a steep gradient of NO_3^--N through the soil profile of CTRL from 2 mg litre^{-1} at 2 cm soil depth to 69 mg litre^{-1} at 18 cm soil depth. The presence of residues increased the amount of N, particularly at 10 cm soil depth, which was much more important for SURF than for INC. Over time, the mineral N concentration at 18 cm soil depth gradually increased for all treatments to an average of 107 mg NO_3^--N litre^{-1} at R9.

The distribution of NO_3^--N in the different soil layers at the end of each evaporation period (before re-wetting) is shown in Figure 3.8. The amounts of NH_4^+-N were always < 1 mg kg^{-1}. A strong depletion in the nitrate content was observed in the 0-5 cm soil layer for the INC treatment compared to CTRL and SURF, which persisted over the 9-week incubation. During this period, SURF showed the largest amounts of nitrate in all soil layers. The net mean N mineralization rate was 0.10, 0.17 and 0.06 mg NO_3^--N kg^{-1} day^{-1} for CTRL, SURF and INC respectively, which expressed on an area basis, is equivalent to 20 kg NO_3^--N ha^{-1} for CTRL, 35 kg NO_3^--N ha^{-1} for SURF and 11 kg NO_3^--N ha^{-1} for INC.

Table 3.2 Distribution of ^{13}C and ^{15}N in the fine (<2 mm) and coarse (>2 mm) fraction with surface applied residues (SURF) or residues incorporated in the 0-10 cm soil layer (INC), expressed as % of added C and N (mean values, with standard errors in parentheses, n = 3).

		SURF					
		^{13}C			^{15}N		
		Week 3 / %	Week 6 / %	Week 9 / %	Week 3 / %	Week 6 / %	Week 9 / %
surface	>2 mm	84.3 (1.6)	79.2 (1.0)	73.8 (0.7)	55.9 (3.9)	51.2 (3.4)	43.1 (2.3)
0-5 cm	<2 mm	5.0 (0.1)	6.2 (0.7)	6.3 (0.2)	26.0 (0.9)	29.7 (2.4)	31.2 (0.8)
5-10 cm	<2 mm	1.6 (0.1)	1.6 (0.2)	1.5 (0.0)	10.5 (0.2)	9.7 (1.0)	10.1 (0.2)
10-17.5 cm	<2 mm	0.0 (0.0)	0.1 (0.0)	0.0 (0.0)	2.6 (0.4)	3.3 (0.4)	4.2 (0.5)
17.5-25 cm	<2 mm	0.0 (0.0)	0.0 (0.0)	0.0 (0.0)	0.0 (0.0)	0.6 (0.1)	3.2 (0.2)
0-25 cm	total	91.0 (2.7)	87.1 (3.0)	81.6 (1.5)	95.1 (6.7)	94.6 (2.3)	91.8 (2.8)

		INC					
		^{13}C			^{15}N		
		Week 3 / %	Week 6 / %	Week 9 / %	Week 3 / %	Week 6 / %	Week 9 / %
0-5 cm	>2 mm	29.9 (1.4)	15.0 (0.9)	11.2 (0.3)	9.0 (1.0)	6.9 (0.3)	6.3 (0.1)
	<2 mm	10.7 (0.2)	13.1 (0.5)	11.9 (1.3)	24.8 (0.8)	29.4 (0.5)	30.8 (2.7)
5-10 cm	>2 mm	15.8 (2.5)	9.9 (0.5)	9.5 (0.4)	8.4 (1.0)	6.8 (0.4)	7.1 (0.1)
	<2 mm	10.7 (0.3)	12.4 (0.6)	10.5 (0.5)	32.2 (0.4)	35.7 (1.1)	32.5 (0.8)
10-17.5 cm	<2 mm	1.9 (0.3)	2.3 (0.2)	2.3 (0.4)	9.9 (1.7)	10.9 (1.0)	11.5 (1.3)
17.5-25 cm	<2 mm	0.0 (0.0)	0.1 (0.0)	0.0 (0.0)	0.3 (0.1)	1.8 (0.3)	3.1 (0.3)
0-25 cm	total	69.1 (2.7)	52.8 (2.2)	45.3 (1.3)	84.6 (3.2)	91.5 (5.3)	91.2 (3.7)

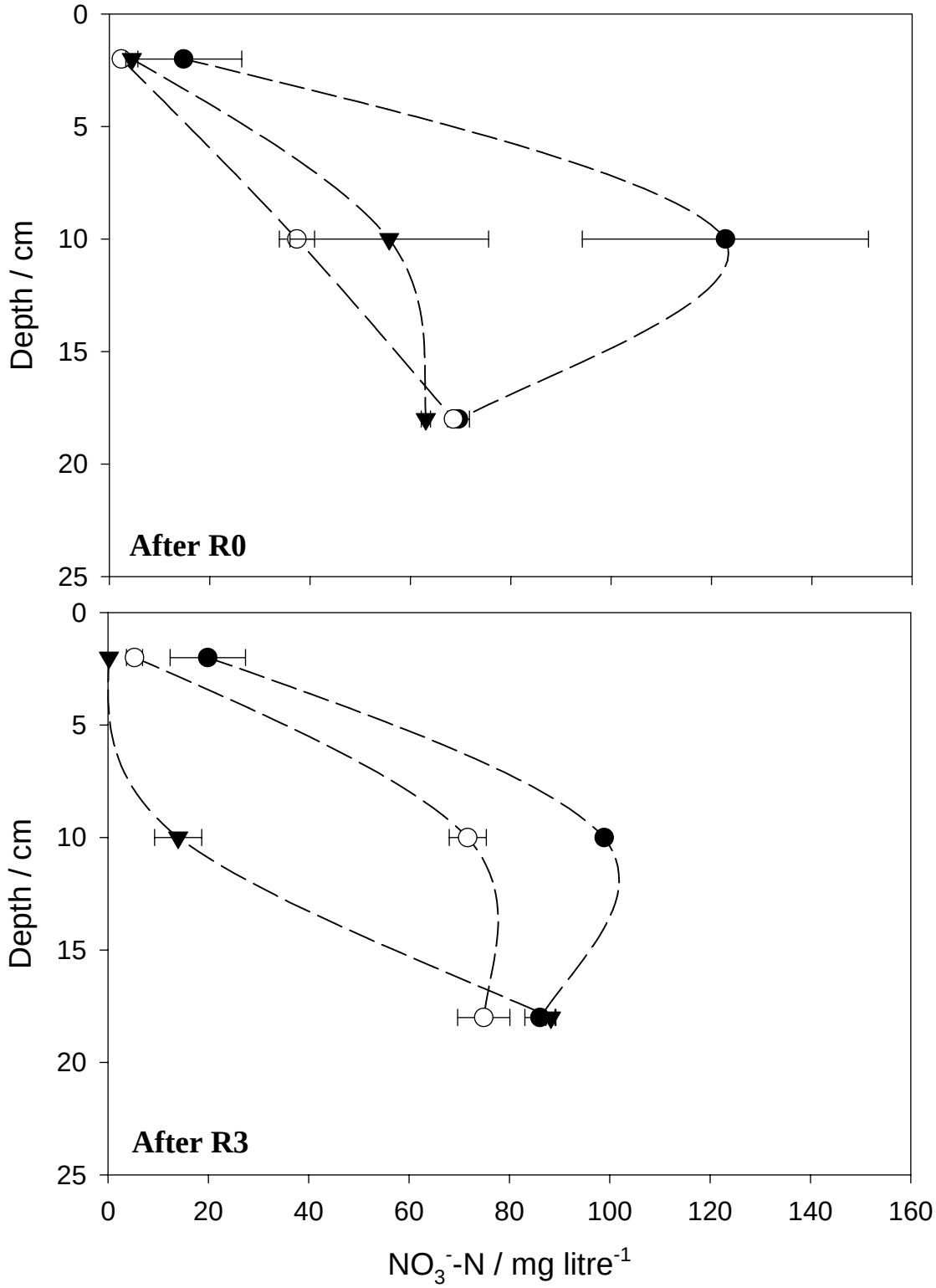

Figure 3.7 (a) The concentration of NO_3^--N in the soil solution at different soil depths after rainfall R0 and R3, for soil without residues (CTRL ○), residues left at the soil surface (SURF ●) or incorporated in the 0-10 cm soil layer (INC ▼) (mean values, bars represent the standard error, n = 2)

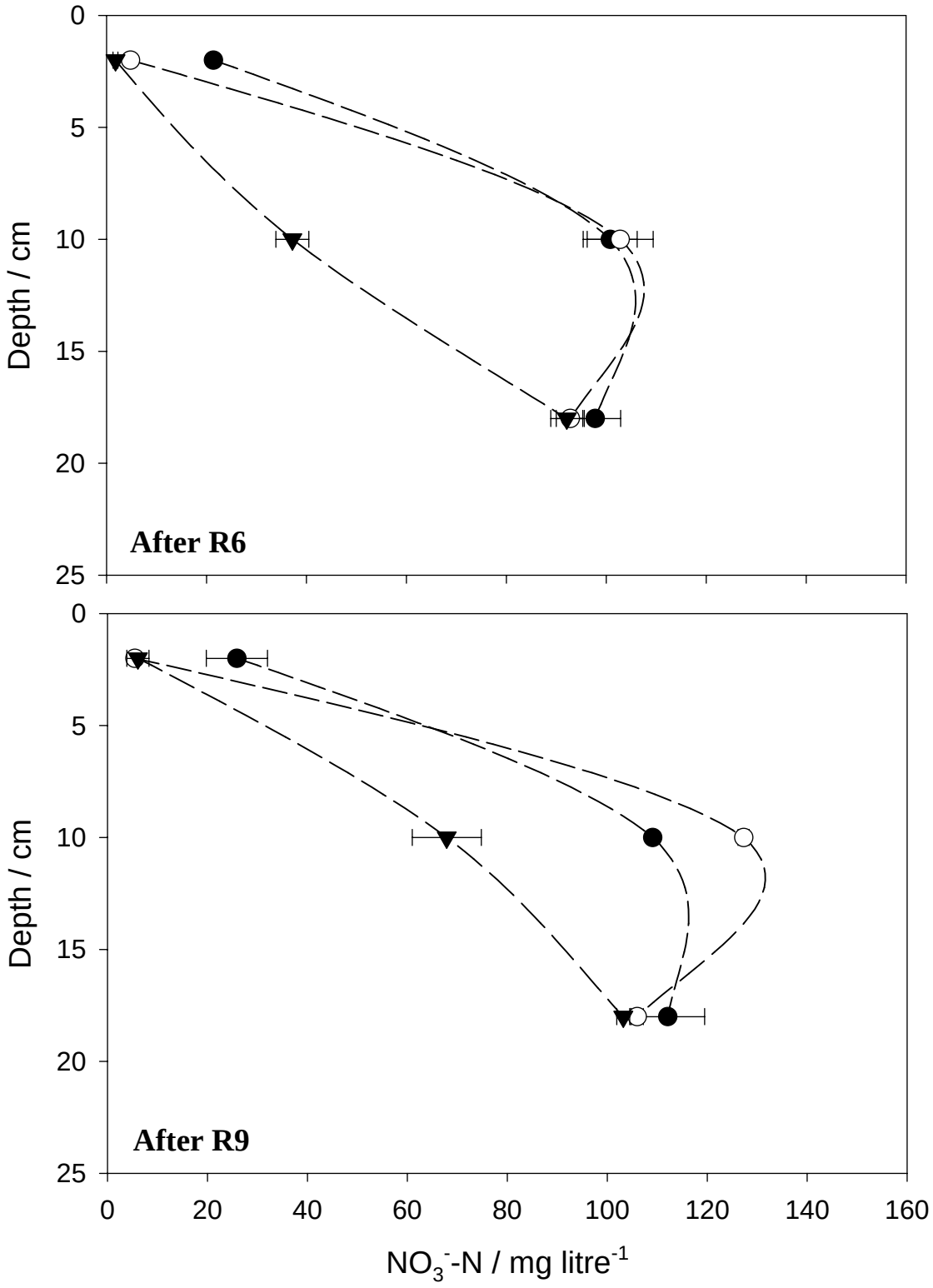

Figure 3.7 (b) The concentration of NO_3^--N in the soil solution at different soil depths after rainfall R6 and R9, for soil without residues (CTRL ○), residues left at the soil surface (SURF ●) or incorporated in the 0-10 cm soil layer (INC ▼) (mean values, bars represent the standard error, n = 2)

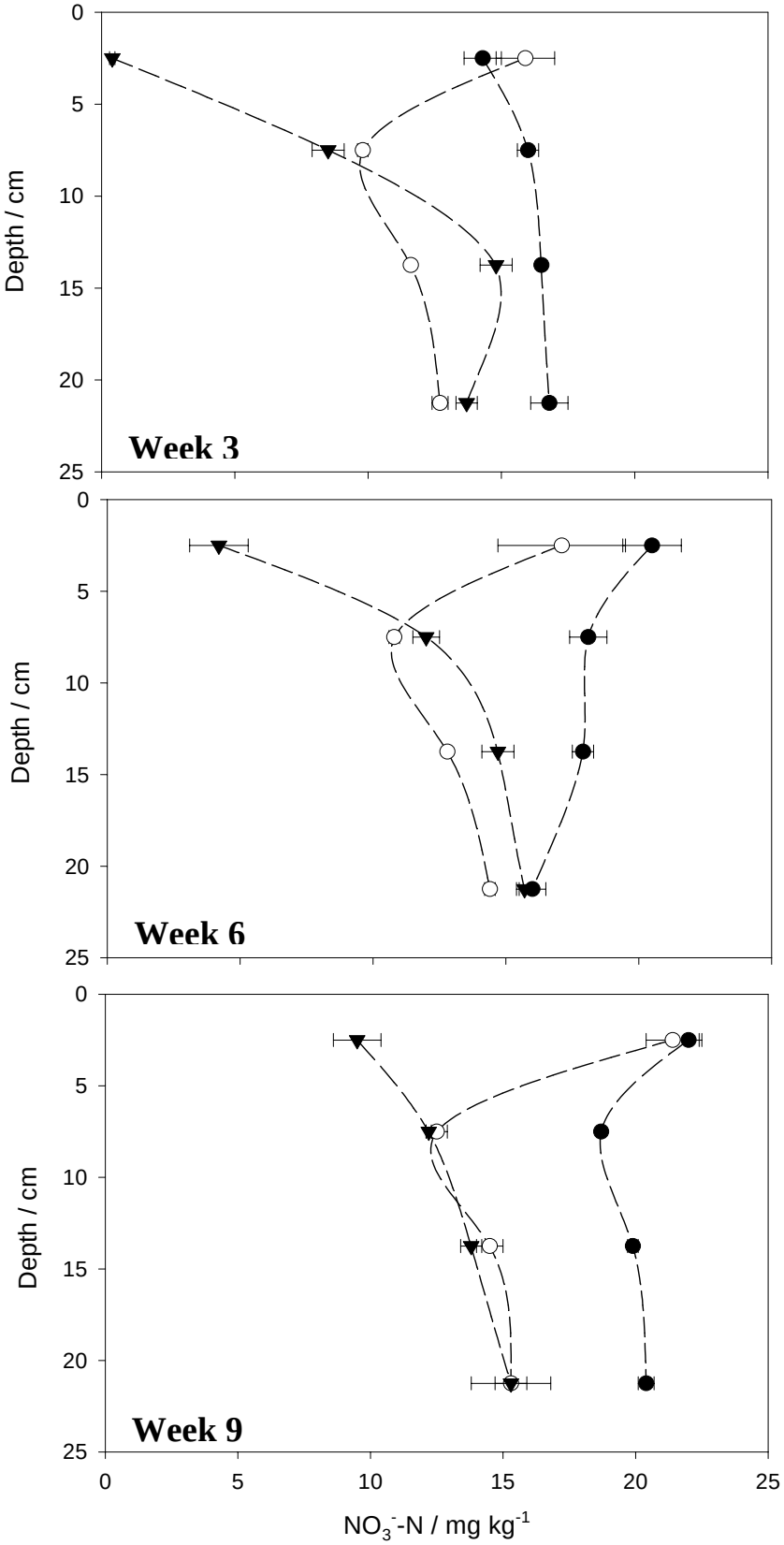

Figure 3.8 Distribution of NO_3^--N in different soil layers after 3, 6 and 9 weeks of incubation (before re-wetting), for soil without residues (CTRL ○), residues left at the soil surface (SURF ●) or incorporated in the 0-10 cm soil layer (INC ▼) (mean values, bars represent the standard error, n = 3)

3.4 Discussion

The experimental set-up allowed the examination of the fate of C and N derived from decomposing crop residues at different locations in the soil, excluding other modifications of soil properties induced by tillage. The different location of the residues had a significant effect on the water dynamics, entailing a strong interaction between location and water regime. The modified soil water dynamics was an important factor determining residue decomposition.

3.4.1 Soil water dynamics

The soil volumetric water content is a main factor influencing the turnover of soil organic carbon (Thomsen *et al.,* 1999). Crop residues left at the soil surface reduced the initial soil water evaporation rate, which resulted on the short term in a higher average moisture content in the soil. Our experiment also showed a significant difference in the water distribution in the soil profile when comparing the mulched soil with a bare one. These differences had an important effect on the microbial activity and decomposition dynamics.

Less is known about the water content of residue mulch during successive periods of wetting and drying. After each successive rain event, a slight increase in the water content of the mulch was observed, while the residue mass had decreased. The increased water storage capacity of the mulch suggested a change in the physical properties of the mulch. The different components of the oilseed rape mixture (leaves, stalks, branches and pods) have been shown to decompose at different rates (Trinsoutrot *et al.*, 2000b), so it can be assumed that mulch properties have changed at each rainfall application. In addition, microbial attack might have modified the porosity of the residue particles. These changes increased the rate of water loss of the mulch during the following evaporation period.

For each evaporation period, maximum CO_2 fluxes were measured at maximum mulch water content and the CO_2 flux decreased with decreasing mulch water content as illustrated in Figure 3.9. Therefore, it is concluded that the water content of the residues is an important factor controlling mulch decomposition.

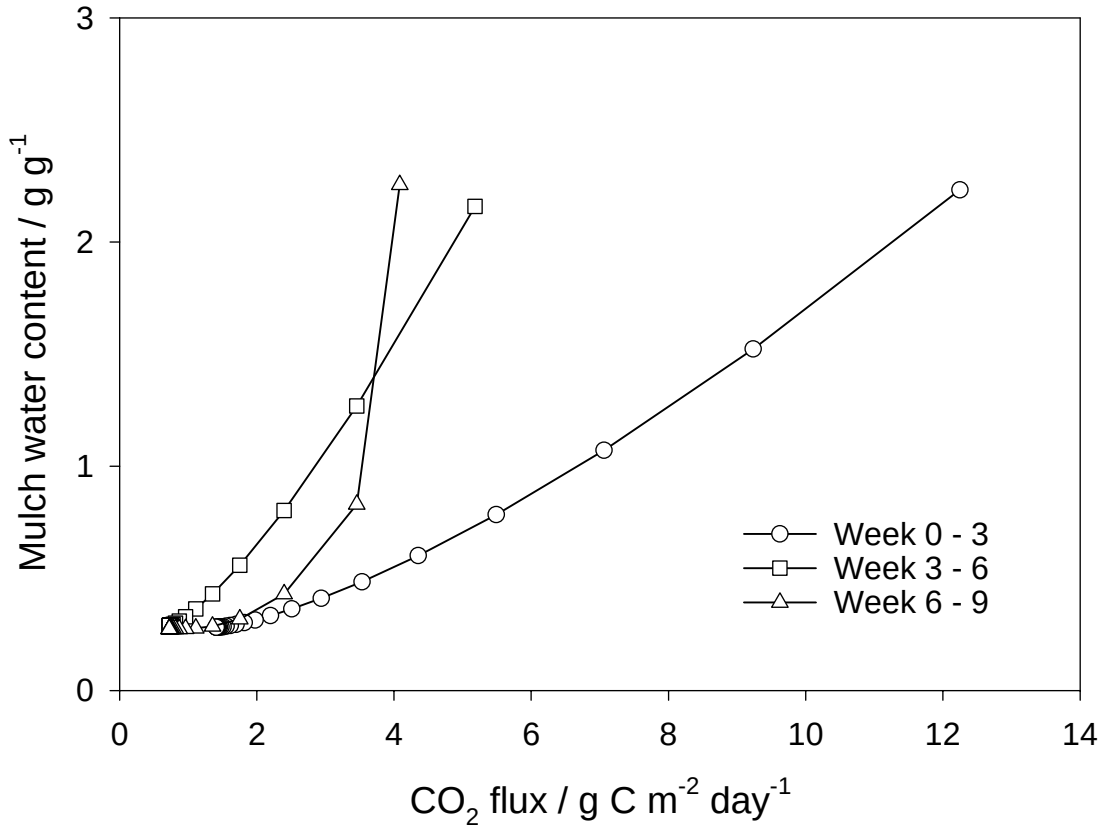

Figure 3.9 Change in CO_2 flux with changing mulch water content during the 3 evaporation periods (Week 0-3, Week 3-6 and Week 6-9).

3.4.2 Soluble carbon

Land use and management practices may significantly influence the amount and the composition of dissolved organic matter, but the processes involved remain largely unknown and observations are often contradictory (Chantigny, 2003). To investigate dynamics of soluble carbon in soil, the mobile dissolved organic carbon (DOC_m) was sampled from the soil solution after each rainfall and the potentially available dissolved organic carbon (DOC_{pa}) was extracted from the soil after 3, 6 and 9 weeks of evaporation. After the first rainfall, a larger amount of DOC_m was measured in the soil with incorporated residues compared to soil with mulch. However, after 3 weeks of evaporation, the total amount of DOC_{pa} in the soil profile with incorporated residues was only 61% of the amount measured in the soil under mulch (0-25 cm). It is suggested that more soluble carbon was liberated from the incorporated residues, but it was decomposed at a faster rate than with residues left at the soil surface. The faster decomposition rate of soluble carbon in soil with incorporated residues is probably due to the larger total microbial activity than in soil under mulch, as measured by SIR. The

combined effect of residue location and water transport regulated the distribution of nutrients for the microbial biomass in the soil profile: the same pattern in distribution of soluble carbon (DOC_m) and SIR was observed.

3.4.3 Residue decomposition

The predominant effect of the initial crop residue location on C and N dynamics was the slower decomposition rate when residues were left at the soil surface. After 9 weeks of incubation, the amount of ^{13}C mineralized from surface applied residues was only 66% of the amount ^{13}C mineralized from incorporated residues. The residue water content was likely the main factor responsible for this difference, as mentioned above. Another factor which influenced the decomposition rate of crop residues was the contact between soil and residue, defining the residue surface area susceptible to microbial attack and the availability of soil nitrogen for the decomposers. When incorporated, all residue particles were surrounded by soil aggregates, while we estimate that only 10% of the 1-cm mulch was in direct contact with the soil. Depending on its biochemical quality, Henriksen & Breland (2002) also observed a faster residue decomposition with increased contact between soil and residue.

Rainfall on surface applied residues resulted in a spatial separation of residue-C and -N, and in a change of the mulch properties. Maximum DOC_m after the first rainfall was measured near the soil surface, while nitrate in the soil solution, originating from the mulch, accumulated at 10 cm soil depth. Transport of residue-C into the soil was less important than the transport of residue-N, resulting in an increased C:N ratio of the mulch. In addition, mineral nitrogen from the upper soil layer was leached down with the rain. In this case, fungal decomposition of residues may be favoured due to the capacity to translocate soil N to the surface litter C by the hyphal network (Frey *et al.*, 2000). The higher C assimilation efficiency and slower turnover rates of the fungal biomass compared to the bacterial biomass (Holland & Coleman, 1987) may have contributed to the slower mineralization rate of the surface placed residue-C.

Homogeneous incorporation of residues in the upper 10 cm of the soil profile did not lead to an equal decomposition in this soil layer. Leaching of nutrients from the 0-5 cm soil layer and the more favourable soil water content for microbial activity in the 5-10 cm soil layer resulted in a faster decomposition rate of the residues in the 5-10 cm soil layer. A greater SIR measured in the 5-10 cm soil layer confirmed these findings.

3.4.4 Distribution of residue-C and –N in soil

The location of crop residues determined the initial distribution of C and N in the soil. With mulch, all of the residue-C and –N was concentrated at the soil surface; while incorporated, it was distributed over the upper 10 cm. According to differences in the location of residue-C, differences are to be expected in the rate of plant material biodegradation, soil respiration or nitrogen immobilization (Balesdent *et al.*, 2000). Gaillard *et al.* (2003) demonstrated in a microcosm incubation experiment the diffusion of residue-C into the 4-5 mm soil surrounding the residues (detritusphere), which could act as hot-spots for microbial activity. Without water infiltration, they only found a negligible amount of residue-C that migrated out of the detritusphere by diffusion. In our experiment however, rainfall resulted in a redistribution of the added C and N over the soil profile, creating large zones of increased microbial activity.
The residue location affected the depth of C and N transport with rain. Given the importance of a rain event on the distribution of residue-C and –N in soil, particularly for the surface treatment, the applied intensity, duration and/or frequency of the rain should have an impact on the observed C and N transport. To our knowledge, this effect has not been reported in the literature. Other experiments under a rain simulator, or computer modelling with different rain scenarios could help to study the influence of different water regimes on the fate of C and N in soil.

3.4.5 Nitrogen mineralization-immobilization

Nitrate measurements in the soil solution sampled after each rainfall indicated that mineral nitrogen was leached out of the upper soil layer. Mineral nitrogen concentrations at 2 cm soil depth were larger with residue mulch than with residue incorporation, because the soil under mulch was replenished with soluble nitrogen leached from the mulch itself. The amount of nitrate in soil extracts after 3, 6 and 9 weeks showed the effect of crop residue location on the nitrogen mineralization-immobilization turnover in soil. The larger soil water content under mulch than with a bare soil surface favoured mineralization of soil N. The physical separation of soil N and surface applied residue-C decreased N immobilization in the 0-5 cm soil layer compared to the incorporation treatment. This resulted in a larger net nitrogen accumulation in the upper soil layer under mulch than with residue incorporation. In the latter, the stimulated microbial activity in the upper 10 cm due to the incorporation of fresh organic matter enhanced nitrogen immobilization compared to the control soil. A much greater immobilization of N for ground and incorporated residues than when cut and surface applied,

was also observed by Corbeels *et al.* (2003). They hypothesised that grinding and mixing the residues affected N dynamics by the combined effect of better accessibility to microbial attack and by increased availability of soil N for immobilization. This is in agreement with our study, which presents the soil water dynamics as an additional factor to explain the nitrogen mineralization-immobilization turnover as a function of crop residue location.

3.5 Conclusion

Oilseed rape residues were incubated in soil columns, incorporated in the 0-10 cm soil layer or left at the soil surface. Under controlled conditions, crop residue location determined the water dynamics in soil and residue. Soil evaporation was reduced with surface placed residues, resulting in a larger soil water content than with residue incorporation. At the same time, fast desiccation of the residue mulch was observed.

Decomposition of crop residues was determined by the interactions between soil and residue water content, and the availability of C and N to the decomposing biomass. Mulch-derived C and N were concentrated near the soil surface, while residue-C and -N were distributed more deeply in the soil profile with residue incorporation. Resulting soluble carbon concentrations in the soil profile were closely related to the distribution of microbial activity. In addition, the decomposition rate of residue mulch decreased with decreasing mulch water content.

Those interactions between water dynamics and nutrient availability resulted in significant differences in C and N mineralization when comparing residue incorporation with surface application. In the short-term (9 weeks), CO_2 emission of the soil with mulch was lower and more residue-C was left in the soil than with residue incorporation. Surface application of residues may also be associated with increased risks of nitrate leaching as mineralization of soil N was stimulated due to an increased soil water content under mulch.

On the short term, significantly more particulate organic matter was recovered with residue mulch than with residue incorporation. However, differences in residue-C recovered in the fine soil fraction (< 2 mm) were less important comparing residue locations. Regarding C storage in the soil on the longer term, it is essential to investigate the fate of particulate organic matter between aggregates e.g. after one cropping season, and how the residue-C that entered the fine soil fraction is distributed over soil micro- and macroaggregates.

Modelling of water and solute transport combined with the biotransformations of C and N, is necessary to better quantify the contribution of the various simultaneous processes (e.g. gross

N mineralization, gross N immobilization, nitrate transport), and will help to interpret the interactions between soil physical and biological properties. Scenario analysis can be used to predict the environmental impact on the longer term of a change in crop residue location associated with the conversion of tillage systems.

Chapter 4

Impact of crop residue location on carbon and nitrogen distribution in soil and in water-stable aggregates

4.1 Introduction

Tillage or the absence of it has a dominant influence on the distribution of carbon through the soil profile (Franzluebbers & Arshad, 1996; Balesdent *et al.*, 2000). First of all, tillage determines where residues are located and consequently decomposed. Secondly, tillage entails mechanical disruption of soil aggregates, with well-documented effects on C dynamics and aggregate formation.

Stable soil macroaggregates are enriched in, and probably stabilized by, recently deposited organic matter (Puget *et al.*, 1995; Angers & Giroux, 1996). In turn, macroaggregates are assumed to protect fresh organic matter from decomposition, in particular in no-tilled soils (Beare *et al*., 1994), where the turnover time of macroaggregates is longer than in conventionally tilled soils (Six *et al*., 1998). A slower turnover allows the formation of stable microaggregates within macroaggregates, in which carbon can be stabilized and sequestered on the long term (Six *et al*., 2000). Most often, however, those effects of tillage on aggregate and organic matter dynamics have been attributed mainly to the absence of mechanical disruption of soil aggregates in a no-till system.

Less is known about the specific contribution of crop residue location to aggregate stability and to the distribution of residue-C and –N in and between soil aggregates, when comparing conventional and no-till systems. Residue location obviously influences important physical and biological soil properties. In Chapter 3 it has been demonstrated that soil water dynamics, the distribution of residue-C and -N in soil and the activity of soil microbial biomass all depend on the initial residue location, which may be important factors in controlling aggregate dynamics. First of all, wetting of a soil can cause disruption of aggregates through slaking (Adu & Oades, 1978), while subsequent drying and rewetting of a soil possibly increases the strength and stability of the remaining aggregates (Materechera *et al*., 1994;

Adapted from: F. Coppens, R. Merckx, S. Recous (submitted) Impact of crop residue location on carbon and nitrogen distribution in soil and in water-stable aggregates. *European Journal of Soil Science*

Denef *et al*., 2001a). Because the intensity of wetting-drying cycles and the development of water gradients through the soil profile were more important with incorporated than with surface applied residues, it is expected that aggregate stability is most influenced by water dynamics with residue incorporation. Secondly, aggregate stability has been related to soil organic carbon content (Carter, 1992; Hermawan & Bomke, 1996), which can act as a binding agent for soil aggregates (Tisdall & Oades, 1982). Given the concentration of organic carbon near the soil surface with residue mulch, it is hypothesized that more stable macroaggregates are formed in the upper soil layer than with residue incorporation. Finally, microbial activity, especially of fungi, plays an important role in the formation and stabilization of macroaggregates (Kinsbursky *et al*., 1989; Bossuyt *et al*., 2001). Fungal biomass has been reported to be more abundant with residue mulch than with residue incorporation (e.g. Holland & Coleman, 1987), which also contributes to an increased aggregate stability near the soil surface under mulch. The interaction between all those factors influences the soil aggregate dynamics and the fate of C and N in the different aggregate fractions.

As part of a larger study that aimed at investigating the specific role of crop residue location on soil water dynamics and the biotransformation of residue-C and –N (Chapter 3), this work examines the short- and medium-term incorporation of residue-C and -N in the different soil aggregate size fractions, as we hypothesize this is key to understand the long term effect on C storage in soils. This level of understanding is required for modelling and predicting the fate of C in soils. To do so, we compared the fate of recently added organic matter in soil with incorporated and surface applied oilseed rape residues, labelled with ^{13}C and ^{15}N. The main questions addressed were: (i) Does the presence of a large residue mass at the soil surface (i.e. the residue mulch) and the slower decomposition rate of this mulch modify the dynamics and concentration of larger macroaggregates in the adjacent soil layer, leading to a larger C stabilization on the long term? (ii) How does the way the new C enters the soil with surface application (leaching of soluble C) vs. incorporation (diffusion of soluble C and residue colonization) modify the distribution of residue-C in the various soil aggregate fractions?

4.2 Materials and methods

4.2.1 Soil and crop residues

Soil was sampled from the experimental site of INRA, Domaine de Brunehaut, Estrées-Mons (Northern France). The soil was a silt loam, Orthic Luvisol (FAO/ISRIC/ISSS, 1998) and has not been cropped since 1994. The 0-25 cm soil layer was sampled, sieved (< 2 mm) at field moist content (0.17 g g^{-1}) and stored in plastic bags at 4°C prior to use. The soil was preincubated for 2 weeks at 20°C before the start of the experiment. The fresh organic matter added to the soil was mature oilseed rape (*Brassica napus* L.), doubly labelled with ^{13}C and ^{15}N. A detailed description of soil and residue characteristics is given in Chapter 3.

4.2.2 Experimental conditions

Plastic cylinders (PVC, 15.4 cm inner diameter, 30 cm length) with perforated bases were filled with 25 cm of soil, compacted at 1.3 g cm^{-3}. Oilseed rape residues were applied at the soil surface (referred to as SURF) or homogeneously mixed in the 0-10 cm soil layer before compaction (referred to as INC) at a rate of 13.8 g dry matter per column, equivalent to a return of 7.4 t ha^{-1}. Control columns without addition of fresh organic matter (referred to as CTRL) were also prepared. At the start of a 33-week incubation period, rain with an intensity of 12 mm $hour^{-1}$ was applied with a rainfall simulator on all the soil columns. The volumetric soil water content was raised from 0.22 to 0.34 cm^3 cm^{-3} after 2.5 hours of rain. Subsequently, the soil columns were transferred in a climate chamber and left uncovered at 20°C and 70% relative air humidity to allow evaporation. Details of soil column preparation and the rainfall simulator are given in Chapter 3.

At week 3, 6 and 9, soil columns were again placed under the rainfall simulator until the water lost by evaporation, as measured by weight loss, was replenished. At week 25, soil water content was adjusted to 0.34 cm^3 cm^{-3} and kept constant until week 33 to stimulate residue decomposition. At week 3, 6 and 9, before re-wetting, three replicate columns of each treatment were used to study short-term organic matter dynamics and aggregate stability; two replicates of CTRL, SURF and INC were analysed after 33 weeks to obtain information on the longer term.

4.2.3 Aggregate separation

After 3, 6, 9 and 33 weeks of incubation, 150 g of soil was sampled from the 0-5 cm and 5-10 cm soil layer of all treatments. The soil was crumbled over an 8 mm sieve along the natural planes of fracture and air-dried at 20°C. A 30 g subsample was used to separate four aggregate fractions by a wet-sieving method adopted from Elliott (1986). First, the soil was submerged for 5 minutes in deionised water to allow slaking. Then, the soil was successively passed through a series of three sieves to separate four fractions: large macroaggregates (>2000 μm), small macroaggregates (2000-250 μm), microaggregates (250-53 μm) and the silt and clay fraction (<53 μm). To obtain the large and small macroaggregates, the sieve was gently moved up and down in the water for 50 cycles in 2 minutes. To separate the microaggregates from the silt and clay fraction, the soil fraction on the 53 μm sieve was washed. We previously checked that the washing water was clear by using 1 litre of water. The aggregate fractions were decanted to remove the particulate organic matter (POM) present between aggregates, which floated on the water, and POM was analysed separately. All aggregate fractions were oven-dried at 60°C. Three replicates of the soil were sieved before incubation, to measure the initial aggregate size distribution. The mean weight diameter, an approximation of the median size of the aggregates, was calculated as:

$$MWD = \frac{\left(\frac{4000+2000}{2}\right)A\% + \left(\frac{2000+250}{2}\right)B\% + \left(\frac{250+53}{2}\right)C\% + \left(\frac{53+0}{2}\right)D\%}{100}$$

were MWD is the mean weight diameter in μm, A% the fraction >2000 μm in wt.%, B% the fraction 250-2000 μm in wt.%, C% the fraction 250-53 μm in wt.% and D% the fraction <53 μm in wt.%.

4.2.4 Soil analysis

The remaining soil of four separate soil layers (0-5 cm; 5-10 cm; 10-17.5 cm; 17.5-25 cm) was passed through a 2-mm sieve to separate the particulate organic matter (> 2 mm) from the soil fraction. Soil and residues were dried, crushed and analysed for total C and N with their atom % excess (% a.e.), using an elemental analyser (NA 1500, Carlo Erba) coupled to a mass spectrometer (Fisons Isochrom, Manchester, UK). The gravimetric soil water content in each soil layer was determined for all treatments. Total C and N, with % a.e., was also measured on

the crushed aggregate fractions (NA 1500, Carlo Erba; Fisons Isochrom, Manchester, UK). Microbial activity (measured by Substrate Induced Respiration, SIR) and soluble carbon in soil extracts (i.e. potentially available dissolved organic carbon, DOC_{pa}) were determined in the 0-5 cm and 5-10 cm soil layer as described in Chapter 3.

4.3 Results

4.3.1 Characteristics of the soil samples

The soil water content, substrate induced respiration rate and soluble carbon (DOC_{pa}) were determined on soil subsamples at the end of each evaporation period, before aggregate separation (Table 4.1).

Table 4.1 Distribution of (a) the soil water content, (b) microbial activity measured by substrate induced respiration and (c) dissolved organic carbon of CTRL, SURF and INC in the 0-5 cm and 5-10 cm soil layer at sampling. Different lowercase letters indicate significant differences over time ($P < 0.05$), for given soil layer and treatment. Different uppercase letters indicate significant differences between treatments and soil layers ($P < 0.05$), at given sampling point.

(a)		Week 3	Week 6	Week 9	Week 33
		Soil water content / g g^{-1}			
CTRL	0-5 cm	0.15 (a,A)	0.16 (b,B)	0.18 (c,AB)	0.24 (d,A)
	5-10 cm	0.16 (a,B)	0.18 (b,C)	0.19 (c,B)	0.23 (d,A)
SURF	0-5 cm	0.23 (a,C)	0.23 (a,D)	0.22 (b,C)	0.24 (c,A)
	5-10 cm	0.23 (abc,C)	0.23 (a,D)	0.22 (b,C)	0.23 (c,A)
INC	0-5 cm	0.14 (a,A)	0.15 (b,A)	0.16 (b,A)	0.24 (c,A)
	5-10 cm	0.16 (a,B)	0.18 (b,C)	0.17 (ab,A)	0.23 (c,A)
(b)					
		Substrate induced respiration / µg C g^{-1} soil $hour^{-1}$			
CTRL	0-5 cm	1.7 (a,A)	1.6 (a,A)	1.6 (a,A)	n.a.
	5-10 cm	1.6 (a,A)	1.8 (b,A)	1.7 (ab,A)	n.a.
SURF	0-5 cm	5.2 (a,CD)	5.3 (a,D)	5.4 (a,D)	n.a.
	5-10 cm	3.6 (a,B)	3.4 (a,B)	3.2 (a,B)	n.a.
INC	0-5 cm	4.1 (a,BC)	4.5 (a,C)	4.3 (a,C)	n.a.
	5-10 cm	6.0 (a,D)	5.6 (a,D)	5.2 (a,D)	n.a.
(c)					
		Soluble carbon / mg DOC_{pa} kg^{-1}			
CTRL	0-5 cm	16.6 (a,B)	14.9 (a,A)	15.3 (a,A)	31.4 (b,A)
	5-10 cm	16.6 (b,B)	14.1 (a,A)	15.5 (ab,A)	31.9 (c,A)
SURF	0-5 cm	43.1 (c,E)	21.3 (a,B)	22.4 (a,B)	37.9 (b,B)
	5-10 cm	31.1 (b,D)	15.7 (a,A)	16.5 (a,A)	33.3 (b,A)
INC	0-5 cm	20.1 (a,C)	29.3 (c,C)	26.1 (b,C)	38.7 (d,BC)
	5-10 cm	14.4 (a,A)	24.0 (b,B)	20.7 (b,B)	39.1 (c,C)

The soil water content in the 0-5 cm and 5-10 cm soil layers of SURF was larger than the soil water content of CTRL and INC at the first three sampling points, without a significant difference in water content between the two layers. For CTRL and INC, soil water content increased with increasing soil depth during the first 9 weeks of incubation. No differences between treatments and soil layers were observed at week 33, where soil was kept artificially at a constant water content.

The application of fresh organic matter stimulated the substrate induced respiration rate of SURF and INC in both soil layers compared to CTRL. For SURF, the maximum respiration was measured in the 0-5 cm soil layer, while the highest respiration rate for INC was found in the 5-10 cm soil layer. No significant differences were observed in the SIR between 3 and 9 weeks.

At week 3, the largest amounts of soluble carbon were measured in the 0-5 and 5-10 cm soil layer of SURF with 43 and 31 mg DOC_{pa} kg^{-1} soil, respectively, while for CTRL and INC amounts varied between 14 and 20 mg DOC_{pa} kg^{-1} whatever the soil layer. Thereafter, higher DOC_{pa} concentrations were observed for INC compared to SURF in both soil layers. The CTRL treatment showed stable values at about 15.0 mg DOC_{pa} kg^{-1} soil, except at week 33 where the concentration was double. The general increase in DOC_{pa} at week 33 compared to week 9, which was also observed for SURF and INC, was attributed to a change in the soil moisture regime between week 9 and 33 (see section Materials and Methods).

4.3.2 Dynamics of residue-C and –N and its distribution in soil

Initially, all of the residue-C and -N was present at the soil surface for SURF, or equally distributed over the 0-10 cm soil layer for INC (Table 4.2). After 33 weeks of incubation, 52.1 % of the residue-C still remained as particulate organic carbon (POM-C, > 2 mm) at the soil surface for SURF, while only 5.2 % of the residue-C was recovered as POM-C for INC (0-10 cm). For INC, POM-C decreased at a faster rate in the 5-10 cm compared to the 0-5 cm soil layer, but at week 33 no significant difference was observed between the two soil layers.

For both residue treatments, the amount of residue-C found in the soil fraction < 2 mm after 33 weeks was to a large extent already present after 3 weeks of incubation. As a result of the initial residue location, a larger amount of residue-C was measured in the soil fraction < 2 mm of the 0-5 cm soil layer compared to the 5-10 cm soil layer for SURF, while the amounts of residue-C in the soil fraction < 2 mm were comparable in both soil layers for INC. Residue-C in the 10-25 cm soil layer was negligible for SURF, while 2.5 % of residue-C was transferred

to the 10-25 cm soil layer for INC. By difference with the total amount of initially added C, cumulative carbon mineralization from residues was calculated as 40.0 % for SURF and 74.1 % for INC after 33 weeks of incubation at 20°C.

At week 33, 30.9 % of the residue-N was still present as POM-N > 2 mm at the soil surface for SURF, while only 2.1 and 3.3 % of the residue-N was recovered as POM-N in the 0-5 cm and 5-10 cm soil layer for INC. Although there was no significant difference in the amount of residue-N between the two soil layers of INC at week 33, a faster initial transfer of residue-N into the soil fraction < 2 mm was observed for the 5-10 cm than for the 0-5 cm soil layer (data not shown). The percentage of residue-N transferred to the 10-25 cm soil layer increased over time to 17.1 % for SURF and 25.3 % for INC. Lack of recovery of residue-N was small, on average 9 % of the added N, and attributed to denitrification losses or sampling errors.

The residue fraction recovered as POM was however not "undecomposed". The C:N ratio of the POM showed an early increase due to the fast release of residue-N into the soil, followed by a continuous decrease due to the microbial colonisation of the residue particles (Table 4.2). In parallel, a decrease in % a.e. ^{15}N of the POM was observed (data not shown), indicative of a dilution of labelled N by unlabelled soil N immobilized by decomposers. Consequently, the N recovered in POM was not anymore residue-N only. At week 33 the relative contribution of soil N represented 35 % (INC, 0-5cm), 28 % (INC, 5-10 cm) and 15 % (SURF) of the measured POM-N. That also means that part of the POM-C recovered in this fraction was microbial biomass-C, but as the almost unique source of C for decomposers was the residue itself, the POM % a.e. ^{13}C did not change over time and the relative contribution of microbial biomass C to the POM-C fraction could only be indirectly estimated from the N data.

4.3.3 Aggregate dynamics

Changes in the mean weight diameter (MWD) resulted mainly from a decrease in the microaggregate fraction (250-53 µm) in favour of the small macroaggregate fraction (2000-250 µm) (Figure 4.1). The amount of large macroaggregates (> 2000 µm) was very small, irrespective of the time, with at most 1.4 % and 0.2 % of large macroaggregates formed for INC and SURF respectively, and their contribution to the MWD was negligible.

Table 4.2 Evolution over time of the distribution of residue-C and –N in particulate organic matter (> 2 mm) and the bulk soil (< 2 mm), for SURF and INC. Values between parentheses indicate the standard error.

Residue-C		SURF / %				INC / %				
	week	0	3	6	9	33	0	3	6	9	33
surface	>2mm	100.0 (-)	84.3 (1.6)	79.2 (1.0)	73.8 (0.7)	52.1 (1.1)	0.0 (-)	0.0 (-)	0.0 (-)	0.0 (-)	0.0 (-)
0-5 cm	>2mm	0.0 (-)	0.0 (-)	0.0 (-)	0.0 (-)	0.0 (-)	50.0 (-)	29.9 (1.4)	15.0 (0.9)	11.2 (0.3)	2.4 (0.9)
	<2mm	0.0 (-)	5.0 (0.1)	6.2 (0.7)	6.3 (0.2)	6.5 (0.3)	0.0 (-)	10.7 (0.2)	13.1 (0.5)	11.9 (1.3)	10.0 (0.8)
5-10 cm	>2mm	0.0 (-)	0.0 (-)	0.0 (-)	0.0 (-)	0.0 (-)	50.0 (-)	15.8 (2.5)	9.9 (0.5)	9.5 (0.4)	2.8 (1.4)
	<2mm	0.0 (-)	1.6 (0.1)	1.6 (0.2)	1.5 (0.0)	1.4 (0.0)	0.0 (-)	10.7 (0.3)	12.4 (0.6)	10.5 (0.5)	8.2 (0.2)
10-25 cm	<2mm	0.0 (-)	0.0 (-)	0.1 (0.0)	0.0 (0.0)	0.1 (0.0)	0.0 (-)	1.9 (0.3)	2.4 (0.2)	2.3 (0.4)	2.5 (0.4)
Not accounted for		0.0 (-)	9.0 (1.5)	12.9 (1.7)	18.4 (0.8)	40.0 (1.4)	0.0 (-)	30.9 (1.5)	47.2 (1.3)	54.7 (0.8)	74.1 (1.4)

Residue-N		SURF / %				INC / %				
	week	0	3	6	9	33	0	3	6	9	33
surface	>2mm	100 (-)	55.9 (3.9)	51.2 (3.4)	43.1 (2.3)	30.9 (3.5)	0.0 (-)	0.0 (-)	0.0 (-)	0.0 (-)	0.0 (-)
0-5 cm	>2mm	0.0 (-)	0.0 (-)	0.0 (-)	0.0 (-)	0.0 (-)	50.0 (-)	9.0 (1.0)	6.9 (0.3)	6.3 (0.1)	2.1 (0.9)
	<2mm	0.0 (-)	26.0 (0.9)	29.7 (2.4)	31.2 (0.8)	30.0 (1.8)	0.0 (-)	24.8 (0.8)	29.4 (0.5)	30.8 (2.7)	31.2 (2.0)
5-10 cm	>2mm	0.0 (-)	0.0 (-)	0.0 (-)	0.0 (-)	0.0 (-)	50.0 (-)	8.4 (1.0)	6.8 (0.4)	7.1 (0.1)	3.3 (1.8)
	<2mm	0.0 (-)	10.5 (0.2)	9.7 (1.0)	10.1 (0.2)	10.8 (0.6)	0.0 (-)	32.2 (0.4)	35.7 (1.1)	32.5 (0.8)	30.5 (0.9)
10-25 cm	<2mm	0.0 (-)	2.6 (0.4)	4.0 (0.5)	7.4 (0.5)	17.1 (0.2)	0.0 (-)	10.2 (1.7)	12.7 (1.0)	14.6 (1.4)	25.3 (0.9)
Not accounted for		0.0 (-)	4.9 (3.9)	5.4 (1.3)	8.2 (1.6)	11.3 (4.7)	0.0 (-)	15.4 (1.8)	8.5 (3.0)	8.8 (2.1)	7.6 (0.9)

C:N of POM		SURF / -					INC / -				
	week	0	3	6	9	33	0	3	6	9	33
surface	>2mm	29.0 (-)	43.6 (3.1)	43.5 (3.2)	47.9 (2.9)	41.9 (1.2)	-	-	-	-	-
0-5 cm	>2mm	-	-	-	-	-	29.0 (-)	87.3 (6.1)	52.4 (4.4)	39.2 (1.2)	22.7 (0.2)
5-10 cm	>2mm	-	-	-	-	-	29.0 (-)	43.2 (2.8)	33.2 (0.4)	29.0 (1.3)	18.2 (0.1)

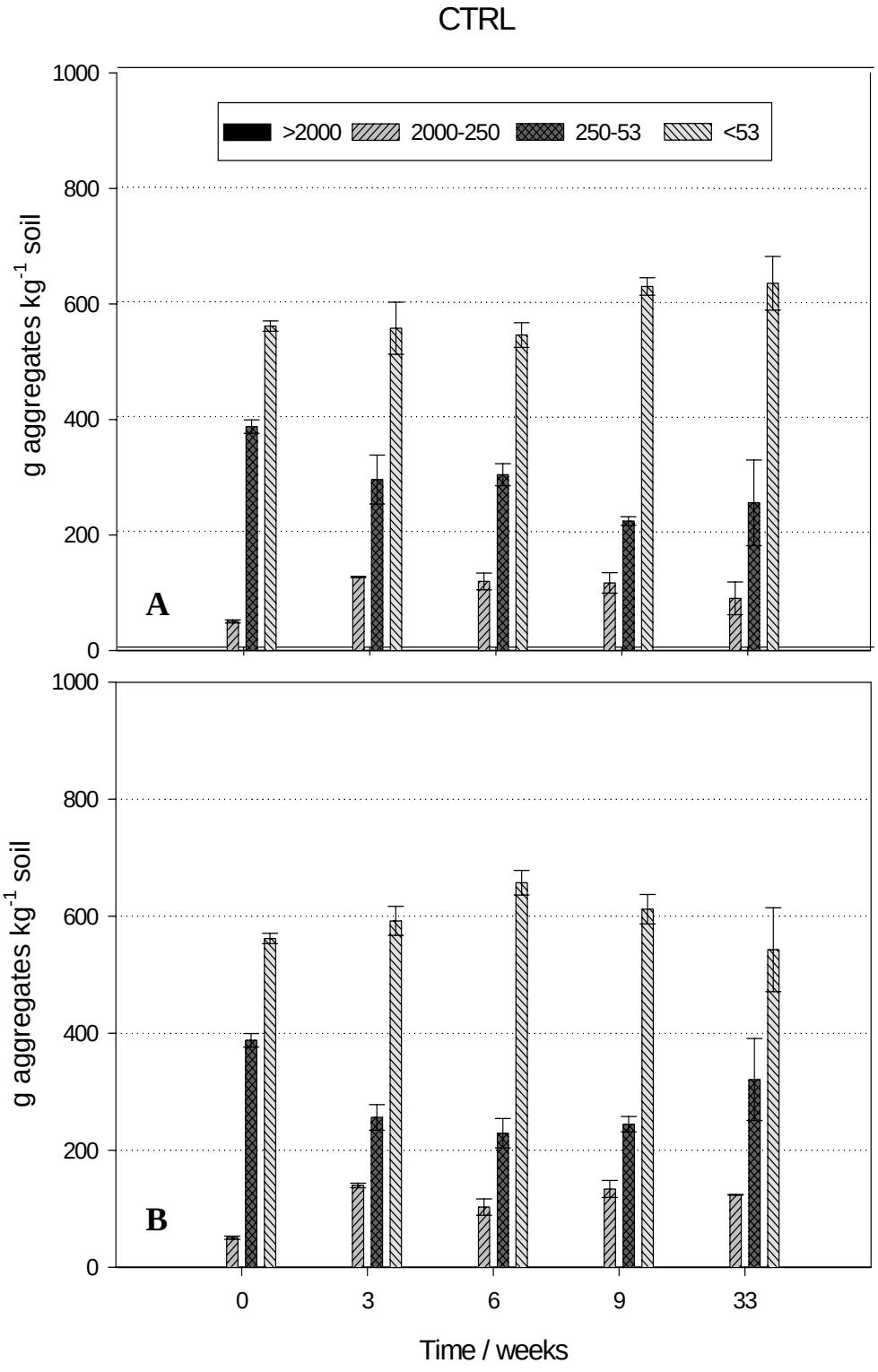

Figure 4.1 (a) Evolution of the distribution of aggregate fraction mass over time for the large macroaggregates (> 2000 µm), small macroaggregates (2000-250 µm), microaggregates (250-53 µm) and the silt and clay fraction (< 53 µm), for (A) the 0-5 cm and (B) the 5-10 cm soil layer of CTRL. Error bars show the 95% confidence interval.

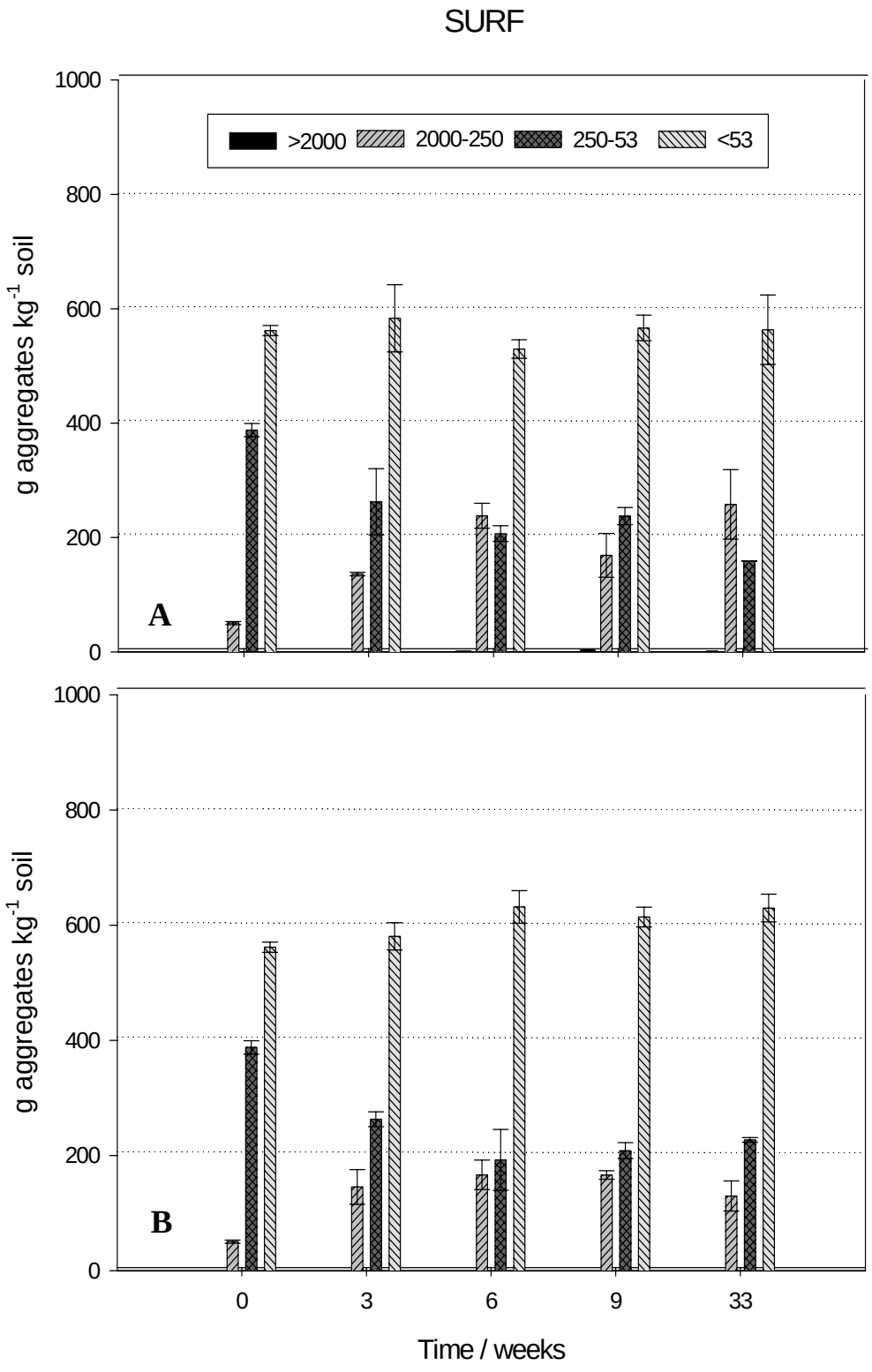

Figure 4.1 (b) Evolution of the distribution of aggregate fraction mass over time for the large macroaggregates (> 2000 µm), small macroaggregates (2000-250 µm), microaggregates (250-53 µm) and the silt and clay fraction (< 53 µm), for (A) the 0-5 cm and (B) the 5-10 cm soil layer of SURF. Error bars show the 95% confidence interval.

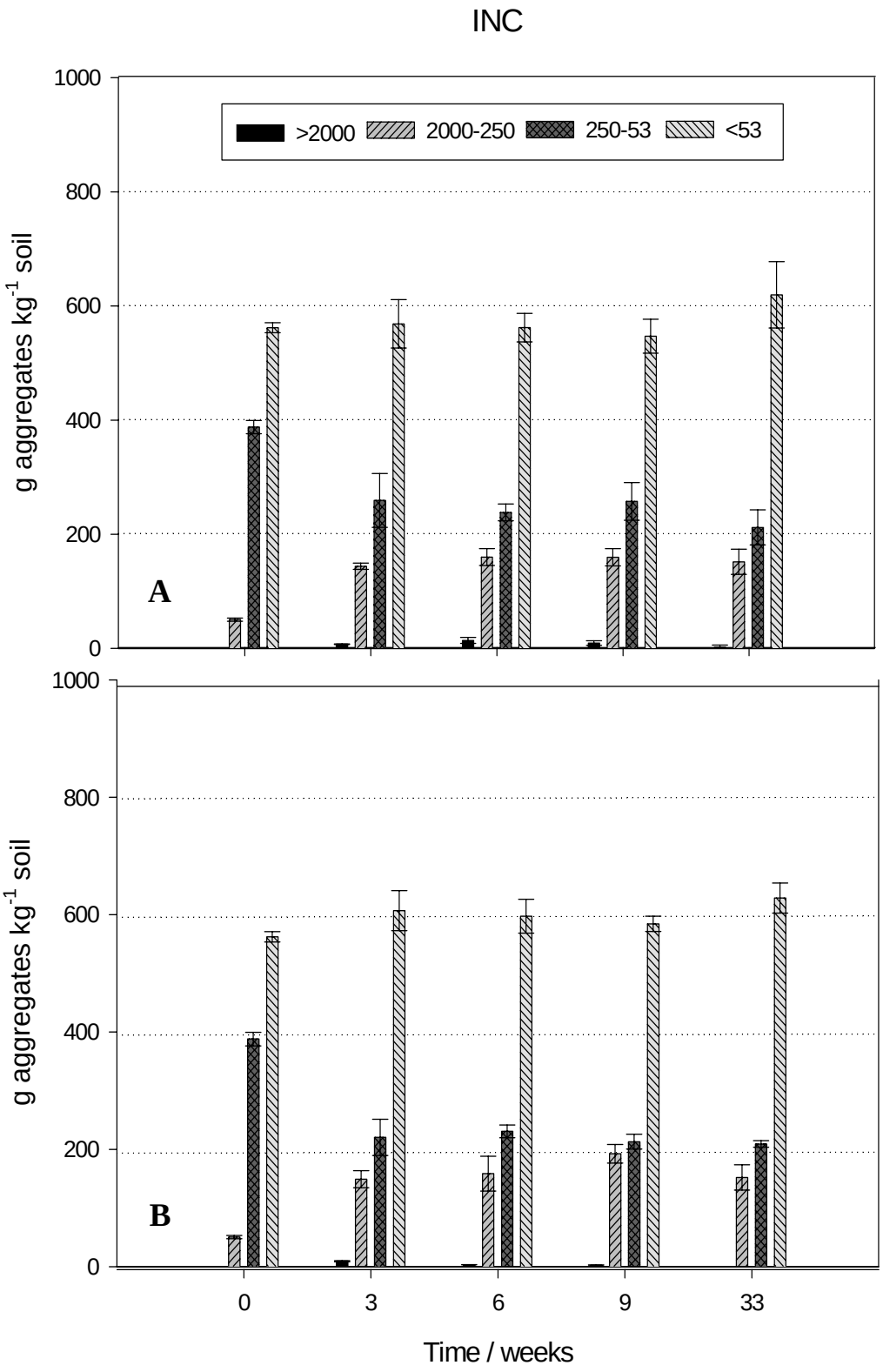

Figure 4.1 (c) Evolution of the distribution of aggregate fraction mass over time for the large macroaggregates (> 2000 µm), small macroaggregates (2000-250 µm), microaggregates (250-53 µm) and the silt and clay fraction (< 53 µm), for (A) the 0-5 cm and (B) the 5-10 cm soil layer of INC. Error bars show the 95% confidence interval.

In the 0-5 cm soil layer, the initial MWD increased for all treatments by at least 56% during the first 3 weeks of incubation, with a significantly larger MWD for INC compared to CTRL and SURF (Table 4.3). From week 6, both residue treatments had a significantly larger MWD compared to CTRL. This difference was maintained until week 33. At this point, the MWD of CTRL had significantly decreased compared to week 3 and the MWD of SURF was significantly larger than the MWD of INC.

In the 5-10 cm soil layer, the initial MWD also increased for all treatments during the first 3 weeks of incubation, with only a significantly larger MWD for INC compared to CTRL. At week 6 and 9, the MWD of SURF and INC was larger than the MWD of CTRL, but after 33 weeks, no significant difference in MWD was observed between treatments, which was similar to the values obtained at week 3.

In both soil layers, and for all treatments, the MWD after 33 weeks was still larger than the MWD before incubation. For CTRL and INC, no significant differences in MWD were observed between the 0-5 cm and 5-10 cm soil layer, while for SURF a larger MWD was calculated in the 0-5 cm than in the 5-10 cm soil layer at week 6 and 33.

Table 4.3 Evolution of the mean weight diameter (MWD) of soil aggregates in the 0-5 cm and 5-10 cm soil layer of CTRL, SURF and INC. Different lowercase letters indicate significant differences over time ($P < 0.05$), for given soil layer and treatment. Different uppercase letters indicate significant differences between treatments and soil layers ($P < 0.05$), at given sampling point.

		MWD / μm				
	Week	0	3	6	9	33
CTRL	0-5 cm	130 (a,A)	203 (c,A)	195 (c,AB)	182 (bc,A)	157 (b,A)
	5-10 cm	130 (a,A)	212 (c,A)	168 (b,A)	204 (c,AB)	202 (bc,AB)
SURF	0-5 cm	130 (a,A)	208 (b,A)	315 (c,D)	248 (bd,BCD)	334 (cd,C)
	5-10 cm	130 (a,A)	219 (bc,AB)	233 (bc,C)	235 (c,C)	197 (b,AB)
INC	0-5 cm	130 (a,A)	233 (b,B)	273 (c,CD)	261 (c,D)	226 (bc,B)
	5-10 cm	130 (a,A)	245 (bc,B)	235 (bc,BC)	269 (c,D)	220 (b,B)

4.3.4 Aggregate enrichment with ^{13}C and ^{15}N

In the 0-5 cm soil layer of SURF, an enrichment in ^{13}C was measured in the small macroaggregate (2000-250 μm), microaggregate (250-53 μm) and silt and clay fraction (< 53 μm) right from week 3 (Figure 4.2). This enrichment slightly increased up to week 33 without a significant difference between the three fractions. Conversely at week 6, the large macroaggregate fraction (> 2000 μm) appeared and immediately turned strongly enriched in ^{13}C compared to the other fractions, up to 1 % a.e. ^{13}C, indicating that about one third of the large macroaggregate-C was residue-derived. In the 5-10 cm soil layer of SURF, as expected from the low total residue-C recovered (cf. Table 4.2), the % a.e. ^{13}C was very small for all fractions without any significant change over time. No large macroaggregates were formed in this soil layer.

For the INC treatment, the situation was rather different than for SURF. All fractions, including the large macroaggregate fraction (> 2000 μm), were already labelled at week 3, with a decrease in % a.e. ^{13}C with decreasing aggregate size. This reflected the smaller relative contribution of labelled residue-C to larger amounts of C in the fraction < 53 μm. There were no significant differences in enrichment between week 3 and week 33 for each fraction, indicating little or no redistribution of initial ^{13}C over time into the different aggregate sizes, or, that ^{13}C mineralized from the soil aggregates was substituted. Similar patterns were observed for the 5-10 cm layer, except that the large macroaggregate fraction tended to be slightly more enriched in ^{13}C than in the 0-5 cm soil layer.

Similar patterns as for the ^{13}C enrichment were observed for ^{15}N enrichment across treatments and layers (Figure 4.3). In both treatments and layers, the large macroaggregate fraction (> 2000 μm) again showed a strong enrichment in ^{15}N, indicating that 20 to 30 % of this fraction N was residue-derived.

4.3.5 Distribution of residue-C and -N in aggregate fractions at week 33

The distribution of residue-C and -N in different aggregate size fractions of the 0-5 and 5-10 cm soil layer was calculated at each date and for each layer from the aggregate fraction mass, its carbon and nitrogen content and the atom % excess of ^{13}C and ^{15}N. Initial C and N distribution in the aggregate fractions of CTRL is given in Table 4.4. As expected from the changes in mass (cf. Figure 4.1) and in enrichment (cf. Figures 4.2 and 4.3), no major evolution in the distribution of ^{13}C across the various aggregate sizes was observed over time, and therefore only the data obtained at week 33 are commented here in detail (Table 4.5).

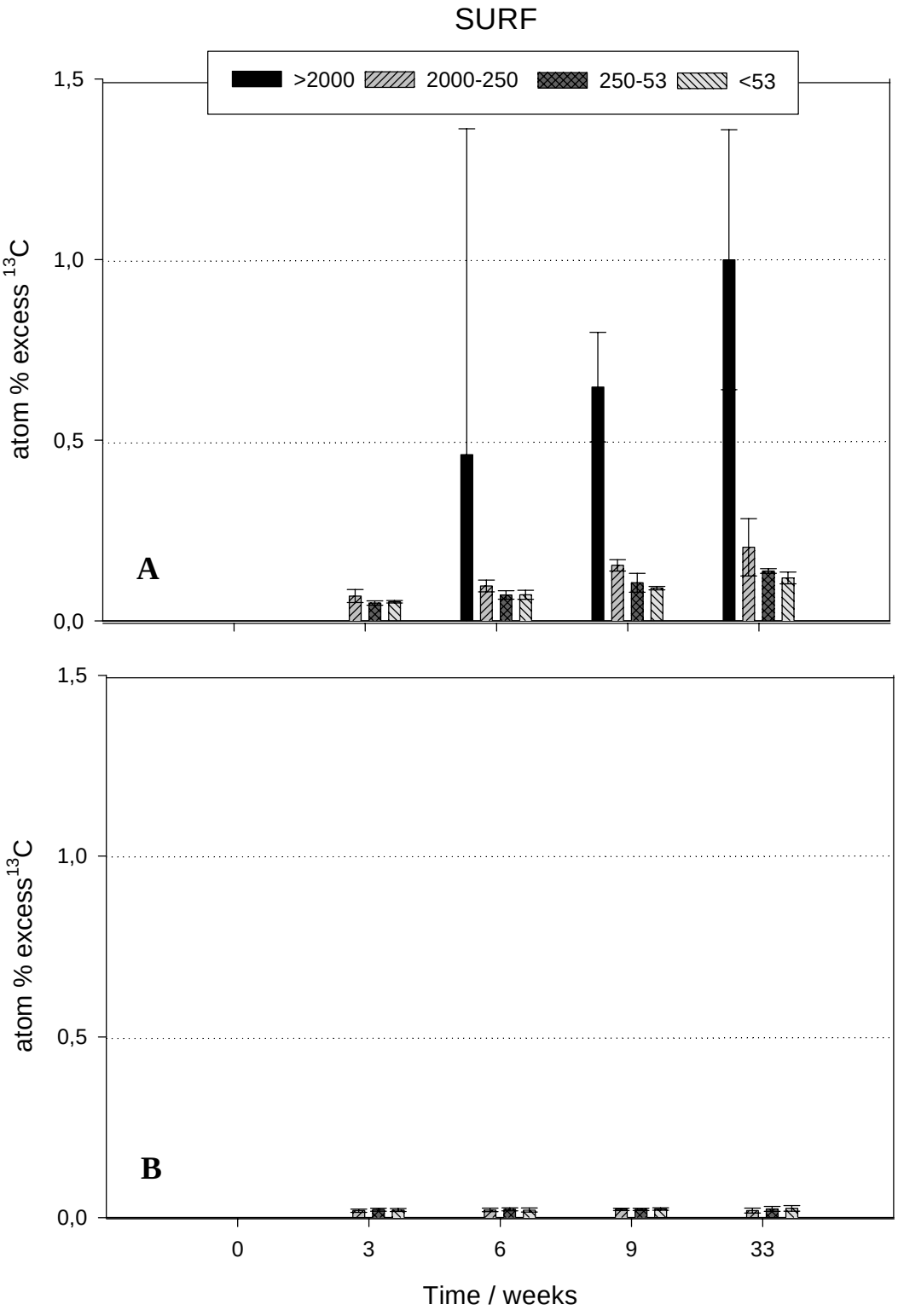

Figure 4.2 (a) Evolution of the ^{13}C atom % excess over time, measured in the large macroaggregates (> 2000 µm), small macroaggregates (2000-250 µm), microaggregates (250-53 µm) and the silt and clay fraction (< 53 µm), for (A) the 0-5 cm and (B) the 5-10 cm soil layer of SURF. Error bars show the 95% confidence interval.

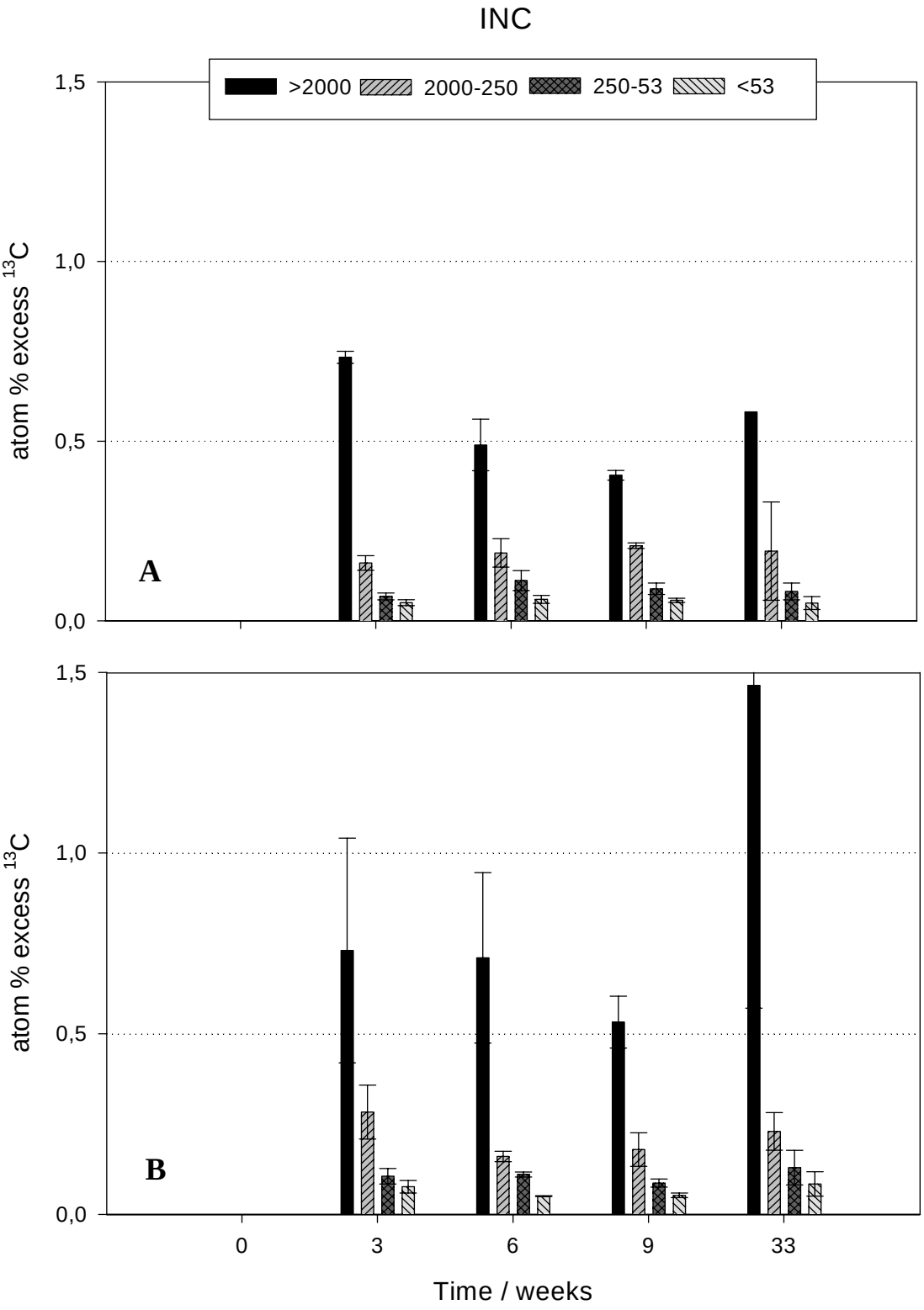

Figure 4.2 (b) Evolution of the ^{13}C atom % excess over time, measured in the large macroaggregates (> 2000 µm), small macroaggregates (2000-250 µm), microaggregates (250-53 µm) and the silt and clay fraction (< 53 µm), for (A) the 0-5 cm and (B) the 5-10 cm soil layer of INC. Error bars show the 95% confidence interval.

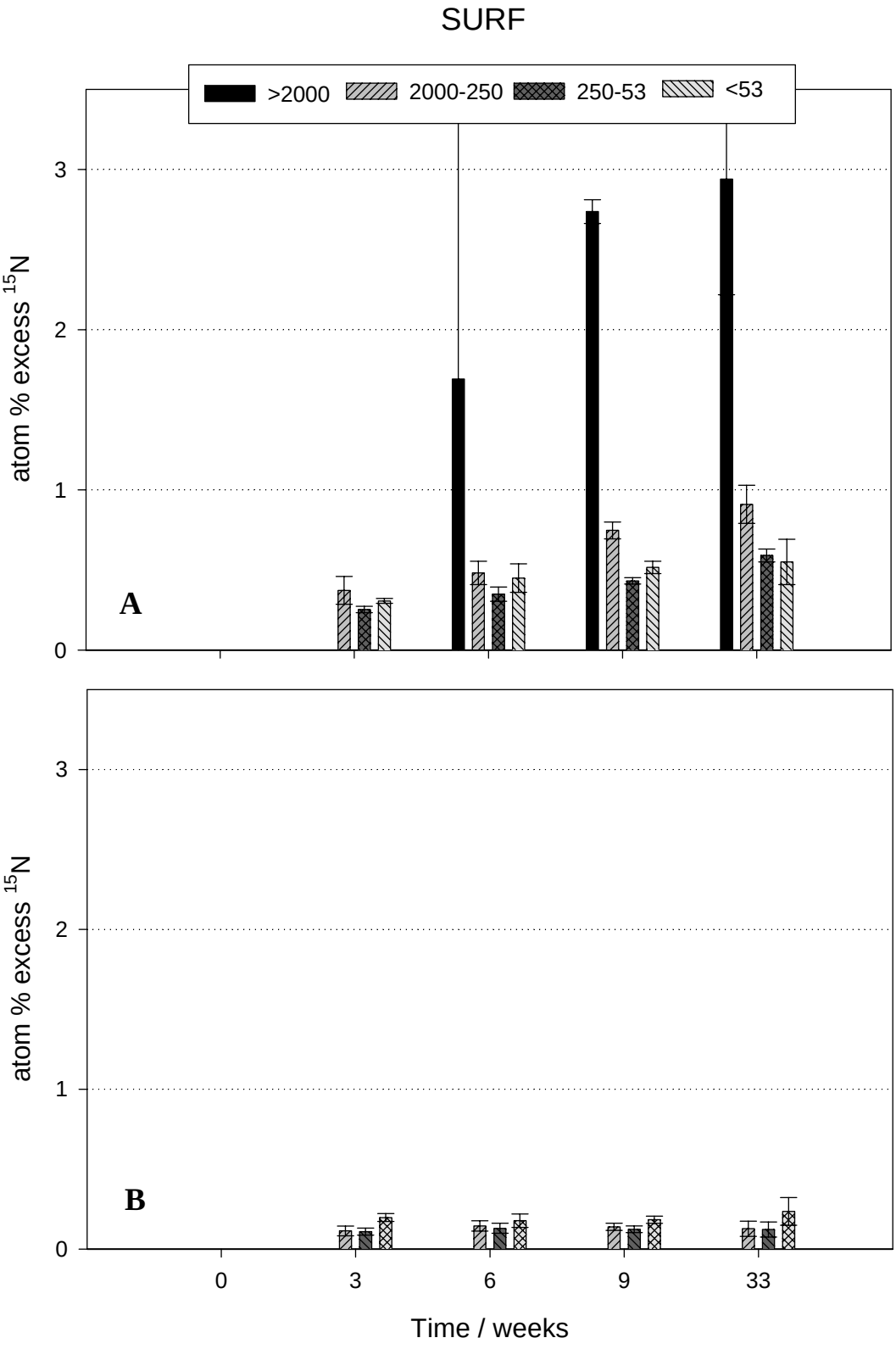

Figure 4.3 (a) Evolution of the ^{15}N atom % excess over time, measured in the large macroaggregates (> 2000 µm), small macroaggregates (2000-250 µm), microaggregates (250-53 µm) and the silt and clay fraction (< 53 µm), for (A) the 0-5 cm and (B) the 5-10 cm soil layer of SURF. Error bars show the 95% confidence interval.

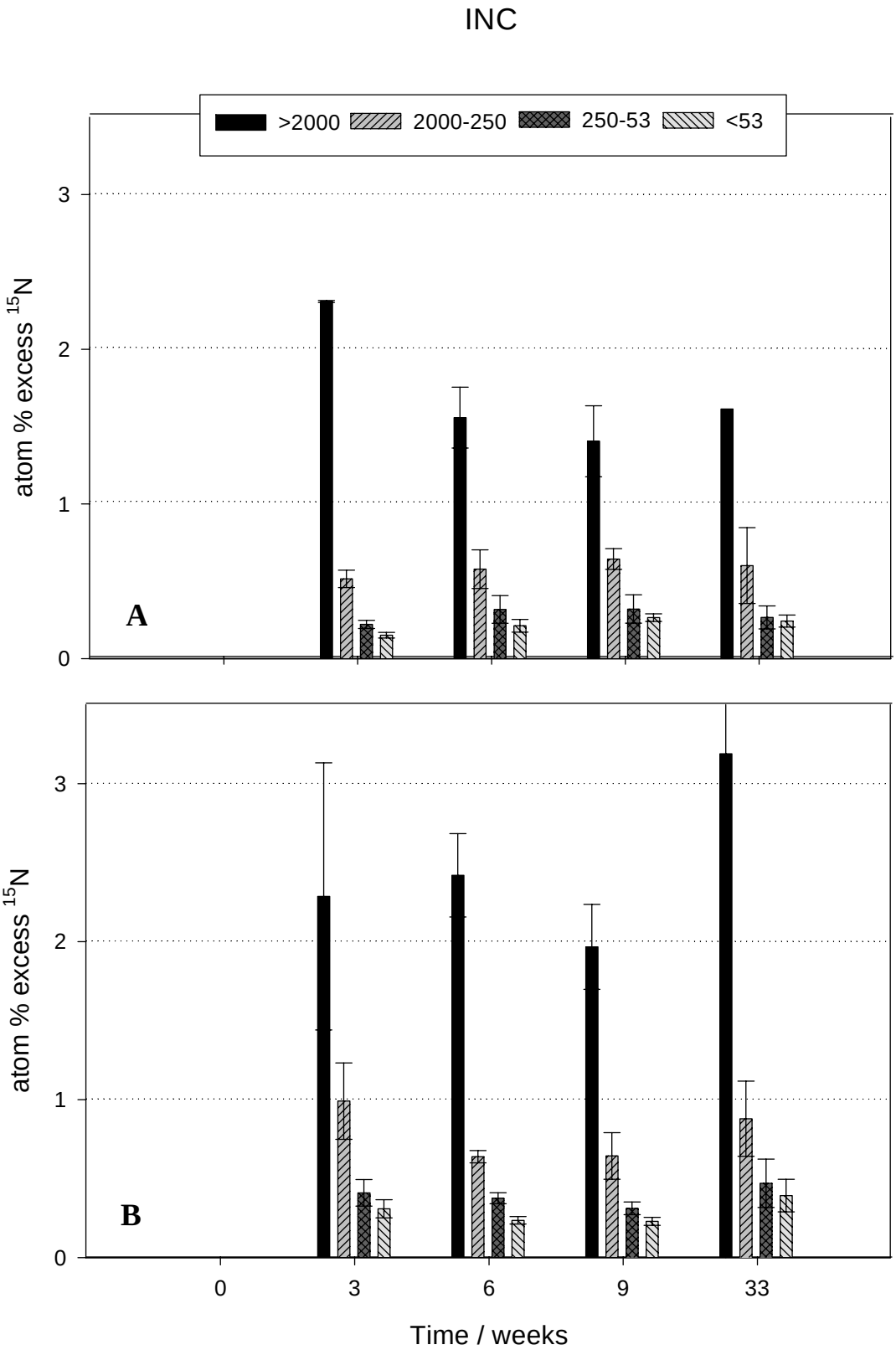

Figure 4.3 (b) Evolution of the ^{15}N atom % excess over time, measured in the large macroaggregates (> 2000 µm), small macroaggregates (2000-250 µm), microaggregates (250-53 µm) and the silt and clay fraction (< 53 µm), for (A) the 0-5 cm and (B) the 5-10 cm soil layer of INC. Error bars show the 95% confidence interval.

Table 4.4 Initial mass distribution and total C and N in the large macroaggregates (> 2000 µm), small macroaggregates (2000-250 µm), microaggregates (250-53 µm) and the silt and clay fraction (< 53 µm) of the control soil.

	mass	C		N		C:N
	/ g kg^{-1} soil	/ g kg^{-1} fraction	/ g kg^{-1} soil	/ g kg^{-1} fraction	/ g kg^{-1} soil	
> 2000 µm	0.0	0.0	0.0	0.00	0.00	-
2000-250 µm	50.4	11.3	0.6	1.05	0.05	10.8
250-53 µm	387.8	10.1	3.9	1.04	0.40	9.7
< 53 µm	561.9	7.2	4.0	0.84	0.47	8.6

Table 4.5 Recapitulative of the distribution of residue-C and -N in soil aggregate and particulate organic matter (POM) fractions in the 0-5 cm and 5-10 cm soil layer, after 33 weeks of incubation. In this table, there is no overlap between residue-C and -N in soil aggregates and POM. Residue-C present at the soil surface as mulch is not taken into account. Values between parentheses indicate the standard error.

			Residue-C / % added		Residue-N / % added	
			SURF	INC	SURF	INC
0-5 cm	Soil aggregates	> 2000 µm	0.2 (0.0)	0.2 (-)	0.4 (0.1)	0.4 (-)
		2000-250 µm	4.3 (0.9)	2.6 (0.9)	15.1 (2.6)	5.7 (1.6)
		250-53 µm	1.8 (0.0)	1.2 (0.3)	6.4 (0.2)	3.4 (0.7)
		< 53 µm	3.2 (0.2)	1.4 (0.2)	15.7 (2.0)	7.3 (1.2)
		Total	9.5 (1.1)	5.4 (1.4)	37.6 (4.8)	16.8 (1.3)
	POM	> 2000 µm	0.0 (-)	1.6 (0.8)	0.0 (-)	1.7 (0.8)
		2000-250 µm	0.0 (0.0)	1.4 (0.6)	0.0 (0.0)	1.6 (0.6)
		250-53 µm	0.0 (0.0)	0.3 (0.2)	0.0 (0.0)	0.5 (0.2)
		Total	0.0 (0.0)	3.3 (1.2)	0.0 (0.0)	3.8 (1.2)
5-10 cm	Soil aggregates	> 2000 µm	0.0 (-)	0.1 (0.0)	0.0 (-)	0.1 (0.0)
		2000-250 µm	0.2 (0.1)	2.8 (0.6)	1.1 (0.3)	8.2 (1.7)
		250-53 µm	0.4 (0.1)	1.9 (0.3)	1.8 (0.4)	6.1 (1.0)
		< 53 µm	0.8 (0.1)	2.4 (0.5)	7.7 (1.6)	11.7 (1.4)
		Total	1.4 (0.2)	7.2 (1.4)	10.6 (2.3)	26.1 (4.2)
	POM	> 2000 µm	0.0 (-)	1.8 (0.3)	0.0 (-)	2.0 (0.4)
		2000-250 µm	0.0 (0.0)	2.2 (2.0)	0.0 (0.0)	2.6 (2.3)
		250-53 µm	0.0 (0.0)	0.2 (0.1)	0.0 (0.0)	0.3 (0.0)
		Total	0.0 (0.0)	4.2 (1.8)	0.0 (0.0)	4.9 (2.0)
0-10 cm	Soil aggregates + POM	Total	10.9 (1.3)	20.1 (0.5)	48.2 (7.1)	51.6 (3.5)

For SURF, no POM at all was recovered in neither aggregate size fraction, indicating that ^{13}C recovered in those fractions originated from soluble ^{13}C leached from the mulch or that ^{13}C was translocated by fungal hyphae. In total 9.5 % of the added residue-C was present in the sum of the four aggregate fractions, with a minor contribution of the large macroaggregate fraction (> 2000 μm). In the 5-10 cm soil layer of SURF, the % of residue-C increased with decreasing particle size, but in total only 1.4 % of ^{13}C was recovered in these fractions. In the 0-10 cm soil layer, 10.7% of the added C was recovered. This analyse does not take into account the amount of residue-C in the mulch still left at the soil surface (i.e. 52.1% of the added C at week 33).

For INC, the ^{13}C was almost homogeneously distributed within the two soil layers due to the initial incorporation of half the residue-C in each layer. No significant difference in the distribution of residue-C over the small macroaggregate (2000-250 μm), microaggregate (250-53 μm) and silt and clay fraction (< 53 μm) was observed comparing week 3 with week 33. At that time 5.4 % (0-5cm) to 7.2 % (5-10 cm) of residue-C was recovered in the sum of the four aggregate fractions, with most of this residue-C being measured in the small macroaggregate fraction (2000-250 μm). The same trends were observed in the 5-10 cm soil layer. In total for the 0-10 cm layer, the recovered ^{13}C in the aggregate fractions amounted to 20.1 % of the added C (POM included).

Although the distribution of residual ^{13}C within the two soil layers was very different according for SURF and INC, the relative distribution of residual ^{13}C within the aggregate fractions was similar for SURF and INC with 46-48 % of the ^{13}C in the small macroaggregate (2000-250 μm) fraction, 19-22% in the microaggregate fraction (250-53 μm) and 34-26 % in the silt and clay fraction (< 53 μm) at week 33.

More residue-N entered the soil aggregates compared to residue-C, however the same trends were observed (Table 4.5). For SURF, the % of residue-N incorporated in aggregates increased from 16.9 % (week 3) to 37.6 % (week 33) in the 0-5 cm soil layer but did not differ significantly over time in the 5-10 cm soil layer (8.8 % – 10.6 % of residue-N). For INC, the % of residue-N present in soil aggregates after 33 weeks of incubation was 16.8 % in the 0-5 cm and 26.1 % in the 5-10 cm soil layer.

4.4 Discussion

4.4.1 Soil aggregation

Previous studies concerning aggregate dynamics and distribution of C and N in aggregates often use soils that are recently brought into cultivation and consequently still relatively rich in organic C (e.g. Elliott, 1986; Six *et al.*, 1998). Agricultural soils of Northern France on the other hand have been cultivated for several hundreds of years and are often poor in native organic matter (e.g. Angers *et al.*, 1997). Soils from this region are highly susceptible to stresses induced by rapid wetting of air-dried aggregates (Le Bissonnais, 1988), resulting in the collapse of most macroaggregates by slaking. In addition, the silt loam soil used in this study did not receive organic inputs since 1994 and was strongly depleted in organic C. The initial aggregate MWD of this soil was small and formation of large macroaggregates was weak compared to other aggregation studies (e.g. Blair, 2000; Six *et al.*, 2001). A single application of fresh organic matter only resulted in small and short term effects, although the hierarchical model of aggregate build-up (Tisdall & Oades, 1982) could be confirmed. Macroaggregates were formed out of microaggregates, and particulate organic matter was mainly associated with large macroaggregates.

Summarizing the observed effects in the two soil layers over time, adding oilseed rape residues resulted in an increased MWD in the 0-10 cm soil layer compared to the control soil after 33 weeks of incubation, without significant differences between SURF and INC. However, in the 0-5 cm soil layer of SURF, more small macroaggregates (2000-250 µm) and a larger MWD were found than for INC.

Several factors contributed to the increase in MWD over time. The influence of physical processes is demonstrated by the evolution of the MWD in CTRL, which was not affected by the addition of residue-C. Aggregate disruption and redistribution of soil particles after a rain event (Adu & Oades, 1978) and 'soil aging' during subsequent wetting and drying of the soil (Horn & Dexter, 1989; Shainberg *et al.*, 1996) had an impact on the stability of aggregates. Those physical processes may be responsible for the initial increase in MWD from week 0.

In addition, microbial activity and residue decomposition are biological processes favourable to aggregate stability (Tisdall, 1994; Martens, 2000), with a particular role of fungi in the formation of macroaggregates (Molope *et al*., 1987; Guggenberger *et al*., 1999; Denef *et al*., 2001b). Although the maximum microbial activity for SURF and INC was not significantly different, it has been shown that important variations exist in the ratio bacterial/fungal

biomass (Bossuyt *et al*., 2001). In particular, the fungal biomass has been reported to be more abundant when residues are placed on the surface than when incorporated (Holland & Coleman, 1987), because of their capacity to translocate soil-N to the surface residue with their hyphal network (Frey *et al*., 2000). The here observed dilution of residue-N by N originating from the soil supports this hypothesis. Therefore, it is expected from the high concentration of POM at the soil surface of the SURF treatment that more macroaggregates are formed in the 0-5 cm soil layer of SURF compared to CTRL and INC.

After the first dry/wet cycle, however, no significant differences were found between the MWD of CTRL and SURF, treatments in which macroaggregates were not yet slaking resistant. For INC, the large macroaggregates that could be recovered were found attached to the fresh organic matter, which is in agreement with Buyanovsky *et al*. (1994) who suggested that large macroaggregates are organized around plant residue particles. At the end of the second dry/wet cycle, the MWD of SURF had significantly increased in the 0-5 cm soil layer, which can be related to the pulse of microbial activity after the application of rain at week 3, as reported in Chapter 3.

For SURF, the long incubation period between 9 and 33 weeks without aggregate disruptive forces (i.e. rain events) and with favourable conditions for decomposition, is supposed to make the aggregates more slaking resistant. In contrast, the MWD for INC tended to decrease between week 9 and 33 and this was probably due to the more advanced decomposition state of the incorporated residues (74% of residue-C mineralised for INC compared to 40% for SURF), that already implied a reduction in microbial activity. The combination of these factors explains the larger MWD in the 0-5 cm soil layer of SURF compared to INC at week 33.

Since residue-C for SURF is concentrated at the soil surface, observed differences in aggregation between SURF and INC are diluted by the considered depth of the upper soil layer (5 cm). Consequently, differences between treatments would be more pronounced when reducing the depth of the upper soil layer. It is expected that those differences in C and aggregate distribution also significantly modify physical and biological properties of the upper cm of soil (e.g. soil structural stability, hydraulic conductivity, microbial activity, oxygen concentration), determining environmental impacts other than total C storage.

4.4.2 Residue-C and –N stored in aggregate fractions

The initial location of crop residues affected dramatically the dynamics of residue decomposition as discussed in Chapter 3. This resulted into a slower decomposition and a large amount of residue particles left at the soil surface for SURF, representing 52 % of the added C at week 33, while almost all of the residue particles were decomposed in the INC treatment. However as discussed earlier, this mulch of residue particles was not 'untouched': (i) the soluble C and N were leached down by rain in an early stage and entered the adjacent soil layer as shown by the dynamics of ^{13}C and ^{15}N in the soil fractions, and (ii) the mulch particles were colonized by the decomposing microbial biomass, as shown by the changes in C:N ratio and ^{15}N labelling of the residual mulch. The total residual ^{13}C in the INC treatment (20.1 % of added ^{13}C) after 33 weeks at 20°C, which corresponds to about 1.4 years at 10°C (Q_{10} = 2.2), is in the range of values obtained in field conditions on the same soil (e.g. Aita *et al*., 1997). By comparing the total residual ^{13}C in the soil (INC) or mulch + soil (SURF), it is concluded that a first main result of having crop residues decomposing at the soil surface is a large POM fraction that is maintained at the soil surface, due to a reduced soil-residue contact that slows down the decomposition.

Basically, the two treatments differ in the way the carbon enters the soil. With the residues left at the soil surface (SURF), some of the residue-C entered the soil possibly by diffusion at the soil-residue interface near the soil surface (as observed by Gaillard *et al*., 1999), but more likely by convective transport after rain, as demonstrated by the large increase in soluble C in the soil solution just after the rainfall (Chapter 3). This is corroborated by the observation that for SURF no POM-C (> 2000 μm) is found in the soil or associated with aggregate fractions. For the INC treatment, all of the POM-C (> 2000 μm) was initially present in the soil and it decreased rapidly as decomposition proceeded. Little residue-C remained as POM associated with aggregate fractions at week 33 (3-4 % of added ^{13}C in each layer).

Although differences exist in the way residue-C enters the mineral soil fraction, the total amount of ^{13}C in the 2000-250 μm, 250-53 μm and < 53 μm aggregate fractions was rather low both for SURF and INC, equivalent to 10.6-12.3 % of the added residue-C at week 33, with no significant difference between the two treatments. However, this carbon was mostly located in the upper layer for SURF, while, as expected, it was almost equally distributed over the two soil layers in which the residues where initially incorporated for INC.

Surprisingly, the relative distribution of ^{13}C in the various aggregate fractions at week 33 did not differ between the two treatments, despite the completely different way for new C to enter

the soil, i.e. despite the mixing of residue particles with the soil in the INC treatment. On the short-term (0-9 weeks), particulate organic matter may have been incorporated into the macroaggregates of INC, in addition to diffusion of soluble carbon and nitrogen into the aggregates as observed for SURF. This initially resulted in larger amounts of residue-C and -N in the larger aggregate fractions of INC compared to SURF, but this effect was only transient. Our findings confirm the hypothesis of Smucker *et al*. (2003), who suggested that diffusion of soluble carbon is the main process for enriching soil aggregates with recently deposited residue-C. Furthermore over time (3-33 weeks) little change was observed for the residue-C recovered in aggregates suggesting that the association of residue-C with the soil aggregates was established very early, during the first 3 weeks of its decomposition after which it was protected against mineralization. This suggests that, despite nearly 50% of the added C was still left at the soil surface as POM in the SURF treatment, it is unlikely that much more ^{13}C would enter the soil and be stabilized within the soil aggregates as POM will decompose, or anyhow that this transfer of ^{13}C is very slow. This supports the concept of a two-compartment system with a soluble fraction of crop residues that diffuses early and is stabilised - before or after being assimilated by the microbial biomass -, and a non-soluble residue fraction (in the soil or at the soil surface) that supports the growth of colonisers, contributes more to net C mineralization and has little interaction with the soil matrix. This conceptual schema was already proposed by Ladd *et al*. (1996) and Gaillard *et al*. (2003).

As observed by Angers *et al*. (1997), more of the added residue-N than –C was recovered in the soil aggregates, for both residue treatments. Except from small denitrification losses, all residue-N remained in the soil while residue-C disappeared as CO_2 through mineralization. While residue-C for SURF was mainly preserved in particulate organic matter at the soil surface, the largest part of residue-N at week 33 was found in the soil aggregate fractions. The larger amount of N in the soluble residue fraction (71 % N compared to 39 % C) resulted in a larger accumulation of residue-N than -C in the soil aggregates. This also corresponded with Angers *et al*. (1997), who attributed the initial difference in distribution of residue-N to the presence of soluble N in the residues.

4.5 Conclusion

In experimental conditions that simulate wetting-drying conditions of field situations, oilseed rape residues were applied as mulch or incorporated in the 0-10 cm soil layer. Spatial separation of soil and surface placed residues slowed down the decomposition rate compared to residue incorporation. This resulted on the short term in a large fraction of particulate organic matter (POM) at the soil surface, while almost all of the POM had disappeared with residue incorporation. The distribution of residue-C and the associated microbial activity determined the dynamics and concentration of macroaggregates in soil: residue addition increased the aggregate mean weight diameter (MWD) compared to the control soil, and a larger MWD was obtained in the 0-5 cm soil layer under mulch than with residue incorporation.

In contrast to the larger amount of residual POM for soil with residue mulch than with residue incorporation, the total amount of ^{13}C recovered in the aggregate fractions did not significantly differ between treatments and was rather low, about 11% of added C. However, this carbon was mostly located in the upper soil layer with mulch, while it was almost equally distributed over the two soil layers with residue incorporation. Despite the different way for new C to enter the soil (i.e. leaching of residue-C after rainfall with mulch vs. diffusion of residue-C and residue colonization with incorporation), the relative distribution of ^{13}C in the various aggregate fractions did not differ between the two treatments at week 33 - probably because in both treatments residue-C mainly entered the aggregate fractions as soluble C.

On the medium to long-term, the distribution of residue-C in soil aggregate fractions at week 33 suggests the following scenario:

(i) Residue-C enters the aggregate fractions as soluble C either after being transported from the residue mulch with water infiltration (after rain) or, with water infiltration and by diffusion from the surrounded residue particles in the case of residue incorporation. The incorporation of residue-C in soil aggregates occurs early and does not change much over time, and the decomposition of POM (> 2000 μm) in the soil does not seem to have any significant impact on C storage in aggregates.

(ii) Therefore, as the main factor determining the storage of residue-C into the soil on the medium to long term would be the initial quality of the crop residue (i.e. the amount of soluble C), the initial residue location has no significant impact on long term C storage in soil, at least not through a differential incorporation into stable aggregate fractions. On the longer term, the fate of mulch-C accumulated at the soil surface should be examined.

(iii) Although the effect of crop residue location on soil aggregation was negligible when expressed as a function of the amount of residue added, our results clearly showed a higher concentration of residue-C and N and increased aggregation near the soil surface with residue mulch. This enhanced aggregation at the soil surface may contribute to increased stabilization of residue-C in soil on the longer term.

CHAPTER 5

Comparing water, carbon and nitrogen dynamics in soil columns with incorporated or surface applied crop residues using the PASTIS model

5.1 Introduction

Crop residue management in agricultural soils has received much attention in the control of soil erosion and the evaluation of carbon sequestration. One option to aim at a more sustainable agriculture is a change towards reduced or no tillage. This change in management of fresh organic matter influences hydrodynamic fluxes and the dynamics of carbon and nitrogen in soil. Tillage practice determines the initial location of added organic matter in soil that, in turn, acts directly on soil physical properties (e.g. water flux, solute transport and soil temperature). In addition, crop residue location - incorporated or left at the soil surface - pre-determines gradients in the organic matter content of the soil, and likewise so in the decomposing microbial biomass and activity.

The rate of crop residue decomposition and nutrient release in soil is also influenced by the biochemical quality of the residues (e.g. Trinsoutrot *et al.*, 2000b). For a given quality, however, the microclimatic conditions imposed on the residues are the main factors regulating decomposition, as suggested by Abiven & Recous (submitted). The residue location in soil imposes these conditions and determines the availability to water and nutrients. All these soil physical and biological changes interact, and influence the decomposition of soil organic matter and the associated biotransformations of carbon and nitrogen (see Chapter 3). It has been observed that residues left at the soil surface in the field decompose at a slower rate than when incorporated in the soil (e.g. Douglas *et al.*, 1980).

The model PASTIS (Garnier *et al.*, 2003) was used as a tool to examine the interactions between crop residue location and quality, and their consequences on the decomposition process. This mechanistic, deterministic model couples the transfer of water and solutes in soil with the biotransformation of carbon and nitrogen. A recently added submodel simulating

residue mulch decomposition is described in Appendix A. This submodel adopted the concept of two stacked mulch layers, where only the layer in contact with the soil is subject to decomposition (Thorburn *et al.*, 2001). Although several empirical parameters still are optimized on observed data, model simulations are essential for understanding the interaction between crop residue quality and its location in soil.

The aim of this work is to study the influence of crop residue location on water, carbon and nitrogen dynamics in soil, in interaction with residue quality. Modelling allowed to calculate cumulative carbon mineralization, gross fluxes of nitrogen mineralization and nitrate transport in soil, processes that otherwise were not accessible.

5.2 Materials and methods

5.2.1 Experimental set-up

The influence of crop residue location on water, carbon and nitrogen dynamics in soil was investigated for oilseed rape (referred to as RAPE) and rye residues (referred to as RYE). A detailed description of the RAPE experiment is given in Chapter 3, the RYE experiment was conducted following the same protocol.

The soil was sampled from the experimental site of INRA, Mons-en-Chaussée, Northern France, on 10/04/2002 (RAPE) and 25/09/2002 (RYE). Temporal and spatial variability of soil sampling induced small changes in soil properties (Table 5.1). The soil was a silt loam, Orthic Luvisol, and has not been cropped since 1994. The 0-25 cm soil layer was sampled, sieved (< 2 mm) at field moisture content (0.17 g g^{-1} for RAPE and 0.14 g g^{-1} for RYE) and stored in plastic bags at 4°C prior to use. The soil was preincubated for 2 weeks at 20°C before the start of the experiments.

The fresh organic matter added to the soil was mature oilseed rape (*Brassica napus* L.) and young rye (*Secale cereale*), both labelled ^{13}C and ^{15}N. The oilseed rape and rye crops were grown under hydroponic conditions in a labelling plant growth chamber, with enriched ^{13}C-CO_2 atmosphere and in a nutrient solution with ^{15}N-KNO_3 (Trinsoutrot *et al.*, 2000a). The oilseed rape residue consisted of a mixture of leaves, stalks, branches and pods. For the rye residue, only the green leaves were used. Both residues were chopped at 1 cm before application to the soil. The C and N content of the residues with their atom % excess and the

biochemical composition determined by proximate analysis (Van Soest, 1963) are given in Table 5.2.

Table 5.1 Selected soil properties of the soil sampled at the experimental site in Mons-en-Chaussée (France)

			RAPE	RYE
soil texture	clay	/ g kg^{-1}	134	166
	fine silt	/ g kg^{-1}	320	321
	coarse silt	/ g kg^{-1}	496	469
	fine sand	/ g kg^{-1}	38	34
	coarse sand	/ g kg^{-1}	12	9
organic C		/ g kg^{-1}	6.7	6.9
total nitrogen		/ g kg^{-1}	0.9	0.8
total carbonate		/ g kg^{-1}	7.0	6.0
CEC		/ $cmol_c$ kg^{-1}	8.1	8.6
pH (water)			8.2	8.3

Table 5.2 Selected chemical and biochemical properties of the oilseed rape and rye residues

RAPE	mass / %	C / %[a]	C / %[b]	^{13}C / % a.e.[c]	N / %[a]	N / %[b]	^{15}N / % a.e.[c]	C/N
Total residue	99.9	42.2	99.9	2.88	1.45	100.0	9.73	29
Soluble fraction	45.6	35.5	39.0	n.a.	1.75	71.0	n.a.	20
Hemicellulose	14.4	36.4	12.6	n.a.	0.75	9.6	n.a.	49
Cellulose	33.2	48.3	38.7	n.a.	0.39	11.4	n.a.	125
Lignin + ash	6.7	59.2	9.6	n.a.	1.33	8.0	n.a.	44

RYE	mass / %	C / %[a]	C / %[b]	^{13}C / % a.e.[c]	N / %[a]	N / %[b]	^{15}N / % a.e.[c]	C/N
Total residue	100.0	43.4	100.1	2.90	2.70	100.1	9.50	16
Soluble fraction	52.5	39.2	47.5	n.a.	2.65	51.7	n.a.	15
Hemicellulose	24.9	49.2	28.2	n.a.	4.61	42.6	n.a.	11
Cellulose	21.2	46.3	22.7	n.a.	0.46	3.6	n.a.	101
Lignin + ash	1.4	53.4	1.7	n.a.	4.44	2.2	n.a.	12

[a] % C and N in mass of biochemical fraction; [b] % of total residue-C and -N; [c] atom % excess

Plastic cylinders (PVC, 15.4 cm inner diameter, 30 cm high) with perforated bases were used to contain 25 cm of soil, compacted at 1.3 g cm^{-3}. Oilseed rape or rye residues were applied at the soil surface (referred to as SURF) or homogeneously mixed in the 0-10 cm soil layer before compaction (referred to as INC) at a rate of 13.8 g dry matter per column, equivalent to a return of 7.4 t ha^{-1}. Control columns without addition of fresh organic matter (referred to as CTRL) were prepared. At the start of a 9-week incubation period, rain with an intensity of 12 mm $hour^{-1}$ was applied with a rainfall simulator on all of the soil columns to raise the

volumetric soil water content to 0.34 cm^3 cm^{-3}. No drainage was observed. Subsequently, the soil columns were transferred in a climate chamber and left uncovered at 20°C and 70% relative air humidity to allow evaporation. After 3, 6 and 9 weeks of incubation, soil columns were placed again under the rainfall simulator until the water lost by evaporation was replenished. Details of the experimental conditions and rainfall simulator are described in Chapter 3. Table 5.3 summarizes the initial experimental conditions.

Table 5.3 Description of initial conditions for the RAPE and RYE experiment

Parameter	**RAPE**	**RYE**
Amount of soil (kg column^{-1})[a]	6.022	6.022
Initial N-NO_3^- in soil (mg kg^{-1} soil)	9.80	29.85
Amount of residues added (g column^{-1})[a]	13.78	13.78
N added by residue (g column^{-1})	0.12	0.37
C added by residue (g column^{-1})	5.82	5.98
Initial mulch thickness for SURF	1 cm	2 cm
Depth of incorporation for INC treatment	from 0 to 10 cm	from 0 to 10 cm
Temperature (°C)	20	20
Incubation time (d)	64	64
Days for rain application (d)	0, 21, 42, 63	0, 21, 42, 63

[a] dry weight

For each treatment (CTRL, SURF, INC) of both residues (RAPE, RYE), two columns were used for semi-continuous measurements (i.e. total of 12 columns). At 6 and 14 cm soil depth, the volumetric water content was measured by horizontally inserted TDR-probes (3 rods, 8 cm). The measurements were registered every hour on a TRASE system (Soilmoisture Equipment Corp.). At the same soil depth, the soil water potential was determined using tensiometers with porous cups of 5 cm (RhizoCera ø 3 mm, Rhizosphere Research Products), connected to differential pressure sensors (CZ5022/2, EuroSensor). Measurements of the soil water potential were stored on a CR10X data logger (Campbell Scientific). Mass loss of the columns was used to calculate daily evaporation rates.

The flux of CO_2 from the soil surface to the atmosphere was calculated from the accumulation rate of CO_2 in the headspace of the columns. During a 3-min period, the columns were sealed with a cover connected to an infrared gas analyser (UNOR 610, Maihak). A fan inside the 'closed chamber' provided homogenous mixing of the air. The slope of a linear regression through the increase of CO_2 concentration over time was used to calculate the CO_2 flux. Measurements were performed on a daily base in the beginning of every evaporation cycle and every 2 or 3 days after the initial flush of microbial activity.

For the SURF treatment, three separate columns per residue were constructed with 'detachable' mulch (i.e. total of 6 columns): residues were placed on a 1-mm mesh to allow measurements of the mulch mass. These data were used to calculate the gravimetric water content of the mulch, after correction of the mass for leached and mineralized C.

Finally, nine columns for each treatment (CTRL, SURF, INC) of both residues (RAPE, RYE) were dedicated for destructive measurements (i.e. total of 54 columns). After 3, 6 and 9 weeks of evaporation, three replicate columns of CTRL, SURF and INC were sliced in four soil layers: 0-5 cm, 5-10 cm, 10-17.5 cm and 17.5-25 cm. For the SURF treatment, the mulch was removed and dried at 60° C; for the INC treatment, the coarse residue fraction (> 2 mm) was separated from the fine fraction (< 2 mm) and also dried at 60°C. Immediately after destruction, the gravimetric water content was determined on each soil layer (24 hours at 105° C). Soil mineral nitrogen was extracted with 1 *M* KCl (30 minutes shaking, soil-to-solution ratio 1/2.5). Soil extracts were centrifuged (20 minutes at 5800 *g*), filtered and stored at –20° C until analysis. Mineral nitrogen (NO_3^--N and NH_4^+-N) was measured by continuous flow colorimetry (TRAACS 2000, Bran & Luebbe). The total C and N content of soil and recovered plant residues, with atom % excess, were determined using an elemental analyser (NA 1500, Carlo Erba) coupled to a mass spectrometer (Fisons Isochrom, Manchester UK). Soil adhering to the recovered residues was detached and analysed separately for C and N.

5.2.2 Model description

Transport of water and nitrate in soil was simulated with the one-dimensional mechanistic model PASTIS (Prediction of Agricultural Solute Transport In Soil: Lafolie, 1991; Garnier *et al.*, 2001). The submodel CANTIS (Carbon and Nitrogen Transformations In Soil) simulated the biotransformations of carbon and nitrogen in soil. The PASTIS model, originally designed for incorporated residues, was adapted to take into account the physical effects of mulch on rain interception and evaporation (Findeling *et al.*, submitted), and the specific dynamics of

mulch decomposition (see Appendix A). In contrast to models used for prediction (e.g. Roth-C), PASTIS is considered as a research tool to study mechanisms in residue decomposition and transport processes.

The PASTIS model has previously been calibrated for incorporated residues (Garnier *et al.*, 2003). The present data for incorporated RAPE and RYE were used for model validation. Only soil-specific hydraulic parameters and soil- and residue-dependent biological parameters were optimized on experimental data, while all other model parameters were used from Garnier *et al.* (2003). The adapted model, $PASTIS_{mulch}$, is actually one of the only models conceptualizing residue mulch decomposition. However, mechanisms are not yet fully understood and mulch decomposition is still based on a number of empirical parameters. The decomposition rate of mulch is considered as a function of the mass fraction of the residues in contact with the soil, its volumetric water content and its temperature. In $PASTIS_{mulch}$, soil nitrogen for the zymogenous biomass is supplied from a superficial soil layer with given depth. The supply of the pool of residue mass in contact with the soil with residues not in contact with the soil is also regulated by an empirical factor. Obtained data for mulch decomposition of RAPE and RYE were used for model calibration, which has not been done before.

5.2.3 Boundary conditions

The $PASTIS_{mulch}$ model is applied to the 25-cm monoliths of the SURF and INC treatment of RAPE and RYE. Depth is set to zero at the soil surface. Rain intensity and actual evaporation are imposed to the model as the surface boundary condition for water. When the topsoil water potential reaches a limit, $h_{lim} = -1.0 \times 10^8$ Pa, this potential is set as a Dirichlet condition at the soil surface. At the bottom, a zero flux condition is imposed. A zero flux boundary condition is set as well for solutes at the soil surface and at the bottom of the soil columns, which means that there is no drainage. Temperature is constant and set to 20°C in the whole system. The equations of $PASTIS_{mulch}$ are solved by using numerical finite elements technique on a discrete mesh of linear elements (0.5 cm) and a time step between 0.001 and 360 s.

5.2.4 Initial conditions

Initial water conditions of $PASTIS_{mulch}$ were given by a constant volumetric water content in the soil profile: 0.22 m^3 m^{-3} for RAPE and 0.18 m^3 m^{-3} for RYE. Soil solutes were initialized

with constant concentration profiles: $[NO_3^-]$ = 0.257 mg cm^{-3} for RAPE, $[NO_3^-]$ = 0.783 mg cm^{-3} for RYE and $[NH_4^+]$ = 0.001 mg cm^{-3} for both residues.

The initial conditions of organic pools and microbial biomass in the CANTIS submodel are listed in Table 5.4. The soluble fraction (SOL) of the added residues was extracted by shaking in cold water for 30 minutes. The neutral detergent fraction (NDF), hemicelluloses (HEM), cellulose (CEL), and lignin (LIG) fractions were determined by proximate analysis (Van Soest, 1963). The rapidly decomposable material (RDM) is the difference NDF-SOL. The amount of fresh organic matter (FOM) in CANTIS is defined as the sum of RDM, HEM, CEL and LIG. The concentrations of total C and N in the SOL, NDF, HEM, CEL and LIG fractions were determined with an elemental analyzer (NA1500, Carlo Erba).

The microbial biomass C was determined by a modified fumigation-extraction method proposed by Vance *et al.* (1987). We calculated the microbial biomass C from difference in soluble C between fumigated and unfumigated soil, and dividing by a coefficient K_{EC} = 0.38. The initial amount of biomass C in soil was 128.3 mg C kg^{-1} for RAPE and RYE. The N:C ratio of the zymogenous biomass for RAPE and RYE was obtained by fitting the model to experimentally obtained C and N mineralization curves of soil with incorporated rape and rye residues, as described in Appendix A.

Table 5.4 Initial conditions of the organic pools and microbial biomass used in the PASTIS model (SOIL refers to parameters used by PASTIS, MULCH refers to parameters used by the submodule $PASTIS_{mulch}$)

	RAPE		RYE	
	INC	SURF	INC	SURF
Amount of fresh organic matter (FOM) - SOIL / mg C kg^{-1} soil	2086.0	104.5	1690.0	104.5
- MULCH / g C m^{-2}		237.9		190.8
Proportion of rapidly decomposable material in FOM - SOIL / g C g^{-1} C	0.258	0.500	0.177	0.500
- MULCH / g C g^{-1} C		0.258		0.177
Proportion of hemicelluloses in FOM - SOIL / g C g^{-1} C	0.153	0.000	0.441	0.000
- MULCH / g C g^{-1} C		0.153		0.441
Proportion of cellulose in FOM - SOIL / g C g^{-1} C	0.471	0.500	0.355	0.500
- MULCH / g C g^{-1} C		0.471		0.355
Proportion of lignin in FOM - SOIL / g C g^{-1} C	0.118	0.000	0.027	0.000
- MULCH / g C g^{-1} C		0.118		0.027
Amount of soluble organic compounds - SOIL / mg C kg^{-1} soil	460.7	31.2	929.7	31.2
- MULCH / g C m^{-2}		51.5		108.2
Amount of zymogenous microbial biomass - SOIL / mg C kg^{-1} soil	32.10	16.05	32.10	16.05
- MULCH / mg C kg^{-1} soil		16.05		16.05
Amount of autochthonous microbial biomass / mg C kg^{-1} soil	96.2	96.2	96.2	96.2
Amount of humified organic matter / mg C kg^{-1} soil	8372	8372	8372	8372
N:C ratio of rapidly decomposable material - SOIL / g N g^{-1} C	0.0304	0.0448	0.0852	0.0448
- MULCH / g N g^{-1} C		0.0304		0.0852
N: C ratio of hemicelluloses - SOIL / g N g^{-1} C	0.0454	-	0.1018	-
- MULCH / g N g^{-1} C		0.0454		0.1018
N: C ratio of cellulose / g N g^{-1} C	0.0000	0.0000	0.0000	0.0000
N: C ratio of lignin - SOIL / g N g^{-1} C	0.0224	-	0.0804	-
- MULCH / g N g^{-1} C		0.0224		0.0804
N: C ratio of soluble organic pool - SOIL / g N g^{-1} C	0.0720	0.0667	0.0620	0.0667
- MULCH / g N g^{-1} C		0.0720		0.0620
N: C ratio of zymogenous microbial biomass / g N g^{-1} C	0.0815[a]	0.0815[a]	0.1032[a]	0.1032[a]
N: C ratio of autochthonous microbial biomass / g N g^{-1} C	0.1250	0.1250	0.1250	0.1250
N: C ratio of humified organic matter / g N g^{-1} C	0.1056	0.1056	0.1056	0.1056

[a] obtained by optimization

5.2.5 Parameter optimization: water flow parameters

The soil water retention curve $h(\theta)$ was obtained for each soil treatment using TDR and tensiometer measurements in the columns (matric potential in the range of -5.0×10^3 to -3.0×10^4 Pa) and the pressure extractor method (Klute & Dirksen, 1986) for lower matric potentials (-5.0×10^4, -1.0×10^5, -3.0×10^5 and -1.5×10^6 Pa). The experimental data were fitted with the model of Van Genuchten (1980). The hydraulic conductivity curve $K(\theta)$ was obtained by inverse modelling with PASTIS, also using the Van Genuchten equation (1980). Details of the fitting procedure are given in Appendix A.

5.2.6 Parameter optimization: biological parameters

Soil- and residue-specific biological parameters of the CANTIS submodel were acquired by fitting the model to experimentally obtained mineralization curves of C and N. The decomposition rate of the autochthonous biomass (k_A) and humified organic matter (k_H), and the humification coefficient by the autochthonous biomass (h_A) were optimized with mineralization data of native organic matter in the control soil; the decomposition rate of the zymogenous biomass (k_Z) and the humification coefficient by the zymogenous biomass (h_Z) were optimized with mineralization data from incorporated rape and rye residues. The incubation experiment and justification of selected parameters are described in Appendix A.

5.2.7 Model efficiency coefficient

The model was evaluated graphically and statistically. Simulated soil matric potential, residual ^{13}C, CO_2 fluxes and the amount of NO_3^--N in the different soil layers were compared with measured data. The efficiency, E_f (-), was used to assess model performance (Smith *et al*., 1996):

$$E_f = \frac{\sum_{i=1}^{n}(m_i - \bar{m})^2 - \sum_{i=1}^{n}(s_i - m_i)^2}{\sum_{i=1}^{n}(m_i - \bar{m})^2}$$

where m_i and s_i are the measured and simulated results, and $\bar{m}$ is the average of the n measured results.

5.3 Results

5.3.1 Water dynamics

For the SURF treatment, water loss from the soil columns by evaporation was reduced with 47 – 59 % for RAPE and with 57 – 68 % for RYE, compared to CTRL (Table 5.5). For the INC treatment, water loss was for both residues and at all times comparable to CTRL. The largest reductions in evaporation for SURF were observed in the beginning of the incubation, when the entire soil surface was covered with mulch. Over time, mulch decomposed and water evaporation from the soil surface became less restricted. Differences in soil evaporation between RAPE and RYE are attributed to physical differences in the applied mulch. For RAPE, mulch components were of relatively large volume compared to RYE leaves and the irregular shapes of oilseed rape stalks, branches, leaves and pods resulted in a considerable 'porosity' of the mulch layer. In contrast, mulching leaves of young rye completely covered the soil surface, physically separating soil from atmosphere.

Table 5.5 Distribution of the soil water content in the soil profile after 3, 6 and 9 weeks of incubation, for CTRL, SURF and INC of the RAPE and RYE treatment. Values are the average of 3 replicates; maximum standard error was 0.01 $cm^3\ cm^{-3}$.

	CTRL			SURF			INC		
RAPE	/ $cm^3\ cm^{-3}$			/ $cm^3\ cm^{-3}$			/ $cm^3\ cm^{-3}$		
Soil layer	Week 3	Week 6	Week 9	Week 3	Week 6	Week 9	Week 3	Week 6	Week 9
0-5 cm	0.15	0.16	0.18	0.23	0.23	0.22	0.14	0.15	0.16
5-10 cm	0.16	0.18	0.19	0.23	0.23	0.22	0.16	0.18	0.17
10-17.5 cm	0.18	0.19	0.20	0.23	0.23	0.22	0.17	0.18	0.18
17.5-25 cm	0.20	0.19	0.21	0.24	0.24	0.22	0.18	0.19	0.19

	CTRL			SURF			INC		
RYE	/ $cm^3\ cm^{-3}$			/ $cm^3\ cm^{-3}$			/ $cm^3\ cm^{-3}$		
Soil layer	Week 3	Week 6	Week 9	Week 3	Week 6	Week 9	Week 3	Week 6	Week 9
0-5 cm	0.15	0.13	0.12	0.23	0.22	0.21	0.16	0.16	0.15
5-10 cm	0.17	0.15	0.16	0.23	0.21	0.21	0.18	0.19	0.17
10-17.5 cm	0.18	0.17	0.17	0.23	0.21	0.21	0.20	0.19	0.18
17.5-25 cm	0.18	0.17	0.18	0.23	0.22	0.21	0.21	0.20	0.19

Differences in soil evaporation between SURF on the one hand, and CTRL and INC on the other hand, induced differences in the distribution of water through the soil profile. Without mulch, the gravimetric soil water content increased with increasing soil depth for CTRL and INC. For SURF, a higher gravimetric soil water content was observed in the soil profile than for CTRL and INC, and smaller water gradients between top and bottom of the columns were measured. The higher soil water content in the 0-5 cm soil layer for RYE compared to RAPE indicates a limitation in the evaporation rate of soil water to the atmosphere. These findings confirm the hypothesis that the mulch from RYE acts more as a barrier against evaporation than mulch from RAPE.

The experimentally obtained water retention curves, by combining data of TDR probes and tensiometers, did not show significant differences between residue treatments (CTRL, SURF, INC) for RAPE and RYE (data not shown). Although no significant effect was found of residue location on water retention in soil, the $PASTIS_{mulch}$ model was not able to simulate the change in soil matric potential over time for each treatment with one common set of hydraulic parameters. Therefore, water transport in the model was calibrated on tensiometer data of each individual treatment, which resulted in very good simulations of the water potential over time (Figure 5.1), as indicated by the model efficiency coefficients (Table 5.6). This was essential for further model evaluation, because water dynamics regulate the transport of nitrates in the soil and the decomposition rate of organic matter is coupled to the soil water potential. Water flow parameters used for modelling are listed in Table 5.7.

Table 5.6 Model efficiency coefficients (E_f) for evaluation of $PASTIS_{mulch}$

	Soil matric potential	Residual ^{13}C	CO_2 flux [a]	CO_2 flux [b]	NO_3^--N (0-5 cm)
RAPE INC	0.876	0.978	-4.935	0.567	-0.813
RAPE SURF	0.963	0.813	-0.121	0.904	0.795
RYE INC	0.897	0.974	-4.729	0.856	-5.351
RYE SURF	0.915	0.924	-9.132	0.225	0.725

[a] all observations included; [b] with abstraction of initial decomposition phase

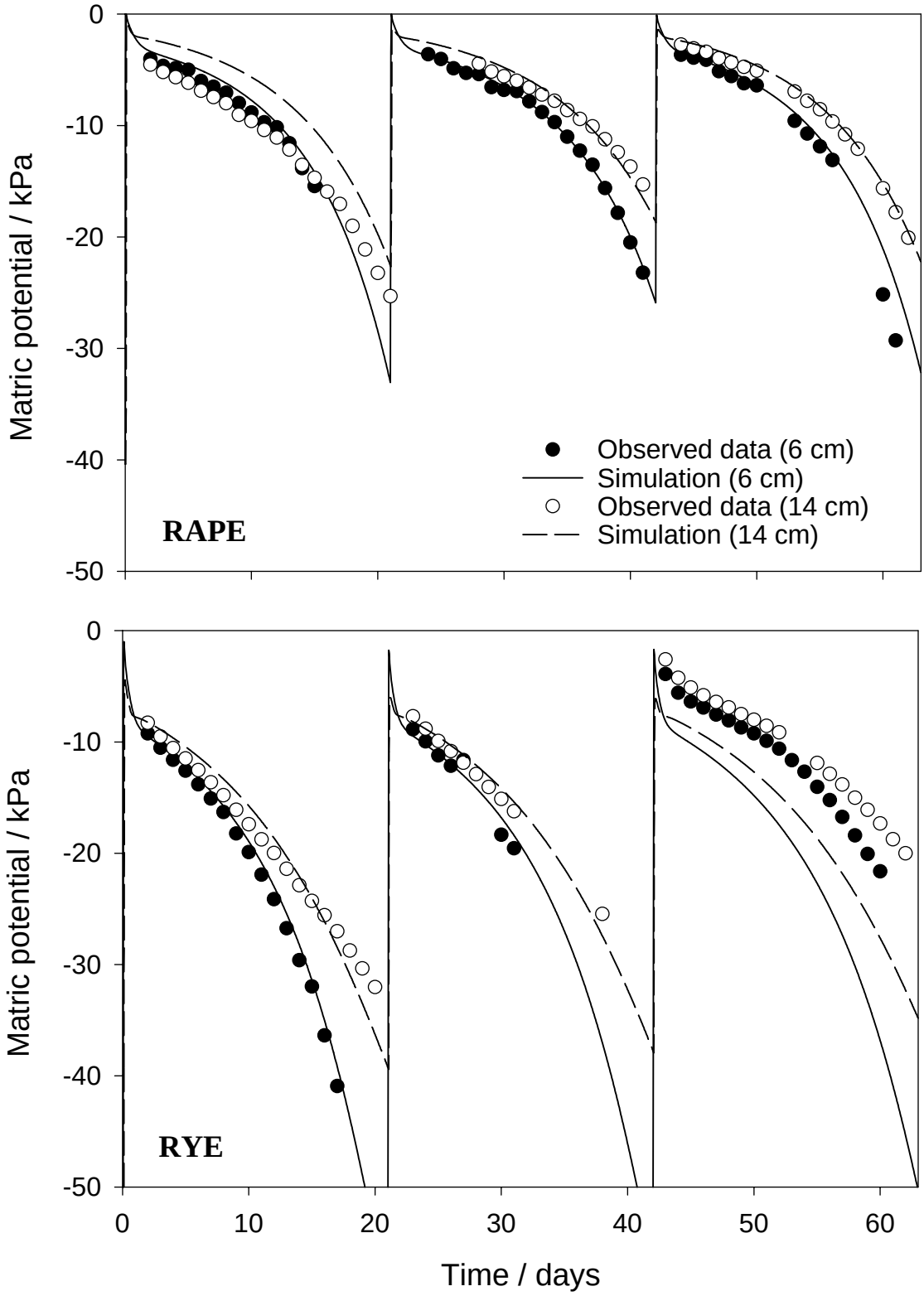

Figure 5.1 (a) Comparison between the observed and simulated change in soil matric potential over time, determined at 6 cm and 14 cm soil depth, with incorporation (INC) of RAPE and RYE residues.

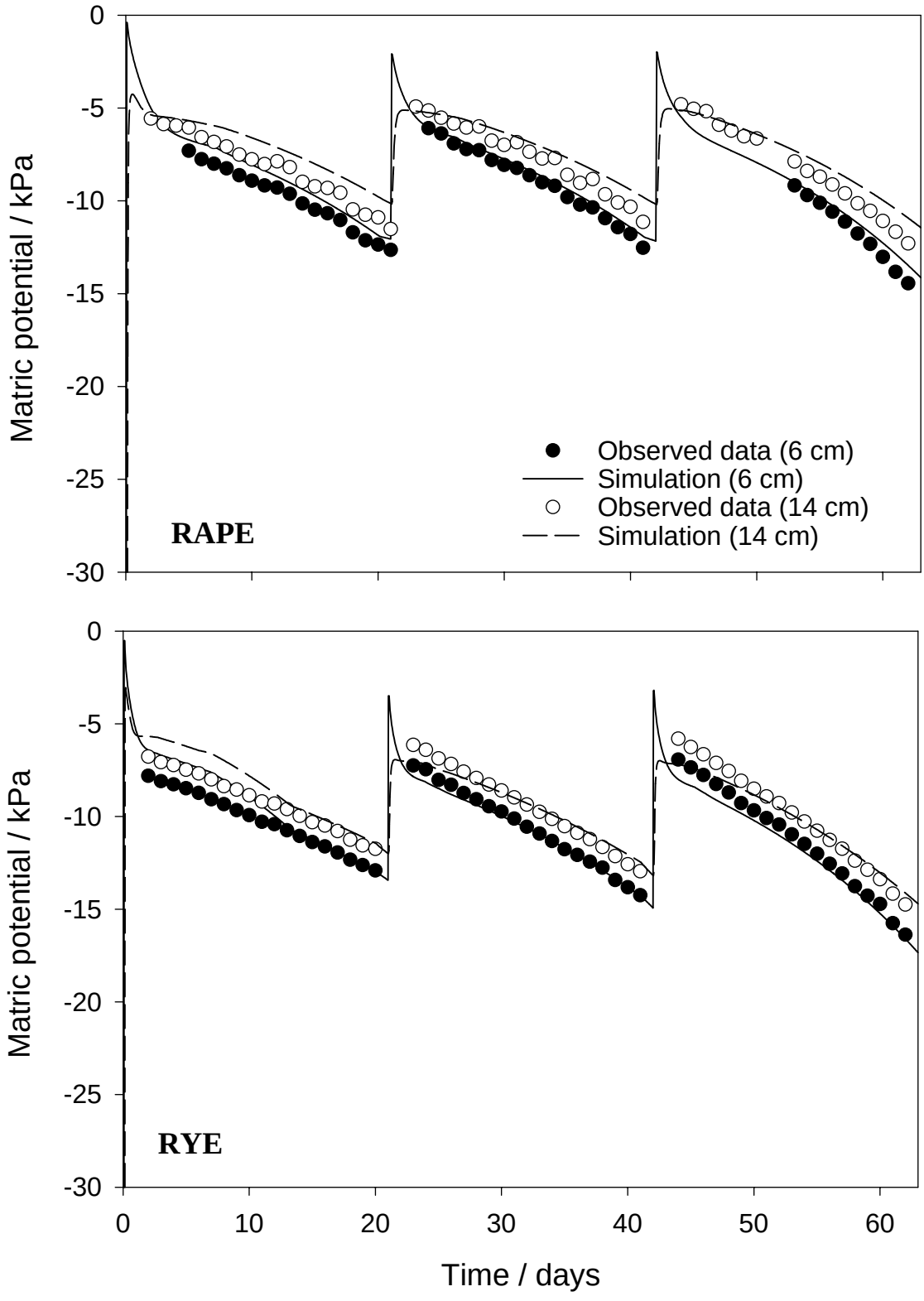

Figure 5.1 (b) Comparison between the observed and simulated change in soil matric potential over time, determined at 6 cm and 14 cm soil depth, with surface application (SURF) of RAPE and RYE residues.

Table 5.7 Hydraulic parameters of soil retention and soil conductivity curves for RAPE and RYE used in $PASTIS_{mulch}$

Function	Hydraulic parameters	Soil columns			
		RAPE		RYE	
		INC	SURF	INC	SURF
$h(\theta)$	θ_s / $cm^3\ cm^{-3}$	0.420	0.535	0.530	0.500
	θ_r / $cm^3\ cm^{-3}$	0.000	0.000	0.000	0.000
	α / cm^{-1}	0.258	0.259	0.107	0.107
	n	1.142	1.185	1.228	1.228
$K(\theta)$	K_s / cm $hour^{-1}$	3.20	6.00	30.00	15.00
	m	1.25	1.29	1.25	1.25

5.3.2 Residue decomposition

Measured from residual ^{13}C in soil, 82 % (SURF) and 45 % (INC) of the residue-C for RAPE, and 66 % (SURF) and 32 % (INC) of the residue-C for RYE was still present in the soil after 9 weeks of incubation (Figure 5.2). For INC, residue-C gradually decreased with every sampling point in the RAPE treatment, while the maximum amount of residue-C was already mineralized during the first 3 weeks of the RYE treatment. For SURF, more residue-C with RYE was mineralized during the first 3 weeks of incubation than after 9 weeks with RAPE. Differences in C mineralization between RAPE and RYE are mainly explained by the differences in residue quality. The lower C:N ratio, a larger amount of the soluble fraction and less lignin in the rye leaves compared to the oilseed rape residues contributed to faster and more advanced residue decomposition in RYE than in RAPE after 9 weeks of incubation.

Optimized biological parameters for the $PASTIS_{mulch}$ model are summarized in Table 5.8. The model simulated well residual ^{13}C in the soil (Table 5.6). For RYE, although final values of simulated residual ^{13}C were in accordance with measured values, the model was not able to simulate the initial fast residue decomposition for INC.

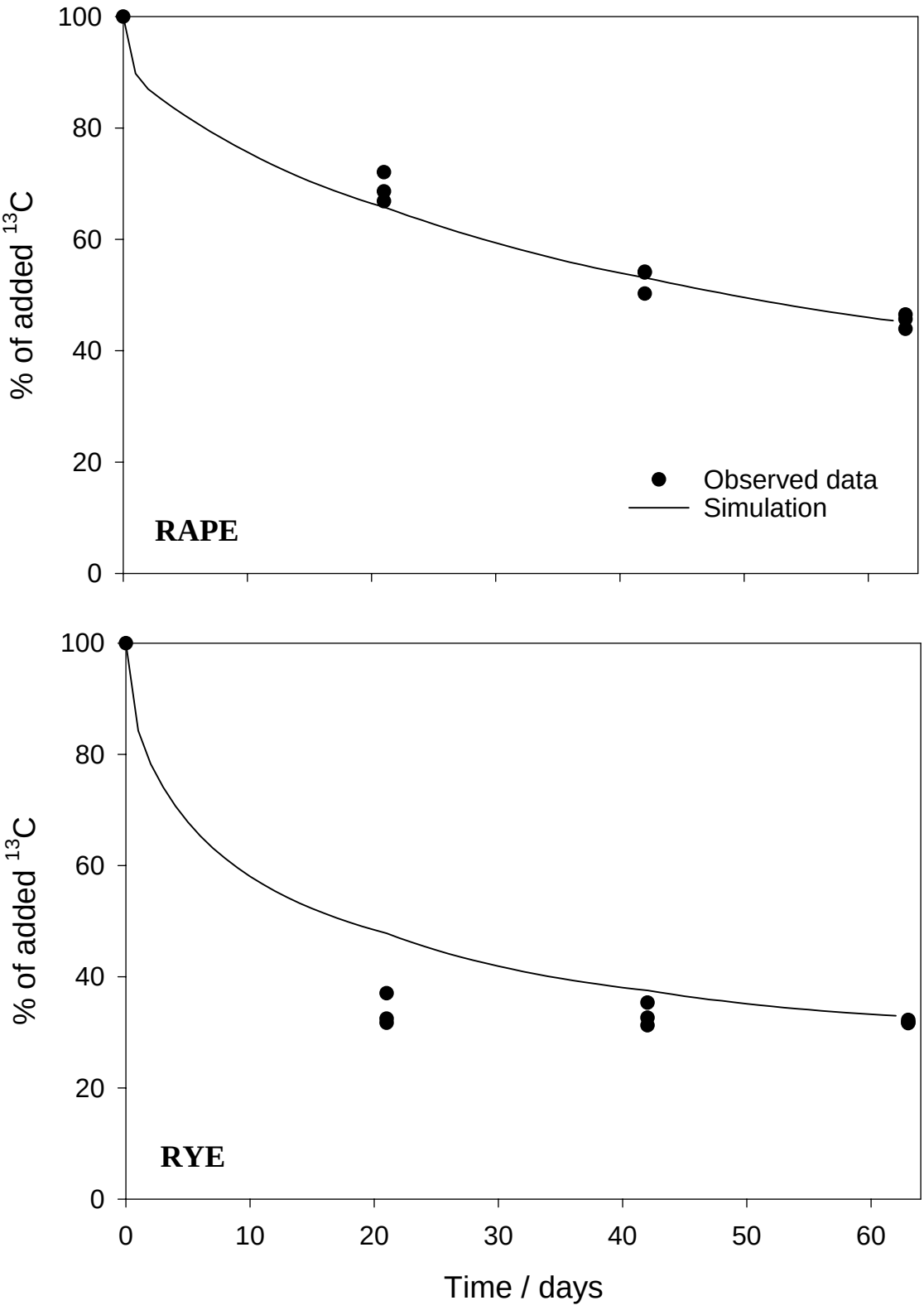

Figure 5.2 (a) Comparison between the observed and simulated change in total residual ^{13}C over time, expressed in % of added ^{13}C, with incorporation (INC) of RAPE and RYE residues.

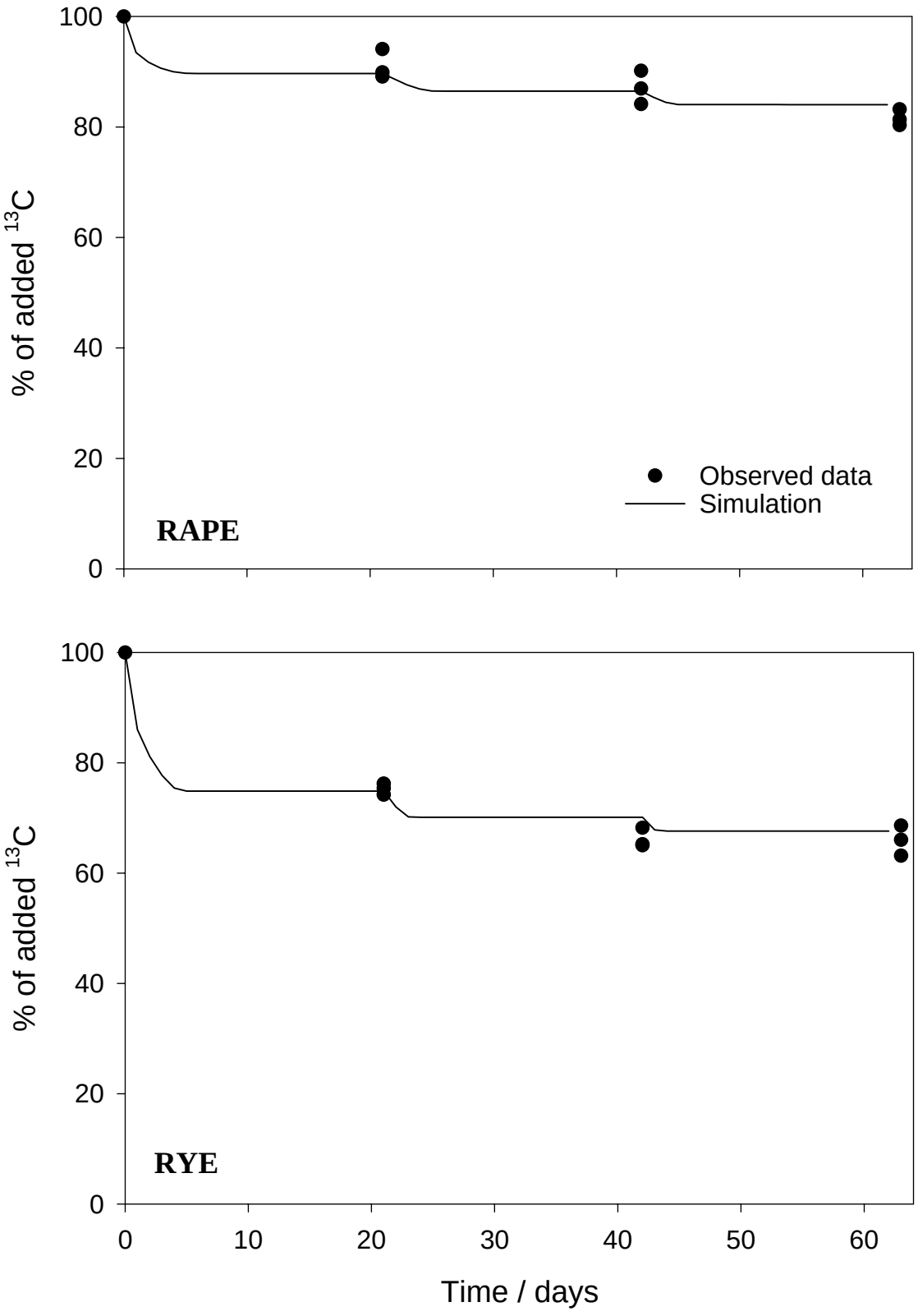

Figure 5.2 (b) Comparison between the observed and simulated change in total residual ^{13}C over time, expressed in % of added ^{13}C, with surface application (SURF) of RAPE and RYE residues.

Table 5.8 Symbols, units and values of biological parameters used in $PASTIS_{mulch}$

Symbol	Parameter	RAPE		RYE	
		INC	SURF	INC	SURF
k_A	Decomposition rate of autochthonous biomass (AUB) (d^{-1})	4.885×10^{-3}			
k_H	Decomposition rate of humified organic matter (HOM) (d^{-1})	0.253×10^{-3}			
h_A	Humification coefficient by AUB (-)	0.3761			
k_Z	Decomposition rate of zymogenous biomass (ZYB) (d^{-1})	0.0206		0.0490	
h_Z	Humification coefficient by ZYB (-)	0.1403		0.2629	

5.3.3 Carbon dioxide fluxes

The general pattern in the evolution of the CO_2 flux over time was correctly simulated for both residue locations of RAPE and RYE (Figure 5.3). However, a large difference was observed between measured and simulated CO_2 flux during the first days of decomposition. This difference is mainly attributed to an increased water-filled porosity near the soil surface, forcing CO_2 diffusion into water, which strongly reduced and delayed emission of CO_2 from soil to atmosphere. The same decrease in CO_2 flux measurements was observed after each rain event for INC, in spite of the stimulated microbial activity due to the increased soil water content. For SURF, this effect was of less importance, because most of the CO_2 produced from the mulch does not interact with the soil. With abstraction of the initial phase of decomposition, good model efficiency coefficients were obtained (Table 5.6), excepted for RYE-SURF. In this treatment, larger CO_2 flux measurements than simulated values are indicative for a priming effect, given the correct simulation of residue-C mineralization as observed with residual ^{13}C. Stimulation of microbial activity by leaching of soluble compounds of the mulch may have enhanced mineralization of native organic matter. This effect was not observed for RAPE, probably due to the smaller fraction of soluble compounds compared to RYE. Priming effect is not taken into account by the model, which means that the simulated CO_2 flux from [soil + residues] may be underestimated.

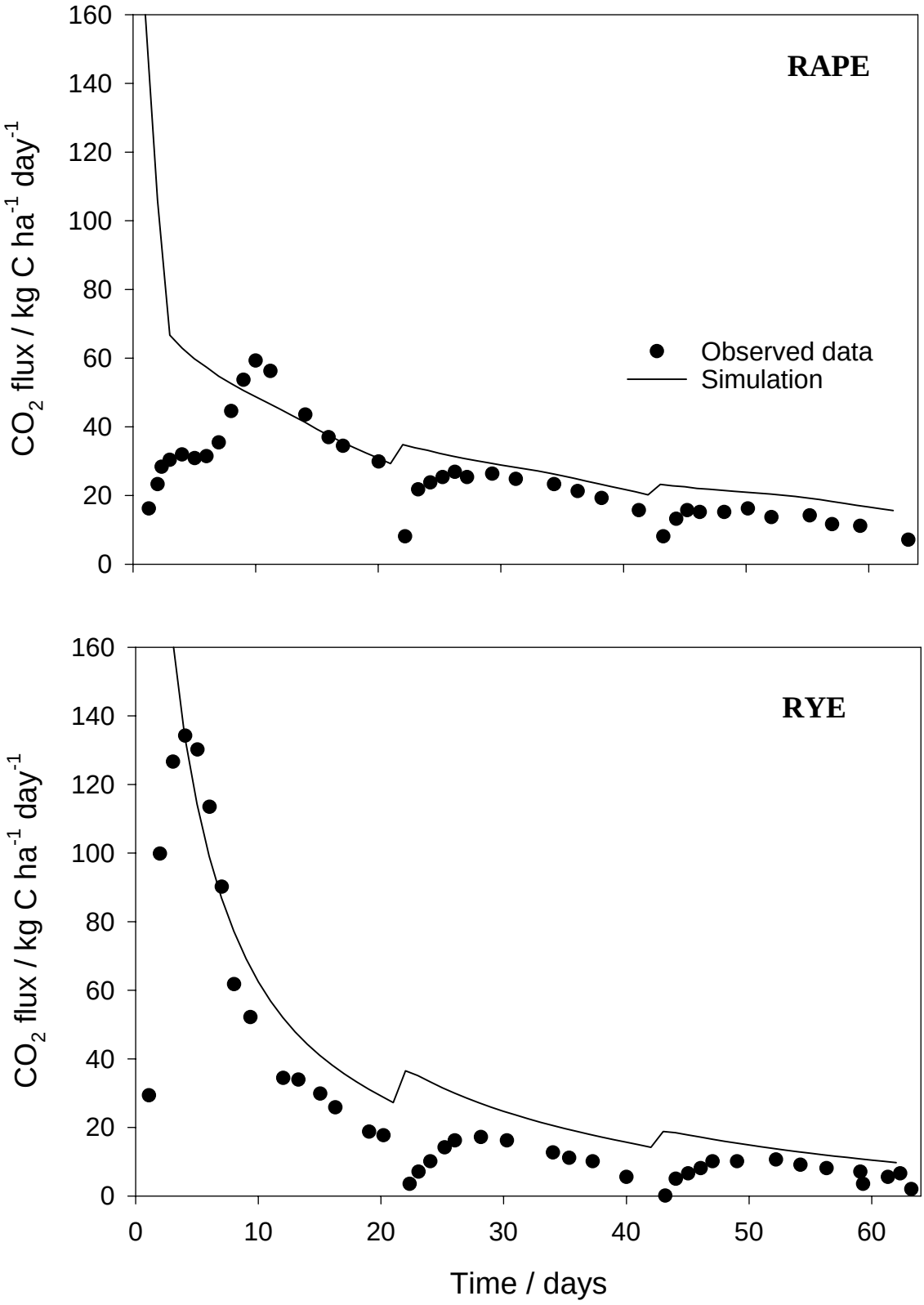

Figure 5.3 (a) Comparison between the observed and simulated change in CO_2 fluxes over time, expressed in kg C ha^{-1} day^{-1}, with incorporation (INC) of RAPE and RYE residues.

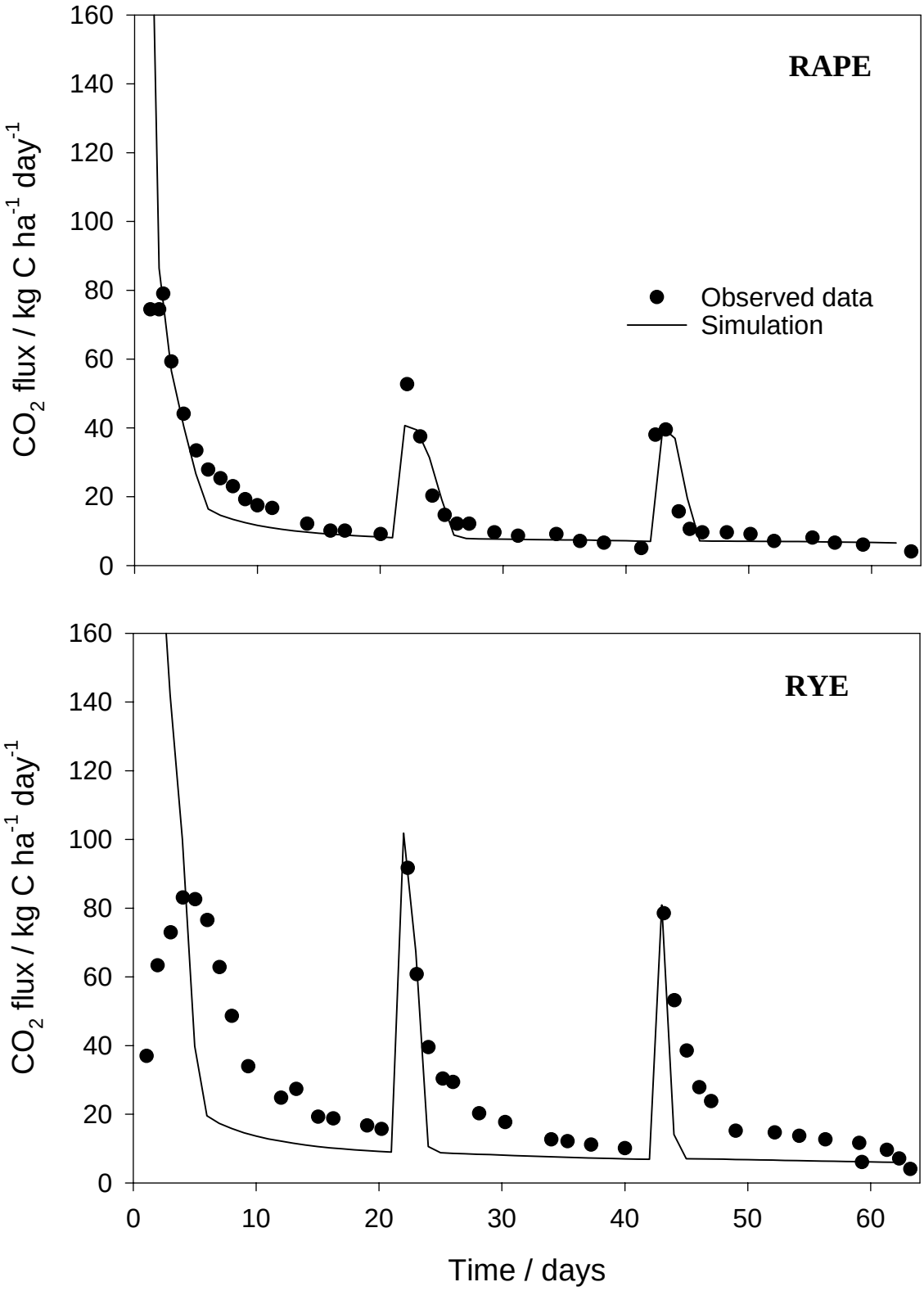

Figure 5.3 (b) Comparison between the observed and simulated change in CO_2 fluxes over time, expressed in kg C ha^{-1} day^{-1}, with incorporation (INC) of RAPE and RYE residues.

5.3.4 Nitrogen dynamics

Nitrate measurements in each soil layer (0-5 cm, 5-10 cm, 10-17.5 cm and 17.5-25 cm) supplied information over net N accumulation in soil at the end of each evaporation period (Table 5.9). Amounts of NH_4^+-N were negligible. For RAPE, a strong depletion in the NO_3^--N content was observed in the 0-5 cm soil layer for the INC treatment compared to SURF, which persisted over the 9-week incubation. During this period, SURF showed the largest amounts of nitrate in all soil layers. For RYE, in contrast to RAPE, larger amounts of nitrate were measured in the 0-5 cm soil layer of INC compared to SURF.

Simulation of nitrate accumulation in the different soil layers with $PASTIS_{mulch}$ is illustrated for the 0-5 cm soil layer (Figure 5.4). The general evolution in nitrogen dynamics was well simulated, although the model efficiency coefficients were quite low for the INC treatment (Table 5.6). Model efficiency was better for SURF than for INC, because in the SURF treatment additional optimizations were performed on the observed data to obtain specific parameters for mulch decomposition in $PASTIS_{mulch}$ (see Appendix A).

Table 5.9 Distribution of the amount of NO_3^--N in the soil profile after 3, 6 and 9 weeks of incubation, for CTRL, SURF and INC of the RAPE and RYE treatment. Values are the average of 3 replicates; standard errors are indicated between parentheses.

RAPE	CTRL / mg NO_3^--N kg^{-1}			SURF / mg NO_3^--N kg^{-1}			INC / mg NO_3^--N kg^{-1}		
Soil layer	Week 3	Week 6	Week 9	Week 3	Week 6	Week 9	Week 3	Week 6	Week 9
0-5 cm	15.9 (1.1)	17.1 (2.4)	21.4 (1.0)	14.3 (0.7)	20.5 (1.1)	22.0 (0.5)	0.4 (0.1)	4.2 (1.1)	9.5 (0.9)
5-10 cm	9.8 (0.2)	10.8 (0.2)	12.5 (0.4)	16.0 (0.4)	18.1 (0.7)	18.7 (0.1)	8.5 (0.6)	12.0 (0.5)	12.2 (0.1)
10-17.5 cm	11.6 (0.1)	12.8 (0.0)	14.5 (0.5)	16.5 (0.1)	17.9 (0.4)	19.9 (0.2)	14.8 (0.6)	14.7 (0.6)	13.8 (0.4)
17.5-25 cm	12.7 (0.3)	14.4 (0.2)	15.3 (1.5)	16.8 (0.7)	16.0 (0.5)	20.4 (0.3)	13.7 (0.4)	15.7 (0.3)	15.3 (0.6)

RYE	CTRL / mg NO_3^--N kg^{-1}			SURF / mg NO_3^--N kg^{-1}			INC / mg NO_3^--N kg^{-1}		
Soil layer	Week 3	Week 6	Week 9	Week 3	Week 6	Week 9	Week 3	Week 6	Week 9
0-5 cm	17.6 (0.5)	23.4 (1.9)	32.0 (1.9)	16.2 (2.6)	34.3 (5.4)	59.7 (2.6)	30.5 (6.7)	55.1 (2.9)	79.6 (6.4)
5-10 cm	22.0 (1.1)	17.9 (1.9)	23.7 (1.5)	18.4 (2.8)	20.2 (2.1)	36.8 (1.3)	28.0 (3.6)	27.5 (1.3)	34.8 (3.8)
10-17.5 cm	34.7 (1.9)	26.5 (2.3)	32.8 (2.1)	32.2 (1.5)	22.0 (0.9)	42.1 (5.4)	33.0 (2.6)	27.3 (1.7)	34.1 (4.3)
17.5-25 cm	41.2 (2.1)	32.6 (2.6)	37.9 (2.3)	29.2 (5.5)	20.5 (2.0)	44.1 (9.2)	43.9 (2.8)	30.9 (1.9)	31.3 (4.2)

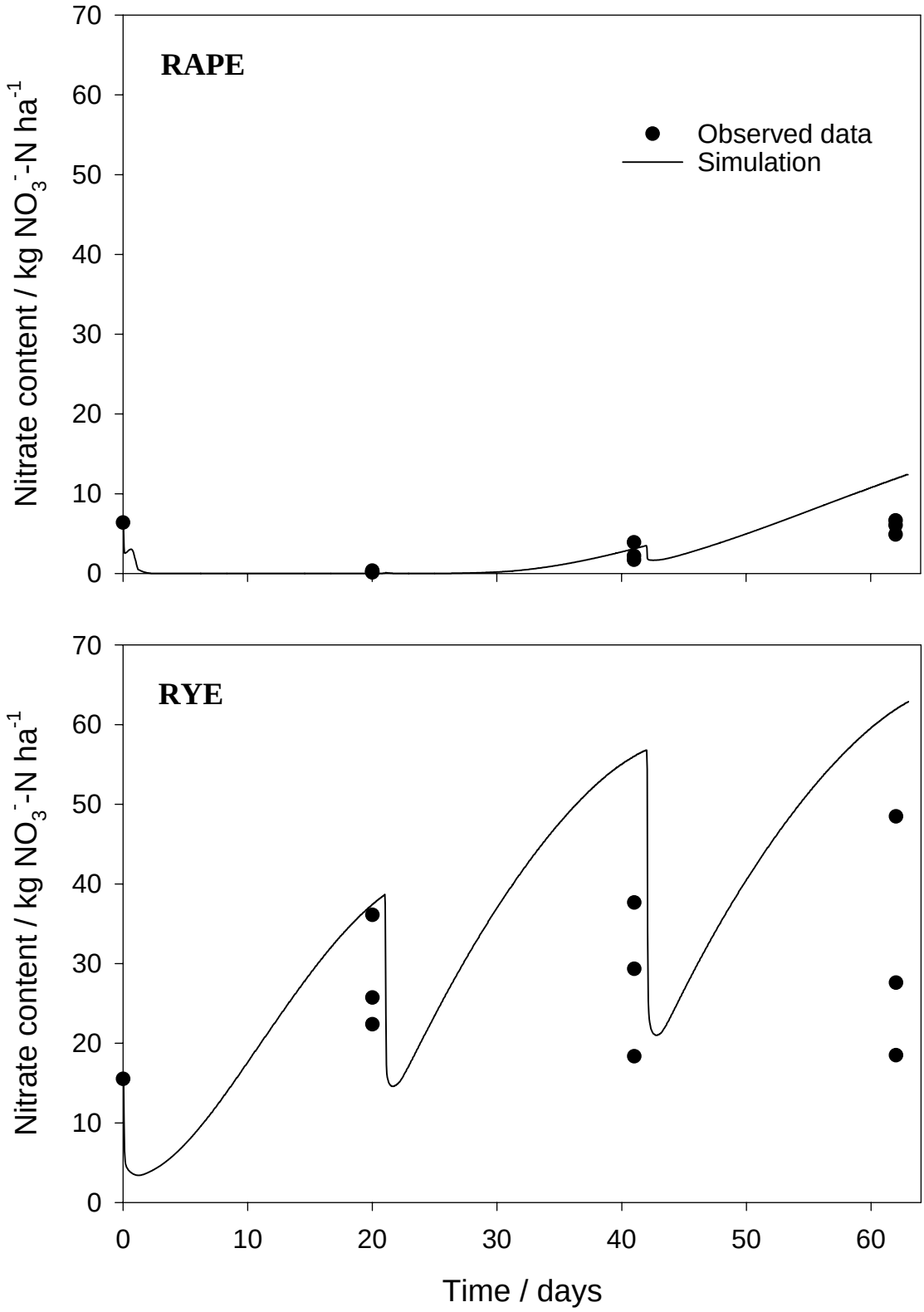

Figure 5.4 (a) Comparison between the observed and simulated change in the amount of nitrate in the 0-5 cm soil layer, expressed in mg NO_3^--N kg^{-1}, with incorporation (INC) of RAPE and RYE residues.

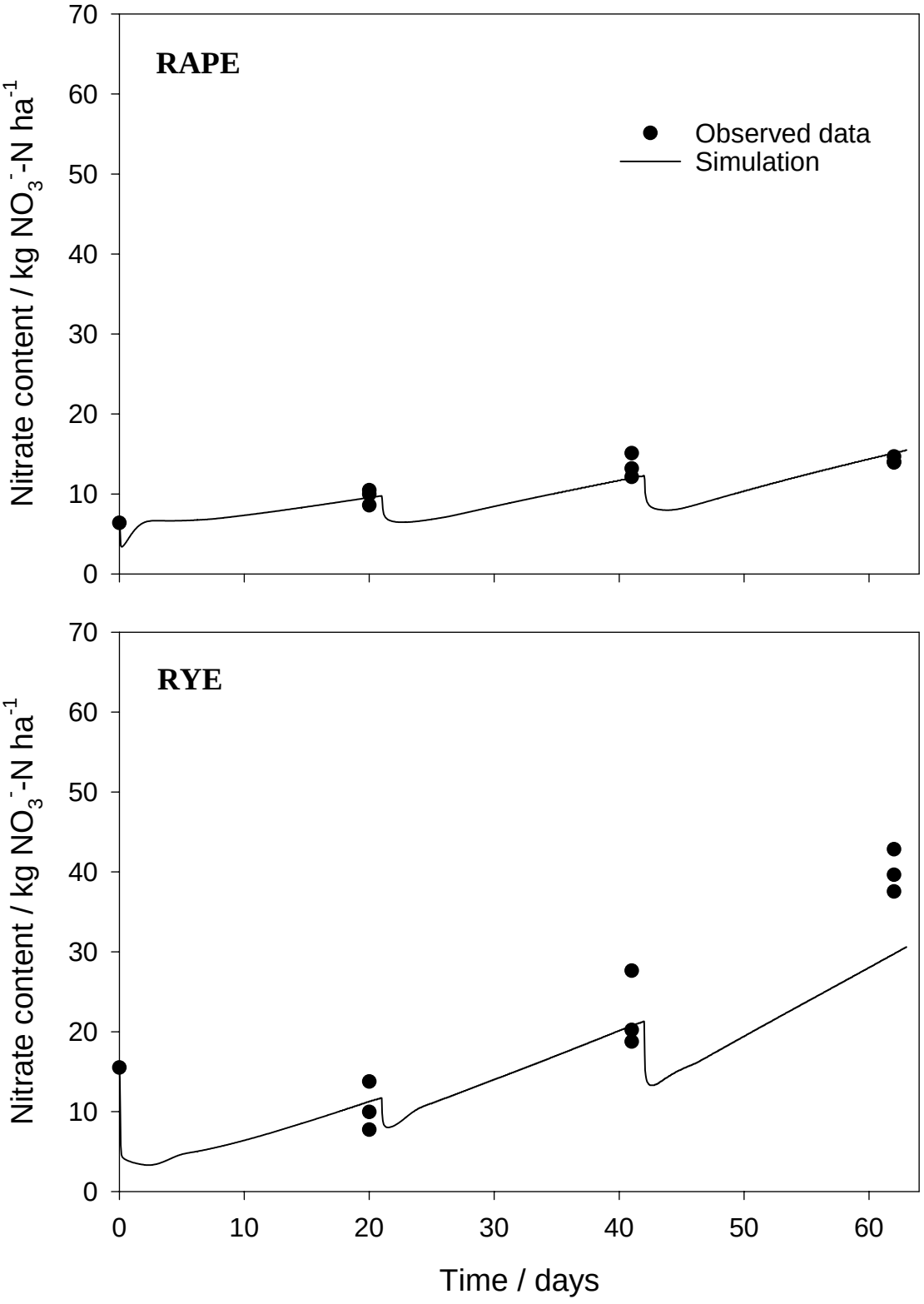

Figure 5.4 (b) Comparison between the observed and simulated change in the amount of nitrate in the 0-5 cm soil layer, expressed in mg NO_3^--N kg^{-1}, with surface application (SURF) of RAPE and RYE residues.

5.4 Discussion

The main objective of this work was to evaluate how crop residue location and physical and biochemical quality interact, affect water dynamics and consequently influence the decomposition process with associated C and N fluxes. To do so, the use of a mechanistic model such as PASTIS was crucial: firstly, to access gross fluxes (e.g. gross mineralization and gross immobilization) that cannot be easily determined and from which depends the net mineralization of nitrogen; then, to estimate nitrate transport in the soil and potential leaching down the soil profile; and lastly, to extrapolate some fluxes to the entire experimental period, e.g. to calculate cumulative C mineralization.

5.4.1 Influence of residue location and quality on water dynamics

Crop residue location affected significantly water dynamics in soil. Evaporation was reduced when residues were left at the soil surface and the degree of reduction was controlled by crop residue quality. Also the water content of the mulch depended on its quality and on the decomposition state of the applied residues. Our results did not indicate significant differences in soil hydraulic properties due to residue placement or quality. Therefore the main interaction between residue quality and location appeared through the characteristics of the mulch itself, which deeply influenced both mulch water content and the soil water content under the mulch. As demonstrated in Appendix A, the water storage capacity after a rain significantly increased during the decomposition of RYE mulch, while it remained constant for RAPE mulch. Physical changes of the mulch during decomposition and a dense network of fungal hyphae at the soil-residue interface holding together the residue particles, in function of residue quality, may have contributed to this increased water storage capacity. However, in $PASTIS_{mulch}$, minimum and maximum volumetric water content of the mulch are fixed values that do not change over time. In result, the mulch water content for RYE after successive rain events was largely underestimated.

5.4.2 Effects of residue location and quality, and their interactions

The initial location of crop residues significantly affected the decomposition rate of the residues as shown by the rates of CO_2 mineralization, demonstrating a much faster mineralization with incorporated than surface placed residues as expected from literature referring to field conditions (e.g. Curtin *et al.*, 1998). In our experimental conditions, this

difference in mineralization was mainly due to the fast drying of the mulch soon after rain applications. Our results are in contradiction with other laboratory data showing little or no effect of surface vs. incorporated placement on decomposition (e.g. Abiven & Recous, submitted). This further supports the initial assumption that 'soil-residue contact' may not be as such the key factor in controlling decomposition, and that other processes (e.g. water dynamics) may interact under actual conditions of decomposition. Whatever the quality of the residue, the difference in total residual ^{13}C between incorporation and surface decomposition was 34 %- 36 % of added C.

The difference in mineralization when comparing incorporation of RAPE with incorporation of RYE, or surface application of RAPE with surface application of RYE was attributed to differences in biochemical residue quality. The larger N availability for decomposition of RYE (C:N = 16) compared to RAPE (C:N = 29) resulted in a more advanced decomposition of about 15 % in favour of RYE, irrespective of the residue placement. Regarding to decomposition kinetics, much faster decomposition was observed with RYE compared to RAPE with incorporation: in this situation, water availability was no longer the driving variable, and differences in C substrate mainly controlled the decomposition rate. As expected, the more biodegradable residue (RYE) decomposed faster than the more recalcitrant one (RAPE). In that case, it is noticeable that the model was unable to simulate for RYE the fast disappearance of ^{13}C from the soil within the first 3 weeks of decomposition. The decrease was followed by a plateau, surprisingly showing that no further significant mineralization occurred with RYE residue incorporation after week 3. On the other hand, both the kinetics and the rate of disappearance of RAPE ^{13}C were well predicted by the model. This suggests that with RYE, with abstraction of the large soluble fraction, the remaining residue-C was not so easily degradable. As the model was calibrated for its biological parameters on experimental data of laboratory incubations performed for each type of residue, this suggests that some parameters either describing residue quality (like morphology), or the mean characteristics of the decomposing biomass (e.g. bacterial/fungal ratio) or the contact between zymogenous biomass and soil (K_{MZ}) may interact with residue quality and could be modified when translating "optimised" soil incubations to columns.

Comparison between simulated cumulative C mineralization and calculation by integration of the measured CO_2 fluxes indicated that our CO_2 flux measurements of INC treatments were underestimated, as suggested before (results not shown). The cumulative amount of mineralized C simulated with $PASTIS_{mulch}$ for CTRL, INC and SURF (Figure 5.5) was supposed to be closer to the actual mineralization rate than our measurements, (i) particularly

after a rain event, when the high soil water content prevented the CO_2 to be evolved from the soil, but (ii) also because integration of non-continuous measurements may introduce errors. For SURF treatments, differences between observed and simulated cumulative C mineralization were less important, and we assume that this is due to the fact that most of the CO_2 evolved was coming directly from the mulch layer without any interaction with the soil.

From the simulations we conclude that crop residue location and quality had an impact on the amount of total emitted carbon dioxide. Less carbon was mineralized from [soil + residue] by leaving crop residues at the soil surface than when incorporated in the soil: -1217 kg C ha^{-1} for RAPE and -1108 kg C ha^{-1} for RYE over the 9-week period and this was due to slower decomposition with mulch. Also more carbon was mineralized with RYE than with RAPE: +597 kg C ha^{-1} for surface applied and +489 kg C ha^{-1} for incorporated residues. Modelling should reveal if those differences are maintained over one cropping season, or if carbon mineralization from RAPE and RYE on the one hand and mineralization for SURF and INC on the other hand converge over time. The outcome of this scenario analysis will provide essential information of how crop residue location and quality interact and how this interaction affects on the longer term carbon accumulation in soil.

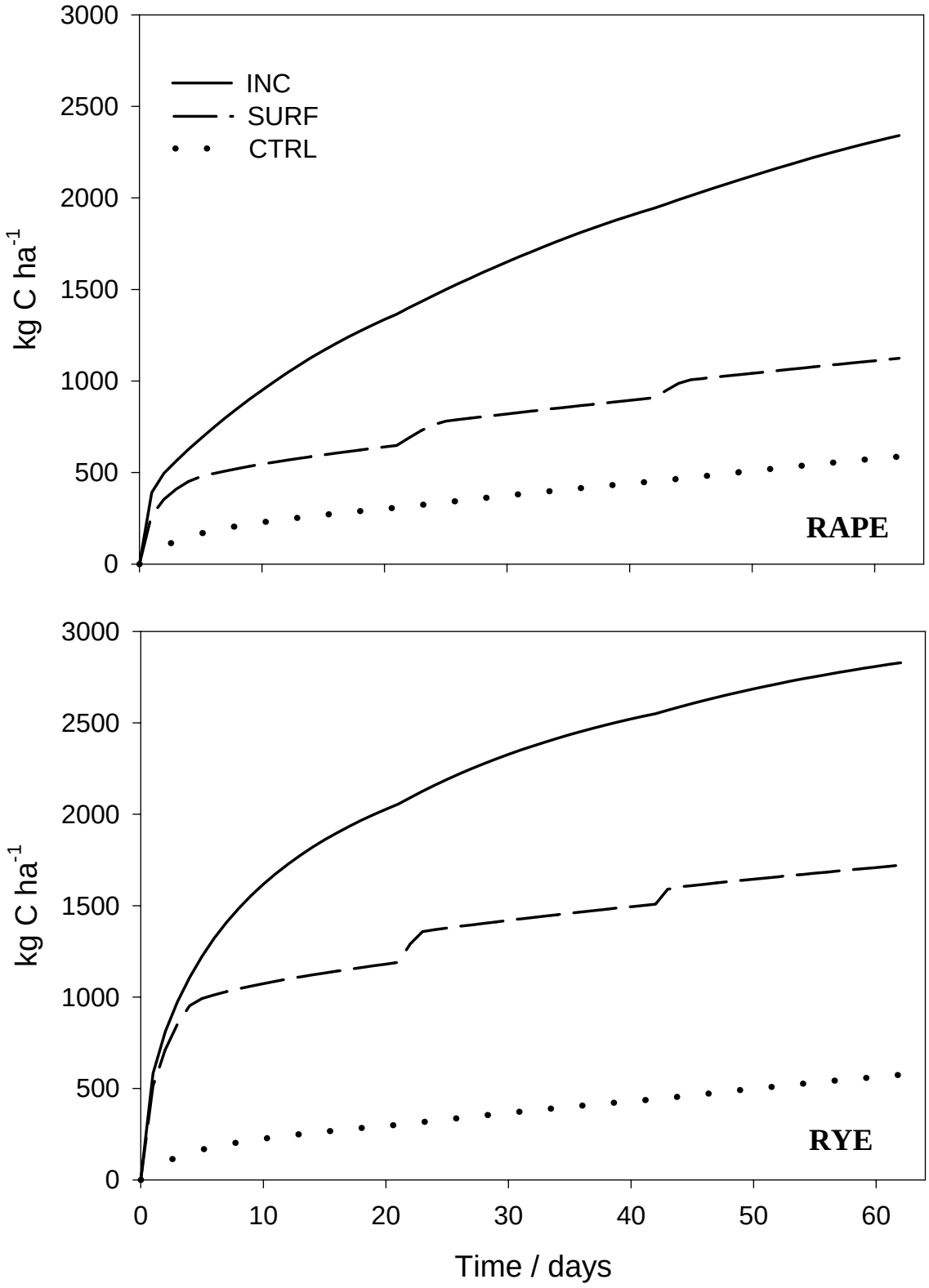

Figure 5.5 Simulation of the cumulative carbon mineralization for the control (CTRL), surface (SURF) and incorporation (INC) treatment with RAPE and RYE residues.

5.4.3 Combined effects of residue location and quality on soil nitrogen dynamics and transport

Crop residue location had a significant effect on nitrogen dynamics in soil that largely depended on residue quality (Figure 5.6). In general, larger gross N fluxes were simulated for INC than for SURF, which is in accordance with the faster residue decomposition observed for INC. Residue location may also influence net N mineralization, as observed for RAPE: the larger soil water content under mulch favoured N mineralization of native organic matter, and the physical separation of the soil-N from the surface applied residue-C decreased N immobilization in the upper soil layer compared to the incorporation treatment. This resulted in a larger net nitrogen accumulation in soil under mulch than with residue incorporation, which was confirmed by the experimental measurements. In contrast, for RYE no significant difference was observed in the final nitrate content measured in the soil, illustrating the interaction of residue quality with the effects of residue location. Simulation of N fluxes in the RYE treatment was not in correspondence with the measured data, and therefore the model could not be used for interpreting the results. Further investigation is required to elucidate this problem.

The distribution of NO_3^--N in the different soil layers resulted from transport processes (leaching with rain and upward transport during evaporation) and the nitrogen mineralization-immobilization turnover. Variations in nitrate concentration over time depend both on residue location and quality, as illustrated for the first wetting-drying cycle (Figure 5.7). Modelling of gross N fluxes helped to explain these changes in nitrate concentration over the soil profile.

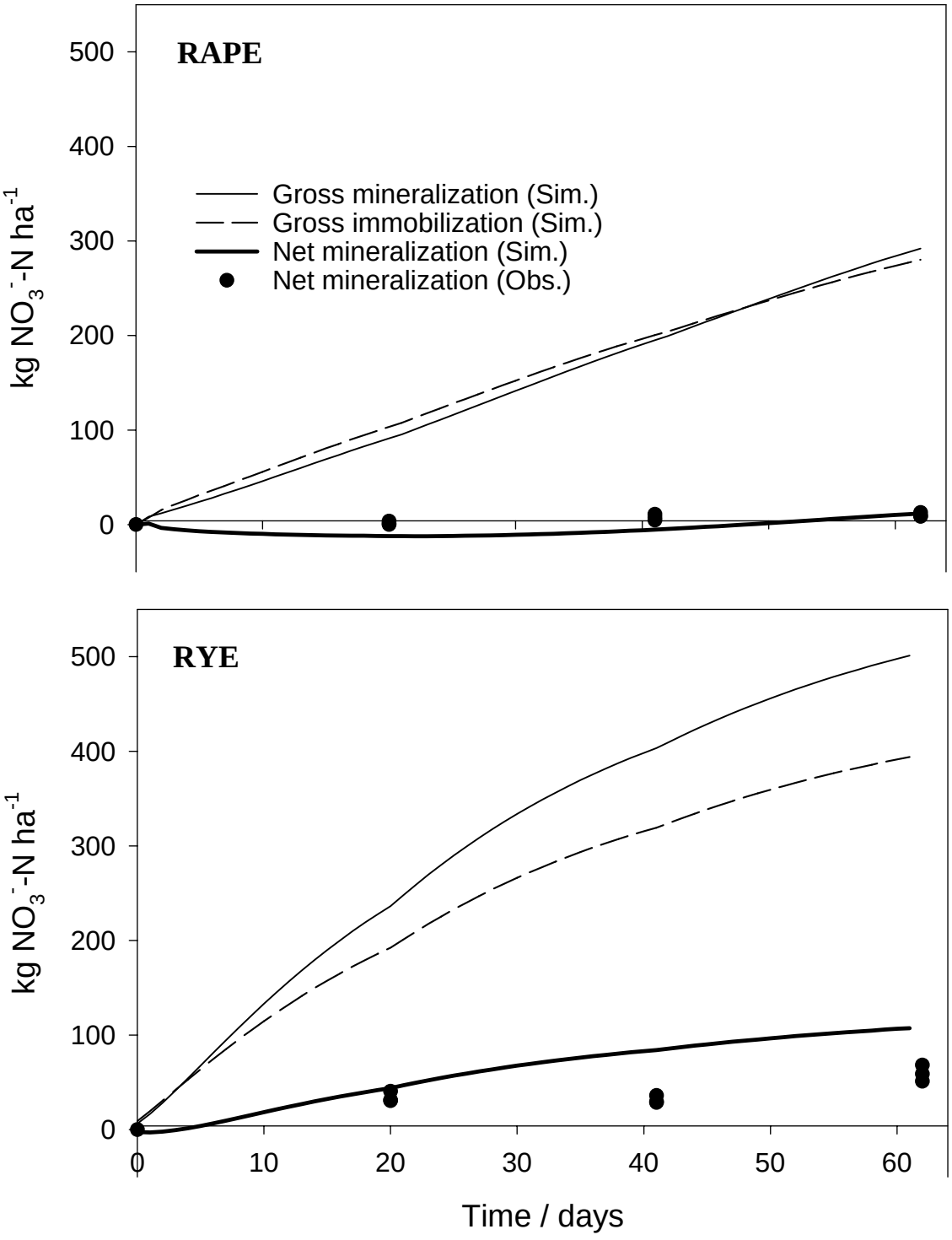

Figure 5.6 (a) Evolution of the simulated gross fluxes of nitrogen mineralization and immobilization, and comparison between simulated and observed net nitrogen mineralization in the 0-25 cm soil layer with incorporation (INC) of RAPE and RYE residues.

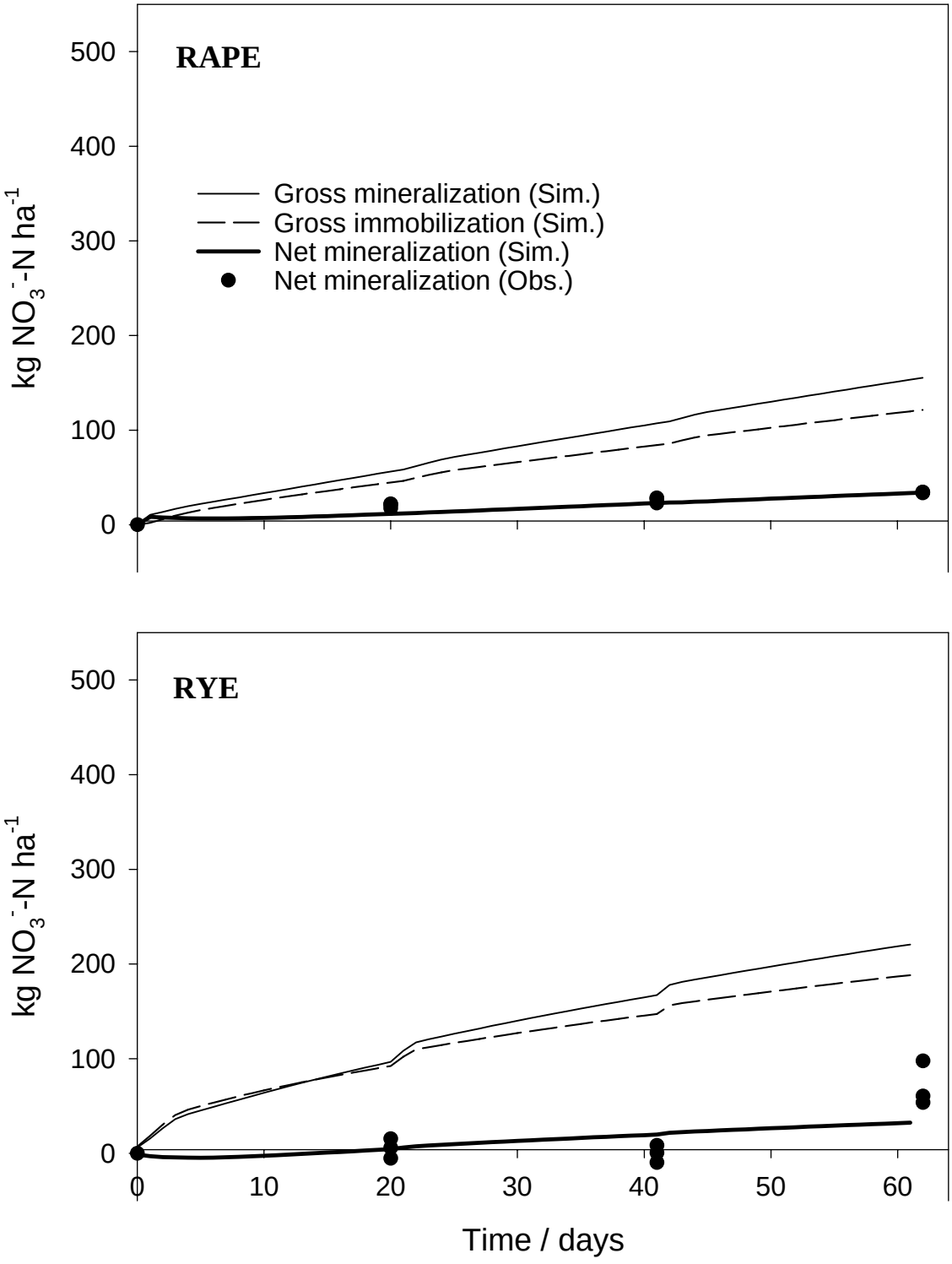

Figure 5.6 (b) Evolution of the simulated gross fluxes of nitrogen mineralization and immobilization, and comparison between simulated and observed net nitrogen mineralization in the 0-25 cm soil layer with surface application (SURF) of RAPE and RYE residues.

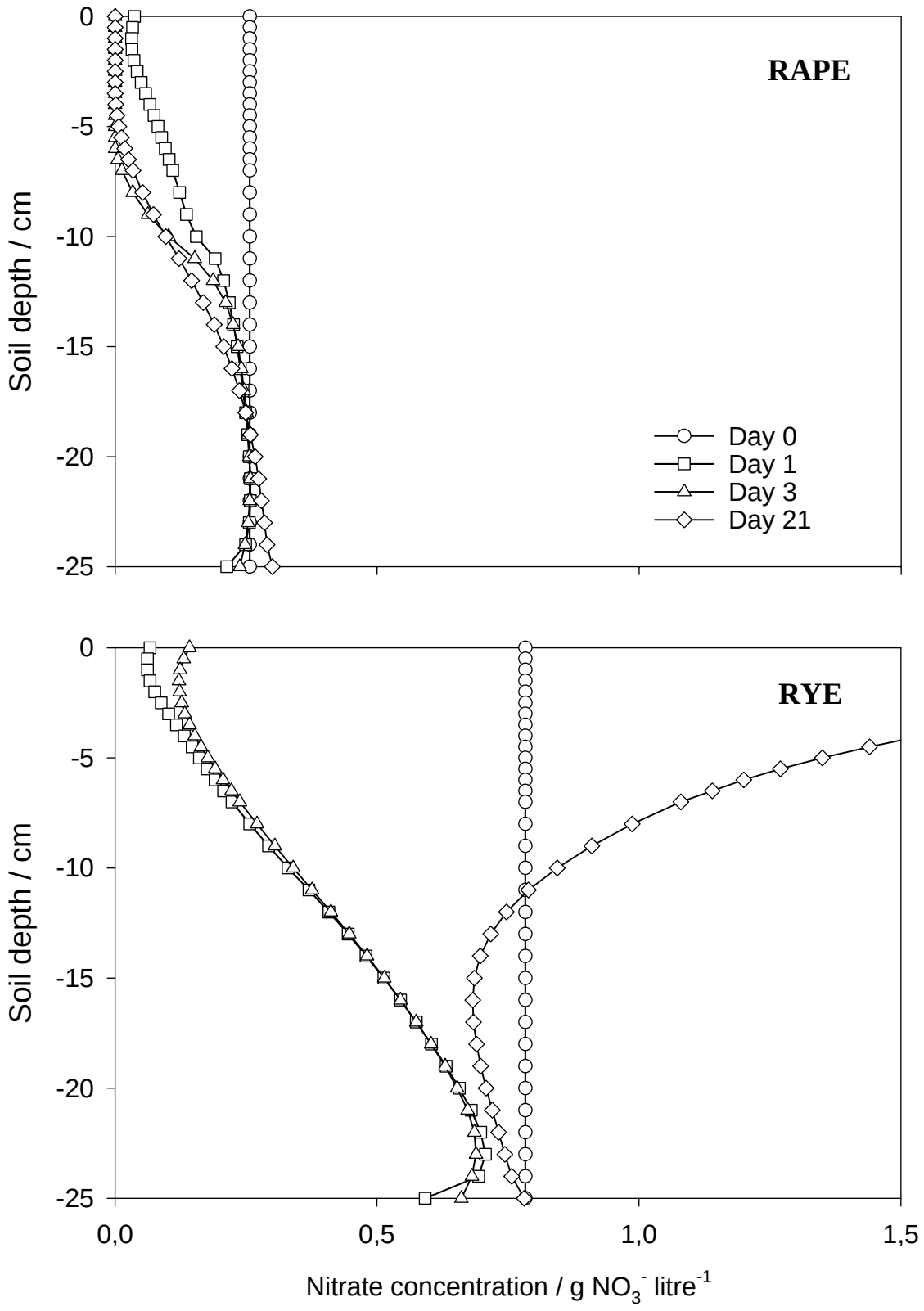

Figure 5.7 (a) Simulation of the nitrate concentration through the soil profile after 0, 1, 3 and 21 days of evaporation, with incorporation (INC) of RAPE and RYE residues.

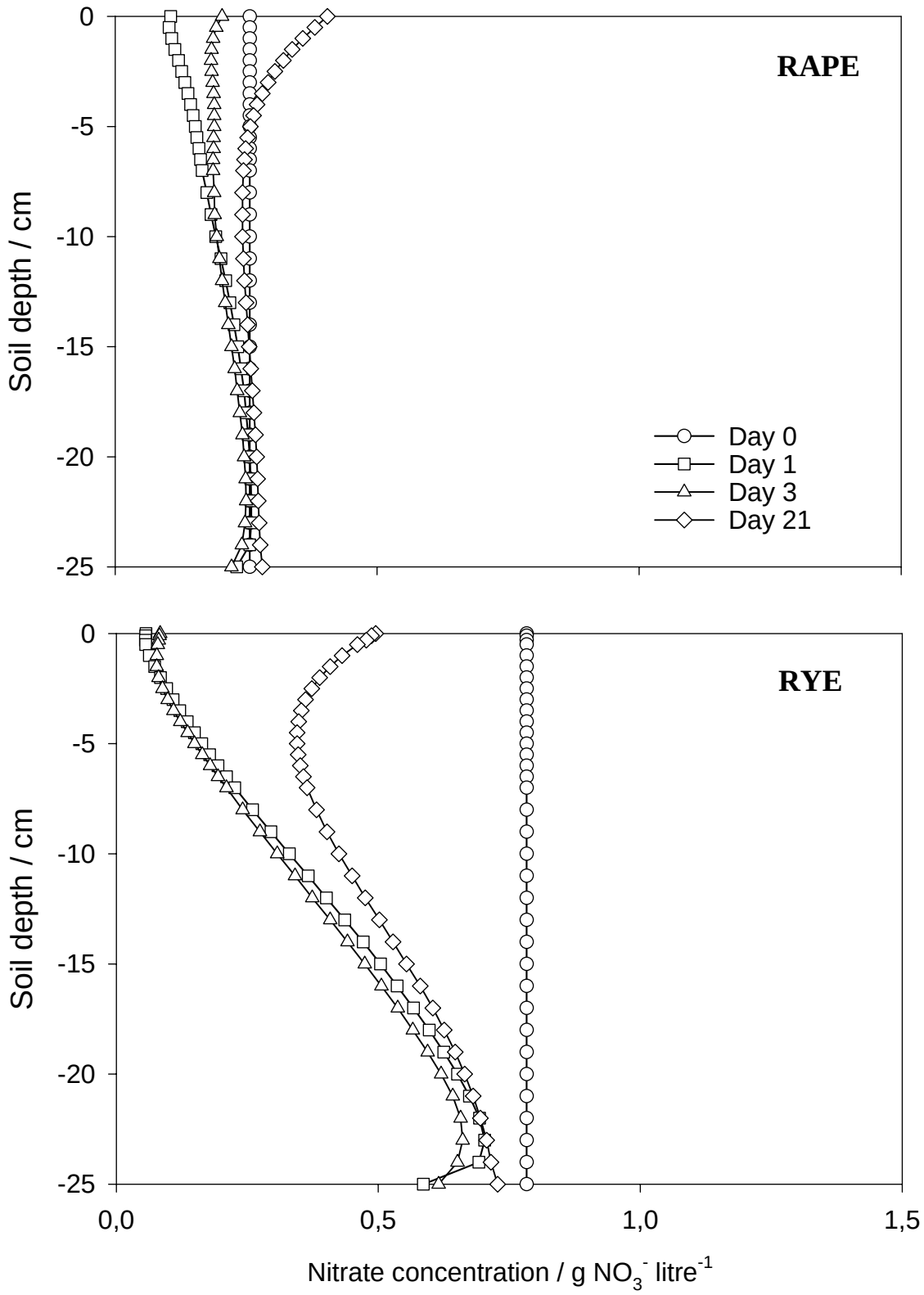

Figure 5.7 (b) Simulation of the nitrate concentration through the soil profile after 0, 1, 3 and 21 days of evaporation, with surface application (SURF) of RAPE and RYE residues.

For the INC treatment of RAPE, the $PASTIS_{mulch}$ model simulated after the first rain a large decrease in the nitrate concentration of the upper soil layer caused by nitrate leaching and N immobilization. The nitrate concentration in the upper part of the soil column further decreased over time, due to N immobilization as observed from the gross N fluxes. For SURF - RAPE however, the initial phase of nitrate leaching was immediately followed by net N mineralization, resulting in nitrate accumulation near the soil surface. For the RYE treatment, the same reduction in nitrate concentration was simulated for INC as for SURF in the first 3 days after rain application, as the same amount of water was applied and no differences in net N mineralization were observed. After 21 days however, the increase in nitrate concentration in the 0-10 cm soil layer simulated for INC largely exceeded the concentration simulated for SURF, which is in accordance with its significant larger net N mineralization. Finally, modelling learned that variations in the concentrations of nitrogen mainly took place in the upper 15 cm of the soil profile. In Chapter 3 it has been demonstrated that microbial activity was stimulated in the 0-17.5 cm soil layer for INC and in the 0-10 cm soil layer for SURF. Changes in nitrate concentration in the soil profile after the initial leaching correspond well to these observed depths of influence.

From this data we conclude that compared to incorporation, in the case residue mulching results in a larger soil water content under mulch (more gross N mineralization) and substrate availability is limiting (less gross N immobilization), in combination with a larger transport of soluble N into the soil after a first rain event (see Chapter 3), leaving crop residues at the soil surface increases the risk on nitrate leaching in soil.

5.5 Conclusion

Crop residue location clearly influences water, carbon and nitrogen dynamics in soil, in interaction with residue quality. Residue mulch significantly reduced soil water evaporation, the extent of reduction depended on physical properties of the mulch layer. Changes in mulch water content, assumed as the main factor controlling surface residue decomposition, also depended on (physical) residue quality. When incorporated, C mineralization kinetics were mainly influenced by biochemical residue quality, e.g. C:N ratio and soluble compounds. The strongest interactions between residue location and quality were observed in the N dynamics: net N mineralization was determined by the interaction between soil water content (depending on residue location) and N availability (depending on residue quality). Modelling allowed to

access gross N fluxes, to estimate nitrate transport and potential leaching in the soil profile and to quantify the impact of residue location and quality on C and N mineralization in soil.

Several scenario analyses can be proposed for a better understanding of mechanisms in surface residue decomposition and to predict the fate of C and N on the longer term - assumed that model description is correct:

(i) Scenarios with rainfall differing in frequency, intensity or duration and where all other conditions are kept constant will allow to verify the hypothesis that water is the main factor in the decomposition of surface placed residues.

(ii) Crop residues of other quality than rape and rye can be characterized by adjusting the biochemical properties in the model (i.e. initial conditions of the organic pools), allowing further investigation of the interactions between crop residue location and quality.

(iii) Simulation on the longer term (e.g. one cropping season) under 'real' meteorological conditions (rain, temperature), with boundary conditions characteristic for a field situation, will permit a more realistic approach in the prediction of decomposition and nitrate leaching from incorporated and surface applied crop residues.

General discussion and perspectives

6.1 Objectives

This work was developed in the general context of the evaluation of land use and management on carbon and nitrogen dynamics in soil. Soils of different ecosystems (e.g. agro-, pasture and forest ecosystem) generally differ in characteristics like organic matter content or microbial biomass. Each ecosystem has also a return of specific plant residues (e.g. crop residues, grass roots, tree leaves), which accumulate over time and define the nature of residual organic matter in the soil. Controversies exist about the effect of soil type on plant residue decomposition, in particular concerning adaptation of indigenous micro-organisms to the added sources of organic matter. Therefore, the effect of soil type was examined on carbon and nitrogen mineralization, in interaction with plant residue quality. It was also investigated if the relationships established between characteristics of arable crop residues and their decomposition rate are valid for plant residues of different origin, largely varying in physical and biochemical quality.

Further, management of plant residues is an important factor influencing carbon dynamics in soil. For example, no-tillage has been shown to be an effective strategy in increasing the carbon stock of arable soils. In this view, crop residue location is a decisive parameter that needs more investigation. The main objectives of this work are to identify the soil physical and biological processes that are affected by crop residue location, how these processes interact and in turn affect the decomposition of fresh organic matter. The contradictory results found in literature between decomposition of surface placed residues under controlled, laboratory conditions and in field conditions demonstrate the need for a fundamental research of the mechanisms controlling the decomposition of mulched residues. Principal factors that explain the contrasting results between laboratory and field conditions are differences in water and/or nitrogen availability, residue particle size and the lack of transport processes in classical laboratory incubations. In addition, residue placement in field situations is determined by specific tillage operations (conventional tillage, reduced tillage, no-tillage) that modify physical soil properties (e.g. soil density, infiltration rate, aggregation) and on the longer term result in the development of gradients in organic matter and microbial biomass. In contrast, soil in laboratory incubation studies is generally sieved and homogenized. All the

factors mentioned above contribute to the observed differences in decomposition of surface placed and incorporated residues, but are not necessarily the immediate consequence of residue placement.

We wanted to examine how residue location affects the fate of carbon and nitrogen in soil and in water-stable soil aggregates. Macroaggregates are assumed to protect fresh organic matter from decomposition, in particular in no-tilled soils, but effects of tillage on aggregate and organic matter dynamics have been attributed mainly to the absence of mechanical disruption of soil aggregates in a no-till system. Little information is available on the specific contribution of crop residue location to the distribution of carbon and nitrogen in aggregates. An understanding of these mechanisms is however essential to explain soil aggregate stabilization and storage of organic C in soil. The influence of residue mulch at the soil surface on aggregate dynamics and the impact on C stabilization on the long term was investigated. In addition, it was examined how the distribution of residue-C in the various soil aggregate fractions is influenced by the way residue-C enters the soil with surface applied and incorporated residues.

The final objective was to evaluate interactions between crop residue location and physical and biochemical residue quality. The PASTIS model was used to compare and quantify the influence of crop residue biochemical composition and mulch characteristics on water dynamics and decomposition. Modelling gives access to extra information that cannot be measured directly, i.e. cumulative C mineralization, nitrate transport in soil and gross fluxes of N mineralization and immobilization, which are essential factors to assess the environmental consequences of a change in residue management.

6.2 General conclusion

Land use and management have a significant influence on the carbon and nitrogen dynamics in soil. The potential contribution to C storage in soil of grass roots and beech leaves is larger than of oilseed rape and rye residues, irrespective of the soil type in which they decompose. The quality of added plant residues is determined by the plant species, which partly depends on land use, and is the first factor that influences the kinetics of residue decomposition. In contrast, soil type has little or no effect on the short-term dynamics of decomposition of residues in soils. On the longer term however, mineralization of residue-C is slightly influenced by soil type, which is probably due to differences in the capacity to stabilize

soluble carbon and/or microbial derived carbon. The 'classical' relationship that is observed between carbon mineralization of the five residues and their biochemical composition (e.g. soluble compounds, lignin content) demonstrate that a general approach can be used to characterise and model the effects of biochemical quality of plant residues originating from different agro-ecosystems. The negligible effect of soil type on the short term kinetics of C mineralization allows that one soil type can be used when investigating the influence of residue quality on short term C fluxes.

Crop residue location determines largely the water dynamics in soil and residue, and it affects the distribution of carbon and nitrogen in soil. Interactions between water content of soil and residues, and the availability of C and N for the decomposing biomass, control the microbial activity and consequently the decomposition rate of the fresh organic matter in soil. This results in significant differences in C and N mineralization of residues incorporated or left at the soil surface. Emission of carbon dioxide from soil with mulch was lower than with incorporated oilseed rape residues, while nitrate accumulation was larger in soil under mulch than with incorporated residues.

Spatial separation of surface placed residues from the soil reduces the residue decomposition rate compared to incorporated residues, resulting on the short term in a large fraction of residual particulate matter on the soil surface. Although the impact of residue location on aggregate dynamics is small when considered over the 0-10 cm soil layer, a significant larger concentration of residue-C and -N and an increased aggregate stability is observed near the soil surface under mulch. Residue-C enters the aggregate fractions as soluble C, either after being transported from the residue mulch with water infiltration or, additionally, by diffusion from the surrounding residue particles in the case of incorporated residue. Incorporation of residue-C in aggregate fractions occurs in the early phase of decomposition and does not change much over time. Decomposition of the particulate organic matter apparently has no significant impact on C storage in the aggregates. The soluble fraction of crop residues diffuses early and is stabilised, the particulate fraction contributes more to net C mineralization and has little interaction with the soil matrix. Consequently, the initial location of crop residues has no significant impact on long term C storage in soil, at least not through a differential incorporation into stable aggregate fractions. On the longer term, the fate of surface placed residue-C that accumulates at the soil surface should be examined.

Finally, crop residue location and quality interact and significantly influence water, carbon and nitrogen dynamics in soil. Water is identified as the main factor controlling decomposition of residue mulch, itself influencing the soil water content. Leaving crop

residues at the soil surface reduces soil evaporation rate by about 50 %, the extent of reduction is influenced by residue quality. The mulch water storage and retention capacity also depend on physical residue quality and the degree of residue decomposition. Although in field conditions soil hydraulic parameters are affected by the applied tillage system (Fuentes *et al.*, 2004), we do not observe a significant contribution of crop residue location to these differences. With incorporation, biochemical residue quality (e.g. N availability, soluble compounds) becomes more important in the control of C mineralization kinetics. The strongest interactions between residue location and quality are observed in the N dynamics.

Our data contributed to the development and calibration of a submodule of the PASTIS model, describing surface residue decomposition. Modelling with PASTIS allows to access gross N fluxes, to estimate nitrate transport and potential leaching in the soil profile and to quantify the impact of crop residue location in soil on carbon and nitrogen dynamics, in interaction with residue quality. Over the period of 9 weeks following residue addition, mulching of oilseed rape reduces CO_2 emission by about 1700 kg C ha^{-1} compared to incorporation of rye residues. Rye incorporation also results in largest net nitrogen mineralization and potential nitrate leaching, which increases by about 100 kg N ha^{-1} compared to incorporation of oilseed rape. It has been demonstrated that under specific conditions of soil water content and substrate availability, residue mulching increases potential nitrate leaching. Using the PASTIS model with an adapted climate scenario will allow extrapolation of these results over one cropping season. Actually, an evaluation study of the impact of land management on residue decomposition in the field is going on, that can contribute to the validation of our modelling results (cf. K. Oorts, INRA).

6.3 Evaluation of research strategy

To identify the processes affected by residue location and how they influence residue decomposition, we conducted a laboratory experiment with repacked soil columns. Soil was sieved before homogenous compaction at field density to eliminate the influence of specific soil characteristics induced by tillage when comparing the decomposition of surface placed and incorporated residues. Residues were left at the soil surface or incorporated homogeneously in the 0-10 cm soil layer to simulate respectively no-tillage and reduced tillage situations. In real conditions, residues are heterogeneously incorporated in the soil, which certainly has an influence on the contact between soil and residues. When a large mass

of residues is concentrated in the soil as illustrated in Picture 6.1, only the outer part of the residue mass is in close contact with the soil particles. However, subsequent tillage operations will fractionate and homogenise the incorporated residues, so our experimental approach of residue incorporation is acceptable. In addition, to imitate soil-residue contact as observed in field situations, the ratio between the size of soil aggregates and residue particles was maintained. In field conditions of our particular soil, most of the soil aggregates were found in the range of 10-20 mm (Figure 6.1), while most of the residue particles had a size between 40 and 60 mm (Figure 6.2). In our soil columns, this proportion was maintained by adding residue particles chopped at 10 mm in soil sieved at 2 mm. Scaling down the residue size from 50 to 10 mm hardy influences its decomposition kinetics, as reported by Angers & Recous (1997).

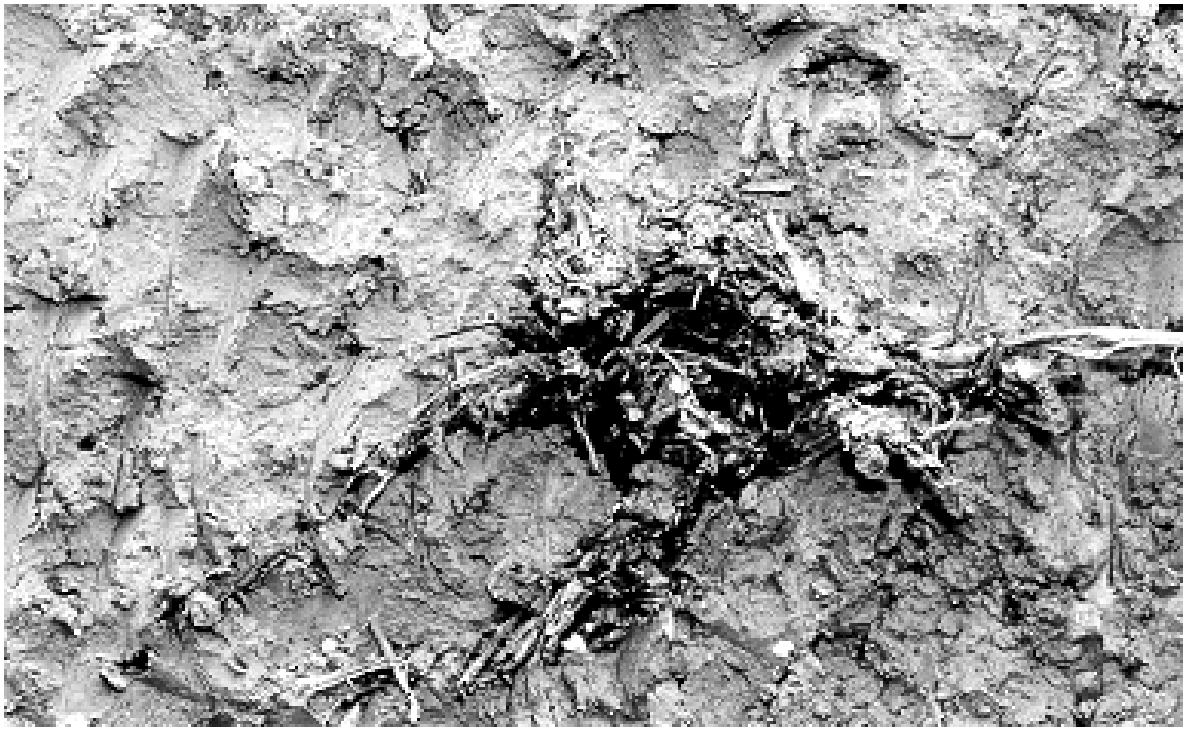

Picture 6.1 Heterogeneous incorporation of wheat straw in soil after ploughing

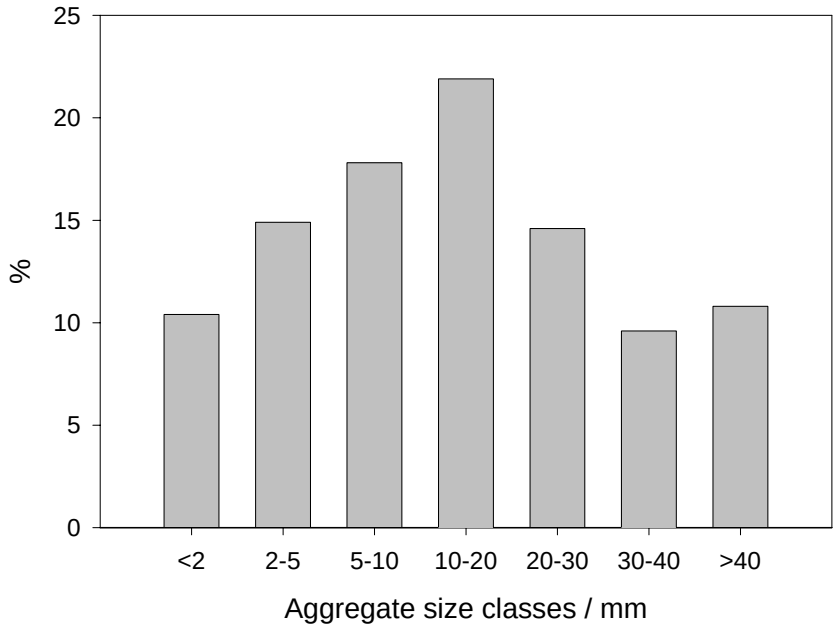

Figure 6.1 Soil aggregate size distribution as observed in the field (Mons)

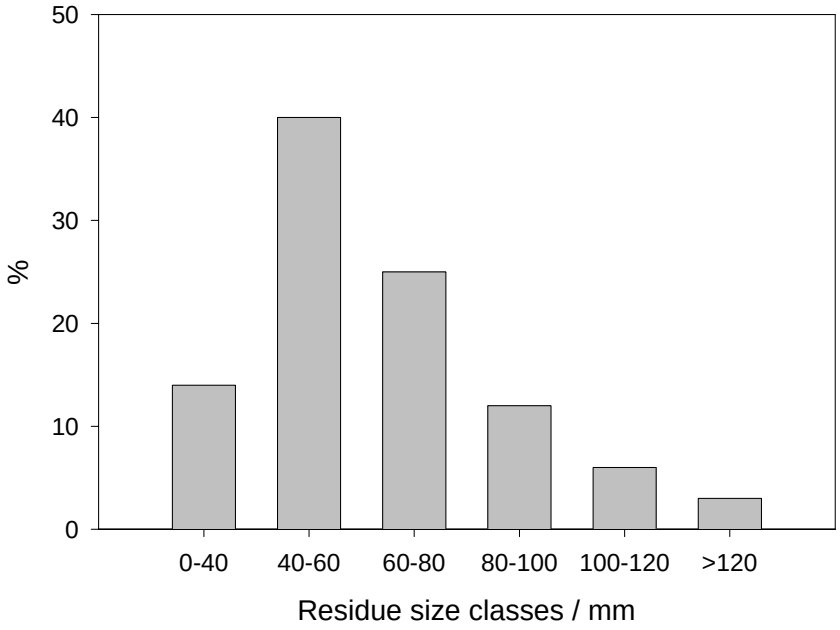

Figure 6.2 Residue particle size distribution as observed in the field (wheat straw)

Decomposition of the added residues was evaluated by evolved CO_2 or residual C, however we are still ignorant of the dynamics in microbial biomass. The global microbial activity was assessed by substrate induced respiration, but no information was obtained on changes in the composition of the microbial population and on the quantification of bacteria and fungi in the soil in function of residue location. Nevertheless, knowledge of these parameters will

contribute to a better understanding of mulch decomposition. An attempt was made to identify changes in the bacterial/fungal ratio, by coupling selective inhibition of fungi and bacteria to the substrate induced respiration method (West, 1986; Bailey *et al.*, 2002), but our experimental set-up did not allow to obtain useful results due to the variations in organic matter content over the soil profile. Other methods can be adopted (e.g. epifluorescence microscopy), but quantification of the bacterial and fungal biomass remains problematic.

In our study, two different models are used: the Roth-C model allows to simulate C mineralization from plant residues on the longer term, while the PASTIS model is privileged for relating transport processes in soil with biotransformations of carbon and nitrogen. In addition, PASTIS has a specific submodule for modelling the decomposition of surface placed residues and simulates processes that otherwise cannot be examined (e.g. transport of nitrate in soil, gross fluxes of nitrogen mineralization / immobilization). Large differences exist in the concepts of both models used for describing the decomposition process. For example, fresh organic matter is characterised by 2 pools in Roth-C (DPM and RPM), while new carbon in PASTIS is distributed over 5 pools (SOL, RDM, HEM, CEL and LIG). Despite those differences, both models are able to simulate satisfactory the mineralization of residue-C, indicating that a mechanistic, explanatory model with numerous parameters like PASTIS not necessarily results in a better performance than a predictive model based on more elementary formalisms.

Although mechanistic decomposition models aim to conceptualize the physical and biological soil processes, empirical parameters or functions still exist as not all soil processes are clearly understood. In PASTIS, the parameter taking into account soil-residue contact (K_{MZ}) is an example of such a factor. To reduce uncertainty in this function, it is proposed to develop a function that defines K_{MZ} from residue particle size and quality. Other parameters in PASTIS have to be optimized on experimentally obtained C and N mineralization data. For this purpose, plant residues are finely chopped (1-3 mm) and incubated under constant temperature and moisture conditions. Although nitrogen dynamics are well simulated when optimizing on the preliminary incubation data, the model overestimated initial nitrogen immobilization and the subsequent nitrogen mineralization rate when compared to the nitrate measurements of the column experiment, even in the control columns without residue addition. Differences in incubation conditions that are not taken into account by the model (e.g. transport of soluble carbon) can explain the bias.

6.4 Perspectives

With our experimental set-up we succeeded in simulating more realistic field conditions than in classical incubation experiments without water fluxes. However, still some additional factors typical for real field situations may interfere with our observations. In the first place, water dynamics in soil - identified as the principal factor for mulch decomposition - largely depend on meteorological conditions. Our conclusion that soil moisture content is larger in soil under mulch than in soil with a bare surface can be inversed when a long period of dryness is followed by small rain events. Surface placed residues intercept the water that otherwise can infiltrate in the soil. Therefore, one of the priorities for future research would be to use modelling to simulate different rain scenarios, so that the impact of rain duration, frequency and intensity on residue decomposition can be investigated.

Secondly, our experimental set-up intentionally does not take into account the impact of different tillage practices on soil properties. Differences in soil aggregation, gradients of soil organic matter or microbial biomass does not exist in the repacked soil columns before application of the crop residues, but those factors will play in the translation of our results to field conditions. We propose to conduct a similar experiment (same crop residues) with intact soil columns taken from arable land under conventional and no-tillage. Differences in the decomposition kinetics and in the fate of carbon and nitrogen in the soil or soil aggregates can thus be contributed to the soil history, in particular the applied tillage practice.

Another difference between our experiment and field conditions is the absence of soil macrofauna (e.g. earthworms) in the soil columns. Earthworms are found to be more abundant in no-tillage systems (Jordan *et al.*, 1997), creating large macropores that favour water infiltration. In addition, they transport particulate organic matter from the soil surface into the soil, while we conclude that only soluble carbon from the mulch enters the soil fraction. Earthworms reduce residue particle size and carbon from fresh organic matter is rapidly incorporated into newly formed stable microaggregates within earthworm casts (Bossuyt *et al.*, 2004), in addition to the aggregate enrichment in residue-C by diffusion that we observed. In the end, these interactions of physical soil properties and residue decomposition with macrofaunal activity should be investigated in real field situations.

Finally, more research is needed for the conceptualization of mulch degradation in decomposition models. Several empirical factors in the mulch module of PASTIS indicate a lack of knowledge in the formalisms for decomposing surface placed residues. Therefore, physical and biological properties of the mulch and their changes during decomposition

should be characterized. For example, changes in water storage and retention capacity of the mulch over time must be taken into account given the importance of the residue water content for its decomposition. In addition, studying microbial colonization of the mulch will allow to describe which fraction of the mulch is directly subject to decomposition (i.e. validation or disproof of the two-layer concept in PASTIS) and to which extent nitrogen from the upper soil layer is used by the microbial biomass. A better understanding in these processes will lead to a more realistic description and will reduce uncertainty in the prediction of mulch residue decomposition.

Appendices

Appendix A - Description PASTIS$_{mulch}$

Modeling water, carbon and nitrogen dynamics in soil covered with decomposing mulch

A. Findeling [a, *] P. Garnier [b], F. Coppens [b, c], F. Lafolie [d], S. Recous [b]

[a] *CIRAD, Unité Propre de Recherche Risque Environnemental Lié à l'Intensification et au Recyclage, avenue Agropolis, 34398 Montpellier Cedex 5, France.*

[b] *INRA, Unité d'Agronomie, rue Fernand Christ, 02007 Laon Cedex, France.*

[c] *Laboratory for Soil and Water Management, Department of Land Management, K.U.Leuven, Kasteelpark Arenberg 20, 3001 Heverlee, Belgium.*

[d] *INRA, Unité de Science du Sol, Site Agroparc, 84914 Avignon Cedex 9, France.*

[*] Corresponding author. E-mail: antoine.findeling@cirad.fr

tel.: +33 (0)4 67 61 71 72

fax: +33 (0)4 67 61 56 42

Submitted to:

Soil Science Society of America Journal

Abstract

A decomposing mulch of residues on the soil surface affects strongly the water, carbon and nitrogen cycling in soil. Two contrasted types of residues were tested to estimate the role of mulch physical and biochemical properties on these effects: rape residues made of large elemental pieces with a C:N ratio of 29 and rye residues consisting of smaller pieces with a lower C:N ratio of 16. Soil columns covered with a mulch of either residue were incubated in laboratory conditions at 20°C during 3 wetting-drying cycles of 21 days each. Measurements provided the evolution of i) matric potential and water content of the soil, ii) water content, dry mass and carbon content of mulch, and iii) NO_3^- content and CO_2 flux from the soil columns. The PASTIS$_{mulch}$ model was developed to account for mulch effects and simulate the columns experiments. It splits the mulch into a decomposable layer in contact with the soil and a not decomposable layer which 'feeds' the former. Calibration of PASTIS$_{mulch}$ on experimental data showed that parameters were dependent on the type of residue. The model, runned with calibrated parameters, provided good simulations of the water, carbon and nitrogen dynamics, with global efficiencies higher than 0.8. The sensitivity analysis carried out on seven key parameters showed that the total mulch dry mass and the proportion of this dry mass in contact with the soil were decisive parameters. PASTIS$_{mulch}$ highlighted that mulch decomposition was not a continuous process but occurred in form of successive pulses corresponding to favorable abiotic conditions.

Introduction

In the context of global warming, management of agricultural practices has been proposed as one way to mitigate CO_2 emissions by increasing C storage in agricultural soils (Paustian *et al*., 1997). They should favor the input of exogenous organic matter into the soils and/or delay the carbon output due to mineralization. Amongst several options depending on the agro-ecosystem considered, the return of crop residues to the soil, in combination with conservation tillage, has been shown to be an effective strategy to increase the C level in cropped soils (Balesdent *et al*., 2000; West & Marland, 2002). However reducing tillage intensity not only increases total C storage, but also dramatically changes C distribution into the soil, soil physical and chemical properties and the associated microbial activities (Holland & Coleman, 1987; Chapter 3 of this thesis). This is the result of combined effects of the presence of a mulch of residues decomposing at the soil surface and of a lack of disturbance of the soil structure. Furthermore it has been suggested that the beneficial effect of soil C storage with conservation tillage could be counterbalanced by other impacts such an increase in N_2O emissions or NO_3^- leaching associated with changes in dynamics and distribution of water, C and N in soil (Ball *et al*., 1999; Six *et al*., 2002). Therefore the development of models that enable to predict simultaneously the transformations of organic matter and the flows of heat and mass in soils is crucial to assess the various environmental impacts of soil management.

Many soil-plant-atmosphere models have been developed to describe the dynamics of water and temperature with a residue mulch at the soil surface (Bristow *et al*., 1986; Sui *et al*., 1992; Tuzet *et al*., 1993; Bussière & Cellier, 1994; Gonzalez Sosa *et al*., 1999; Findeling *et al*., 2003a; Findeling *et al*., 2003b). They were mainly used to assess the impact of a mulch on physical processes such as water runoff, soil thermal regime, erosion and evaporation. There are only few models that have been designed to simulate the decomposition of a residue mulch and the associated C and N dynamics (CERES, Quemada *et al*. (1997); APSIM, Thorburn *et al*. (2001); EXPERT-N, Berkenkamp *et al*. (2002)). These models have in common a specific *mulch module* that split the mulch into two layers, one being in close contact with the soil while the upper layer is 'feeding' the former as a function of external factors (management, climatic event,…). However there is a general agreement about a lack of knowledge on the mechanisms that drive mulch decomposition. The effect of abiotic factors (mulch temperature, mulch water content, nitrogen limitations and contact between

mulch and soil) on the dynamics of decomposing microorganisms is poorly documented. Consequently modeling mulch decomposition remains a challenging issue.

This work aims at understanding and modeling better mulch decomposition processes. Based on the PASTIS model (Lafolie, 1991; Garnier *et al*., 2003) that simulates water, heat and solute transport and C and N cycling in bare soil, a new model, namely PASTIS$_{mulch}$, was developed to take the mulch into account. Its originality lies in a coupling between biological mulch decomposition processes and mass and heat flows, and in a description of abiotic factors by laws currently used for incorporated residues but, to our knowledge, not for residue mulch.

The main objective of the study was to identify and simulate the physical and biological effects of a decomposing residue mulch and its quality on water, carbon and nitrogen dynamics in a mulch-soil system. Two contrasted types of mulch were tested: a mulch of rape residues made of large elemental pieces with a C:N ratio of 29 versus a mulch of rye residues consisting of smaller pieces with a lower C:N ratio of 16. The experiments were conducted under laboratory conditions for both residues. The strategy adopted relied on 3 steps: 1) obtaining for both residues a set of experimental data that describes the water, carbon and nitrogen dynamics in a mulched soil, 2) developing the mulch module of PASTIS$_{mulch}$ to simulate the effect of the mulch on the water, carbon and nitrogen dynamics, and 3) calibrating and evaluating the model and assessing its sensitivity to some key parameters of the mulch.

Theoretical background

The PASTIS model

The one-dimensional mechanistic model PASTIS (Prediction of Agricultural Solute Transfer In Soils), described by Lafolie (1991), Garnier *et al*. (2001) and Garnier *et al*. (2003), simulates the transport of water, solutes and heat using classical equations, i.e. Richard's equation for water flow, the convection-dispersion for solute transport and the convection-diffusion equation for heat flow:

$$C_h \frac{\partial h}{\partial t} = \frac{\partial}{\partial z}\left(K\left(\frac{\partial h}{\partial z} - 1 \right) \right) \quad (1)$$

$$\frac{\partial (\theta C)}{\partial t} = \frac{\partial}{\partial z}\left(\theta D \frac{\partial C}{\partial z} - qC \right) \quad (2)$$

$$C_T \frac{\partial T}{\partial t} = \frac{\partial}{\partial z}\left(\lambda_T \frac{\partial T}{\partial z} - qC_w T \right) \quad (3)$$

where $C_h = \left(\frac{\partial \theta}{\partial h} \right)_T$ is the soil capillary capacity (m^{-1}), h is the matric potential of soil water (m), t is the time (s), z is the vertical coordinate (m), K is the soil hydraulic conductivity ($m\ s^{-1}$), C is the solute concentration ($kg\ m^{-3}$), θ is the soil volumetric water content ($m^3\ m^{-3}$), D is the dispersion coefficient ($m^2\ s^{-1}$), q is the Darcy water flux ($m\ s^{-1}$), C_T is the soil volumetric thermal capacity ($J\ m^{-3}\ K^{-1}$), T is the soil temperature (K), λ_T is the soil thermal conductivity ($W\ m^{-1}\ K^{-1}$), C_w is the water volumetric thermal capacity ($J\ m^{-3}\ K^{-1}$). The model does not consider vapor phase transport, hysteresis of hydraulic properties, or preferential flow. Dirichlet or Neumann conditions can be applied at the top and bottom of the soil for water, solutes and temperature.

The CANTIS submodel (Carbon And Nitrogen Transformations In Soil) simulates the transformations of carbon and nitrogen (Figure A.1). It considers the decomposition of organic matter, mineralization, immobilization, nitrification and humification. The model makes the distinction between gross mineralization, gross immobilization and net mineralization. The gross mineralization is the production of inorganic N from the organic pool of N due to microbial activity. The gross immobilization is the conversion of inorganic N into organic N: it includes microbial immobilization and humification of N. The net mineralization is the difference between gross mineralization and gross immobilization. Soil organic matter is divided into three non-living organic pools: fresh, soluble and humified organic matter, and two living pools. The microbial population is split into an autochthonous biomass that decomposes humified organic matter and a zymogenous biomass that decomposes fresh and soluble organic matter. The meanings of the parameters are listed in Table A.1. Decomposition of fresh or soluble organic matter is assumed to follow first-order kinetics as:

$$\frac{dC_i}{dt} = -k_i C_i f_T f_W f_N f_B \qquad (4)$$

where C_i is the carbon content of the organic matter pool i, k_i is the decomposition rate constant of that pool, f_T is the temperature function, f_W is the moisture function, f_N is the nitrogen limitation function, and f_B is the biomass-dependent function. These functions have been described previously (Garnier *et al*., 2001). A sink/source term is introduced in equation **(** 2 **)** to account for mineralization or immobilization of N by micro-organisms.

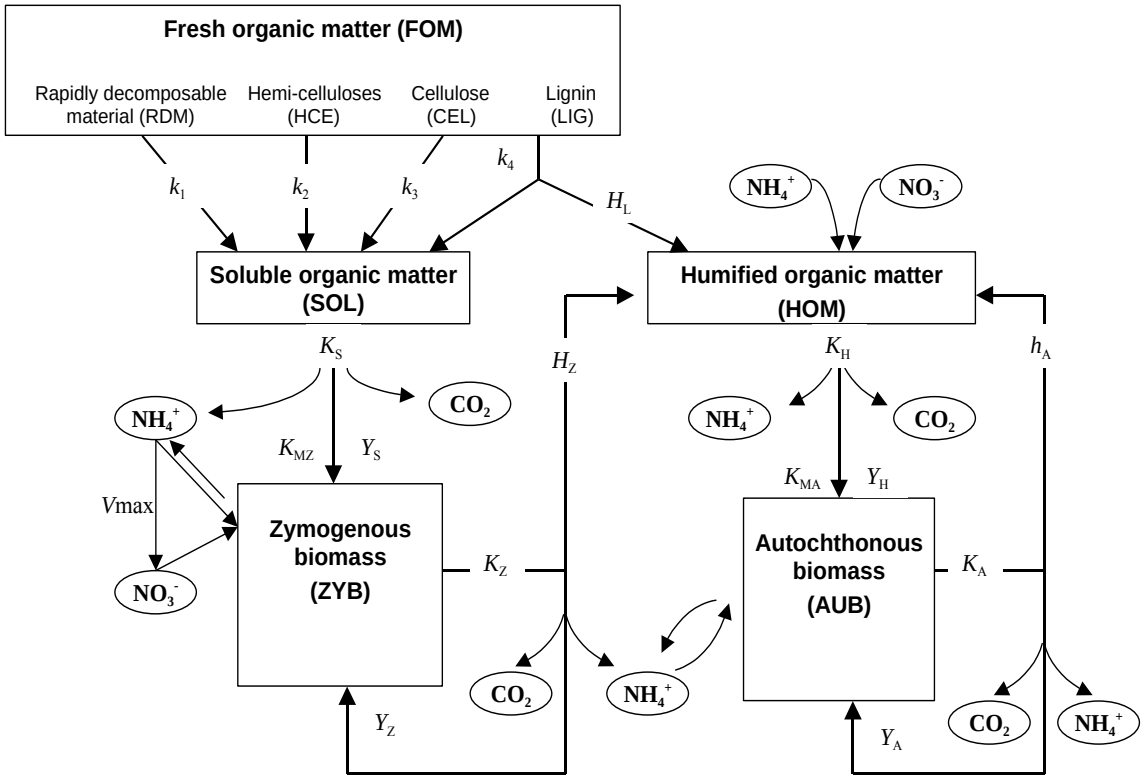

Figure A.1 Flow diagram of the CANTIS (Carbon And Nitrogen Transformations In Soil) submodel from Garnier *et al*.(2003).

Table A.1 Biological parameters used in the CANTIS (Carbon And Nitrogen Transformations In Soil) submodel

Symbol	Parameter	Rape	Rye
k_1	Decomposition rate of rapidly decomposable material (RDM) (d^{-1})	0.2531	
k_2	Decomposition rate of hemicelluloses (HCE) (d^{-1})	0.1013	
k_3	Decomposition rate of cellulose (CEL) (d^{-1})	0.1535	
k_4	Decomposition rate of lignin (LIG) (d^{-1})	0.00222	
k_S	Decomposition rate of soluble compounds (SOL) (d^{-1})	1.495	
k_Z	Decomposition rate of zymogenous biomass (ZYB) (d^{-1})	0.0206	0.0490
k_A	Decomposition rate of autochthonous biomass (AUB) (d^{-1})	0.00489	
k_H	Decomposition rate of humified organic matter (HOM) (d^{-1})	0.00025	
h_Z	Humification coefficient by ZYB (-)	0.1403	0.2629
h_A	Humification coefficient by AUB (-)	0.3761	
h_L	Humification coefficient of lignin (-)	1	

Adaptation of PASTIS model

PASTIS is originally designed for incorporated residues. In this work, the model is adapted to the case of a surface residue mulch to take into account the physical effects of the mulch on rain interception and evaporation (Findeling, 2001), and the specific dynamics of decomposition of the latter. The new model is referred to as PASTIS$_{mulch}$ and the introduced parameters are listed in Table A.2.

For rain interception, the mulch as a porous medium can intercept rainfall up to a maximum value $R_{m,max}$ (m) defined as:

$$R_{m,max}(t) = \frac{\theta_{me,max}}{\rho_{me}} DM_m(t) \qquad (5)$$

where $\theta_{me,max}$ is the mulch element maximum volumetric water content ($m^3\ m^{-3}$), ρ_{me} is the density of mulch elements ($kg\ m^{-3}$) and DM_m is the mulch dry mass ($kg\ m^{-2}$).

Table A.2 Mulch parameters used in the mulch module of PASTIS$_{mulch}$ (Prediction of Agricultural Solute Transfer In mulched Soils) model

Symbol	Parameter	Rape	Rye
$DM_m(0)$	Initial dry mass (g m^{-2})	552.8	417.4
$DM_{m,c}(0)$	Initial dry mass in contact (g m^{-2})	**To be calibrated**	
z_m	Mulch thickness (cm)	1	2
α_{feed}	Mulch feeding rate (d^{-1})	**To be calibrated**	
$\theta_{me,max}$	Maximal vol. water content of mulch elements (m^3 m^{-3})	0.212	0.700
$w_{me,max}$	Maximal grav. water content of mulch elements (g g^{-1})	2.078	2.000
$R_{m,max}$	Maximal mulch water storage (cm)	0.13	0.10
$\theta_{me,res}$	Residual vol. water content of mulch elements (m^3 m^{-3})	0.030	0.105
α_m	Mulch propensity to water recharge (-)	0.25	0.25
ρ_{me}	Mulch element density (g cm^{-3})	0.102	0.350
$z_{m,zyb}$	Max. depth for available N for mulch decomposition (cm)	**To be calibrated**	

Mulch water storage, R_m (m), is calculated as:

$$\Delta R_m = \begin{cases} \Delta R \exp\left(-\alpha_m \dfrac{R_{m,max} - R_{m,res}}{R_{m,max} - R_m} \right) & \text{if } R_m < R_{m,max} \\ 0 & \text{if } R_m = R_{m,max} \end{cases} \quad (6)$$

where R is the cumulative rainfall (m), α_m is the mulch propensity to water recharge (-), and $R_{m,res}$ is the residual mulch water content (m) calculated from the residual mulch volumetric water content $\theta_{me,res}$ (m^3 m^{-3}) as in equation (5). The amount of rain which is not intercepted

by the mulch is transmitted to the soil. When the flux of water reaching the soil exceeds the Darcy's infiltration flux, ponding water is stored and infiltrated later on in the soil.

For evaporation, the mulch acts as a physical barrier to convective and diffusive vapor fluxes between the soil and the atmosphere (Findeling *et al*., 2003a). As a consequence, the total potential evaporation rate, E^{pot} (kg m^2 s^{-1}), is split into the potential evaporation rate of the mulch, E_m^{pot} (kg m^2 s^{-1}), and the soil, E_s^{pot} (kg m^2 s^{-1}):

$$\begin{aligned} E_m^{pot} &= \xi E^{pot} \\ E_s^{pot} &= (1-\xi) E^{pot} \end{aligned} \qquad (7)$$

where $\xi = 0.352$ is the propensity of the mulch to reduce soil evaporation demand (Findeling, 2001). E_s^{pot} is applied to the soil. E_m^{pot} is applied to the mulch to evaporate its water storage:

$$\Delta R_m = -\min(E_m^{pot}\Delta t; R_m) \qquad (8)$$

For decomposition, residue decomposition is highly dependent on the contact with micro-organisms and the available mineral nitrogen resource (Henriksen & Breland, 2002; Garnier *et al*., 2003). In the case of mulch, the residue elements which are closely in contact with the soil will decompose more easily because micro-organisms from the soil can colonize them and fungi can use their hyphae to absorb mineral nitrogen in the soil to decompose efficiently the residue. On the contrary, the upper elements which are not in contact with the soil will hardly decompose because of water limitation which hinders micro-organisms activity. Based on an approach similar to that of Thorburn *et al*. (2001) in APSIM-Residue model, we define two compartments for the mulch (Figure A.2):

$$DM_m(t) = DM_{m,c}(t) + DM_{m,nc}(t) \qquad (9)$$

where $DM_{m,c}$ is the mulch dry mass in contact with the soil (kg m^{-2}) and $DM_{m,nc}$ is the mulch dry mass not in contact with the soil (kg m^{-2}). The former can decompose whereas the latter is assumed unavailable for decomposition. $DM_{m,nc}$ is set to an initial value and then decreases exponentially with time to account for the progressive rearrangement of the mulch due to climatic action (rain and wind). This decrease corresponds to an equivalent increase in $DM_{m,c}$:

$$\Delta DM_{m,c}(t) = \alpha_{feed} DM_{m,nc}(t)\Delta t \qquad (10)$$

where α_{feed} is the feeding rate (d^{-1}) of the decomposable mulch compartment by the non decomposable mulch compartment. Decomposition of $DM_{m,c}$ is based on the CANTIS model. $DM_{m,c}$ is split into fresh and soluble organic matter like incorporated organic matter in PASTIS. However, mulch decomposition is controlled by specific abiotic functions (equation (4)). The mulch temperature ($T_{me} = 20\,°C$, constant in this experiment) and the mulch element volumetric water content, θ_{me} ($m^3\ m^{-3}$), are used to calculate respectively f_T and f_W in the mulch. Only a limited topsoil layer can be involved in mulch decomposition since the influence of the zymogenous biomass, which decomposes the mulch, is limited by the maximum length of the fungi hyphae (Figure A.2). This limit is imposed by setting a maximum extension depth of the zymogenous biomass, $z_{m,zyb}$ (m), and considering that N immobilization for mulch decomposition is restricted to the topsoil layer of thickness $z_{m,zyb}$. f_N is calculated from the available amount of mineral N in this layer. Finally, mineralized N from the mulch is assumed to be produced in the same topsoil layer.

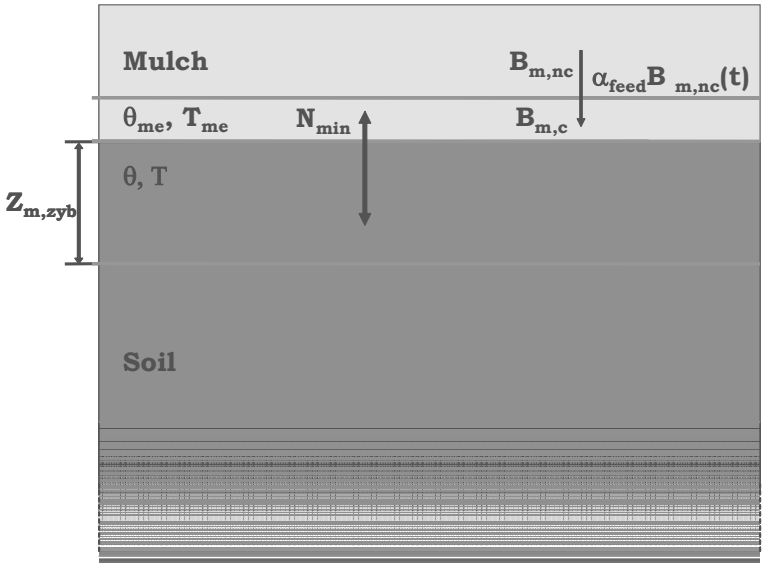

Figure A.2 Conceptual diagram of mulch decomposition processes based on a two mulch compartments approach.

Materials and methods

Main experiment

Experimental set-up

The soil used in the experiment was a silt loam, Typic Hapludalf (Orthic Luvisol), obtained from the experimental site of INRA, Mons-en-Chaussée, Northern France (Table A.3). The top 25 cm soil layer was sampled, sieved (< 2 mm) at field moist content, and stored in plastic bags at 4°C prior to use. Soil storage at 4°C for the rye experiment was 10 months longer than for the rape experiment. The low storage temperature did not completely inhibit C and N mineralization in the soil (Table A.4). Therefore nitrate concentration was higher in soil used for the rye than for the rape experiment (0.783 g l^{-1} for rye *vs.* 0.257 g l^{-1} for rape). Soil storage also modified soil aggregation.

Table A.3 Characteristics of the used soil, rape and the rye residues

Parameter	Soil	Rape residue	Rye residue
C content (%)	0.85	42.2	43.4
N content (%)	0.09	1.45	2.7
C:N ratio (-)	9.47	29.1	16.1
Clay (%)	13.4	/	/
Silt (%)	81.6	/	/
Sand (%)	5.0	/	/
pH H_2O	8.2	/	/

Two contrasted types of crop residues were used to form the mulch in this experiment: i) a moderately decomposable residue, namely mature oilseed rape (*Brassica napus* L.) with a C:N ratio of 29, and ii) an easily decomposable residue, namely young rye (*Secale cereale*) with a C:N ratio of 16 (Table A.3). Both residues were labeled ^{13}C. For the rape, the residues consisted of a mixture of leaves, stalks, branches and pods. For the rye residue, the sample consisted only of green leaves, as the growth of rye crop was stopped before elongation stage. Both residues were chopped in 1 cm- pieces with scissors, before application onto the soil. The ^{13}C atom excess % was 2.88 for both residues.

Table A.4 Description of experimental conditions for the rape and rye experiments

Parameter	Rape experiment	Rye experiment
Amount of soil† (kg column^{-1})	6.022	
Initial N-NO_3^- in soil (mg kg^{-1} soil)	9.80	29.85
Amount of residues† added (g column^{-1})	13.78	13.78
N added by residue (g column^{-1})	0.12	0.37
C added by residue (g column^{-1})	5.82	5.98
Temperature (°C)	20	
Duration (d)	64	
Days for rain application (d)	1, 21 and 42	

† amount expressed in dry mass.

Plastic cylinders (15.4 cm diameter and 30 cm length) were used to pack soil over 25 cm depth at 1.3 g cm^{-3} (equivalent to 6.022 kg of dry soil per column). We built a total of 28 columns, 14 by residue type. For each residue experiment, two replicates were dedicated to continuous measurements, three replicates were dedicated to mulch water content measurement and 9 columns were dedicated to destructive measurements (3 replicate columns were destroyed after each rain). For each residue experiment, a dry mass of 13.78 g (equivalent to 7.4 t ha^{-1}) was applied at the surface of each cylinder as mulch.

The experiment lasted 9 weeks and included 3 rain applications followed by 3 drying periods (Table A.4). Artificial rain was applied every 3 weeks on the columns at days 0, 21 and 42 from a rain simulator. The first rain had an intensity of 12 mm h^{-1} during 2.5 hours. For the second and third rain, the columns were left under the rain simulator at the same intensity until the water lost during the current evaporation period was compensated. During the drying periods, the columns were kept in a climate chamber at 20°C and 70% relative air humidity to allow evaporation.

Measurements during incubation

Measurements were the same for the rape and the rye experiments. Two columns were equipped with probes to provide information about the transport of water and solutes. At -6

and -14 cm below the soil surface, the volumetric water content was measured by horizontally placed TDR-probes (3 rods, 8 cm). The measurements were registered every hour on a TRASE system (Soilmoisture Equipment Corp.). At the same level of the column, the soil water potential was determined with tensiometers equipped with RhizoCera porous cups (3 mm diameter and 5 cm length, Rhizosphere Research Products) connected to differential pressure sensors (CZ5022/2, EuroSensor). Measurements of the soil water potential were stored in a CR10X data logger (Campbell Scientific). Soil solution was sampled 12 hours after the application of each rain at –2 cm below the soil surface, using Rhizon MOM soil solution samplers (10 cm length, Rhizosphere Research Products). The samples were stored at -20°C and later analyzed for mineral nitrogen (TRAACS 2000, Bran & Luebbe). Mass loss of the columns was used to calculate daily evaporation rates.

The flux of CO_2 from the soil surface to the atmosphere was calculated from the accumulation rate of CO_2 in the headspace of the columns. During a 3-min period, the columns were sealed with a cover connected to an infrared gas analyzer (UNOR 610, Maihak). A fan inside the 'closed chamber' provided homogenous mixing of the air. The slope of a linear regression between the increase of CO_2 concentration and the elapsed time was used to calculate the CO_2 flux. Measurements were performed on a daily base at the beginning of every evaporation cycle and every 2 or 3 days after the initial flush of microbial activity.

The columns dedicated to mulch water content measurement (3 for each residue) were constructed with detachable mulch. The residues were placed on a 1-mm mesh to allow measurements of the mulch mass. These data were used to calculate the water content of the mulch, after correction of the mass for leached and mineralized C.

Measurements at destructive soil samplings

After 3, 6 and 9 weeks, three soil columns of each residue were destroyed for analysis. The mulch was removed and dried at 60°C during 48 hours. The soil columns were sliced in four parts: 0-5, 5-10, 10-17.5 and 17.5-25 cm. The soil adhering to the recovered residues was detached with a needle and analysed separately. The soil gravimetric water content was determined in each layer (24 h at 105°C) immediately after destruction. Soil mineral nitrogen was extracted with 1 *M* KCl (30 minutes shaking, soil-to-solution ratio 1/2.5). Soil extracts for mineral N were centrifuged (20 minutes at 5800 *g*), filtered and stored at -20°C until analysis.)

Specific soil incubations

Specific incubations were carried out to derive the biological parameters of CANTIS submodel. Those incubations were done with the same batch of soil, at a constant temperature (20°C) and matric potential (-5.0 × 10^4 Pa) in non-limiting mineral nitrogen conditions (N-NO_3^- = 77 mg N kg^{-1}soil) for 172 days. The soil was incubated either alone (control) and with plant residues. The residues were finely chopped (1-3 mm) and mixed thoroughly with soil aggregates, at the rate of 2 g dry matter kg^{-1}soil. The mineralization of C was continuously measured by trapping CO_2 evolved into NaOH, with the traps renewed daily at the beginning of the experiment then weekly when the rate of mineralization slowed down, with in total 27 interval measurements. The trapped CO_2 was analyzed by back titration with HCl. At 12 sampling dates, soil was destructively sampled and the mineral N in soil was extracted with 1 *M* KCl and analyzed by continuous flow colorimetry as described above.

Analytical methods

The amount of fresh organic matter (FOM) added to the soil was determined for both residues. The soluble fraction (SOL) of the added residues was extracted by shaking in cold water for 30 minutes. The neutral detergent fraction (NDF), hemicelluloses (HEM), cellulose (CEL), and lignin (LIG) fractions were determined by proximate analysis (Van Soest & Wine, 1967). The rapidly decomposable material (RDM) is the difference NDF-SOL. The concentrations of total C and N in the SOL, NDF, HEM, CEL and LIG fractions were determined with an elemental analyzer (NA1500, Carlo Erba).

The microbial biomass carbon was determined by a modified fumigation-extraction method proposed by Vance *et al*. (1987). The soluble carbon from soil samples, unfumigated or fumigated with chloroform, was extracted by 0.03 *M* K_2SO_4 (soil:extractant ratio = 1:4), followed by centrifuging (20 minutes at 5800 *g*) and storage at -40°C. The concentration of soluble carbon in the extracts was measured by an oxidation method at 100°C in a persulphate medium, the CO_2 produced being measured by infrared spectrometry. The microbial biomass carbon was calculated as the difference between the soluble C in the fumigated and the unfumigated soil, and dividing by a coefficient K_{EC} = 0.38 (Vance *et al*., 1987).

The mineral nitrogen (NO_3^--N and NH_4^+-N) contained in the soil water solution and in the soil KCl extracts was measured by continuous flow colorimetry (TRAACS 2000, Bran & Luebbe). The total C content of the soil and the recovered plant residues and its atom excess

^{13}C, was determined using an elemental analyser (NA 1500, Carlo Erba) coupled to a mass spectrometer (Fisons Isochrom).

Modeling conditions

PASTIS$_{mulch}$ is applied to the 25-cm monoliths of soil covered by the mulch of rye and rape of constant thickness, z_m (m). Depth is set to zero at the soil-mulch interface. Rain intensity and actual evaporation are imposed to the model as the surface boundary condition for water. When the topsoil water potential reaches a limit potential, h_{lim} = -1.0 × 10^8 Pa, this potential is set as a Dirichlet condition at the soil surface. At the bottom, the water boundary condition is Neumann zero flux condition. A third-type flux condition is set for solutes at the soil surface and a free drainage condition is imposed at the bottom. Temperature is constant and set to 20°C in the whole system. The equations of PASTIS$_{mulch}$ are solved by using a finite differences technique with regular node spacing of 0.5 cm and a time step between 0.001 and 360 s.

Model parameters

Initial conditions

The initial conditions were derived from measurements for each experiment. The initial water condition of PASTIS$_{mulch}$ was given by a constant volumetric water content profile: 0.217 m^3 m^{-3} for the rape experiment and 0.176 m^3 m^{-3} for the rye experiment. Solutes in soil were initialized with constant concentration profiles: [NO_3^-] = 0.257 mg cm^{-3} for the rape experiment, [NO_3^-] = 0.783 mg cm^{-3} for the rye experiment, [NH_4^+] = 0.001 mg cm^{-3} for both residues. The initial values for the CANTIS submodel are listed in Table A.5.

Water flow parameters

The soil water retention curve $h(\theta)$ was obtained for each residue mulch experiment using TDR and tensiometer measurements in the column (matric potential in the range of -5.0 × 10^3 to -3.0 × 10^4 Pa) and the pressure extractor method (Klute, 1986) for lower matric potentials (-5.0 × 10^4, -1.0 × 10^5, -3.0 × 10^5 and -1.5 × 10^6 Pa). The experimental data were fitted with the Van Genuchten (1980) model:

$$S_e(h) = \frac{\theta - \theta_r}{\theta_s - \theta_r} = \left[1 + (\alpha h)^n\right]^{-\left(1-\frac{1}{n}\right)} \qquad (11)$$

where $S_e(h)$ is the effective saturation, θ_r and θ_s are respectively the residual and saturated volumetric water contents ($m^3\ m^{-3}$), α is the scaling factor of matric potential (m^{-1}), and n is an empirical shape parameter (-).

The Van Genuchten (1980) model was selected for the hydraulic conductivity curve $K(\theta)$:

$$K(\theta) = K_s S_e^l \left[1 - \left(1 - S_e^{1/m} \right)^m \right]^2 \qquad (12)$$

where K_s is the saturated soil hydraulic conductivity ($m\ s^{-1}$), m is an empirical shape parameter (-), and l is the tortuosity parameter set to 0.5. Saturated infiltration measurements on an independent sample of the same soil provided a saturated water conductivity of 8.86×10^{-6} m s^{-1}. This value was an estimate of saturated water conductivity of the columns but could not allow prediction of water conductivity for non-saturated water contents. To minimize the discrepancies between soil water simulation and observation we decided to slightly tune the conductivity parameters K_s and m. The best values were determined by non-linear fitting on the simulated soil matric potentials at -6 and -14 cm compared to the corresponding tensiometric measurements. The optimized K_s was of the same order of magnitude as measured K_s and m was reasonably close to estimates derived from the Mualem law ($m = 1 - 1/n$), for both experiments. All the parameters of Equations (11) and (12) are given in Table A.6 for both experiments.

Biological parameters

We estimated the biological parameters of the CANTIS submodel either by fitting the model to the data of the specific incubations (C and N mineralization curves), as already described in Garnier *et al*. (2003), or by taking default values from literature (Table A.1).

The incubation data obtained in the soil without residue (control) were used to estimate three parameters for the decomposition of humified organic matter: the decomposition rates, k_A and k_H, and the humification coefficient h_A (right hand side of Figure A.1). We determined the parameters by non-linear fitting of model outputs to observed C and N mineralization curves. The assimilation yields by the autochthonous biomass (Y_H and Y_A) were set to 0.62 g C g^{-1} C. The C:N ratio of the autochthonous biomass was assumed to be 8.

Table A.5 Initial condition of organic pools and microbial biomasses used in the CANTIS (Carbon And Nitrogen Transformations In Soil) submodel

Parameter	**Rape**	**Rye**
Amount of fresh organic matter (FOM) (g C m^{-2})	237.91	190.78
C content/dry mass conversion factor of FOM (g C g^{-1} DM)	0.464	0.494
Proportion of rapidly decomposable material in FOM (g C g^{-1} C)	0.26	0.18
Proportion of hemicelluloses in FOM (g C g^{-1} C)	0.15	0.44
Proportion of cellulose in FOM (g C g^{-1} C)	0.47	0.35
Proportion of lignin in FOM (g C g^{-1} C)	0.12	0.03
Amount of soluble organic compounds (g C m^{-2})	51.51	108.2
Amount of zymogenous microbial biomass (mg C kg^{-1} soil)	32.1	32.1
Amount of autochthonous microbial biomass (mg C kg^{-1} soil)	96.2	96.2
Amount of humified organic matter (mg C kg^{-1} soil)	8372	8372
C:N ratio of rapidly decomposable material (g C g^{-1} N)	32.89	11.74
C:N ratio of hemicelluloses (g C g^{-1} N)	22.03	9.82
C:N ratio of cellulose (g C g^{-1} N)	$+\infty$	$+\infty$
C:N ratio of lignin (g C g^{-1} N)	44.64	12.44
C:N ratio of soluble organic pool (g C g^{-1} N)	13.89	16.13
C:N ratio of zymogenous microbial biomass (g C g^{-1} N)	12.26	9.69
C:N ratio of autochthonous microbial biomass (g C g^{-1} N)	8.00	8.00
C:N ratio of humified organic matter (g C g^{-1} N)	9.47	9.47
C:N ratio of total residue (g C g^{-1} N)	29.10	16.10

Table A.6 Hydraulic parameters of soil retention and soil conductivity curves for the rape and the rye experiments

Symbol	Parameter	Rape experiment	Rye experiment
Retention curve *h(θ)*			
θ_s	Saturated volumetric water content ($m^3\ m^{-3}$)	0.535	0.500
θ_r	Residual volumetric water content ($m^3\ m^{-3}$)	0.000	0.000
α	Scaling factor of matric potential (m^{-1})	25.9	10.7
n	Empirical shape parameter (-)	1.185	1.228
Conductivity curve *K(θ)*			
K_s	Saturated water conductivity ($m\ s^{-1}$)	1.67×10^{-5}	4.17×10^{-5}
m	Empirical shape parameter (-)	0.225	0.200

The incubation data obtained in the soil with incorporated residues were used to calculate three parameters concerning the decomposition of fresh organic matter: the decomposition rate k_Z, the humification rate h_Z and the C:N ratio of the zymogenous biomass (left hand side of Figure A.1). The assimilation yields by the zymogenous biomass (Y_S and Y_Z) were set to 0.62 g C g^{-1} C. The size of the zymogenous biomass was initialized at 32.1 mg C kg^{-1}, which represented 25% of the total microbial biomass (Table A.5).

We assumed that decomposition rates in incubation experiments did not depend on the size of the biomass, and thus set parameters K_{MA} and K_{MZ} to 0. The model accounts for direct and indirect assimilation of N by microbes (organic and mineral forms respectively). The proportion of direct assimilation by the zymogenous biomass, α_Z, and by the autochthonous biomass, α_A, were set to 1 and 0 respectively (Garnier *et al*., 2003). The nitrification parameters ($V_{max} = 5$ mg N kg^{-1} d^{-1} and $K_N = 3.5$ mg N kg^{-1}) and the partition coefficient between NH_4^+ and NO_3^- immobilization ($\beta = 0.045$) were taken from Garnier *et al*. (2003).

Model calibration and evaluation

Calibration

The PASTIS$_{mulch}$ model was calibrated on three parameters which were introduced in the formalism of mulch decomposition and were not easy to assess accurately by direct measurement or observation: the initial amount of mulch dry mass in contact with the soil $DM_{m,c}(0)$ (g m^{-2}), the mulch feeding rate α_{feed} (d^{-1}), and the maximum soil depth for available nitrogen for mulch decomposition $z_{m,zyb}$ (cm). The efficiency, E_f (-), was used to assess model performance (Smith *et al*., 1996):

$$E_f = \frac{\sum_{i=1}^{n}(m_i - \overline{m})^2 - \sum_{i=1}^{n}(s_i - m_i)^2}{\sum_{i=1}^{n}(m_i - \overline{m})^2} \qquad (13)$$

where m_i and s_i are the measured and simulated results for a given state variable, and $\overline{m}$ is the average of the n measured results. For each residue, the efficiency was calculated for the amount of carbon remaining in the mulch and for the nitrate content of the 0-5 cm topsoil layer. The arithmetical average of these efficiencies, $\overline{E}_f$ (-), was used to identify the best simulation for the rape and the rye experiments. For both experiments the tested values for calibrated parameters were 0, 20, 40, 60, 80 and 100% of $DM_m(0)$ for $DM_{m,c}(0)$, 10^{-1}, 10^{-2} and 10^{-3} d^{-1} for α_{feed}, and 1, 3, 5, 7 and 10 cm for $z_{m,zyb}$.

Evaluation

The model was evaluated with the calibrated mulch parameters for both mulch experiments. The simulations of the water, nitrogen and carbon dynamics were analyzed and discussed for the soil and the mulch.

Sensitivity analysis

A one-at-a-time analysis of sensitivity of PASTIS$_{mulch}$ was carried out on the three calibration parameters plus four additional parameters: the initial dry mass, $DM_m(0)$, the maximal and residual volumetric water content of mulch elements, $\theta_{me,max}$ and $\theta_{me,res}$ respectively, and the mulch propensity to water recharge, α_m. The relative variation of the parameters, $\Delta X_i(j)$ (-), was defined as:

$$\Delta X_i(j) = \frac{X_i^j - X_i^*}{X_i^*} \quad (14)$$

where $X_{1\le i\le 7} \in \left\{DM_m; DM_{m,c}; \alpha_{feed}; z_{m,zyb}; \theta_{me,sat}; \theta_{me,res}; \alpha_m\right\}$ stands for the tested parameter, X_i^* and X_i^j are the optimum value and current value j of parameter X_i respectively. Model sensitivity was studied through three significant output variables related to mulch effects: the cumulative CO_2 flux, $CO_{2,cum}$ (kg C ha^{-1}), the final carbon amount remaining in the mulch, $C_{m,fin}$ (mg C m^{-2}), and the final nitrate content in the 0-5 cm topsoil layer, $NO_{3,fin}^-$ (kg N ha^{-1}). The sensitivity, ζ (-), was expressed for each parameter and each variable as:

$$\zeta\left(X_i, j, Y_k\right) = \frac{1}{2}\left\{\left[\frac{Y_k^{rape}\left(X_1^*,\text{K},X_i^j,\text{K},X_7^*\right)}{Y_k^{rape}\left(X_1^*,\text{K},X_i^*,\text{K},X_7^*\right)} - 1\right] + \left[\frac{Y_k^{rye}\left(X_1^*,\text{K},X_i^j,\text{K},X_7^*\right)}{Y_k^{rye}\left(X_1^*,\text{K},X_i^*,\text{K},X_7^*\right)} - 1\right]\right\} \quad (15)$$

where $Y_{1\le k\le 3} \in \left\{CO_{2,cum}; C_{m,fin}; NO_{3,fin}^-\right\}$ is the type of simulated variable.

Results and discussion

Model calibration

The values of calibrated parameters (Table A.7) show two different patterns for the rape and the rye experiments. For the rape, the optimal value of $DM_{m,c}(0)$ was only 20% of total initial mulch dry mass. The larger size of the rape mulch elements impeded a close contact between the soil and the mulch elements, especially those from the upper part of the mulch. For the rye, we found an optimal value of $DM_{m,c}(0)$ of 80% of total initial mulch dry mass. This result can be explained by the smaller size of the elemental pieces of the rye mulch which were clumped together by the fungal hyphae and by a more intimate contact between the base of the mulch and the soil. The mulch feeding rate, α_{feed}, took the highest value of the calibration range and was the same for both kinds of residue. This parameter had little influence on simulation, which will be discussed in the sensitivity analysis section. The maximum soil depth for available nitrogen for mulch decomposition, $z_{m,zyb}$, revealed another difference between the residues. For the rape this parameter took a high value of 5 cm. This suggests that fungi had an important role in rape mulch decomposition, which is in good agreement with the high C:N ratio of this residue. The fungal hyphae probably facilitated the

colonization of the poorly clumped mulch elements and allowed the deep absorption of nitrate in soil as already observed by Frey *et al*. (2000). For the rye $z_{m,zyb}$ took a small value of 1 cm. The close contact of this residue with the soil and its low C:N ratio made it easier for microorganisms to decompose and required less mineral nitrogen. Finally, no significant correlation was observed between parameters $DM_{m,c}(0)$ and $z_{m,zyb}$ for the rape or the rye experiment, which means that parameters were independent and specific of the decomposition processes they encompassed.

The simulations performed with the calibrated parameters were satisfactory (Table A.7), with global efficiencies of 0.813 and 0.924 for the rape and the rye experiments respectively. Carbon in mulch was well simulated for both residues with efficiencies higher than 0.8, good regression statistics despite a small bias of 5.1 mg C m^{-2} for the rye. PASTIS$_{mulch}$ reproduced fairly well the nitrate dynamics in the 0-5 cm topsoil layer for the rape which provided good values for all statistical criteria. The model performed satisfactorily for the rye in spite of a larger bias of -3.3 kg N ha^{-1}. The linear correlation between simulation and observation was high ($R^2 = 0.930$) but the regression was far from the Y=X axis. These discrepancies will be discussed in the model evaluation section.

Model evaluation

Matric potential in soil

Measured soil matric potential showed a strong increase when rain was applied and then a gradual decrease with a typical downward gradient during the evaporation stages, for both experiments. However the evaporation limitation caused by the mulch kept the soil matric potential in a reduced range (ψ > -2.0 × 10^4 Pa) which corresponded to a soil volumetric water content higher than 0.25 m^3 m^{-3} during the whole experiment.

The retained soil hydraulic parameters provided good simulations of soil matric potential for the rape and the rye experiments (Figure A.3), with efficiencies of 0.963 and 0.916 respectively. The slight difference in hydraulic properties between both experiments is attributed to the changes in soil aggregation during the storage period (soil storage for the rye experiment was 10 months longer than for the rape experiment).

Table A.7 Optimal value of the parameters and statistical performance of the calibrated model for the rape and the rye experiments

Symbol	Parameter, variable	Rape	Rye
$DM_{m,c}(0)$	Initial mulch dry mass in soil contact (g m^{-2})	110.6	333.9
$DM_{m,c}(0) / DM_m(0)$	Initial proportion of mulch dry mass in soil contact (%)	20	80
α_{feed}	Mulch feeding rate (d^{-1})	0.1	0.1
$z_{m,zyb}$	Depth for available N for mulch decomposition (cm)	5	1
Global performance			
$\overline{E}_f$	Average model efficiency (-)	0.804	0.825
Carbon in mulch			
E_f	Model efficiency for carbon (-)	0.813	0.924
Slope	Slope of linear regression (-)	0.711	0.876
Origin	Origin of linear regression (mg C m^{-2})	80.5	34.1
σ_{res}	Residual standard deviation (mg C m^{-2})	6.1	6.7
R^2	Determination coefficient (-)	0.832	0.955
B	Bias (mg C m^{-2})	0.8	5.1
Nitrate in soil (0-5cm)			
E_f	Model efficiency for nitrate (-)	0.795	0.725
Slope	Slope of linear regression (-)	0.914	0.579
Origin	Origin of linear regression (kg N ha^{-1})	0.8	6.6
σ_{res}	Residual standard deviation (kg N ha^{-1})	1.3	2.0
R^2	Determination coefficient (-)	0.813	0.930
Bias	Bias (kg N ha^{-1})	-0.2	-3.3

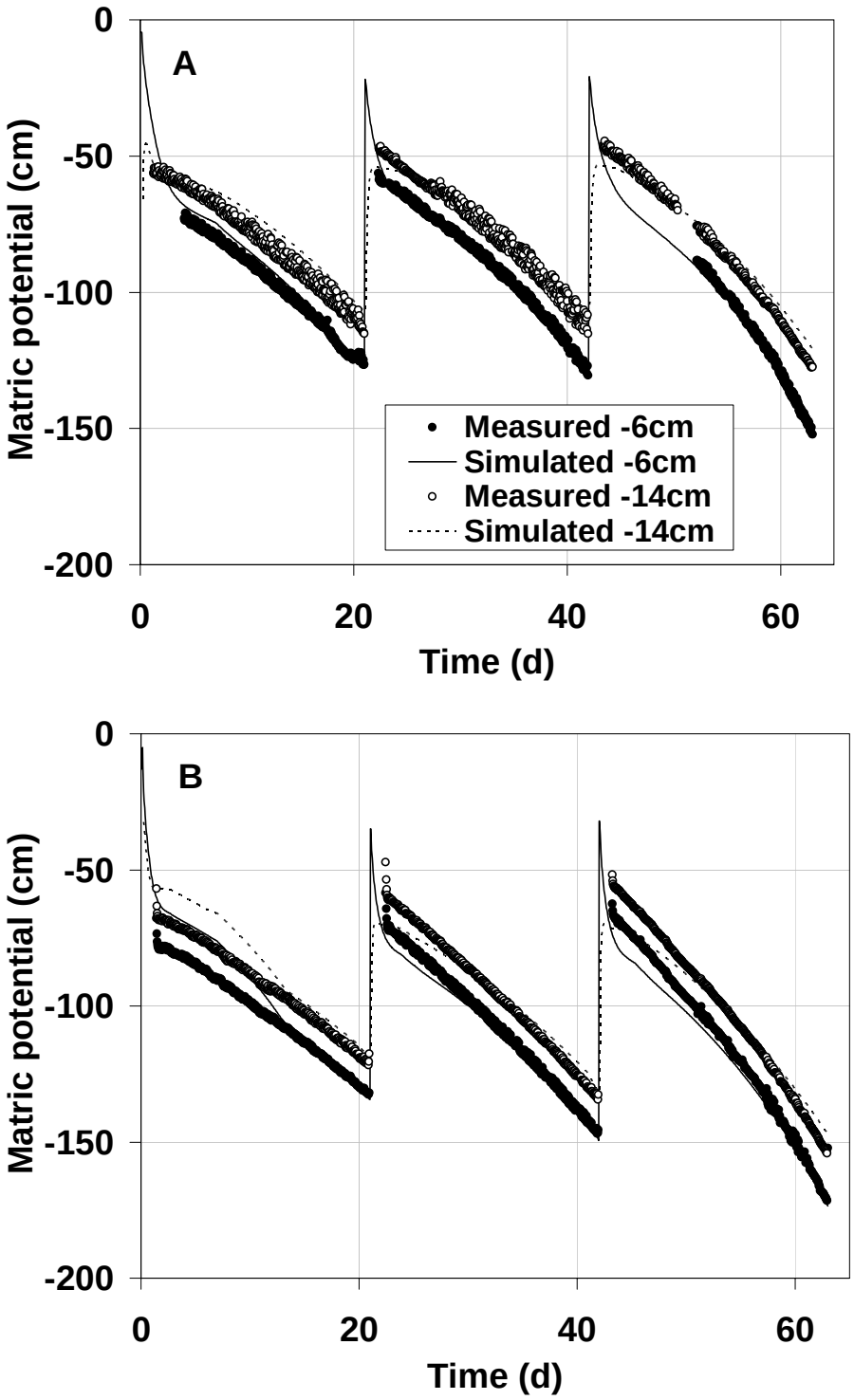

Figure A.3 Simulated and measured matric potentials in the soil at -6 and -14 cm: (A) rape experiment and (B) rye experiment (1 cm of water = 100 Pa).

Mulch evolution

Water content of mulch

Gravimetric measurements showed the successive mulch wetting-drying cycles (Figure A.4): gravimetric water content of mulch elements, w_{me} (g g^{-1}), quickly increased during the rain application and then decreased gradually during the evaporation stage. 5 or 6 days after rain application w_{me} reached a minimal value of 0.3 g g^{-1} for both residues, which corresponded to the mulch residual water content $\theta_{me,res}$ (Table A.2). The time necessary to reach this minimal value decreased along mulch decomposition because the residue mass and thus the maximal mulch water storage decreased. The initial maximal observed gravimetric water content was close to $w_{me,max}$ for both residues (Table A.2) and then slightly increased for the rape and dramatically increased for rye. This increase was probably due to an alteration of mulch physical properties as a consequence of decomposition processes. Observation showed that the development of the fungi hyphae in the mulch clumped the rye leaves and formed a decomposing humus-like organic layer that could store more water per unit weight than fresh residues.

The model simulated well the water dynamics of the rape mulch ($E_f = 0.852$). The successive wetting and drying cycles were well reproduced. However, some discrepancies were observed for the rye mulch ($E_f = 0.529$) for which the model underestimated the maximal mulch water content and the time necessary for the mulch to dry. This problem was partly due to the evolution of the mulch properties during decomposition. PASTIS$_{mulch}$ could not account for an increase of maximal gravimetric water content during simulation. Also, the close contact between the small elements of the rye mulch and the soil may have facilitated mulch water recharge by capillary rise. This phenomenon was not taken into account in the model.

Dry mass of mulch

Observed dry mass of mulch decreased strongly during the first three weeks and then more slowly for both residues (Figure A.5). The decrease was faster and higher for rye mulch (-305 g dry mass m^{-2}) than for rape mulch (-250 g dry mass m^{-2}), partly because of the amount of soluble compounds in the rye. Simulated dry mass of mulch was calculated by summing dry mass of FOM and ZYB which originated from the mulch and remained intimately linked to the residue. The former was calculated from carbon content divided by a conversion factor

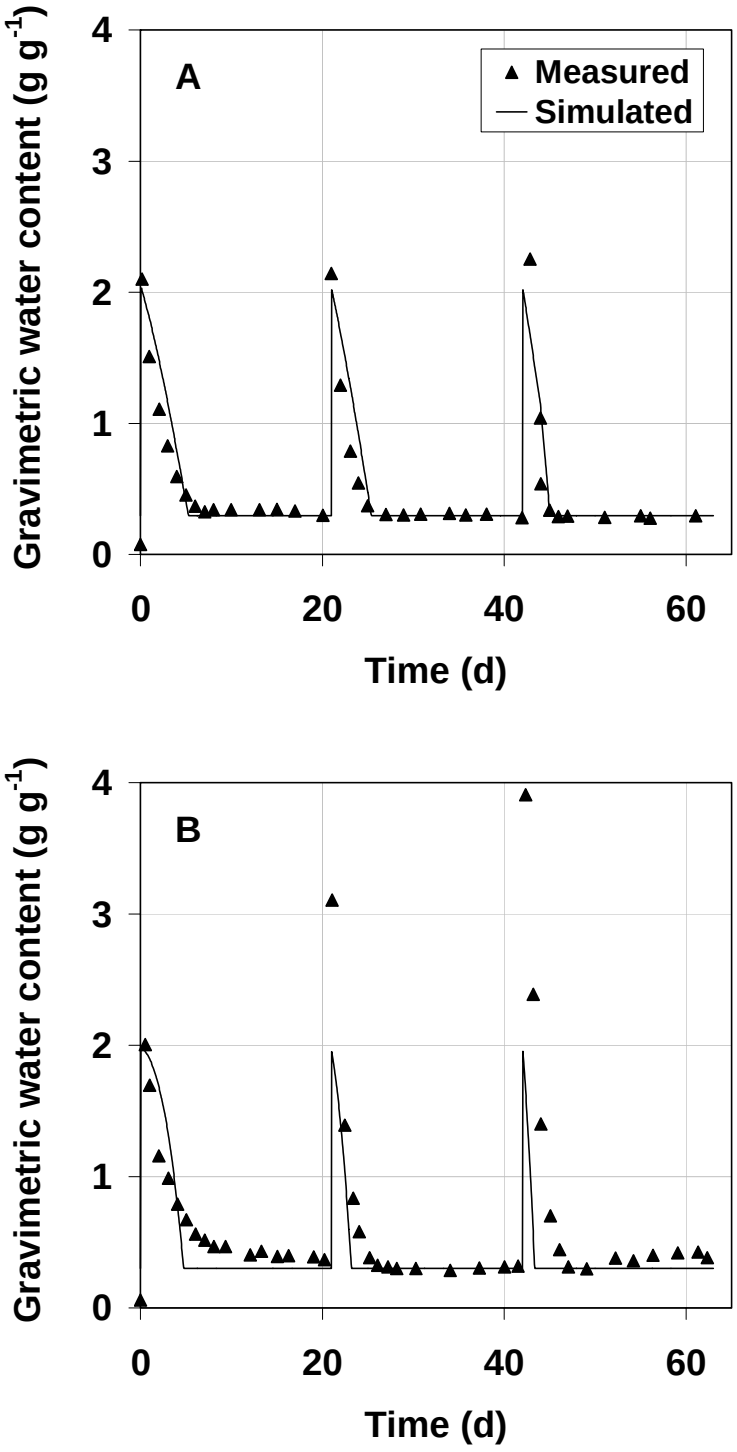

Figure A.4 Simulated and measured gravimetric water content: (A) rape experiment and (B) rye experiment.

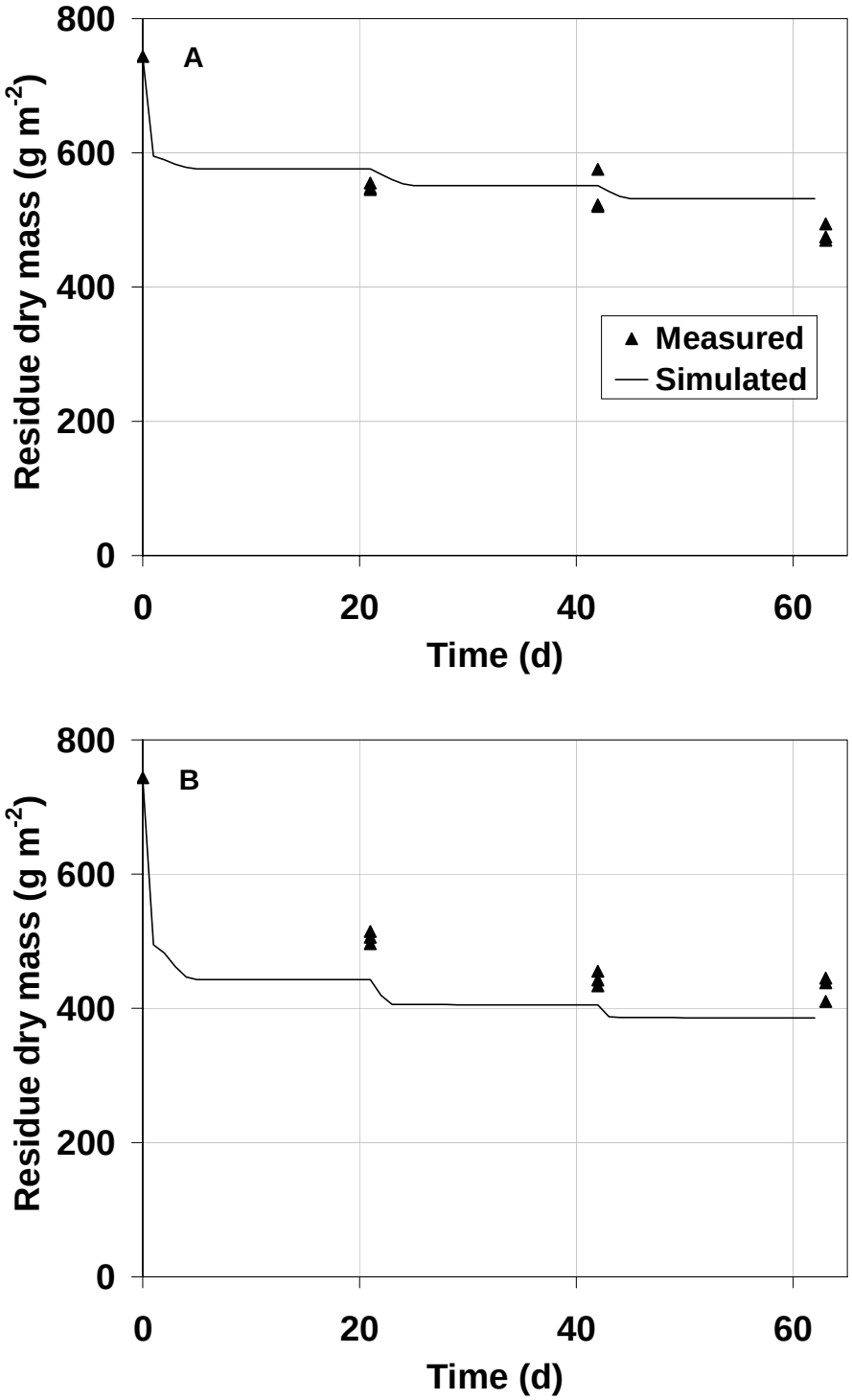

Figure A.5 Simulated and measured total dry mass of mulch: (A) rape experiment and (B) rye experiment.

provided by the Van Soest fraction analysis (Table A.5). The latter was estimated from ZYB carbon content by using a 0.5 conversion factor (Taylor *et al*., 2002). Simulated dry mass was in good agreement with experimental data with efficiencies for rape and rye experiments of 0.761 and 0.718 respectively. Differences between simulation and observation were always lower than 72 g m^{-2} in absolute terms for both residues. The model simulated a substantial decrease in dry mass during the 5-6 days following every rain and then an almost constant dry mass for both residues (Figure A.5). The strongest decrease during the first wetting-drying cycle, especially for rye mulch, was well simulated by the model although no measurement permitted to validate its kinetics. Also, dry mass decrease was strongly correlated to the mulch water content (Figure A.4). These results highlighted the importance of the type of residue in the decomposition processes.

Carbon and nitrogen dynamics

Carbon mineralization

Measured and simulated total (soil and mulch) CO_2 fluxes are represented in Figure A.6. Measured CO_2 fluxes were higher during and just after the rain application and then decreased during the evaporation period, for both residues (Figure A.6). This trend is correlated to the evolution of gravimetric water content of the mulch. The CO_2 production was stimulated by a high water content of the mulch. For the rape experiment, the CO_2 peak tended to decrease over time (80, 52 and 40 kg C ha^{-1} d^{-1} for the first, second and third peaks respectively), while the peaks for the rye experiment tended to remain constant over time with a rate between 80 and 90 kg C ha^{-1} d^{-1}. This behavior can be partly explained by the higher amount of soluble organic compound of the rye mulch (Table A.5) which generated larger and more lasting CO_2 emissions. Also the higher water content of the rye mulch during second and third rain (Figure A.4) facilitated mulch decomposition. Minimum CO_2 flux measured before each rain was higher for the rye experiment than for the rape experiment.

The peaks of CO_2 production were rather well described by the model except at the beginning of simulation where the model strongly overestimated CO_2 flux during one day for the rape and three days for the rye. Global efficiencies were poor for both experiments ($E_f < 0$), but became more satisfactory when removing the early overestimated simulation points from calculation ($E_f = 0.9$ for the rape and $E_f = 0.4$ for the rye experiment).

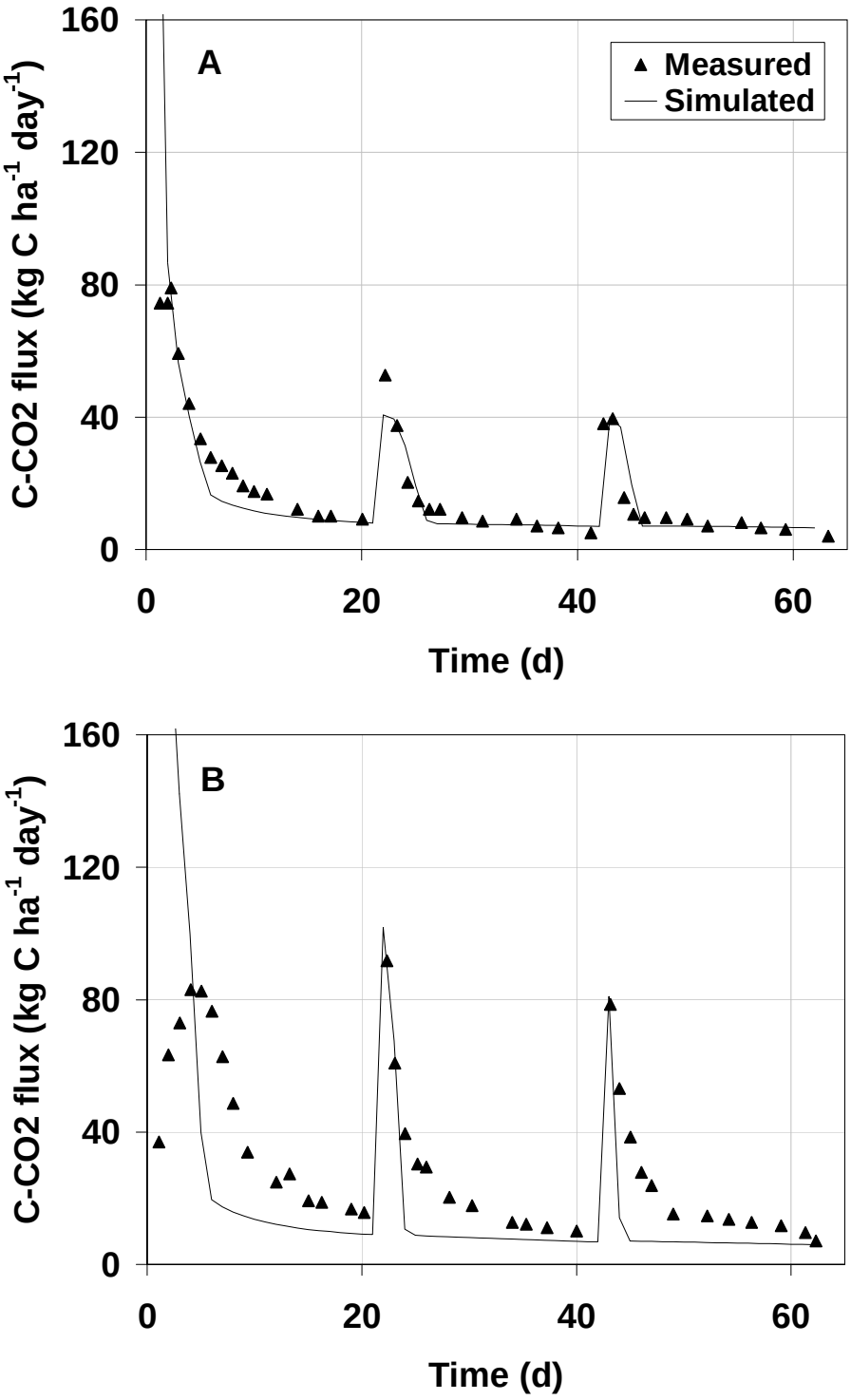

Figure A.6 Simulated and measured total CO_2 fluxes: (A) rape experiment and (B) rye experiment.

During the first wetting-drying cycle and when the topsoil layer was close to saturated water content, the CO_2 diffusion occurred mainly in water which dramatically reduced and delayed CO_2 flux. The measurements of CO_2 flux from the mulched soil to the atmosphere underestimated the real production of CO_2 in the whole column. The model considered that carbon mineralization resulted in an immediate CO_2 flux at the soil surface, without diffusion limitation in soil, and consequently provided higher maximum CO_2 flux than measurements. Also, PASTIS$_{mulch}$ simulated decomposition rates as independent on the size of the microbial biomass. This assumption is questionable at the beginning of the experiment when the zymogenous biomass strongly developed to colonize the residues, and can partly explain the overestimation of simulated CO_2 flux.

Additional observation on bare soil showed that only the first rain caused a mineralization flush leading to a CO_2 peak, whereas during the second and third rain the CO_2 emission from the soil remained constant. Consequently, the second and third peaks of the mulched columns probably resulted from a CO_2 flux mainly from the mulch, which emitted directly in the atmosphere without transfer limitation. PASTIS$_{mulch}$ could simulate those peaks more accurately in spite of a slight underestimation that can be correlated to the underestimation of gravimetric water content calculated by the model compared to experimental data (Figure A.4). When water content was underestimated, the moisture factor f_w was also underestimated and the simulated rate of CO_2 emission was reduced.

The biological parameters used for decomposing humified organic matter were the same for the rape and the rye experiments. Consequently, the minimal CO_2 flux simulated just before each rain was the same for both experiments which was not in agreement with measurements that showed, over the time interval, a greater mineralization rate for the rye experiment. The difference between simulated and observed CO_2 fluxes for the rye experiment may result from a priming effect induced by the leaching of soluble carbon into the soil (Table A.5), which was not taken into account in the model.

Mulch decomposition

Decomposition of rye mulch was faster than decomposition of rape mulch (Figure A.7). At day 64, measurement showed that only 66% on average of ^{13}C remained in the mulch of rye residue versus up to 83% in the mulch of rape residue. As already observed for dry mass (Figure A.5) and CO_2 flux (Figure A.6), mulch decomposition mainly occurred after rain when mulch was wet and was more intense just after the first rain.

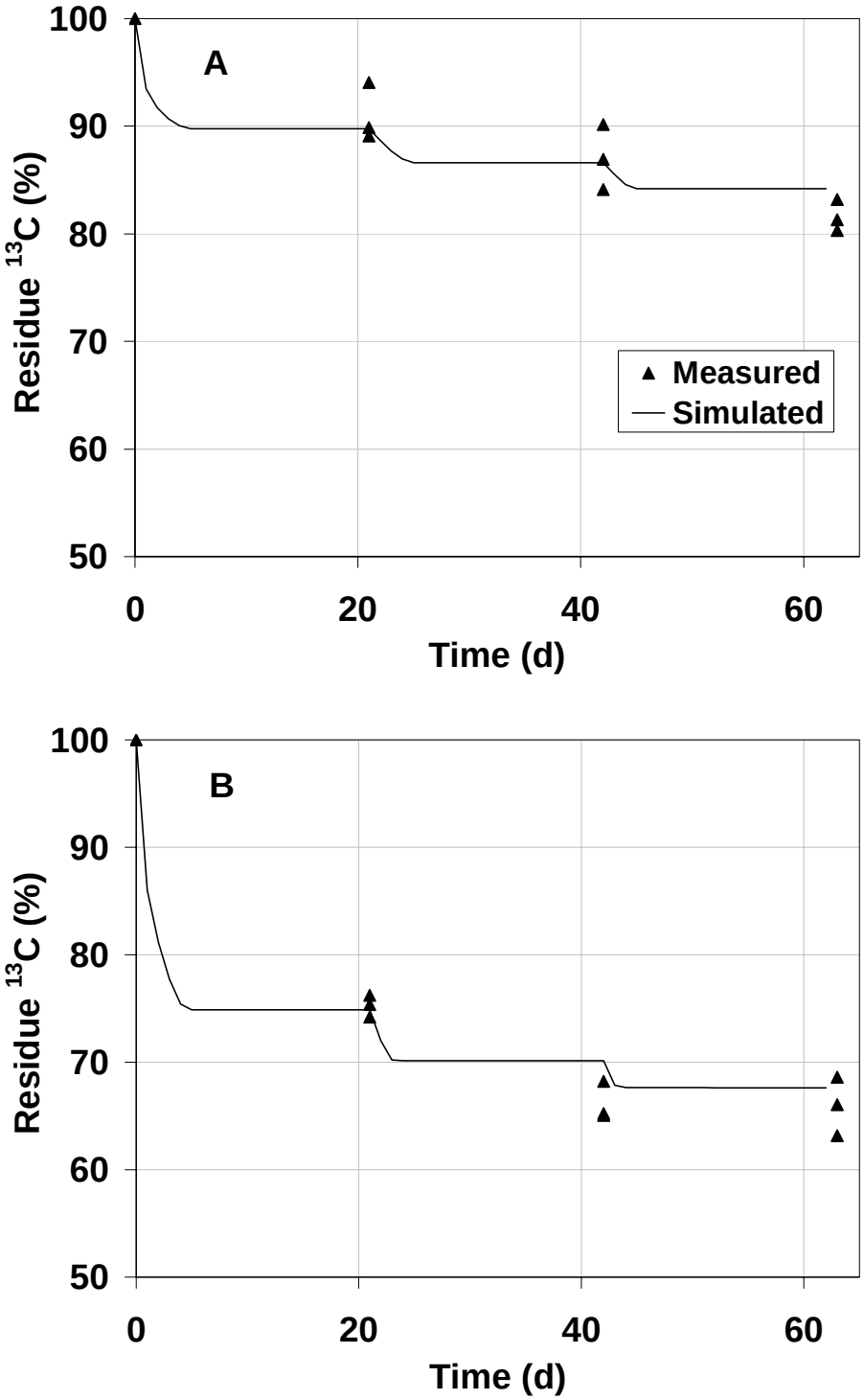

Figure A.7 Simulated and measured ^{13}C remaining in mulch: (A) rape experiment and (B) rye experiment.

The higher decomposition of rye can be explained by a lower total C:N ratio, a higher proportion of soluble organic compounds (Table A.5) and a better contact between mulch and soil for this residue (Table A.7).

PASTIS$_{mulch}$ reproduced well the two different decomposition dynamics with efficiencies of 0.813 and 0.924 for the rape and the rye respectively, and differences between simulation and observation always smaller than 5.1% (0.5 g C m^{-2}) in absolute terms.

We observed a good agreement between simulated and experimental data of remaining ^{13}C although the model underestimated the CO_2 flux for the rye experiment (Figure A.6B). In the specific rye incubations, which were used to optimize CANTIS biological parameters (Table A.1), we observed no priming effect: the difference between the final and initial C contents in the residue was close to the difference between the cumulative CO_2 emission from the incubated soil with rye residues and the cumulative CO_2 emission from the incubated bare soil. PASTIS$_{mulch}$ was run with the biological parameters of Table A.1 and simulated correctly the mulch decomposition, which confirms that the discrepancy between simulation and observation for the basal CO_2 emission was due to an additional soil emission term that PASTIS$_{mulch}$ could not simulate.

Nitrogen dynamics

Measured N-NH_4^+ content in soil was always lower than 1 mg N kg^{-1} soil, which was negligible compared to N-NO_3^- content. Consequently, we only considered nitrate as inorganic nitrogen. Measurements of N-NO_3^- amounts in the topsoil layer (0-5 cm) are presented in Figure A.8 for the end of each drying period. An increase in nitrate amount over time was observed for both residues. This increase can result from mineralization of humified organic matter of the soil, nitrate leaching from the mulch, and convective transport of nitrate by capillary rise of water in the soil during evaporation stages. The mulch created favorable moisture conditions for mineralization of soil organic matter as shown in Figure A.3 where the matric potential was always higher than -2.0×10^4 Pa. The increase of N-NO_3^- over time was higher for the rye experiment than for the rape experiment. This was mainly due to a greater release of nitrogen by the rye mulch which decomposed more than the rape mulch (Figure A.7) and whose nitrogen content was substantially higher (C:N of 16 for the rye and 29 for the rape).

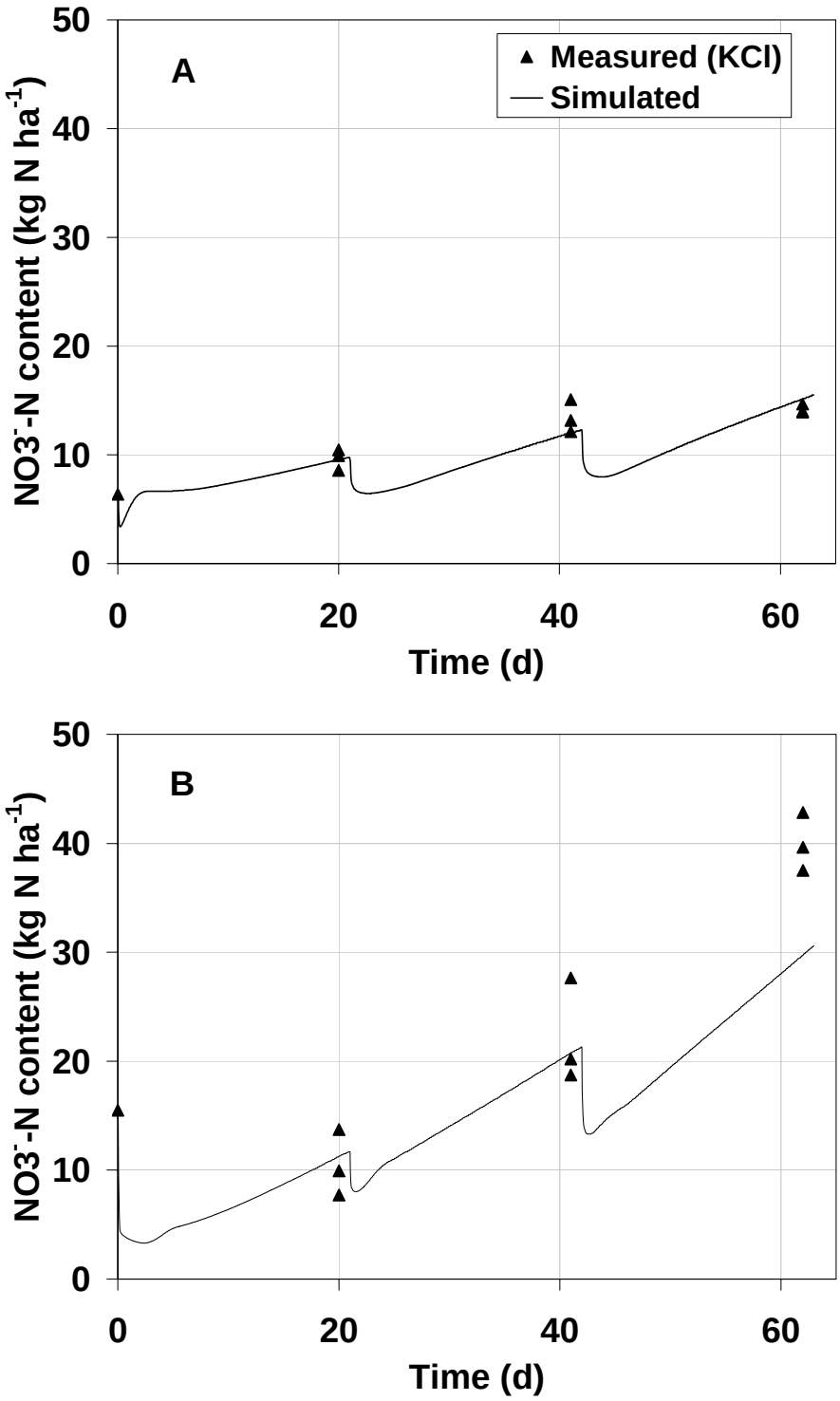

Figure A.8 Simulated and measured nitrate content in the 0-5 cm topsoil layer: (A) rape experiment and (B) rye experiment.

Measured and simulated values were in good agreement for both experiment (Figure A.8) with efficiencies higher than 0.725. The main discrepancy was found for the amount of N-NO_3^- of the rye experiment (Figure A.8B). The model slightly underestimated the data at the end of the third evaporation period. This discrepancy can be related to the assumption made previously to explain the high CO_2 flux of rye experiment (see previous comment for Figure A.6). The soluble organic compounds coming from rye mulch which increased basal carbon mineralization by priming effect also increased nitrogen mineralization of soil organic matter which led to a higher release of mineral nitrogen in soil.

Figure A.9 shows measured N-NO_3^- concentration in the soil solution at -2 cm below the mulch just after the rain. Nitrate concentration stayed nearly constant over time under the rape mulch whereas it increased substantially under the rye mulch. This increase was in agreement with experimental data in Figure A.8B and was attributed to the priming effect and the most complete decomposition of the rye residue (Figure A.7)

The model simulation of nitrate concentration at –2 cm was satisfactory for the rye ($E_f = 0.494$) but overestimated the experimental data for the rape experiment ($E_f < 0$). This overestimation was counterbalanced by an equivalent underestimation at -10cm and was possibly the consequence of a preferential downward convective transport of nitrate during the rain which the model could not account for. Simulation showed that nitrate concentration changed dramatically over time for both residues. For each wetting-drying cycle, simulated nitrate concentration decreased during rain application due to nitrate leaching and dilution effect and then increased during evaporation period due to capillary rise, mineralization and concentration effect caused by water depletion. The nitrate dynamics was more marked when expressed in concentration (Figure A.9) than in quantity (Figure A.8) because concentration was sensitive to the changes in water content at -2cm in addition to transport and mineralization/immobilization processes.

The global N balance terms are represented in Figure A.10 for the whole column (0-25 cm soil layer) for both experiments. For the rape experiment, simulated gross mineralization was always larger than gross immobilization, which resulted in a positive net mineralization that tended to increase to reach a maximum of 32.8 kg N ha^{-1} on day 63. For the rye experiment the gross mineralization was 42% larger on average than for the rape and reached 220 kg N ha^{-1}.The gross immobilization of the rye experiment was also greater (55% on average) and represented 188 kg N ha^{-1} in the end of the experiment. From day 1 to day 14 the gross immobilization prevailed and the net mineralization was negative. During the first rain a

substantial part of the soluble fraction of the rye residue was leached into the soil. This amount was greater for the rye residue than for the rape residue. Besides, although the total C:N ratio was higher for the rape than for the rye (Table A.5), the C:N ratio of the soluble organic compounds was higher for the rye than for the rape (16.1 versus 13.9 respectively) and induced a greater immobilization of soil inorganic N by the microbial biomass. After day 14 the net mineralization became positive and increased regularly to reach 36.5 kg N ha^{-1} on day 63.

PASTIS$_{mulch}$ simulation of nitrate content in soil was globally in good agreement with the data from rhizon samples and KCl extractions (Figure A.10). The simulation efficiencies, calculated without rhizon measurements of day 1, were 0.565 for the rape experiment and 0.747 for the rye experiment. Rhizon measurements were strongly impacted by the initial leaching of the mulch during first rain (organic and inorganic N), which the model could not simulate. However this discrepancy disappeared within the first drying period and simulated and observed nitrate content became comparable at day 20. Also, we observed a slight underestimation of late soil nitrogen content for the rye experiment. This behavior was again the consequence of the previously described priming effect that occurred for this experiment. The final net mineralization was larger for the rape experiment than for the rye experiment. This result may appear surprising because the C:N ratio of the rape residue is higher than that of the rye residue (29.1 versus 16.1 respectively – Table A.5). However, we saw that the rye residue had more soluble organic compounds with a higher C:N residue than the rape (Table A.5). Consequently, mineralization of the rye residue required an initial 20-days immobilization stage to decompose these soluble compounds leached into the soil since the first rain. Afterwards, the zymogenous biomass decomposed almost exclusively the non soluble fraction of the residue of lower C:N ratio which led to a net mineralization of 36.5 kg N ha^{-1} in 49 days (0.74 kg N ha^{-1} d^{-1} on average). During this stage the net mineralization flux of the rye experiment was higher than that of the rape experiment (0.52 kg N ha^{-1} d^{-1} on average), and would provide more mineralized N if the experiment lasted more.

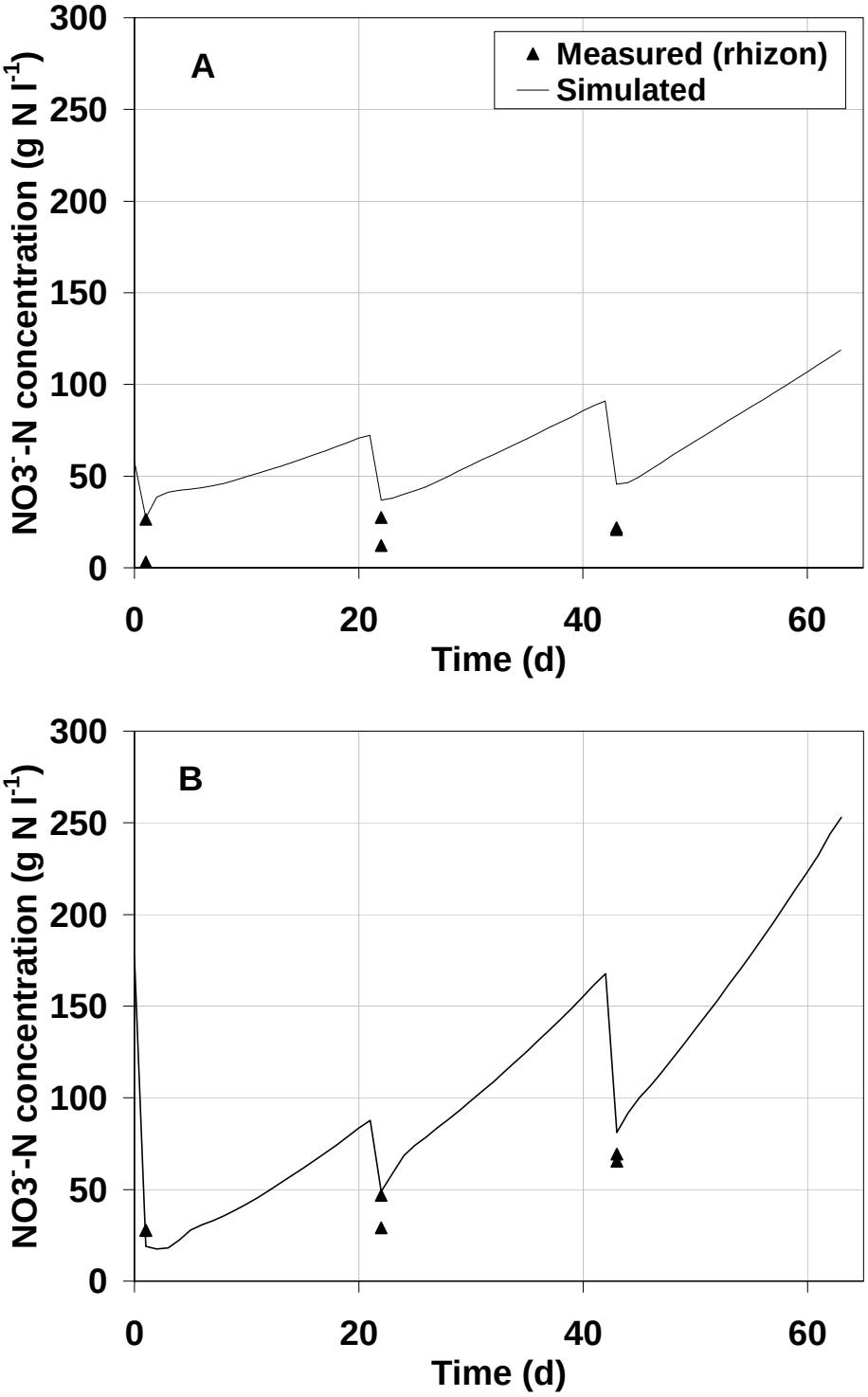

Figure A.9 Simulated and measured nitrate concentration in soil solution at -2 cm: (A) rape experiment and (B) rye experiment.

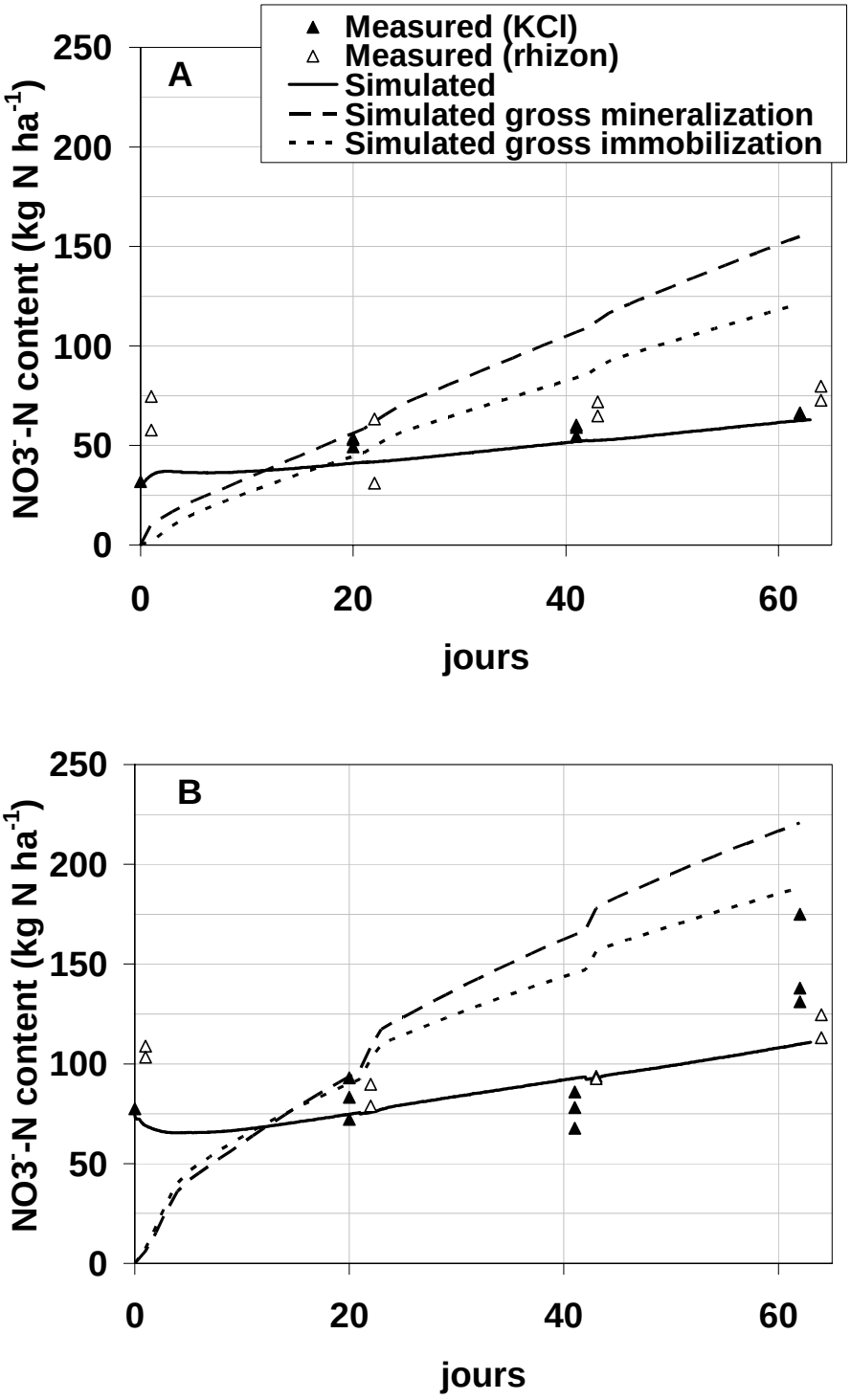

Figure A.10 Simulated and measured nitrate content in the 0-25 cm topsoil layer: (A) rape experiment and (B) rye experiment.

Sensitivity analysis

The model sensitivity, ζ (-), is presented for the cumulative CO_2 flux, the final carbon amount remaining in the mulch and the final nitrate content in the 0-5 cm topsoil layer (Figure A.11), for all tested parameters except the residual volumetric water content of mulch elements ($\theta_{me,res}$) and the mulch propensity to water recharge (α_m). For these two parameters ζ was lower than 4% for the three model outputs and all relative variations of parameter from -100% up to +200%. The highest sensitivity was observed for the total initial dry mass of mulch ($\zeta(DM_m(0))$ up to 127%), the initial dry mass of mulch in contact with the soil ($\zeta(DM_{m,c}(0))$ up to 55%) and the maximal volumetric water content of mulch elements ($\zeta(\theta_{me,max})$ up to 52%). ζ variation was moderate for the maximum depth for available N for mulch decomposition ($\zeta(z_{m,zyb})$ up to 16%), and limited for mulch feeding rate ($\zeta(\alpha_{feed})$ up to 7%). For output variables cumulative CO_2 flux and final carbon amount remaining in the mulch (Figure A.11A-B), the results were sound since a decrease of the carbon content in the mulch corresponded to an increase of CO_2 emission. The parameters $DM_{m,c}(0)$ and $DM_m(0)$ which defined the amount of directly or indirectly available fresh organic matter for decomposition had the greatest impact on model C outputs (up to 55 and 127% respectively). The model C outputs were also very sensitive to $\theta_{me,max}$ (up to 52%), that quantified the water storage capacity of the mulch and, consequently, the number of days during which the mulch was wet and could decompose. As already explained in the mulch decomposition section, the decomposition of the mulch was highly correlated to its water content (Figures A.4 and A.7). $z_{m,zyb}$ had logically little influence on C cycle since it drove topsoil inorganic N dynamics. Also, only very small values of α_{feed} had an impact on C model outputs in these laboratory conditions. For N output variable (Figure A.11C), the model sensitivity was moderate for $DM_{m,c}(0)$ and strong for $DM_m(0)$, up to 18 and 59% respectively, which emphasized the link between the carbon and nitrogen cycles in the mulch decomposition processes. $z_{m,zyb}$ had a moderate impact of up to 16% on model sensitivity.

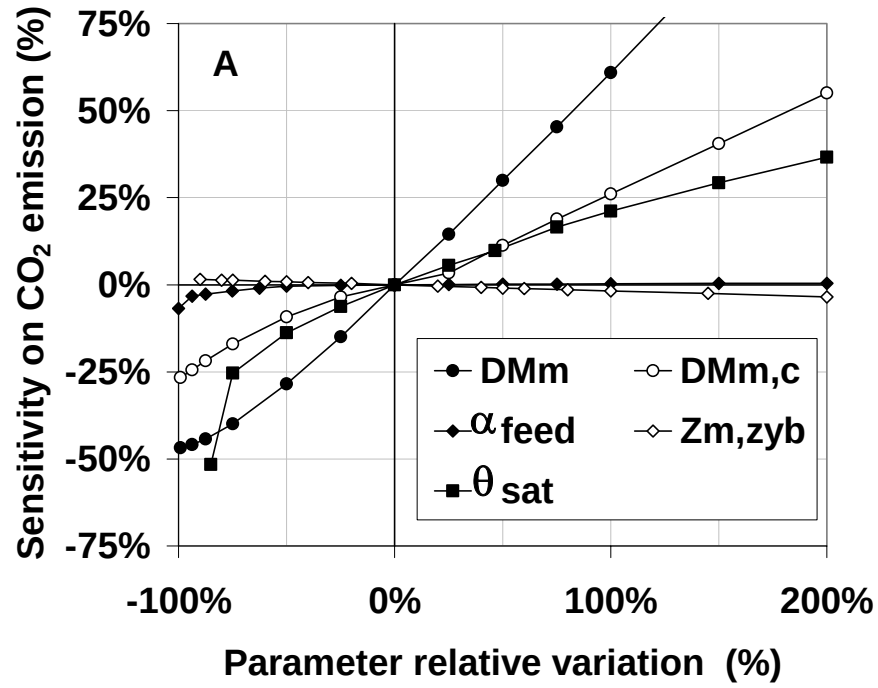
A
75%
50%
25%
0%
-25%
-50%
-75%
Sensitivity on CO_2 emission (%)
DMm
DMm,c
α feed
Zm,zyb
θ sat
-100%
0%
100%
200%
Parameter relative variation (%)

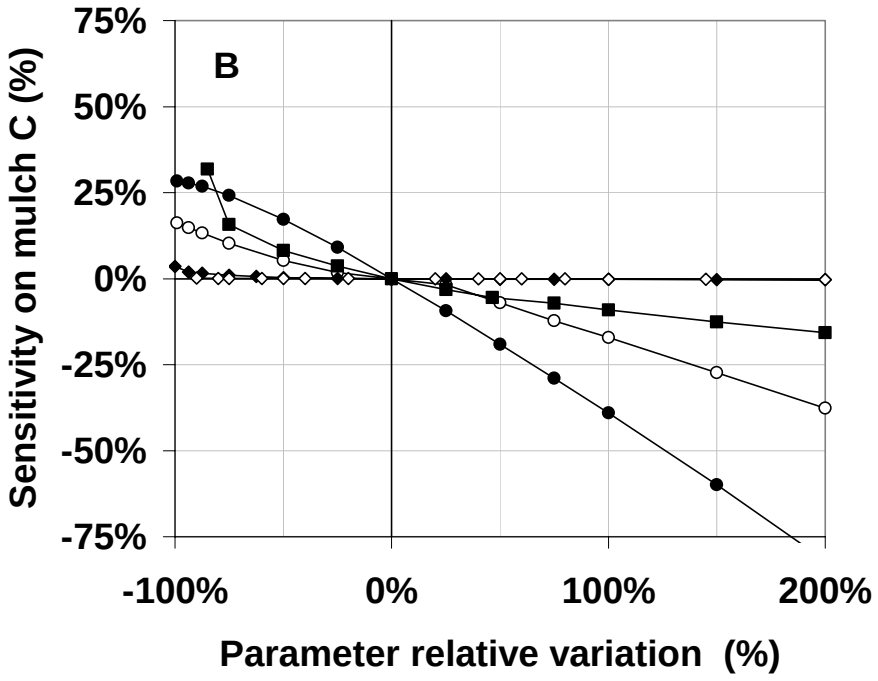
B
75%
50%
25%
0%
-25%
-50%
-75%
Sensitivity on mulch C (%)
-100%
0%
100%
200%
Parameter relative variation (%)

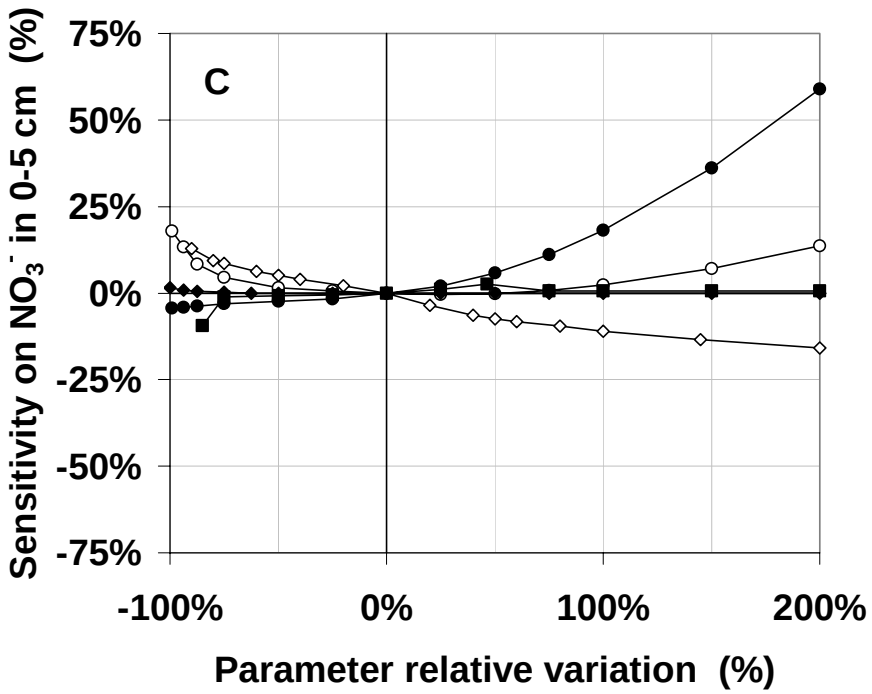

Figure A.11 Sensitivity analysis of the model outputs (cumulative CO_2 emission (A), final mulch residue carbon (B), and final nitrogen content in the 0-5 cm topsoil layer (C)) on 5 key parameters describing the mulch.

Nitrate content in the 0-5 cm topsoil layer decreased with this parameter because more nitrate was used by the zymogenous biomass for mulch decomposition. $\theta_{me,max}$ had little effect on model sensitivity partly because the extra mineralization caused by a $\theta_{me,max}$ increase was counterbalanced by a greater immobilization of the zymogenous biomass whose C:N ratio was lower than that of residue (Table A.5). Finally, the tested N output of the model was almost insensitive to α_{feed} (less than 2%), which can be explained by the controlled laboratory conditions. In real agronomical conditions this parameter could have more influence because weather conditions (wind drag force, heavy and variable rain events, frost and thawing,…) and agronomical treatments (tillage, cattle grazing,…) may influence strongly the structure of the mulch and, in turn, the amount of mulch in contact with soil.

Conclusion

The objective of this work was to identify and model the physical and biological effects of a decomposing residue mulch and its quality on water, carbon and nitrogen dynamics in a mulch-soil system. Experiments conducted for a mulch of rape or rye residues showed that mulch maintained a high soil volumetric water content ($\theta > 0.25$ m^3 m^{-3}) and that mulch water content had quick and sharp variations corresponding to rain application (wet mulch almost completely dried within 5 or 6 days). Mulch dry mass decreased by 34% for the rape experiment and 41% for the rye experiment emphasizing the role of mulch quality and size of elements in the decomposition process. Mulch C decomposition occurred when the residues were wet and was slower and less complete for the rape residues than for the rye residues (66% versus 83% respectively after 64 days) because the rye residues had a greater amount of soluble compounds, a lower total C:N ratio, a higher water content and a better soil-mulch contact. CO_2 fluxes from the mulch-soil system were also highly dependent on mulch water content and were lower for the rape than for the rye experiment. This difference may result from a priming effect induced by the leaching of rye soluble carbon into the soil. N content in the topsoil (0-5 cm) showed an increase due to mulch decomposition and N mineralization along the experiment. This increase was more substantial for the rye experiment as a consequence of the more complete decomposition of rye residues and of the probable priming effect.

The PASTIS$_{mulch}$ model, developed to account for mulch effects, was calibrated on experimental data and evaluated. Calibration of mulch parameters showed that the initial proportion of this dry mass in contact with the soil ($DM_{m,c}(0)$) and the maximal depth for available N for mulch decomposition ($z_{m,zyb}$) were highly dependent on the type of residue, whereas the calibrated mulch feeding rate (α_{feed}) was the same for both residues. The model was run with calibrated parameters and provided good simulation of soil and mulch water regime for both experiment. Mulch dry mass and carbon content were fairly well reproduced, although some discrepancies were observed for CO_2 emission of the rye experiment. These discrepancies were probably due to a priming effect that the model was not able to account for and to an inaccurate description of mulch colonization by the zymogenous biomass at the beginning of the experiment. N content in soil was also well simulated for the rape experiment and again underestimated for the rye experiment where the priming effect increased soil mineralization. The model showed that, at the soil column scale, rape

decomposition led to a positive and increasing net N mineralization throughout the experiment. On the contrary, an early N immobilization stage of 20 days was simulated for the rye experiment, which can be explained by the leaching of the rye soluble compounds of high C:N ratio during the first rain application. This initial stage delayed rye mineral N release which resulted in an equivalent final net mineralization for both experiments (40 kg N ha^{-1}), in spite of a higher net N mineralization flux for the rye experiment after day 20.

The sensitivity analysis of the model highlighted that mulch decomposition processes were highly dependent on the total initial amount of mulch dry mass ($DM_m(0)$) and the initial proportion of this dry mass that was in contact with the soil ($DM_{m,c}(0)$). The water storage capacity of the mulch ($\theta_{me,max}$) and the maximal depth for available N for mulch decomposition ($z_{m,zyb}$) were also decisive parameters of mulch decomposition processes. On the contrary, the minimum mulch water content ($\theta_{me,res}$), the mulch propensity to water recharge (α_m) and the mulch feeding rate (α_{feed}) had little impact on simulation. This latter parameter would probably become more important in real agronomical conditions were the weather and the technical treatments can modify the flux between the non in contact and the in contact compartments.

This work emphasized the role of a mechanistic model to describe simultaneous and complex processes and to provide gross and net C and N fluxes often not available by measurement. It proved that mulch decomposition was not a continuous process as for incorporated residues but occurred in form of successive pulses corresponding to favorable abiotic conditions. This result is in good agreement with field observations on mulch residue turnover that often correlate mulch decomposition with rain events or high temperature periods. However, the modeling approach suffers some weaknesses. PASTIS$_{mulch}$ did not account for priming effect and C transport in soil, which can be an important limitation in the case of surface residue mulch. The assumption that the mulch water content and temperature are the good parameters to describe abiotic factors f_W and f_T is questionable since the mulch-soil interface is a transition zone with strong mass and energy gradients. A weighted average of topsoil and mulch conditions would probably be more adapted. Also, the dynamics of the mulch zymogenous biomass was assumed to follow the same laws as the zymogenous biomass in the soil, whereas the mulch can be submitted to dramatic changes in temperature, water content and available topsoil mineral nitrogen. Research on mulch-soil interface may help to understand better the role of mulch properties (size distribution of elemental pieces, lying or

standing residues, biochemical residue quality,…) in local microclimate and associated decomposition process to define robust functions to be introduced in models. Finally, PASTIS$_{mulch}$ was tested in laboratory conditions, and should be tested in real farming conditions. This last point will be addressed in a following paper.

Acknowledgements

We greatly appreciate the laboratory assistance of F. Barrois, O. Delfosse, G. Alavoine and S. Millon. Thanks to E. Grehan, F. Bornet and F. Schoovaerts for technical support and Y. Duval and F. Mahu for their help with the rain simulator. This work was funded by an INSU ECCO-PNBC project involving INRA and CIRAD and the GICC 2002 project involving INRA and Région Picardie. The collaboration between INRA and K.U.Leuven was supported by the bilateral French - Flemish Tournesol Project (T2001.013).

Appendix B - Illustration experimental design

Picture A.1 Experimental setup for the incubation of soil columns under controlled conditions in a climate chamber. Columns were equipped with TDR probes, tensiometer suction cups and soil solution samplers. Daily CO_2 flux measurements were performed with an infrared gas analyzer.

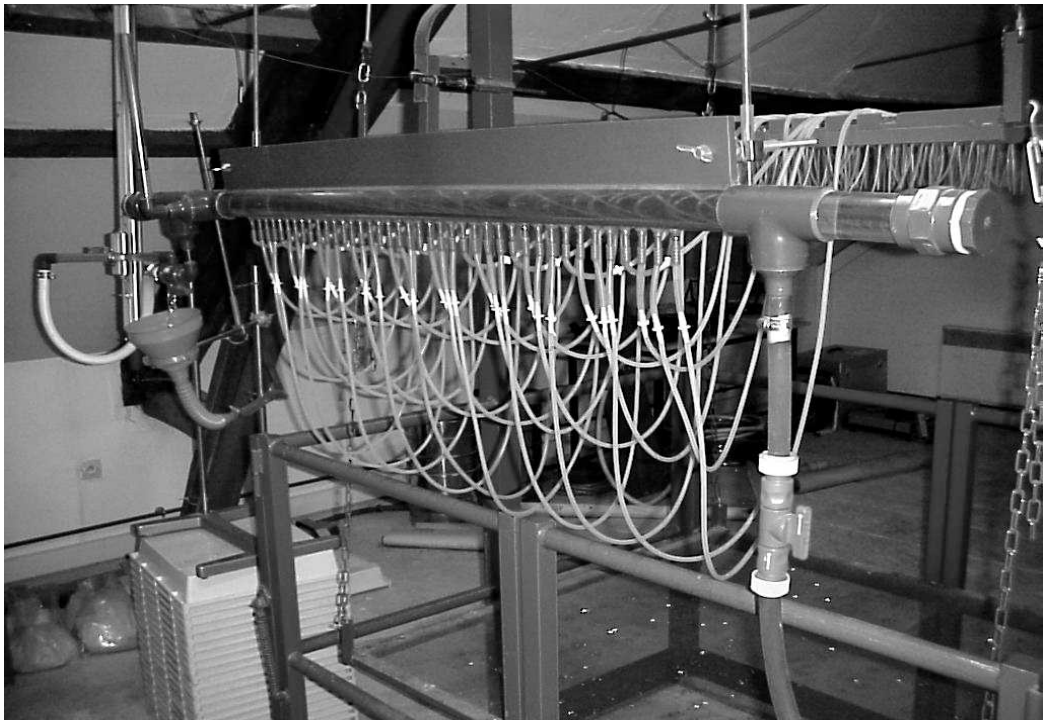

Picture A.2 Simulator that was used to periodically apply an artificial rain on the soil columns (rain intensity: 12 mm $hour^{-1}$)

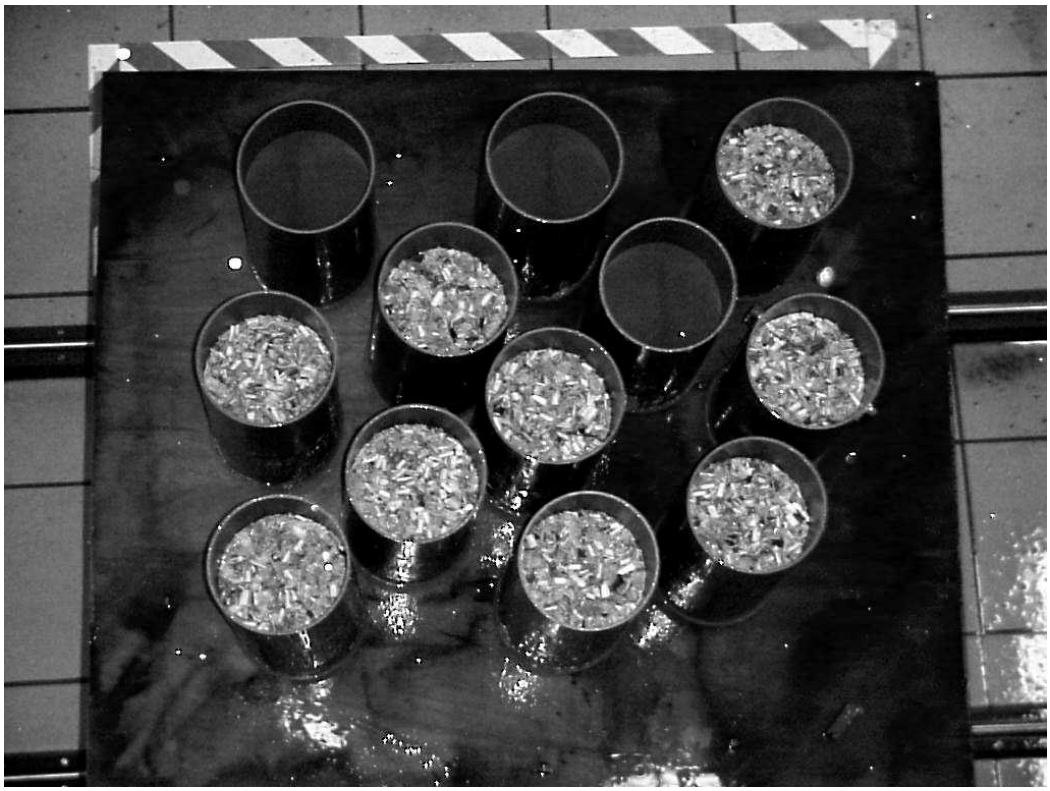

Picture A.3 View of the soil columns (30 cm length and diameter of 15 cm) placed under the rain simulator, with residues left at the soil surface or incorporated in the upper 10 cm of the soil

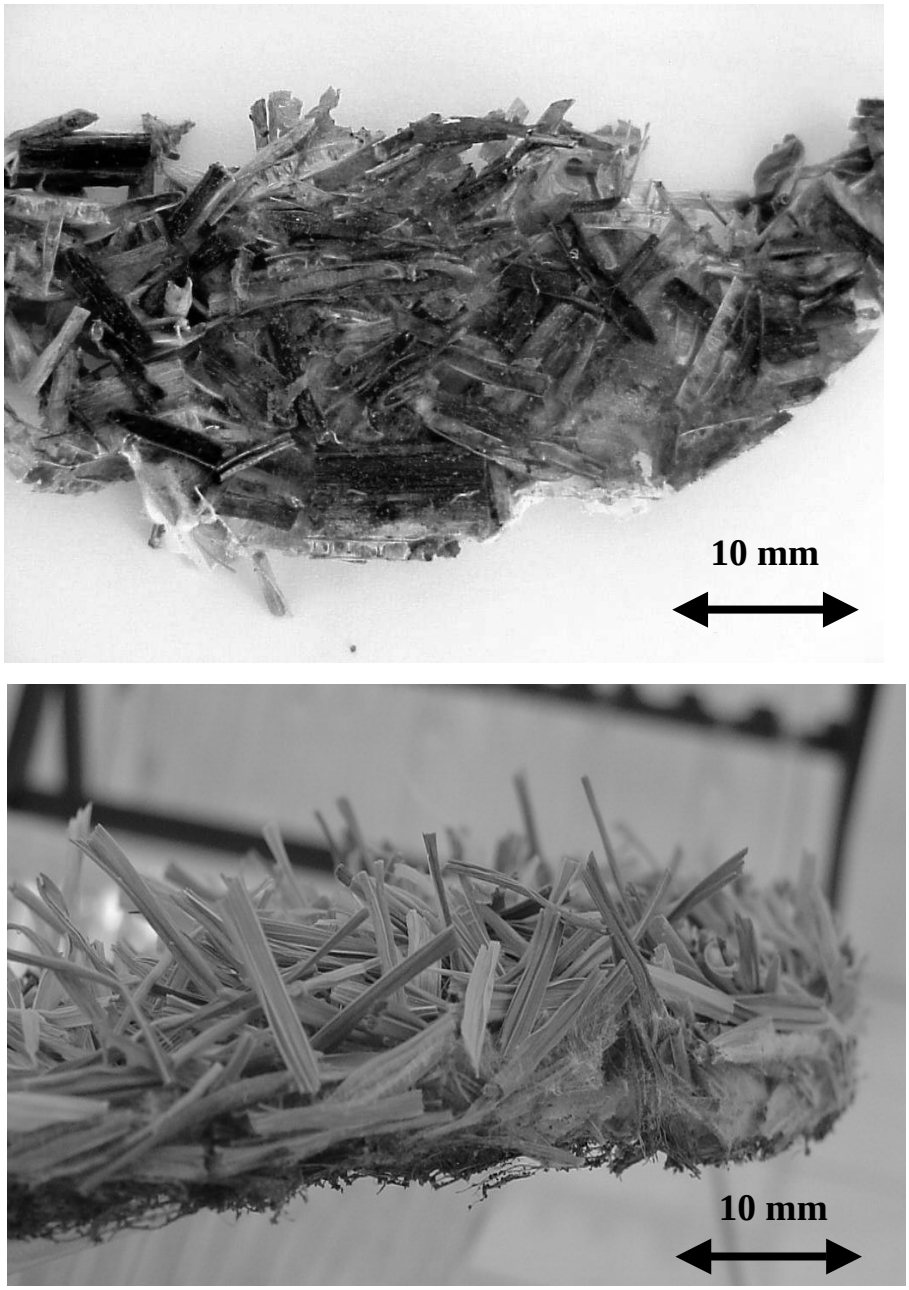

Picture A.4 Detail of oilseed rape mulch (above) and rye mulch (under) after 3 weeks of incubation

Appendix C - Bibliography

Abiven, S. & Recous, S. submitted. Mineralization of crop residues placed at the soil surface or incorporated. *Biology and Fertility of Soils*.

Abiven, S., Recous, S., Reyes, V. & Oliver, R. 2002. Impact of residue quality and location in soil on the C and N mineralisation of residues from cropping systems from Cerrados, Brazil. 17th World Congress of Soil Science, Bangkok.

Adu, J.K. & Oades, J.M. 1978. Physical factors influencing decomposition of organic materials in soil aggregates. *Soil Biology & Biochemistry*, **10,** 109-115.

Aita, C., Recous, S. & Angers, D.A. 1997. Short-term kinetics of residual wheat straw C and N under field conditions: Characterization by $^{13}C^{15}N$ tracing and soil particle size fractionation. *European Journal of Soil Science*, **48,** 283-294.

Ambus, P. & Jensen, E.S. 1997. Nitrogen mineralization and denitrification as influenced by crop residue particle size. *Plant and Soil*, **197,** 261-270.

Anderson, J.P.E. & Domsch, K.H. 1978. A physiological method for the quantitative measurement of microbial biomass in soils. *Soil Biology & Biochemistry*, **10,** 215-221.

Angers, D.A. & Giroux, M. 1996. Recently deposited organic matter in soil water-stable aggregates. *Soil Science Society of America Journal*, **60,** 1547-1551.

Angers, D.A. & Recous, S. 1997. Decomposition of wheat straw and rye residues as affected by particle size. *Plant and Soil*, **189,** 197-203.

Angers, D.A., Recous, S. & Aita, C. 1997. Fate of carbon and nitrogen in water-stable aggregates during decomposition of $^{13}C^{15}N$-labelled wheat straw *in situ*. *European Journal of Soil Science*, **48,** 295-300.

Arrouays, D., Balesdent, J., Germon, J.C., Jayet, P.A., Soussana, J.F. & Stengel, P. (eds) 2002. *Mitigation of the greenhouse effect. Increasing carbon stocks in French agricultural soils? An assessment report compiled by the French Institute for Agricultural Research (INRA) on the request of the French Ministry for Ecology and Sustainable Development*. INRA, France.

Aulakh, M.S., Doran, J.W., Walters, D.T., Mosier, A.R. & Francis, D.D. 1991. Crop residue type and placement effects on denitrification and mineralization. *Soil Science Society of America Journal*, **55,** 1020-1025.

Bailey, V.L., Smith, J.L. & Bolton Jr., H. 2002. Fungal-to-bacterial ratios in soils investigated for enhanced C sequestration. *Soil Biology & Biochemistry*, **34,** 997-1007.

Balesdent, J. 1996. The significance of organic separates to carbon dynamics and its modelling in some cultivated soils. *European Journal of Soil Science*, **47,** 485-493.

Balesdent, J., Chenu, C. & Balabane, M. 2000. Relationship of soil organic matter dynamics to physical protection and tillage. *Soil & Tillage Research*, **53,** 215-230.

Ball, B.C., Scott, A. & Parker, J.P. 1999. Field N_2O, CO_2 and CH_4 fluxes in relation to tillage, compaction and soil quality in Scotland. *Soil and Tillage Research,* **53,** 29-39.

Beare, M.H., Cabrera, M.L., Hendrix, P.F. & Coleman, D.C. 1994. Aggregate-protected and unprotected organic matter pools in conventional- and no-tillage soils. *Soil Science Society of America Journal*, **58,** 787-795.

Bending, G.D. & Turner, M.K. 1999. Interaction of biochemical quality and particle size of crop residues and its effect on the microbial biomass and nitrogen dynamics following incorporation into soil. *Biology and Fertility of Soils*, **29,** 319-327.

Bending, G.D., Turner, M.K. & Jones, J.E. 2002. Interactions between crop residue and soil organic matter quality and the functional diversity of soil microbial communities. *Soil Biology & Biochemistry*, **34,** 1073-1082.

Berkenkamp, A., Priesack, E. & Munch, J.C. 2002. Modelling the mineralisation of plant residues on the soil surface. *Agronomie*, **22,** 711-722.

Blair, N. 2000. Impact of cultivation and sugar-cane green trash management on carbon fractions and aggregate stability for a Chromic Luvisol in Queensland, Australia. *Soil & Tillage Research*, **55,** 183-191.

Blevins, R.L. & Frye, W.W. 1993. Conservation tillage: an ecological approach to soil management. *Advances in Agronomy*, **51,** 33-78.

Bond, J.J. & Willis, W.O. 1969. Soil water evaporation: Surface residue rate and placement effects. *Soil Science Society of America Proceedings*, **33,** 445-448.

Bossuyt, H., Six, J. & Hendrix, P.F. 2004. Rapid incorporation of carbon from fresh residues into newly formed stable microaggregates within earthworm casts. *European Journal of Soil Science*, **55,** 393-399.

Bossuyt, H., Denef, K., Six, J., Frey, S.D., Merckx, R. & Paustian, K. 2001. Influence of microbial populations and residue quality on aggregate stability. *Applied Soil Ecology*, **16,** 195-208.

Bremer, E., van Houtum, W. & van Kessel, C. 1991. Carbon dioxide evolution from wheat and lentil residues as affected by grinding, added nitrogen, and the absence of soil. *Biology and Fertility of Soils*, **11,** 221-227.

Brisson, N., Mary, B., Ripoche, D., Jeuffroy, M.H., Ruget, F., Nicoullaud, B., Gate, P., Devienne-Baret, F., Antonioletti, R., Durr, C., Richard, G., Beaudoin, N., Recous, S., Tayot, X., Plenet, D., Cellier, P., Machet, J.M., Meynard, J.-M. & Delécolle, R. 1998. STICS: a generic model for the simulation of crops and their water and nitrogen balances. I. Theory and parameterization applied to wheat and corn. *Agronomie*, **18,** 311-346.

Bristow, K.L., Campbell, G.S., Papendick, R.I. & Elliot, L.F. 1986. Simulation of heat and moisture transfer through a surface residue-soil system. *Agricultural and Forest Meteorology*, **36**, 193-214.

Bussière, F. & Cellier, P. 1994. Modification of the soil temperature and water content regimes by a crop residue mulch : experiment and modelling. *Agricultural and Forest Meteorology,* **68**, 1-28.

Buyanovsky, G.A., Aslam, M. & Wagner, G.H. 1994. Carbon turnover in soil physical fractions. *Soil Science Society of America Journal*, **58,** 1167-1173.

Cannavo, P., Richaume, A. & Lafolie, F. 2004. Fate of nitrogen and carbon in the vadose zone: in situ and laboratory measurements of seasonal variations in aerobic respiratory and denitrifying activities. *Soil Biology & Biochemistry*, **36,** 463-478.

Carter, M.R. 1992. Influence of reduced tillage systems on organic matter, microbial biomass, macro-aggregate distribution and structural stability of the surface soil in a humid climate. *Soil & Tillage Research*, **23,** 361-372.

Chantigny, M.H. 2003. Dissolved and water-extractable organic matter in soils: a review on the influence of land use and management practices. *Geoderma*, **113,** 357-380.

Chenu, C., Hassink, J. & Bloem, J. 2001. Short-term changes in the spatial distribution of microorganisms in soil aggregates as affected by glucose addition. *Biology and Fertility of Soils*, **34,** 349-356.

Chesson, A. 1997. Plant degradation by ruminants: Parallels with litter decomposition in soils, In: *Driven by nature: Plant litter quality and decomposition* (eds G. Cadisch & K. E. Giller). CAB International.

Coleman, K. & Jenkinson, D.S. 1996. A model for the turnover of carbon in soil, In: *Evaluation of soil organic matter models using existing, long-term datasets* (eds D. S. Powlson *et al.*), pp. 237-246. Springer, Berlin.

Corbeels, M., O'Connell, A.M., Grove, T.S., Mendham, D.S. & Rance, S.J. 2003. Nitrogen release from eucalypt leaves and legume residues as influenced by their biochemical quality and degree of contact with soil. *Plant and Soil*, **250,** 15-28.

Curtin, D., Selles, F., Wang, H., Campbell, C.A. & Biederbeck, V.O. 1998. Carbon dioxide emissions and transformation of soil carbon and nitrogen during wheat straw decomposition. *Soil Science Society of America Journal*, **62,** 1035-1041.

Darwis, D., Machet, J.M., Mary, B. & Recous, S. (1994) Effect of different straw management on the dynamics of nitrogen in soil. Consequences for nitrate leaching. In*: Proc. ISTRO 13th International conference, Aalborg Denmark* (ed. Jensen, H.E.), 201-206 (oral communication)

Denef, K., Six, J., Paustian, K. & Merckx, R. 2001a. Importance of macroaggregate dynamics in controlling soil carbon stabilization: short-term effects of physical disturbance induced by dry-wet cycles. *Soil Biology & Biochemistry*, **33,** 2145-2153.

Denef, K., Six, J., Bossuyt, H., Frey, S.D., Elliott, E.T., Merckx, R. & Paustian, K. 2001b. Influence of dry-wet cycles on the interrelationship between aggregate, particulate organic matter, and microbial community dynamics. *Soil Biology & Biochemistry*, **33,** 1599-1611.

Diels, J., Vanlauwe, B., Van der Meersch, M.K., Sanginga, N. & Merckx, R. 2004. Long-term soil organic carbon dynamics in a subhumid tropical climate: ^{13}C data in mixed C3/C4 cropping and modeling with ROTHC. *Soil Biology & Biochemistry*, **36,** 1739-1750.

Douglas, J., C.L. & Rickman, R.W. 1992. Estimating crop residue decomposition from air temperature, initial nitrogen content and residue placement. *Soil Science Society of America Journal*, **56,** 272-278.

Douglas, J., C.L., Allmaras, R.R., Rasmussen, P.E., Ramig, R.E. & Roager, J., N.C. 1980. Wheat straw composition and placement effects on decomposition in dryland agriculture of the Pacific Northwest. *Soil Science Society of America Journal*, **44,** 833-837.

Elliott, E.T. 1986. Aggregate structure and carbon, nitrogen, and phosphorus in native and cultivated soils. *Soil Science Society of America Journal*, **50,** 627-633.

Engel, T. & Priesack, E. 1993. Expert-N , a building-block system of nitrogen models as resource for advice, research, water management and policy, In: *Integrated Soil and Sediment Research: A Basis for Proper Protection* (eds H. J. P. Eijsackers & T. Hamers), pp. 503-507. Kluwer Academic Publishers, Dodrecht, Netherlands.

FAO. (ed.) 2002. *La séquestration du carbone dans le sol pour une meilleure gestion des terres*, Rome.

FAO/ISRIC/ISSS. 1998. *World reference base for soil resources*. FAO, Rome.

Findeling, A. 2001. Etude et modélisation de certains effets du semis direct avec paillis de résidus sur les bilans hydrique, thermique et azoté d'une culture de maïs pluvial au Mexique, ENGREF, Montpellier.

Findeling, A., Chanzy, A. & de Louvigny, N. 2003a. Modeling heat and water flows through a mulch allowing for radiative and long distance convective exchanges in the mulch. *Water Resources Research,* **39,** 1244.

Findeling, A., Ruy, S. & Scopel, E. 2003b. Modeling the effects of a partial residue mulch on runoff using a physically based approach. *Journal of Hydrology*, **275**, 49-66.

Findeling, A., Lafolie, F., Scopel, E. & Maraux, F. submitted-a. Consequences of direct sowing with residue mulch on crop growth, water and temperature balances: experiments and modeling. *Soil Science Society of America Journal*.

Findeling, A., Garnier, P., Coppens, F., Lafolie, F. & Recous, S. submitted-b. Modelling the physical and biological effects of a decomposing residue mulch on water, carbon and nitrogen dynamics in soil columns.

Flessa, H., Potthoff, M. & Loftfield, N. 2002. Greenhouse estimates of CO_2 and N_2O emissions following surface application of grass mulch: importance of indigenous microflora of mulch. *Soil Biology & Biochemistry*, **34,** 875-879.

Forge, T.A., Hogue, E., Neilsen, G. & Neilsen, D. 2003. Effects of organic mulches on soil microfauna in the rootzone of apple: implications for nutrient fluxes and functional diversity of the soil food web. *Applied Soil Ecology*, **22,** 39-54.

Franzluebbers, A.J. & Arshad, M.A. 1996. Water-stable aggregation and organic matter in four soils under conventional and zero tillage. *Canadian Journal of Soil Science*, **76,** 387-393.

Frey, S.D., Elliott, E.T., Paustian, K. & Peterson, G.A. 2000. Fungal translocation as a mechanism for soil nitrogen inputs to surface residue decomposition in a no-tillage agroecosystem. *Soil Biology & Biochemistry*, **32,** 689-698.

Fruit, L., Recous, S. & Richard, G. 1999. Plant residue decomposition: effect of soil porosity and particle size, In: *Effect of mineral-organic-microorganism interactions on soil and freshwater environments* (eds Berthelin *et al.*). Kluwer Academic / Plenum Publishers, New York.

Fuentes, J.P., Flury, M. & Bezdicek, D.F. 2004. Hydraulic properties in a silt loam soil under natural prairie, conventional till, and no-till. *Soil Science Society of America Journal*, **68,** 1679-1688.

Gaillard, V., Chenu, C. & Recous, S. 2003. Carbon mineralisation in soil adjacent to plant residues of contrasting biochemical quality. *Soil Biology & Biochemistry*, **35,** 93-99.

Gaillard, V., Chenu, C., Recous, S. & Richard, G. 1999. Carbon, nitrogen and microbial gradients induced by plant residues decomposing in soil. *European Journal of Soil Science*, **50,** 567-578.

Garnier, P., Néel, C., Mary, B. & Lafolie, F. 2001. Evaluation of a nitrogen transport and transformation model in a bare soil. *European Journal of Soil Science*, **52,** 1-16.

Garnier, P., Ezzine, N., De Gryze, S. & Richard, G. 2004. Hydraulic properties of soil-straw mixtures. *Vadose Zone Journal*, **3,** 714-721.

Garnier, P., Néel, C., Aita, C., Recous, S., Lafolie, F. & Mary, B. 2003. Modelling carbon and nitrogen dynamics in a bare soil with and without straw incorporation. *European Journal of Soil Science*, **54,** 555-568.

Godwin, D.C. & Jones, C.A. 1991. Nitrogen dynamics in soil-plant systems, In: *Modeling plant and soil systems*, pp. 287-321. American Society of Agronomy, Madison, WI.

Gonzalez Sosa, E., Braud, I., Thony, J.-L., Vauclin, M., Bessemoulin, P. & Calvet, J.-C. 1999. Modelling heat and water exchanges of fallow land covered with plant-residue mulch. *Agricultural and Forest Meteorology,* **97**, 151-169.

Gregory, J.M., McCarty, T.R., Ghidey, F. & Alberts, E.E. 1985. Derivation and evaluation of a residue decay equation. *Transactions of the Asae*, **28,** 98-101.

Guérif, J., Richard, G., Durr, C., Machet, J.M., Recous, S. & Roger-Estrade, J. 2001. A review of tillage effects on crop residue management, seedbed conditions and seedling establishment. *Soil & Tillage Research*, **61,** 13-32.

Guggenberger, G., Elliott, E.T., Frey, S.D., Six, J. & Paustian, K. 1999. Microbial contributions to the aggregation of a cultivated grassland soil amended with starch. *Soil Biology & Biochemistry*, **31,** 407-419.

Gupta, S.C., Dowdy, R.H. & Larson, W.E. 1977. Hydraulic and thermal properties of a sandy soil as influenced by incorporation of sewage sludge. *Soil Science Society of America Journal*, **41,** 601-605.

Hassink, J., Bouwman, L.A., Zwart, K.B. & Brussaard, L. 1993. Relationships between habitable pore space, soil biota and mineralization rates in grassland soils. *Soil Biology & Biochemistry*, **25,** 47-55.

Henriksen, T.M. & Breland, T.A. 2002. Carbon mineralization, fungal and bacterial growth, and enzyme activities as affected by contact between crop residues and soil. *Biology and Fertility of Soils*, **35,** 41-48.

Hermawan, B. & Bomke, A.A. 1996. Aggregation of a degraded lowland soil during restoration with different cropping and drainage regimes. *Soil Technology*, **9,** 239-250.

Holland, E.A. & Coleman, D.C. 1987. Litter placement effects on microbial and organic matter dynamics in an agroecosystem. *Ecology*, **68,** 425-433.

Holland, J.M. 2004. The environmental consequences of adopting conservation tillage in Europe: reviewing the evidence. *Agriculture, Ecosystems & Environment*, **103,** 1-25.

Horn, R. & Dexter, A.R. 1989. Dynamics of soil aggregation in an irrigated desert loess. *Soil & Tillage Research*, **13,** 253-266.

Jensen, E.S. 1994. Mineralization-immobilization of nitrogen in soil amended with low C:N ratio plant residues with different particle sizes. *Soil Biology & Biochemistry*, **26,** 519-521.

Jensen, L.S., Mueller, T., Tate, K.R., Ross, D.J., Magid, J. & Nielsen, N.E. 1996. Soil surface CO_2 flux as an index of soil respiration in situ: a comparison of two chamber methods. *Soil Biology & Biochemistry*, **28,** 1297-1306.

Jensen, L.S., Salo, T., Palmason, F., Breland, T.A., Henriksen, T.M., Stenberg, B., Pedersen, A, Lundström, C. & Esala, M. (in press) Influence of biochemical quality on C and N mineralisation from a broad variety of plant materials in soil. *Plant and Soil*

Jordan, D., Stecker, J.A., Cacnio-Hubbard, V.N., Li, F., Gantzer, C.J. & Brown, J.R. 1997. Earthworm activity in no-tillage and conventional tillage systems in Missouri soils: A preliminary study. *Soil Biology & Biochemistry*, **29,** 489-491.

Keating, B.A., Carberry, P.S., Hammer, G.L., Probert, M.E., Robertson, M.J., Holzworth, D., Huth, N.I., Hargreaves, J.N.G., Meinke, H., Hochman, Z., McLean, G., Verburg, K., Snow, V., Dimes, J.P., Silburn, M., Wang, E., Brown, S., Bristow, K.L., Asseng, S., Chapman, S., McCown, R.L., Freebairn, D.M. & Smith, C.J. 2003. An overview of APSIM, a model designed for farming systems simulation. *European Journal of Agronomy*, **18,** 267-288.

Kinsbursky, R.S., Levanon, D. & Yaron, B. 1989. Role of fungi in stabilizing aggregates of sewage sludge amended soils. *Soil Science Society of America Journal*, **53,** 1086-1091.

Klute, A. & Dirksen, C. 1986. Hydraulic conductivity and diffusivity: laboratory methods, In: *Methods of soil analysis. Part 1. Physical and mineralogical methods* (ed. A. Klute), pp. 687-734. American Society of Agronomy, Inc., Madison, Wisconsin (USA).

Kumar, K. & Goh, K.M. 2000. Crop residues and management practices: effects on soil quality, soil nitrogen dynamics, crop yield, and nitrogen recovery, In: *Advances in Agronomy* (ed. D. Sparks), pp. 197-319. Academic Press, San Diego.

Ladd, J.N., VanGestel, M., Monrozier, L.J. & Amato, M. 1996. Distribution of organic ^{14}C and ^{15}N in particle-size fractions of soils incubated with ^{14}C, ^{15}N-labelled glucose/NH_4, and legume and wheat straw residues. *Soil Biology & Biochemistry*, **28,** 893-905.

Lafolie, F. 1991. Modelling water flow, nitrogen transport and root uptake including physical non-equilibrium and optimization of the root water potential. *Fertilizer Research*, **27,** 215-232.

Le Bissonnais, Y. 1988. Comportement d'agrégats terreux soumis à l'action de l'eau: analyse des mécanismes de désagrégation. *Agronomie*, **8,** 915-924.

Le Bissonnais, Y. & Arrouays, D. 1997. Aggregate stability and assessment of soil crustability and erodibility. 2. Application to humic loamy soils with various organic carbon contents. *European Journal of Soil Science*, **48,** 39-48.

Lin, Q. & Brookes, P.C. 1999. An evaluation of the substrate-induced respiration method. *Soil Biology & Biochemistry*, **31,** 1969-1983.

Lundquist, E.J., Jackson, L.E., Scow, K.M. & Hsu, C. 1999. Changes in microbial biomass and community composition, and soil carbon and nitrogen pools after incorporation of rye into three California agricultural soils. *Soil Biology & Biochemistry*, **31,** 221-236.

Ma, L.W., Peterson, G.A., Ahuja, L.R., Sherrod, L., Shaffer, M.J. & Rojas, K.W. 1999. Decomposition of surface crop residues in long-term studies of dryland agroecosystems. *Agronomy Journal*, **91,** 401-409.

Martens, D.A. 2000. Plant residue biochemistry regulates soil carbon cycling and carbon sequestration. *Soil Biology & Biochemistry*, **32,** 361-369.

Materechera, S.A., Kirby, J.M., Alston, A.M. & Dexter, A.R. 1994. Modification of soil aggregation by watering regime and roots growing through beds of large aggregates. *Plant and Soil*, **160,** 57-66.

Mendham, D.S., Kumaraswamy, S., Balasundaran, M., Sankaran, K.V., Corbeels, M., Grove, T.S., O'Connell, A.M. & Rance, S.J. 2004. Legume cover cropping effects on early growth and soil nitrogen supply in eucalypt plantations in south-western India. *Biology and Fertility of Soils*, **39,** 375-382.

Merckx, R., Den Hartog, A. & Van Veen, J.A. 1985. Turnover of root-derived material and related microbial biomass formation in soils of different texture. *Soil Biology & Biochemistry*, **17,** 565-569.

Molina, J.A.E., Clapp, C.E., Shaffer, M.J., Chischester, F.W. & Larson, W.E. 1983. NC-SOIL - a model of nitrogen and carbon transformations in soil: description, calibration and behaviour. *Soil Science Society of America Journal*, **47,** 85-91.

Molope, M.B., Grieve, I.C. & Page, E.R. 1987. Contributions by fungi and bacteria to aggregate stability of cultivated soils. *Journal of Soil Science*, **38,** 71-77.

Nemati, M.R., Caron, J. & Gallichand, J. 2000. Stability of structural form during infiltration: Laboratory measurements on the effect of de-inking sludge. *Soil Science Society of America Journal*, **64,** 543-552.

Nunan, N., Wu, K., Young, I.M., Crawford, J.W. & Ritz, K. 2003. Spatial distribution of bacterial communities and their relationships with the micro-architecture of soil. *FEMS Microbiology Ecology*, **44,** 203-215.

Pankhurst, C.E., Ophel-Keller, K., Doube, B.M. & Gupta, V.V.S.R. 1996. Biodiversity of soil microbial communities in agricultural systems. *Biodiversity and Conservations*, **5,** 197-209.

Parton, W.J., Schimel, D.S., Cole, C.V. & Ojima, D.S. 1987. Analysis of factors controlling soil organic matter levels in Great Plains grasslands. *Soil Science Society of America Journal*, **51,** 1173-1179.

Paustian, K., Agren, G.I. & Bosatta, E. 1997a. Modelling litter quality effects on decomposition and soil organic matter dynamics, In: *Driven by nature: Plant litter quality and decomposition* (eds G. Cadisch & K. E. Giller). CAB International.

Paustian, K., Andrén, O., Janzen, H.H., Lal, R., Smith, P., Tian, G., Tiessen, H., Van Noordwijk, M. & Woomer, P.L. 1997b. Agricultural soils as a sink to mitigate CO_2 emissions. *Soil Use and Management*, **13,** 230-244.

Powlson, D.S., Smith, P. & Smith, J.W. 1996. *Evaluation of soil organic matter models*. Springer Verlag, Berlin.

Puget, P., Chenu, C. & Balesdent, J. 1995. Total and young organic matter distributions in aggregates of silty cultivated soils. *European Journal of Soil Science*, **46,** 449-459.

Quemada, M. & Cabrera, M.L. 1995. Ceres-N Model Predictions of Nitrogen Mineralized from Cover Crop Residues. *Soil Science Society of America Journal*, **59,** 1059-1065.

Quemada, M. & Cabrera, M.L. 1997. Temperature and moisture effects on C and N mineralization from surface applied clover residue. *Plant and Soil*, **189,** 127-137.

Quemada, M., Cabrera, M.L. & McCracken, D.V. 1997. Nitrogen release from surface-applied cover crop residues: Evaluating the CERES-N submodel. *Agronomy Journal*, **89,** 723-729.

Scott, N.A., Cole, C.V., Elliott, E.T. & Huffman, S.A. 1996. Soil textural control on decomposition and soil organic matter dynamics. *Soil Science Society of America Journal*, **60,** 1102-1109.

Shainberg, I., Goldstein, D. & Levy, G.J. 1996. Rill erosion dependence on soil water content, aging, and temperature. *Soil Science Society of America Journal*, **60,** 916-922.

Sims, J.L. & Frederick, L.R. 1970. Nitrogen immobilization and decomposition of corn residue in soil and sand as affected by residue particle size. *Soil Science*, **109,** 355-361.

Six, J., Feller, C., Denef, K., Ogle, S.M., de Moraes Sa, J.C. & Albrecht, A. 2002. Soil organic matter, biota and aggregation in temperate and tropical soils - Effects of no-tillage. *Agronomie*, **22**, 755-775

Six, J., Elliott, E.T. & Paustian, K. 2000. Soil macroaggregate turnover and microaggregate formation: a mechanism for C sequestration under no-tillage agriculture. *Soil Biology & Biochemistry*, **32,** 2099-2103.

Six, J., Elliott, E.T., Paustian, K. & Doran, J.W. 1998. Aggregation and soil organic matter accumulation in cultivated and native grassland soils. *Soil Science Society of America Journal*, **62,** 1367-1377.

Six, J., Carpentier, A., van Kessel, C., Merckx, R., Harris, D., Horwath, W.R. & Lüscher, A. 2001. Impact of elevated CO_2 on soil organic matter dynamics as related to changes in aggregate turnover and residue quality. *Plant and Soil*, **234,** 27-36.

Smith, J.U., Smith, P. & Addiscott, T.M. 1996. Quantitative methods to evaluate and compare organic matter models, In: *Evaluation of soil organic matter models* (ed. J. Smith), pp. 182-199. Springer-Verlag, Berlin.

Smucker, A.J.M., Dell, C.J. & Santos, D. 2003. Tillage modifications of carbon sequestration within soil aggregates. International Soil Tillage Research Organisation Conference, Brisbane.

Sorensen, P., Ladd, J.N. & Amato, M. 1996. Microbial assimilation of C-14 of ground and unground plant materials decomposing in a loamy sand and a clay soil. *Soil Biology & Biochemistry*, **28,** 1425-1434.

Sui, H., Zeng, D. & Chen., F. 1992. A numerical model for simulating the temperature and moisture regimes of soil under various mulches. *Agricultural and Forest Meteorology,* **61**, 281-289.

Summerell, B.A. & Burgess, L.W. 1989. Decomposition and chemical composition of cereal straw. *Soil Biology & Biochemistry*, **21,** 551-559.

Swift, M.J., Heal, O.W. & Anderson, J.M. 1979. *Decomposition in terrestrial ecosystems*. Blackwell Scientific Publications, Oxford London Edinburgh Melbourne.

Tarafdar, J.C., Meena, S.C. & Kathju, S. 2001. Influence of straw size on activity and biomass of soil microorganisms during decomposition. *European Journal of Soil Biology*, **37,** 157-160.

Taylor, J.P., Wilson, B., Mills, M.S. & Burns, R.G. 2002. Comparison of microbial numbers and enzymatic activities in surface soils and subsoils using various techniques. *Soil Biology & Biochemistry,* **34**, 387-401.

Tebrügge, F. & Düring, R.-A. 1999. Reducing tillage intensity - a review of results from a long-term study in Germany. *Soil & Tillage Research*, **53,** 15-28.

Thomsen, I.K., Schjonning, P., Jensen, B., Kristensen, K. & Christensen, B.T. 1999. Turnover of organic matter in differently textured soils II. Microbial activity as influenced by soil water regimes. *Geoderma*, **89,** 199-218.

Thorburn, P.J., Probert, M.E. & Robertson, F.A. 2001. Modelling decomposition of sugar cane surface residues with APSIM-Residue. *Field Crops Research*, **70,** 223-232.

Tian, G., Brussaard, L., Kang, B.T. & Swift, M.J. 1997. Soil fauna-mediated decomposition of plant residues under constrainted environmental and residue quality conditions, In: *Driven by nature: Plant litter quality and decomposition* (eds G. Cadisch & K. E. Giller), pp. 125-134. CAB International.

Tisdall, J.M. 1994. Possible role of soil microorganisms in aggregation in soils. *Plant and Soil*, **159,** 115-121.

Tisdall, J.M. & Oades, J.M. 1982. Organic matter and water-stable aggregates in soils. *Journal of Soil Science*, **33,** 141-163.

Trinsoutrot, I., Recous, S., Mary, B. & Nicolardot, B. 2000a. C and N fluxes of decomposing ^{13}C and ^{15}N *Brassica napus* L.: effects of residue composition and N content. *Soil Biology & Biochemistry*, **32,** 1717-1730.

Trinsoutrot, I., Recous, S., Bentz, B., Linères, M., Chèneby, D. & Nicolardot, B. 2000b. Biochemical quality of crop residues and carbon and nitrogen mineralization kinetics

under nonlimiting nitrogen conditions. *Soil Science Society of America Journal*, **64,** 918-926.

Tuzet, A., Perrier, A. & Oulid Aissa, A.K. 1993. A prediction model for field drying of hay using a heat balance method. *Agricultural and Forest Meteorology,* **65,** 63-89.

Van Genuchten, M.T. 1980. A closed-form equation for predicting the hydraulic conductivity of unsaturated soils. *Soil Science Society of America Journal*, **14,** 892-898.

Van Soest, P.J. 1963. Use of detergent in the analysis of fibrous feeds. II. A rapid method for the determination of fiber and lignin. *Journal of the Association of Official Agricultural Chemists*, **46,** 829-835.

Van Soest, P.J. & Wine, R.H. 1967. Use of detergents in the analysis of fibrous feeds. IV. Determination of plant cell-wall constituents. *Journal of the Association of Official Agricultural Chemists,* **50**, 50-55.

Vance, E.D., Brookes, P.C. & Jenkinson, D.S. 1987. An extraction method for measuring soil microbial biomass C. *Soil Biology & Biochemistry*, **19,** 703-707.

Vanlauwe, B., Diels, J., Sanginga, N. & Merckx, R. 1997. Residue quality and decomposition: An unsteady relationship?, In: *Driven by nature: Plant litter quality and decomposition* (eds G. Cadisch & K. E. Giller), pp. 157-166. CAB International.

Vestergaard, P., Ronn, R. & Christensen, S. 2001. Reduced particle size of plant material does not stimulate decomposition, but affects the microbivorous microfauna. *Soil Biology & Biochemistry*, **33,** 1805-1810.

Wang, H., Curtin, D., Jame, Y.W., McConkey, B.G. & Zhou, H.F. 2002. Simulation of soil carbon dioxide flux during plant residue decomposition. *Soil Science Society of America Journal*, **66,** 1304-1310.

Watson, R.T. (ed.) 2002. *Climate Change 2001: Synthesis Report*. IPCC, Geneva, Switzerland.

West, A.W. 1986. Improvement of the selective respiratory inhibition technique to measure eukaryote:prokaryote ratios in soils. *Journal of Microbiological Methods*, **5,** 125-138.

West, T.O. & Marland, G. 2002. A synthesis of carbon sequestration, carbon emissions, and net carbon flux in agriculture: comparing tillage practices in the United States. *Agriculture, Ecosystems & Environment*, **91,** 217-232.

Woomer, P.L., Palm, C.A., Qureshi, J.N. & Kotto-Same, J. 1998. Carbon sequestration and organic resource management in African smallholder agriculture, In: *Soil processes and the carbon cycle* (eds R. Lal *et al.*), pp. 153-173. CRC Press, Boca Raton, FL.

Zeller, B., Grehan, E. & Recous, S. in preparation. A simple method to produce large amounts of ^{13}C and ^{15}N labelled beech litter. *Annals of Forest Science*.